Terms and Conditions of Use of Digitised Theses from Trinity College Library Dublin

Copyright statement

All material supplied by Trinity College Library is protected by copyright (under the Copyright and Related Rights Act, 2000 as amended) and other relevant Intellectual Property Rights. By accessing and using a Digitised Thesis from Trinity College Library you acknowledge that all Intellectual Property Rights in any Works supplied are the sole and exclusive property of the copyright and/or other IPR holder. Specific copyright holders may not be explicitly identified. Use of materials from other sources within a thesis should not be construed as a claim over them.

A non-exclusive, non-transferable licence is hereby granted to those using or reproducing, in whole or in part, the material for valid purposes, providing the copyright owners are acknowledged using the normal conventions. Where specific permission to use material is required, this is identified and such permission must be sought from the copyright holder or agency cited.

Liability statement

By using a Digitised Thesis, I accept that Trinity College Dublin bears no legal responsibility for the accuracy, legality or comprehensiveness of materials contained within the thesis, and that Trinity College Dublin accepts no liability for indirect, consequential, or incidental, damages or losses arising from use of the thesis for whatever reason. Information located in a thesis may be subject to specific use constraints, details of which may not be explicitly described. It is the responsibility of potential and actual users to be aware of such constraints and to abide by them. By making use of material from a digitised thesis, you accept these copyright and disclaimer provisions. Where it is brought to the attention of Trinity College Library that there may be a breach of copyright or other restraint, it is the policy to withdraw or take down access to a thesis while the issue is being resolved.

Access Agreement

By using a Digitised Thesis from Trinity College Library you are bound by the following Terms & Conditions. Please read them carefully.

I have read and I understand the following statement: All material supplied via a Digitised Thesis from Trinity College Library is protected by copyright and other intellectual property rights, and duplication or sale of all or part of any of a thesis is not permitted, except that material may be duplicated by you for your research use or for educational purposes in electronic or print form providing the copyright owners are acknowledged using the normal conventions. You must obtain permission for any other use. Electronic or print copies may not be offered, whether for sale or otherwise to anyone. This copy has been supplied on the understanding that it is copyright material and that no quotation from the thesis may be published without proper acknowledgement.

THE INFLUENCE OF FRACTURES ON TOPOGRAPHY AND GROUNDWATER FLOW IN THE BURREN AND GORT LOWLANDS, WESTERN IRELAND.

By Brian Mac Sharry

Department of Geology

Trinity College, Dublin

Submitted to the University of Dublin for the degree of Doctor of Philosophy

December 2005

DECLARATION

This thesis is entirely my own work, except where stated. It has not been submitted for a degree this or any other university. All references are duly acknowledges. I agree that the library of Trinity College, Dublin may lend it on request in accordance with the regulations of Trinity College Dublin.

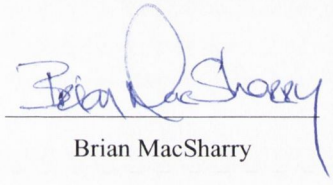

Brian MacSharry

DECLARATION

This thesis has not been submitted as an exercise for a degree at any other university. Except where stated, the work described therein was carried out by me alone.

I give permission for the Library to lend or copy this thesis upon request.

Signed: 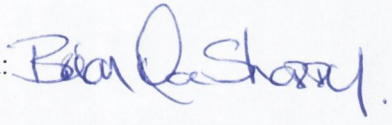

SUMMARY

The primary hypothesis of this thesis is that "Topographic depressions are located along areas of high fracture density" and by association that topographic depressions will identify areas of high fracture density. A secondary, associated, hypothesis is that the "Fracture density controls the flow of fluid in the study area and the morphology of the cave systems". This thesis was examined through the analysis of three separate but inter-linked data sets; the fracture network, the cave systems and the geomorphology of the region, which were collected and analysed using a GIS. The study area chosen was the Burren and Gort Lowlands regions of north Co. Clare and south Co. Galway, due in part to the dramatic variation in topography between these Lower Carboniferous limestone dominated regions. In regions where the matrix is impermeable, such as in this instance, fluid flow is confined to the fracture backbone of the region. In order to understand groundwater flow a detailed understanding of the fracture pattern of the region is essential. Understanding the flow of groundwater in the area is important from an environmental, economic and natural resources point of view.

In order to investigate any influence fractures have on topography it is necessary to map the fracture pattern of the region in detail. When the fracture maps were complete the fracture system was analysed and percolation theory was used to establish the backbone of the system. The terminations of the system were classified into three categories, blind, abutments and cross; from this the connectivity of the system was calculated. The topography of the region was examined through surveyed profiles perpendicular to features and interrogation of a Digital Terrain Model. The length, morphology and orientation of series of cave passages from a number of different caves were analysed. Flow directions of groundwater in the region were obtained. Once the data had been collected it was input into a GIS where the spatial distribution and interactions between the data sets could be examined.

The principal result that comes out of the thesis is the primary importance of the veins rather than the joints in controlling karstic features such as depressions and caves. The veins are preferentially utilised due to the following characteristics, they are clustered, vertically persistent, have a regionally consistent trend, are well connected, have a high rate of intersections per units area, and are horizontally persistent along strike for over 7km. They define narrow zones of increased connectivity that enable flow to transfer across a region. By contrast the joints are regularly spaces, have a lower degree of connectivity, strata-bound and have a regionally variable trend. The veins exert a strong control on the backbone of a fracture system and therefore on regional fluid flow and resulting features. The vertical and horizontal persistence of the vein clusters allows the flow to transfer quickly and effectively between the point(s) of input and discharge. In karstic terrain's dissolution is the primary weathering agent in this region, in bedrock where the matrix is largely impermeable, fractures are the principal pathways of dissolution in the region and thus the resulting dissolution created features will be strongly controlled by the fracture pattern. An analysis of the fracture patterns allows for an understanding of the characteristics of these cave systems and topographic depression, their locations, geometry's and spatial relationships. The two fracture sets, veins and joints, have different attributes and are utilised to differing extents. The cave systems of the region are controlled by two factors, firstly the fracture network and secondly the local hydrological controls. The Caves will preferentially form

along the high connectivity vein dominated sections. Analysing the data within a GIS allows for the spatial distribution of the caves to be evaluated. The topographic depressions are located along vein clusters on a variety of scale from micro, metre level, to macro, kilometre level scale. The depressions mirror the geometrical characteristics of the vein clusters; they are elongate narrow features, which are vertically and horizontally extensive. The surveyed profiles carried out at Cappanawalla and Sheyshmore was compared with the local fracture pattern and it is apparent that the depressions are coincident with the vein clusters. By utilising the different data sets within a GIS the spatial relationships between them can be investigated. When the location of all the surveyed and mapped depressions, obtained from field visits, DTM analysis and literature review, and the mapped cave systems are displayed there is a strong spatial correlation between the data sets.

ACKNOWLEDGEMENTS

I would like to thank John Walsh, Tom Manzocchi and Chris Bonson from the Fault Analysis Group at UCD, for all their selfless help, ideas and encouragement over the last few months, without which this would not have been possible. Thank you. I would like to thank Dr. John Graham for stepping into the breach and being as helpful as possible. I am also indebted to Dr. Alex Densmore, Prof, George Sevastopulo, Dr. Zoe Shipton, Dr. Mike Philcox, Dr David Drew and Dr Pete Coxon of the Geography Dept for many interesting conversations and ideas. I would also like to thank Prof Adrian Phillips, Prof. Geoff Clayton, Dr. Dave Chew, Dr. Ian Sanders, Dr Patrick Wyse Jackson, Dr. Chris Nicolas, and Dr. Val Troll. Prof. David Sanderson was of great help in completing this thesis with his insightful ideas and corrections.

I am especially grateful of all the help from the technicians, Neil for organising anything you need, Frank for his "great" Cork accent, Declan for always being there when you need him, be it for photographs, slides or computer maintenance. I am grateful to Joann Layng for being as helpful as possible when you needed anything. I would like to thank Martin Critchley, Glen Millar and Dave Coller for their help over the years,.

I would like to thank all the post-graduates in the Department, especially those who have escaped over the last few years. A special thanks to Mike Cunningham for all his friendship and help over the years. Also to my former comrade in arms, Duncan, Gerry- thanks for talking me into playing soccer that evening-, Phonsie- for all your friendship and the regular visits as a result of the soccer and the surfing, Stuart, FX, Murray, Malone, Leather- who I still blame for "making me "tackle that guy, I'll get you when you are rich don't worry, Alan –my business partner, we could have been rich (doubtful really), Jamie, Christina, Niamh- thanks for helping me keep sane when I was writing up-Jacqui, Becky, Jackie, Mags, Gemma, Kate, Aileen, Pete, Kirsten, Claire, Rory, the newbie's, Catherine, Eoghan and Marion, the Pearse Street gang- Dave, Mary and Ben- its been great sharing office with you and thanks for the help over the last few days, especially for the chocolate, thanks Mary. Thanks to all of you for your friendship. And to those who have gone off to greener pastures, or in Karl's case sandier pastures, Sarah, Ric, thanks for all the chocolate, Kay, Cruise, Niall, Güven, Craig, thanks for showing me around at the start.

I would like to thank Julie, Monina and Piero for being great house-mates and to Sam, thanks for carrying the surveying equipment up all those hills. A big thank you to Elizabeth for all your help and friendship over that last few years, it has been greatly appreciated and this thesis would be substantially more illegible if not for your superb editing skills, also thanks to Olwyn for your friendship and company. And to my old friends Vicky and Stephen, thanks for all the support over the last few years, you won't have to be buying me drinks anymore wait until the IT gets a hold o f this, front page here I come again. I am grateful to Gay & Mary and co in the Exams office for all the work and to Jackie Akerele. To all those on the GSU committees over the years it was a real pleasure and reality check, we had some great times, especially Ming being released. A big thanks to all at NPWS, especially Gemma, Rebecca and Marian, all the GIS Unit and my colleagues in the National Monuments Section particularly Ann & Con.

Finally a big thank you to my family especially my parents for all their help, financial and emotional over the years, I hope I can pay it back sometime

DEDICATION

This thesis is dedicated to my family for all their support.

"Louit now solicited, through the College Bursar, and finally obtained, a further sum of £50, fondly calculated to defray the expenses of a 6 month research expedition in the county of Clare. His analysis of the risible estimate was as follows

	£	s	d
Travelling	1	15	0
Boots	0	15	0
Coloured beads	5	0	0
Gratifications	0	10	0
Sustenance	42	0	0
	50	00	00

The food necessary for the maintenance of his dog a bull terrier, in the condition of ferocious plethora to which he was accustomed, he generously declared himself willing to pay out of his own pocket and he added, with his usual candour and to great merriment of the Grants Committee that he thought he could rely on O'Connor to live off the country.....Invited through the College Bursar to produce the boots for the return of the 15s.....he declared that they had unfortunately been sucked off his feet by a bog, which in the fading light and the confusion of his senses consequent on his prolonged inanition, he had mistaken for a field of late onions."

Watt, Beckett 1952

"The hard grey beauty of North County Clare"

S. Wall 1993

Table of Content

Chapter 8. Discussion & Conclusions

List of Figures

CHAPTER 2

CHAPTER 3

CHAPTER 4

CHAPTER 5

CHAPTER 6

CHAPTER7

List of Table

CHAPTER 3

CHAPTER 4

CHAPTER 5

CHAPTER 6

CHAPTER 7

CHAPTER 1: INTRODUCTION

1.1: Introduction

The primary hypothesis of this thesis is that "Topographic depressions are located along areas of high fracture density" and by association that topographic depressions will identify areas of high fracture density. A secondary, associated, hypothesis is that the "Fracture density controls the flow of fluid in the study area and the morphology of the cave systems". These hypotheses are based upon observations of the fracture patterns and topography of the Burren and Gort Lowlands, which have a contrasting topography despite having similar geology. The Burren consists of an approximately 360km^2 plateau of Lower Carboniferous Limestone and Upper Carboniferous Shale's and Sandstone's, gently dipping from 200-300 m in the north to 100 m in the south, following the regional dip to the south-south-west. The Gort Lowlands is a region of Lower Carboniferous Limestone bounded to the west by the Burren and to the east by the Slieve Aughty Lower Palaeozoic Inlier. It is a low-lying plain extending from Kinvarra in the north to the Fergus Estuary in the south.

To test these hypotheses the following data sets will be analysed

- Fracture patterns: need to quantify and describe the fracture sets in the region and investigate the spacing, density, connectivity, fill, vertical persistence of the fracture sets.
- Topography: the micro, meso and macro scale topography of the region needs to be mapped and discussed, identify any recurring aspects of the depressions, their length, shape, spatial distribution. As the area of interest is a karstic terrain the processes involved in karstification, the primary weathering agent in this region, need to be discussed.
- Hydrological information is required in the form of flow patterns, flow controls and catchment information.
- Cave systems: need to investigate the distribution of cave systems, their shape, controls on the caves- are they vertically persistent or horizontally persistent, their relationship to each other and to any surface topographic features.
- Regional geology, what units are the features in, does the regional bedrock geology have a control on the features.

The data will be obtained by

- Analysis of remotely sensed imagery, principally aerial photographs at two scales, 1:3,000 and 1:48,000 of selected areas. This will be supplemented by field visits to validate the data and map additional areas.
- A literature review of the topography of the region will be followed up by analysis of stereo-paired aerial photographs, which will be used to identify depressions. Specific locations will be surveyed using a Electronic Distance Metre (EDM) total station, while a Digital Terrain Model (DTM) of the area will be used to locate features and for extraction of topographic profiles of large areas.
- The hydrological controls of the regions will be obtained from a literature review.
- Information regarding cave systems will be obtained via literature review and discussion with speleologist's familiar with the region.

The results from all these different data sets will be incorporated into a Geographic Information System (GIS) (Arc View 3.2) to investigate any spatial correspondences.

Fractures have important mechanical effects on rock masses, governing rock mass stability and strength as has been widely discussed in engineering geology literature, see Zhang & Sanderson (2002) and Odling *et al.* (1999) and references within. It is the influence of fractures on fluid flow and creation of resulting features that will be examined. The chemical weathering process of dissolution of limestone by weak carbonic acid produced by the reaction of water and carbon dioxide is the dominant weathering agent at work on karstic areas. Flow and transport through a karst aquifer is strongly dependent on heterogeneities, such as fractures that have been enlarged by chemical dissolution, these solutionally enlarged conduits provide preferential flow pathways through the system (Kaufmann 2003). As the fractures enlarge due to dissolution, conductivities in the fracture system can increase with time, with fracture conductivity increasing by several orders of magnitude with increasing fracture width (Kaufmann & Braun 1999, Kaufmann & Braun 2000, Kaufmann 2003) with flow routes that acquire increasing discharge accelerate in growth, forming cave passages, while others languish with negligible growth (Palmer 1991). The driving force for flow through the system is groundwater recharge and discharge, as the amount of recharge, either by precipitation (diffuse recharge) or via sinking streams (concentrated inputs), and the heights of the base level of resurgences and rivers (discharges), establish the pressure difference for flow within the aquifer (Kaufmann 2002).

This region was chosen as it is the best-developed karst region in Ireland, contains a wide variety of surface and sub surface karst landforms ranging from micro to macro relief surface features (Section 7.2), an extensive network of cave systems that have been mapped in detail by speleological groups and a well exposed fracture system. In addition there was a large database of water flow traces, depression locations and maps and descriptions of cave systems available for the two regions. The geomorphology, hydrology and the cave systems of the Burren have been described by a number of workers, principally Drew (1973, 1980, 1988, 1990, 1993, 2000, 2003) and by the University of Bristol Spelaeological Society. The hydrology and geomorphology of the Gort Lowlands was subject to an extensive amount of data collection and analysis through the remit of the Office of Public Works (OPW) report entitled "An Investigation of the flooding problems in the Gort–Ardrahan Area of South Galway" (1997). This report was commissioned to investigate the flooding in the region in the vicinity of Gort town, which suffered three "100 year" floods in 1990, 1991 and 1994/1995. These events flooded large areas of this low-lying plain, creating large lakes over much of the region and isolating a number of homes from the outside world. The subsequent damage was estimated at €12.6 million and led to a call for the government to take immediate action to "solve" the problem.

The fracture pattern of the Burren was investigated through a combination of analysis of low-level aerial photographs and field mapping. The fracture pattern for the Gort Lowlands was investigated using a combination of SAR imagery and aerial photographs that were commissioned for the 1997 study of the area. Remote sensing data provided a common database in these two regions.

1.2: Thesis outline

A theme-based approach has been adopted in the presentation of this research. Each chapter presents an introduction to what will be discussed, followed by the relevant information on materials and methods, followed by analysis of the data and discussion of the results. Several appendices are included which contain additional data used in the thesis. These are referenced where appropriate.

This research is based on work carried out on three distinct but interlinked data sets; fracture and lineament data, cave location and passageway data and data on topographic depressions in the region. This analysis has been followed up where appropriate by visits to key locations.

Chapter Two provides the regional geological and structural settings which all have had a strong influence on the landscape of the region. The karstic landscape for which the Burren is famous is a result of solution acting on the Lower Carboniferous limestone. The Namurian strata capped and protected the limestone until recent times (Tratman 1969, Drew 2003). The Galway Granite has had an affect on the geology of the region since its emplacement. It acted as a structural high during Carboniferous times (Hodson 1954, Max *et al* 1978, Max *et al* 1983, Madden 1983 in El Desouky *et al* 1996), subsequently it provided the source of the fluids that filled the veins as evident by the occurrence of fluorite in the veins of the region O'Connor *et al.* (1993). The termination of the Fergus Shear Zone against the granite has had an effect on the entire region, creating a complex fracture pattern in the Gort Lowlands and leaving a structural imprint on the Burren. The hydrology of the Burren and Gort Lowlands is discussed at the end of this chapter. This provides a context for the hydrological setting of the region and describes each area in detail including discussion on surface and subsurface flow and flow paths derived from tracer studies.

Chapter Three deals with the attributes of the fracture sets. The chapter discusses the different fracture sets that occur within the Burren in terms of type, orientation, fill, spacing, vertical persistence and relative timing. The fractures can be divided into two groups, veins and joints, which have different geometrical and spatial characteristic and different controls on the flow through the system.

Chapter Four discusses the fracture network in terms of connectivity, intersection density and percolation theory. This chapter discusses the processes that can control the transport of fluids through a fractured rock mass. A series of fracture networks are analysed and discussed, the spanning cluster and backbone of each network is derived an compared to the original network in order to investigate the role specific fracture orientations (and types) have on controlling flow through the system. It will be shown that the backbone can have different directional characteristics than the network. The results of this analysis are subsequently used to understand and analyse the sub-surface and surface features of the Burren and the Gort Lowlands.

Chapter Five discusses the role of remote sensing in lineament analysis. The different images used in the project are discussed as are the techniques used to enhance and understand the lineament derived from the images. The concept of lineaments analysis is discussed and a conceptual model for the stages in the development of a lineament map is produced.

Chapter Six introduces the sub-surface drainage of the region. Controls on the location of the caves are discussed. The caves are described as layer parallel flow features as the caves are mainly horizontal and confined to individual beds. In situations similar to this where cross layer flow is inhibited two-dimensional fracture patterns can be used to understand three-dimensional flow (Odling 1997). This allows the concepts developed from the interpretation of fracture patterns in Chapter Four to be applied to the cave system. A series of 25 caves from across the Burren are divided into 13 geographic regions. The hydrology and the characteristics of the caves found within each geographic region are discussed individually. The caves are subsequently analysed basis of the orientation of the cave passages and any links with surface features are highlighted and discussed. The results from this allow for an understanding of how the fractures control groundwater flow in the Burren. The caves are also used to elucidate the local fracture pattern of the region in which they occur.

Chapter Seven discusses the geomorphology of the region and the link between fractures and depressions and discusses the features associated with karstic terrains. The role of chemical weathering in the development of the Burren and other karstic terrains is examined. In order to investigate the link between fractures and topography a series of topographic profiles were done at a number of locations and several scales. The methodology and conclusions of these profiles are discussed. The chapter ends by discussing both the surface and subsurface features of the Gort Lowlands.

Chapter Eight provides a discussion of the major questions and conclusions reached from the research. In the chapter the links between each data set are used to answer the questions raised, such as what is the effect of the local hydrological situation, why are veins utilised preferentially to joints, are there links between surface and sub surface features. Recommendations for future work are made in this section.

CHAPTER 2: REGIONAL GEOLOGY.

2.1: Regional Geology

The Burren is composed of a series of Lower Carboniferous (Dinantian) limestones overlain by Upper Carboniferous (Namurian) shales and sandstones. The Namurian deposits are confined to the western and southern extent of the Burren, with the remainder of the Burren being composed of Lower Carboniferous Limestones which produces the characteristic stepped topography of the Burren. The low-lying Galway Batholith Figure 2.1 dominates the north side of Galway Bay). The Galway Batholith extends south south east for several kilometres under Galway Bay where it forms the substrate for Carboniferous Limestone strata of the Burren of north Co. Clare (Hodson 1954, Max *et al* 1978, Max *et al* 1983, Madden 1983 in El Desouky *et al* 1996). The Lower Carboniferous limestone and the Galway Granite Batholith are tectonically juxtaposed in Galway Bay by the EW trending Skerd Rocks Fault, which produces a pronounced topographic scarp on bathymetric maps of Galway Bay. O'Raghallaigh *et al* (1997) describe the off-shore geology of Galway Bay and give a post-Visean age for this fault and incorrectly state that the fault downthrows to the north. This implies that the ancient Skerd Rock Fault, which predates the intrusion of the batholith and brings the South Connemara Group in contact against the Dalradian metagabbro-gneiss suite, (El Desouky *et al* 1996, Crowley & Feely 1997), has been reactivated in post-Visean times. Dewey (2002) postulates that this fault, which he calls the Galway Bay Fault and shows down throwing to the south, was rejuvenated under NW-SE directed compression in Miocene times.

2.1.1: Galway Granite

The Galway Granite Batholith is a late Caledonian Calcalkaline composite intrusion emplaced at c. 400Ma into the 470Ma metagabbro-gneiss suite to the north and into lower Ordovician greenschist facies rocks of the South Connemara Group to the south (Leake 1989, Leake & Tanner 1994, Crowley & Feely 1997, Friedrich *et al* 1997). The 470Ma age was derived from U-Pd dates yielded from the Cashel-Lough Wheelan Gabbro. The intrusion was sited along a major fault the E-W trending Skerd Rocks Fault. The dimensions of the Galway Granite on land are 70km by EW by 30km NS, while a south-south-east extension of several km beneath Galway Bay is indicated by gravity and aeromagnetic studies, where it forms the substrate for Carboniferous Limestone strata of the Burren of north Co. Clare (Hodson 1954, Max *et al* 1978, Max *et al* 1983, Madden 1983 in El Desouky *et al* 1996). The overall dimensions of the Galway Granite Batholith are 90km by 35km with the long axis orientated NNW - SSE (El Desouky *et al* 1996).

The Galway Granite Batholith (Figure 2.2) is cut by two major faults, the NNE trending Shannawona fault and the NNW trending Barna Fault. They define the boundaries of between three principal blocks, the western (west of the Shannawona fault), the central (between the Shannawona Fault and the Barna Fault) and the eastern block (east of the Barna Fault) (Crowley & Feely 1997). Gravity studies by Madden (1983), in Crowley & Feely (1997), show that the central block is 3-4km thinner than the western block. This is in keeping with the assertion by Leake (1978) that the granite to the east of the Shannawona Fault, the Central block, was up-thrown and then eroded now exposing a corresponding deeper intrusive level. The western block comprises lithologies ranging from granodiorite (the Carna Granite) through adamellite (the Errisbeg Townland Granite) to alkali granite (the Murvey Granite)

(Crowley & Feely 1997). The central block exposes a wider spectrum of lithologies ranging from diorite to granodiorite to alkali granite, indicating a relatively less evolved nature for the central block, in fitting with Leake's (1978) assertion.

The western block consists of three major granites, the Carna Granite, Errisbeg Townland Granite and the Murvey Granite and exposes roof zone granites (Leake 1974, 1978, 1990, Crowley & Feely 1997). The margins of the western block are commonly occupied by the evolved leucocratic Murvey Granite, which passes inwards over a few meters into the K- Feldspar megacrystic Errisbeg Townland Granite, which itself passes inwards over c.300m to the Carna Granite. According to Leake (1974) the narrow transitional contact between the Errisbeg Townland Granite and the Murvey Granite is consistent with crystallisation of the Murvey Granite as a layer on top of the Errisbeg Townland Granite with which it is always in contact. The Carna Granite was almost fully crystallised before being emplaced by near vertical upward movement into the Errisbeg Townland Granite Murvey Granite magma (Leake 1974, Crowley & Feely 1997). The western block is separated form the central block by the NNE trending sinistral Shannawona Fault.

2.1.2: Carboniferous

2.1.2.1: Introduction

At the start of the Carboniferous, Ireland was located near the equator on the southern margin of the Old Red Sandstone continent. To the south there was a rapidly transgressing wide shallow ocean (Sevastopulo 1981, Cope *et al* 1992, Sevastopulo & Wyse Jackson 2001). By late Dinantian times the palaeogeography of Ireland was dominated by a wide (c.500km) shallow marine carbonate platform bounded by land to the north and by the South Munster Basin to the south with at least two fault controlled intrapaltform basins, the Dublin Basin and the Shannon Trough (Sevastopulo 1981, Somerville & Strogen 1992, Gallagher 1996). Carbonate sedimentation dominated during Dinantian times. By early Silesian times the sedimentation pattern was dominated by an overall regressive trend in which there was an overall shallowing upwards trend from deeper water deposits to more terrigenous and shallow water cyclothemic deposits of deltaic origins (Anderton 1979, Sevastopulo 1981, Cope *et al* 1992, Goodhue 1996).

2.1.2.2: Lower Carboniferous

The lithological units that make up the exposed limestones of the Burren are late Dinantian (Asbian and Brigantian) in age. Evidence for what might underlie the Burren limestones must come from adjacent areas. Waulsortian limestone banks dominate successions in the late Tournaissian. They are thought to represent accumulations below storm wave base in aphotic conditions, more than 200m deep (Lees & Miller 1995). The Waulsortian Complex in Ireland has the greatest lateral spread (more than 30,000km^2 in the late Tournaissian), and thickness (up to about 100m) known anywhere in the world (Lees & Miller 1995). The Waulsortian formed near the South Munster Basin seems to be situated on a laterally extensive ramp. Stratigraphic and facies relations show that the Waulsortian complex spread from the Shannon area eastwards and northwards following the transgression up the regional paleoslope (Sevastopulo 1982, Cope *et al* 1999, Lees & Millar 1995). Fault related bathymetric features sometimes influenced Waulsortian build-up. Lees (pers. comm. 1999) notes that there is a distinct change in the paleoseafloor

in the region of the Fergus Shear Zone, indicating that the Fergus Shear Zone lineament was an active paleobathymetric feature at the time.

In North Clare and South-West Galway bioclastic shelf limestones persisted throughout the Visean. The Tubber Formation (MacDermot unpub. and Gallagher 1996) comprises the stratigraphic interval between the Waulsortian bank deposits and the base of the overlying Burren Formation (Sleeman & Pracht 1999). The Tubber Formation is characterised by crinoidal medium grey packstone and wackestone (Sevastopulo & Wyse Jackson 2001).

The terraced topographic nature of the limestones in the Burren reflects the subtle lithological changes indicative of the cyclical nature of the Asbian and Brigantian successions (Sevastopulo 1981). The Burren Formation (MacDermot unpub. and Gallagher 1996) passes conformably from the Tubber Formation without significant lithological change (Sleeman & Pracht 1999, Sevastopulo & Wyse Jackson 2001). The formation is typified by a pale grey packstone and wackestone with intervals of dark cherty limestones and oolitic grainstones. Gallagher (1996) interpreted the sequences within each cycle as follows: an initial shallow sub-tidal phase during which peloidal limestones were deposited, followed by: a slight deepening when crinoids became prevalent, this was in turn followed by: a shallowing during which peloidal limestones were deposited (Gallagher 1996, Sevastopulo & Wyse Jackson 2001). The tops of many of the cycles show evidence of emergence in the form of palaeokarstic surfaces and clay wayboards, which were probably palaeosols. The Asbian Burren Formation had been divided into four members by MacDermot, which are seen on the geological map of the Burren, Figure 2.3, and on the stratigraphic column, Figure 2.4. The oldest member is the Blackhead Member, which is a thick to medium, bedded fine-grained limestone. This is followed by the Fanore Member a medium bedded fine-grained limestone with thin shale partings between beds. The Maumcaha Member overlies the Fanore Member, and consists of a massive fine-grained limestone, which is subsequently overlain by the Aillwee Member. The Aillwee Member is the topmost member of the Burren Formation and consists of thick, massive beds fine-grained limestones with a number of clay horizons. MacDermot has divided the Aillwee Member into two divisions an upper and a lower division. The cycles within the Asbian have an average thickness of 12 m (Gallagher 1996). The Burren Formation is overlain by the Brigantian Slievenaglasha Formation (MacDermot unpub. and Gallagher 1996).

The Slievenaglasha Formation is characterised by the development of cyclical crinoidal packstones and grainstones interbedded with darker fine-grained nodular wackestone occurring in the lower and upper parts of the formation, while the middle section is dominated by dark cherty nodular-bedded wackestones and packstones. It has been divided into four distinct members. The lowest member of the formation is the Ballyvoe Member an alternating medium to coarse-grained crinoidal limestones. The Fahee Member is a fine-grained limestone with frequent chert nodules and is marked by a distinct chert bed at it base and it top. These chert layers can be correlated to the Upper and Lower Faunal Zones of Drew (1988). These chert layers act as acquitards for the cave systems in the region. The overlying Ballyelly Member is a crinoidal medium grained limestone with chert layers and chert nodules. The uppermost member of the Slievenaglasha Formation is the Lissylisheen Member, an alternating fine-grained, medium to coarse-grained crinoidal limestone. The cycles within the Brigantian have an average thickness of 6 m, and are deeper sub-tidal in nature compared to the underlying Asbian (Gallagher 1996). The Upper Carboniferous Namurian succession rests unconformably on the Brigantian units.

2.1.2.3: Upper Carboniferous

The Silesian of Western Europe is divided into the Namurian, Westphalian and Stephanian. Within Ireland the Namurian is the most wide spread, with the Westphalian being confined to the Lenister, Slieve Ardagh, Cratloe, Kanturk and Coalisland coal fields and the Kingscourt Inlier; there are no Stephanian sediments in Ireland (Sevastopulo 1981). Throughout the Dinantian and Silesian, subsidence continued and generally basin sizes decreased although many area of non-deposition are recognised and interpreted as upstanding blocks. Some of these blocks are underlain by Devonian granites, which are of low density and are isostaically buoyant. The early Namurian was marked by an overall regressive trend, in which lowering of the sea relative to land level brought an increase in the input of clastic material smothering the carbonate platforms (Goodhue 1996). The largest area of Namurian rocks in Ireland extends from north Co. Clare across the Shannon to Killarney, Co. Kerry, and across to near Mallow Co. Cork, Figure 2.5, (Sevastopulo & Wyse Jackson 2001). Goodhue uses the term West Clare Basin to describe this region; it is the equivalent to the Western Namurian Basin of Collinson *et al* (1996) and the Western Irish Namurian Basin of Wignall & Best (2000).

The differential subsidence and bathymetry initiated in the Dinantian period persisted into the early Namurian. The Namurian of Clare is divided into two groups the Shannon Group and the Central Clare Group (Rider 1974, 1978, Pulham 1989). The Clare Shale Formation is stratigraphically the lowest formation of the Shannon Group The lowest member of the Shannon Group, the Clare Shale Formation, can dramatically illustrate this. In the north of the basin, in, north-west Clare, the Clare Shale Formation is a 10 m thick succession, which rests unconformably, but without obvious angular discontinuity, on an attenuated Dinantian sequence of clean shallow marine shelf bioclastic limestone (Hodson 1954a, Hodson 1954b, Sevastopulo 1981). Southwards towards the depocentre of the basin, a distance of c.60km, the same formation thickens considerably to in excess of 300m. Here the Clare Shale Formation rest conformably on a Dinantian sequence which consists of carbonate breccias passing upwards into interbedded limestones and mudstones of probable deep-water origin. The Clare Shales are the lateral equivalent of the Ross Sandstone Formation that occurs in the central and southern part of the basin. The Ross Sandstone Formation is a turbiditic sandstone that thins away from the axis of the basin. The Gull Island Formation, which reaches a thickness of 130 m in the north, overlies the Ross Sandstone Formation to the south, where the Gull Island Formation is a c.550m thick succession (Collinson et al 1991).

At its depocentre near Ballybunion, Co. Kerry, the thickness of the Namurian exceeds 1600m, whereas in the north at Doolin, the succession is 300m thick. The reason for this disparity is that the NW of Clare is underlain by the southerly extension of the Galway Granite. As granites are less dense and isostatically buoyant, they act as structural highs. In the Carboniferous of the Clare region the Galway Granite acted as a structural high, as indicated by the stratigraphy of the region.

In the north of Clare, the lowest part of the Clare Shale Formation consists of a phosphate sequence. These phosphates occur as a thin veneer of pebbles welded to the top of the Dinantian shelf bioclastic limestone, and as thin laterally extensive lenses as short distance above the limestone (Sevastopulo 1981, Sevastopulo & Wyse Jackson 2001). These phosphates consist of granular apatite and collophane, carbonate apatite, which together with pyrite are set in an apatite and carbonate cement (Sevastopulo 1981, Sevastopulo & Wyse Jackson 2001). Such phosphates are known in other areas as extremely condensed deposits; they also commonly indicate the presence of

submarine highs. In the Clare area they are shown to reflect very slow sedimentation rates (Sevastopulo & Wyse Jackson 2001). The Clare Shale Formation records tranquil anoxic to dysoxic deposition over the West Clare Basin during the early Namurian (Wignall & Best 2000). Wignall & Best (2000) developed a new model for the West Clare Basin arguing that the change from carbonate dominated deposition in the Dinantian to the black shale deposits of the early Namurian coincided with substantial deepening over the Galway High.

The Gull Island Formation is mainly formed of laminated grey siltstone, but contains particularly in its lower parts turbiditic sandstones deposited by channels up to 6 m deep and several hundred meters wide (Collinson *et al* 1991). The siltstones show evidence for extensive syn-depositional slumping (Donath & Parker 1964). The slumps are internally folded into recumbent flow folds; the most striking example of this is the Fisherstreet Slide, which affects the lower beds of the formation near Doolin. As with the Clare Shale Formation, the Gull Island Formation thickens progressively to the south. In the north of the basin the Gull Island Formation is 130m thick and rests on the Clare Shale Formation, in the south of the basin the same formation is approximately 550m thick and rests on a thick sequence of bedded turbidite sandstones, the Ross Sandstone Formation (Sevastopulo 1981, Sevastopulo & Wyse Jackson 2001. The palaeocurrent directions in the Gull Island Formation indicate a general WSW to ENE transport direction (Rider 1969). The facies seen throughout the Gull Island Formation and in overlying cyclothems indicate that there was a major sediment source to the west and northwest. Rider (1974) compares the Namurian sequences of this region to those of the modern day Mississippi Delta.

The overlying Central Clare Group (Rider 1974, 1978, Pulham 1989) is made up of a series of five large-scale cyclothems. Each cyclothem recoding the progradation of a deltaic system that commonly culminates in distributory channel sandstone followed by transgression and development of marine strata (Rider 1974, Pulham 1989, Wignall 2000)

2.2: Fergus Shear Zone

In the western half of Central Ireland, Variscian deformation is characterised by brittle-ductile trans-current shear zones, major open folds and heterogeneous vertical cleavage (Coller 1984). Deformation being the result of NS compression and EW to ENE-WSW dextral shear (Coller 1984). The Fergus Shear Zone marks the western margin of this zone of deformation. The Fergus Shear Zone is a major NNE trending Hercynian age, low strain, and sinistral shear zone. It extends from the Foynes region of West Co. Limerick to the Gort Lowlands of South Co. Galway. It a long narrow feature being over 70km long and between 5 and 15km wide and an overall displacement of c. 10km (Coller 1984, Dolan 1984, Graham 2001). It has a strong negative topographic expression along its length; the Gort Lowlands.

Coller (1984) identified what appeared to be, a deeper expression of the Fergus Shear Zone through a strong aeromagnetic lineament along the northern extent of the shear zone. This deeper level of the Fergus Shear Zone also appears in the Lower Palaeozoic Slieve Aughty Inlier where the strike of the Caledonian cleavage and folds changes parallel to the Fergus Shear Zone. A number of stratigraphic feature indicate a deep-seated control for the Fergus Shear Zone (Sleeman & Pracht 1999). As previously stated (Section 2.1.2.2) Lees, pers. comm. 1999, describes a distinct change in the paleoseafloor in the region of the Fergus Shear Zone, indicating that it was an active paleobathymetric feature during the Lower Carboniferous. A study of gravity gradients in Ireland by Readman *et al*

(1997) shows how the continuity of gravity lineaments across both Caledonian basement and Carboniferous Basins in Central Ireland, suggesting that the older Caledonian faults were reactivated during Carboniferous Basin formation and during dextral transpression at the end of the Variscian orogenic event.

The Fergus Shear Zone terminated to the south in the Foynes / Newcastle area of west Co. Limerick where it is defined by an aerial photograph lineament density high. To the north the Fergus Shear Zone terminates against the southern extent of the, buried, Galway Granite in the Gort Lowlands.

The Fergus Shear Zone is marked by a rotation of folds to the west into the shear zone (Dolan 1984). The Fergus Shear Zone is identified by an anomalous fracture pattern more complex than the regional pattern. The termination of the Fergus Shear Zone against the buried Galway Granite has a strong affect on the geology of the region. The termination of a sinistral shear zone against a rigid body will create a zone of extension on west side and a corresponding zone of compression on the east side. The zone of compression on the east side is manifested by increased folding on the north side of the Slieve Aughty Inlier and by the presence of WNW-ESE fractures on the western side on the shear zone.

2.3 Hydrology:

2.3.1: Introduction

Surface discharge on karst landscapes quickly disappears underground and drainage is dominated by subsurface flow. Flow and transport through a karst aquifer is strongly dependent upon heterogeneities, such as fractures enlarged by chemical dissolution, which provide preferential flowpaths and which respond quickly to recharge events in the catchment area. As the fractures enlarge due to dissolution conductivities in the fracture system can increase with time with fracture conductivity increasing by several orders of magnitude with increasing fracture width (Kaufmann & Braun 1999, Kaufmann & Braun 2000, Kaufmann 2003). The driving force for flow through the system is groundwater recharge and discharge, as the amount of recharge, either by precipitation (diffuse recharge) or via sinking streams (concentrated inputs), and the heights of the base level of resurgences and rivers (discharges), establish the pressure difference for flow within the aquifer (Kaufmann 2002). Flow routes that acquire increasing discharge accelerate in growth, while others languish with negligible growth (Palmer 1991).

Karst groundwater flow may transfer water between surface catchments, a spring in one river catchment may receive water from a sinking stream in another catchment, for example Cullaun 3 is located in the Fergus-Elmvale catchment yet tracer studies show it flows to St Brendan's Well in the adjacent St Brendan's catchment. There is a lack of clear distinction between surface and sub-surface hydrological systems in these areas. (Drew 2003)

2.3.2 Hydrology of the Burren

Drainage of the Burren surface water is confined to ephemeral streams, seasonal turloughs and drainage from adjacent Namurian rocks (Figure 2.6). The Burren is drained almost wholly by underground channels with the exceptions of the Caher River, which reaches the sea at Fanore under most conditions, the Rathborney River and Berneens Stream, which reaches the sea only under wet conditions. The Caher River rises from springs north east of

Slieve Elva, and flows to the sea at Fanore draining northeastern Slieve Elva and northwestern Poulacapple. Initially it flows updip north, north-east, over limestone, before turning westward to Fanore where it cuts a channel through 10-15m thick deposits of drift (Drew 1990). The Rathborney River and Berneens Stream drain into the Ballyvaughan Valley, both streams flow along calcareous drift on parts of their course (Drew 1990). The annual mean precipitation is 1500mm of which 980mm (65%) is not evapotranspired and becomes recharge (Drew 1990).

Recharge to the system is rapid either in the form of concentrated inputs from sinking streams at the Namurian / Lower Carboniferous boundary or via diffuse inputs over the Burren. Discharge of the system is in part to the sea (to the north and west) via submarine or littoral zone springs, partly to the Aille river system via St Brendan's spring (draining the south-western margin of the Burren), partly to the Gort-Kinvarra subsurface drainage system into Galway Bay and for the major part to the Elmvale Spring, the discharge point for the Fergus River catchment which has a has a mean flow of > 3900 l/s (Drew 1990, Drew 2003).

Subsurface drainage is strongly influenced by the geology of the region. Layers of clay, shale and chert (of the Slievenaglasha Formation) which are interbedded with the limestone act as barriers to vertical percolation and encourage sub-lateral flow along bedding planes (Drew 2003) and the fracture network. The majority of explored cave systems have developed above such layers oriented down dip to the WSW often following single bedding layers for considerable distances. The majority of mapped cave systems in the Burren have a vertical extent under 60m, with very few caves breaching these impermeable units.

The major hydrological features of the Burren are shown in Figure 2.6 including surface streams, internal and external springs and the inferred locations of the groundwater basin divides as well as proven lines of sub-surface drainage. The information relating to the catchments varies greatly, ranging from nearly non-existent in the cases of many of the areas draining to the sea to well documented in catchments such as Fergus River, St Brendan's and Ballyvaughan (Drew 1990, Drew 20003). Overall the dominance of north to south/ south to north drainage is very apparent due in part to the well-developed vein sets of that orientation, and in the case of the southerly flow to the regional dip (Drew 1990).

The Fergus River/Elmvale catchment is the largest catchment accounting for approximately 1/3 of the Burren drainage, draining some 120km^2, flow is principally from north to south to the Fergus River spring. Response to rainfall at the spring is rapid, being in the order of 10-48 hours (Drew 2003). Diffuse inputs occur from swallow holes along the eastern edge of the Namurian boundary at Poulacapple and further south as well as swallow holes in the vicinity of Carran and the Seven Streams Cave at Teeskagh from small ephemeral streams which occur on beds of interbedded chert, shale and limestone of the Slievenaglasha Formation, as well as small number of swallow holes that are scattered through out the catchment. In the southeast of the catchment there are a number of monoclinical folds along which flow appears to be focused (Drew 1988, Drew 1990) (e.g. flow from Carran and Seven Streams Cave).

The St Brendan's/Killeany catchment drains the region along the western edge of Poulacapple and the eastern edge of Slieve Elva where a large number of swallow holes and cave systems exist, including Poulnagollum the longest cave system in the region at over 12km in length. Waters sinking in the upper half of the catchment first resurges at the internal spring of Killeany where it sinks before reappearing again at St Brendan's Well 3km down dip to the

southwest. Over 30% of the catchment consists of Namurian strata, there is according to Drew (2003) a proportionately large number of sinking streams feeding the streams which leads to a rapid and dramatic response to rainfall.

The Ballyvaughan catchment drains an area of 45km^2 almost entirely of limestone with the exception of a small (.6% of the total area) of Namurian strata along the northern edge of Poulacapple. Input is from a series of discrete sources such as of swallow holes and ephemeral streams at the summit of Aillwee Hill as well as from the sinkings of the Rathborney river and Berneens stream in addition to diffuse inputs via rainfall over the exposed limestone pavement that makes up a large portion of this region. Flow is primarily south to north up dip to the intertidal springs directly off shore Ballyvaughan. This fact means that water from rain fall and from ephemeral streams at altitude on Aillwee Hill need to vertically traverse 250m of limestone in order to rise again at Ballvaughan (Drew 1990, 2003), implying that flow cuts through the layers of chert and shale that act to prohibit vertical percolation elsewhere. It will be discussed later that a vein cluster responsible for controlling a NNE section of cave passage in Aillwee Cave can be traced vertically 110m to a set of depressions immediately above the cave system and that when rainfall occurs small streams within the cave system recharge quickly via this vertical passageway. An analysis of the geology of this region offers an explanation for this vertical propagation. The bedrock at the summit of Aillwee Hill is the Ballyvoe Member the lowest member of the Slievenaglasha Formation, the chert layers that act, as aquitards are located at the base and top and within the overlying Fahee Member and Ballyelly Member respectably. Flow is able to percolate vertically in this region, as the members containing aquitards are geographically limited and utilises the NNE trending vein clusters to percolate vertically before flowing up dip to the north. Drew (1990) contends that such flow behaviour may have initiated under different hydrodynamic conditions than occur at present.

The remainder of the discharge from the Burren is to the sea (Drew 1990, Drew 2003). On the north coast the springs are associated with the major north-south embayments at Ballyvaughan, Bellharbour, Corranroo and Kinvarra. The marine springs on the west coast occur up to 500m from shore and at depths up to 15m below sea level. The Fisherstreet catchment drains the area to the north of the Aille River, the Fisherstreet/Doolin cave system parallels the Namurian/Lower Carboniferous in this region as well as the course of the Aille River, and discharges to the sea immediately off shore from Doolin. Flow from the Poulsallagh/Derren-Trawee catchments resurges at two large offshore springs. The Caher River rises at the southern extremity of the col that forms the surface divide between the Killeany/St Brendan's catchment and drainage northward into the Atlantic at Fanore (Drew 2003). In its upper reaches it flows northwards, along the strike of the vein clusters, over exposed limestone before flowing over calcareous till northwesterly towards Fanore.

2.3.3. Hydrology of the Gort Lowlands.

The eastern portion of the Gort – Kinvarra catchment is underlain by largely impermeable Old Red Sandstone of the Slieve Aughty inlier which hosts a number of streams that flow onto the limestone bedrock that makes up the remainder of the catchment. The hydrology of the catchment may be divided into 3 distinct zones along a southeast to northwest transect 1) the area of sinking streams, 2) the area of surface water-groundwater interaction, 3) the wholly underground section (Figure 2.7) (Drew 2003)

1) The area of sinking streams: Three rivers drain the Lower Palaeozoic Slieve Aughty upland; from north to south they are the Owenshree, the Ballylee and the Owendalulleegh/Beagh/Gort. Upon reaching the limestone these rivers flow parallel to the upland before sinking underground. Waters from these rivers have been traced to reappear at the springs at Kinvarra and Corranoo 10-15km to the north-west (OPW 1998, Drew 2003). The Owenshree River flows in a southwesterly direction where it sinks in the Blackrock Turlough. Drew (2003) notes that recharge to this turlough after heavy rainfall is swift and the turlough will become a lake 1km in diameter within 36 hours. The Ballylee River flows in a NNE direction after flowing from Slieve Aughty before sinking. The Beagh River alternates between surface and subsurface downstream from Lough Cutra sinking first at the Punchbowl, one of the largest sinks in Ireland, before reappearing and sinking again before it finally re appears at Pollduagh Cave the source of the Gort River which runs NNE for 5km where it sinks at Polltoophill. The majority of water from these 3 rivers emerges at the large Polldeelin spring to the east of Coole Lough before rising and sinking again at two more points prior to flowing into Coole Lough (Drew 2003).

2) Surface water-groundwater interaction: Between the sinking of the rivers at Polldeelin and Caherglassaun Lough 8 km to the west north west the drainage is a combination of surface and sub-surface flow. Coole Lough, which the waters from the sinking streams flows to, is a permanent body of water which acts a swallow hole through which the lake waters flow towards Caherglassaun Lough. A minor amount of flow bypasses the lough as it flows from Polldeelin to the vicinity of Caherglassaun Lough, where flow has a marine-tidal influence. There are a number of turloughs in this region, such as Newtown and Garryland turloughs. This region is subject to periodic flooding of varying magnitudes, and during the 1990's to a series of high magnitude floods, which covered large areas of the region. A number of "1 in 100 year" flood events hit the region in 1990, 1991 and 1994/1995.

3) Underground flow: The area between Caherglassaun Lough and the coast is devoid of surface water. The most distinctive topographic features in this otherwise flat landscape are a series of large enclosed depression (dolines) and cave passages, which lie in a line extending from Caherglassaun Lough to Quinn's Cave (135680 208230) 6.5 km to the west-northwest. A number of the caves along this linear trend have lengths in excess of 1 km, such as Morans Cave (1160m long) and the Pollaloughabo/Pollbehan cave system (1500m long). Drew (2003) contends that the dolines are the result of the collapses into a major, narrow, 25m wide, water filled karst conduit, of which the cave passages are part of, that carries all of the underground drainage from the Gort area. The conduit continues to an "ancient outlet in Galway Bay west of Corranroo"(Drew 2003). The majority of the modern drainage leaves this WNW trending conduit along the Pollaloughabo/Pollbehan cave passage and flows to a series of springs at Kinvarra. During times of high flow the water is discharged from the springs at Corranroo.

Flooding in this region occurs when the sinking streams, sourced on Slieve Aughty, are backed up when the flow exceeds the capacity of the underground flow channels and the enclosed depressions, which fill up with rising ground water, that make up the system. The high magnitude floods of the 1990's were the result of the very high rainfall over a prolonged period, which lead to the finite capacity of the karstic flow of the system being exceeded (OPW 1998).

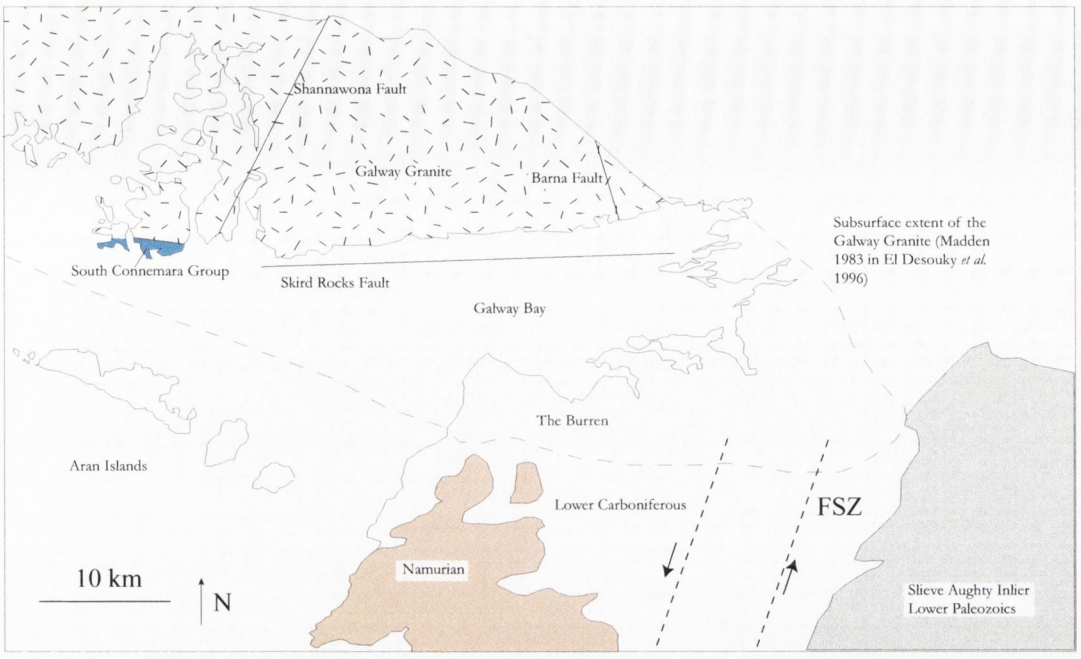

Figure 2.1: Regional Geological Map, showing the location of the Galway Granite Batholith, Lower Palaeozoics, Lower Carboniferous, Upper Carboniferous (Namurian) and Fergus Shear Zone (FSZ).

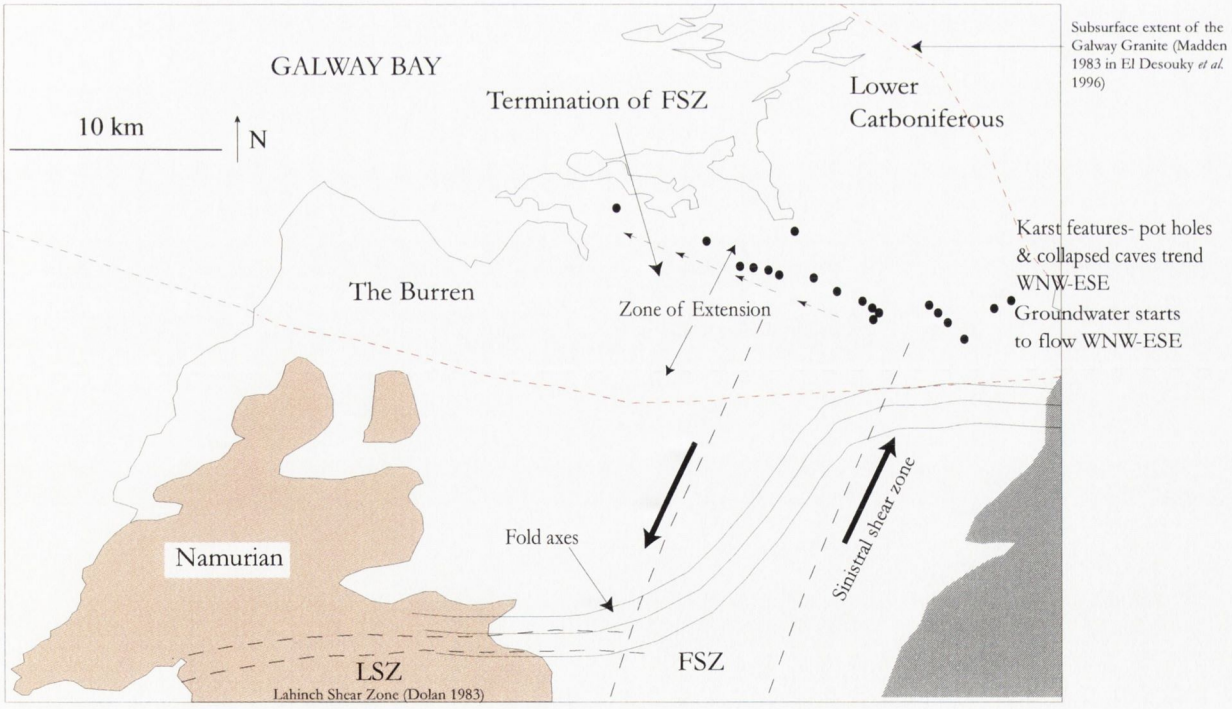

Figure 2.2: Map illustrating the termination of the sinistral Fergus Shear Zone. The shear zone terminates against the southern extent of the subsurface Galway Granite. This resuts in a zone of extension being created. This zone is marked by WNW-ESW trending fractures, WNW-ESE trending groundwater flow and karst features of the same orientation. The Fergus Shear Zone is marked by a series of fold axes that swing into and out of the zone in addition to an anomalous fracture pattern (Dolan 1983, Coller 1984).

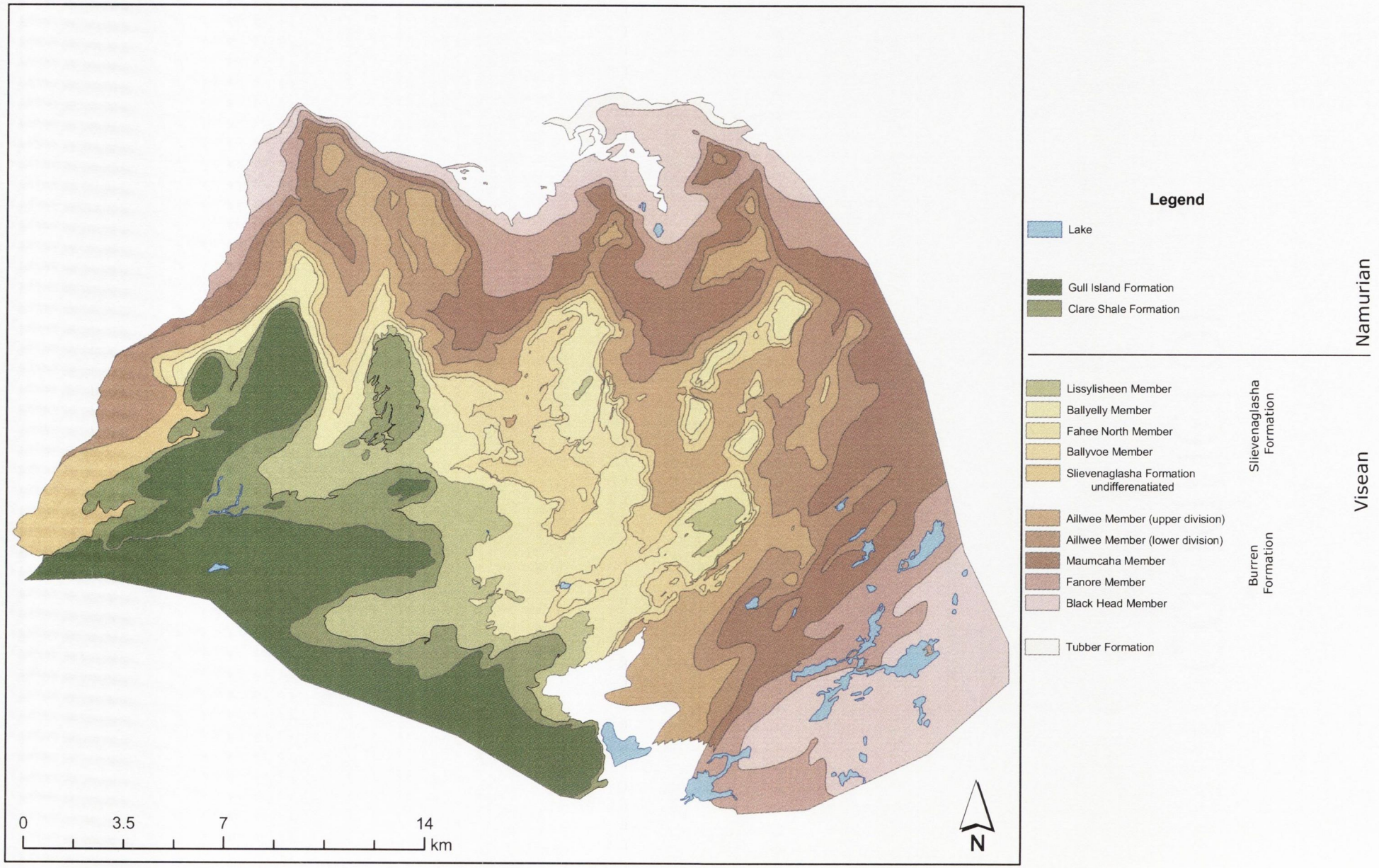

Figure 2.3: Geological map of the Burren region (modified from the Geological Survey Of Ireland).

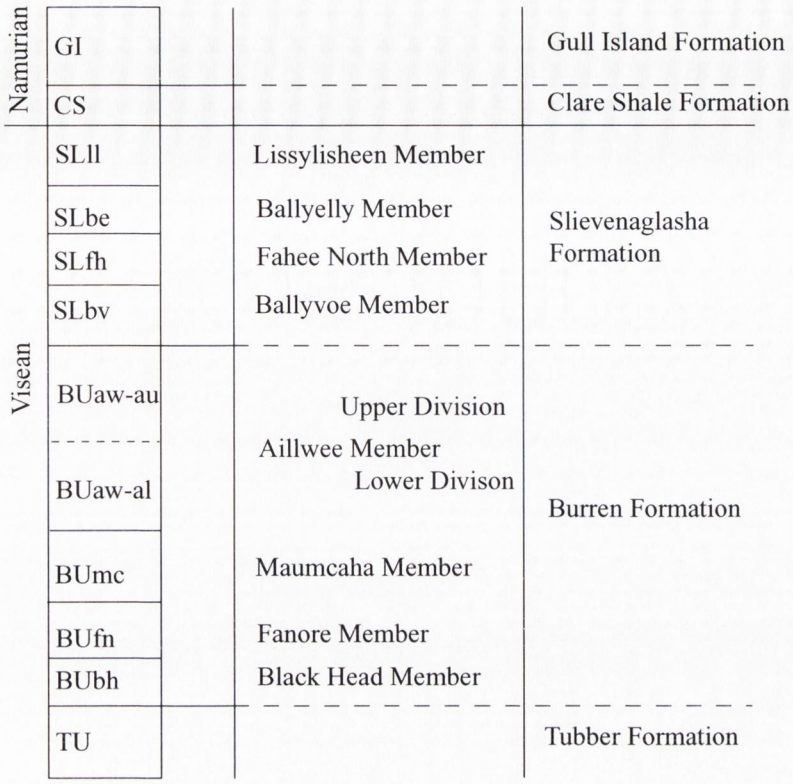

Figure 2.4: Stratigraphic Column of the geology of the Burren. Not to scale

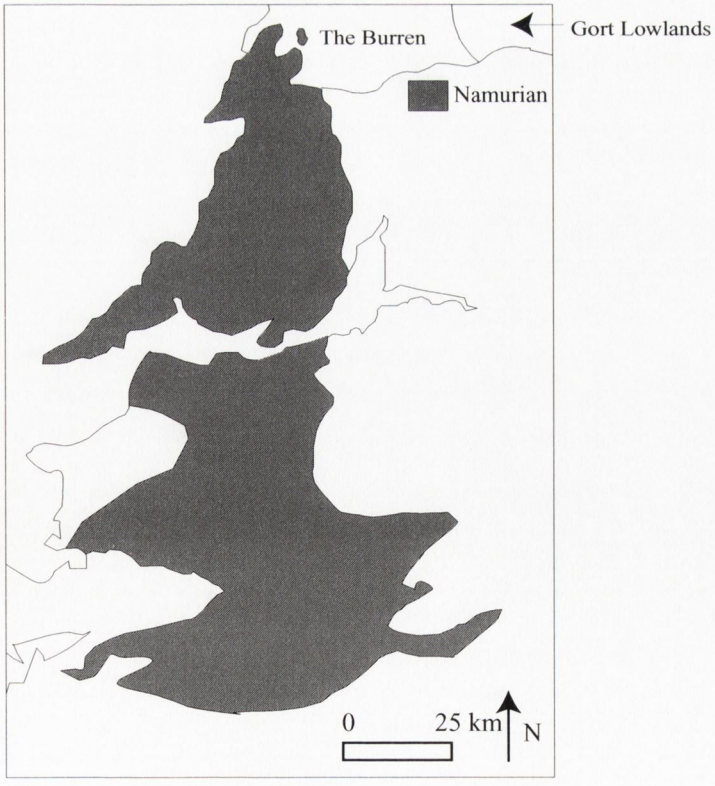

Figure 2.5: Distribution of Namurian rocks in Co. Clare, Co. Kerry and Co. Cork
Modified from Sevastopulo & Wyse Jackson (2001).

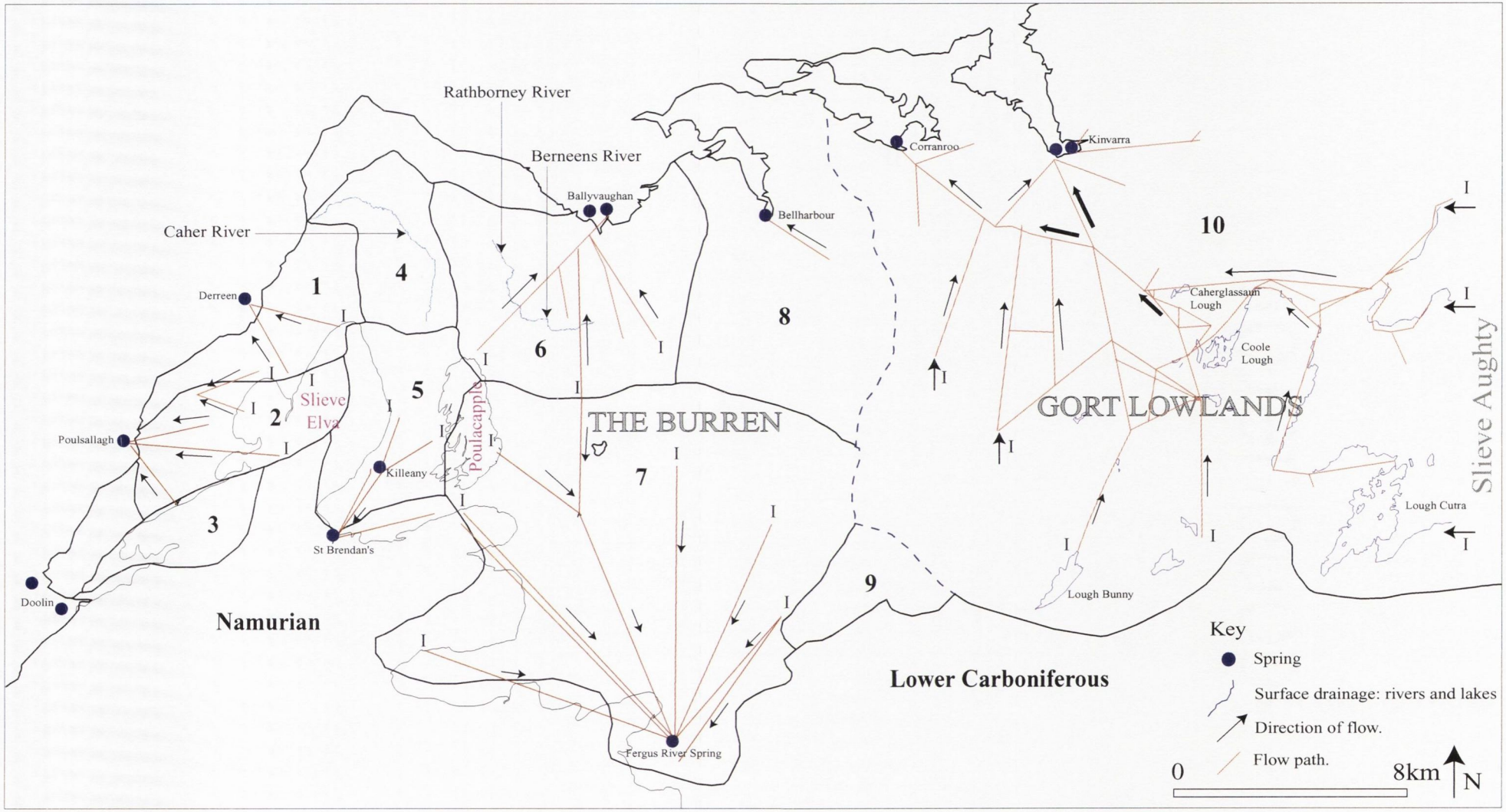

Figure 2.6: Composite flow pathway diagram of the Burren and Gort Lowlands showing surface and sub-surface drainage pathways, catchments, sources/inputs (I) and springs/outputs (●) . Data complied from literature, Tratman (1969), Self (1981), Drew (1988), Drew (1990), OPW (1998), Drew (2003). The dashed line denotes the boundary between the Burren and Gort Lowlands. The catchments are numbered as follows
1: Derren-Trawee, 2: Poulsallagh, 3: Fisherstreet, 4: Caher, 5: Killeany/St Brendans, 6: Ballyvaughan, 7: Fergus River/Elmvale, 8: Bellharbour, 9: Fergus River Lower, 10: Gort-Kinvarra.

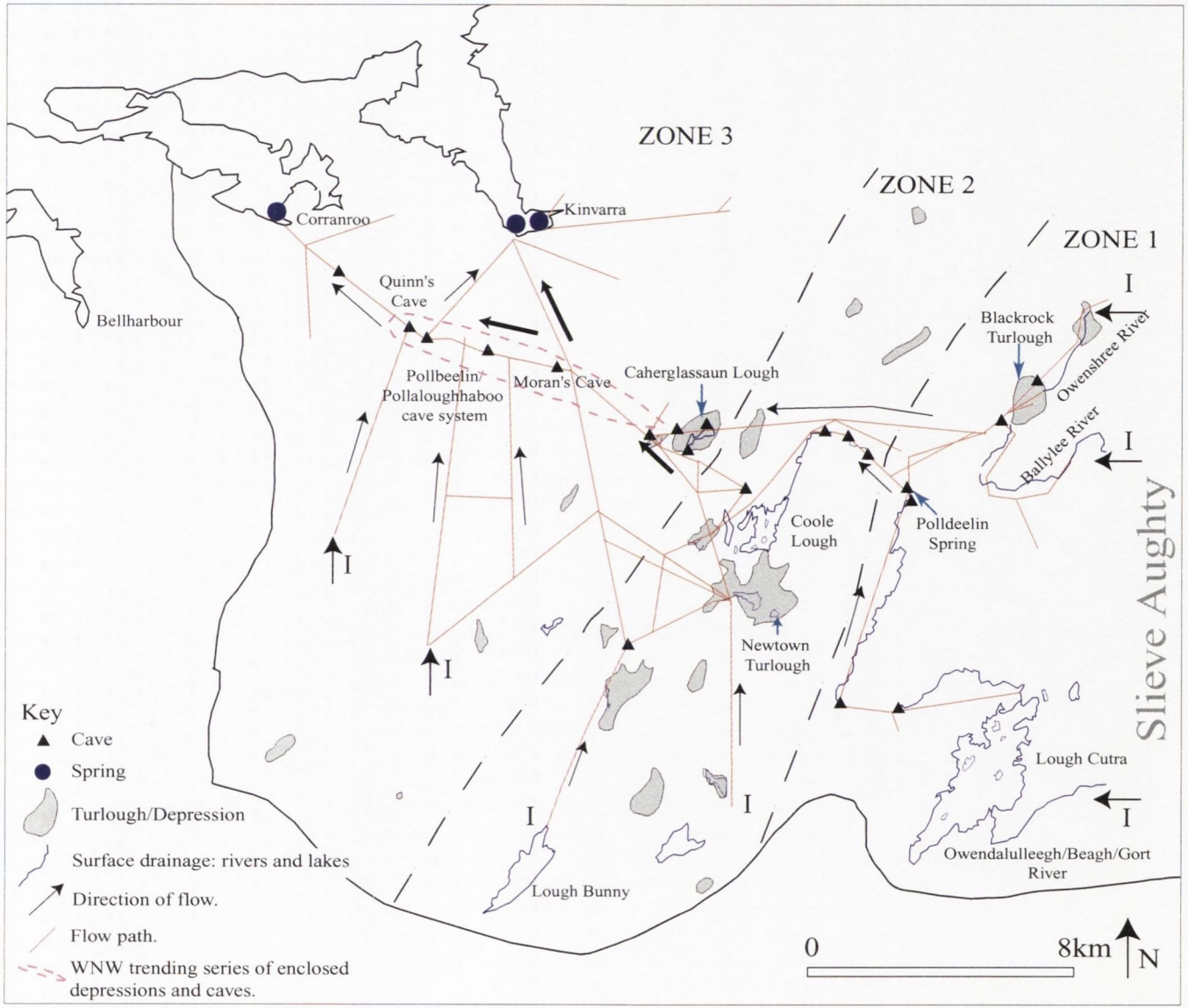

Figure 2.7: Map of hydrology of the Gort Lowlands showing surface and sub-surface drainage pathways, catchment, sources/inputs, turloughs, caves, outputs/springs and division of the area into three zones based on the hydrological conditions (Tratman 1969, Self 1981, Drew 1988, Drew 1990, OPW 1998, Drew 2003).

CHAPTER 3: FRACTURE ATTRIBUTES

3.1 Introduction.

Fractures are the most common structures found in the Earth's crust. The spatial distribution and scaling of fractures varies from those with a small range in size and a regular spacing to fractures with a broad size distribution exhibiting a high degree of clustering. (Laderia & Price 1981, Segall & Pollard 1983, Huang & Angelier 1989, Gross 1993, Becker & Gross 1996, Odling 1997, Gillespie *et al.* 2001). The scaling and spacing of fractures is related to the nature of the host rock, the interaction of the fractures with host rock and each other, and the conditions of deformation (Gross 1993, Cooke & Underwood 2001, Gillespie *et al.* 2001).

In the Burren region of Co. Clare, fracture data were collected from a series of high-resolution, low-level aerial photographs of two target areas consisting of exposed limestone pavements at Cappanawalla and Sheyshmore and from a number of field locations throughout the Burren (Figure 3.1). The aerial photographs were taken from a height of 760m above ground surface, producing high-quality 1:3,000 scale monochromatic images. Solution of the limestone has greatly enlarged the fractures, producing grykes, enhancing the visual signature of the fractures. This allowed for the fractures to be mapped in detail from the low-level aerial photographs at locations at Cappanawalla in the north of the Burren and at Sheyshmore towards the south of the Burren. The joints are unmineralised, regularly spaced, and vertically constrained by bed thickness (strata-bound). The veins are mineralised, clustered, and vertically persistent (non-strata-bound).. The veins have a consistent NNE strike, while the joints show greater strike variation (Gillespie *et al.* 2001).

Characterisation of the fracture systems of a region is vital for understanding how fractures control flow and associated topographic features within a region (Sharp 1993). Fractures form high-permeability pathways that control the flow of fluid and any contaminants that may enter the system. The focus of this chapter is to characterise the two fracture types in the region and understand the interaction between each set.

3.2 Fracture Mechanics

Fractures are surfaces along which rocks have been mechanically broken. Fractures are classified by the relative motion that has occurred across the fracture tips during their formation (Twiss & Moore 1992). Three basic modes of displacement can be recognised at the tips of fractures. Displacement in this instance is the infinitesimal movement that initiates propagation at the fracture tip (Van der Pluijm & Marshry (1997).

- Mode I – Extension or Tensile Fractures: The relative motion is perpendicular to the fracture wall.
- Mode II – Shear Fractures: Motion is a sliding motion perpendicular to the fracture edge.

- Mode III – Shear Fractures: Motion is a sliding motion parallel to the fracture edge (Pollard & Aydin 1987).

Joints have no displacement parallel to the fracture plane, hence they are extension or Mode I fractures. They propagate perpendicular to the least principal stress in the plane of the maximum and intermediate principal stress. Joints are the most common brittle structures in the upper crust, as they are structures that can form under relatively low differential stress (Engelder 1993). They can be divided into systematic and non-systematic joints. Systematic joints are planar regularly spaced features; non-systematic joints are curved and more irregular in their geometry and usually terminate against systematic joints. Veins are mineral-filled Mode I fractures.

To help in the analysis of fractures in a region, fractures are commonly classified according to several parameters.

- ***Orientation.*** The orientation of fractures aids in the identification of fracture sets, inferences on the orientation and extent of the tectonic event that produced them.
- ***Termination style.*** Individual fractures do not have an indefinite extent; they are finite features. Fractures may terminate by simply dying out, by curving and dying out with the stress being taken up by another fracture, by branching and dying out, by curving into another fracture, or by terminating against a pre-existing fracture or surface such as a bedding plane.
- ***Spacing.*** Fracture spacing is a useful method for analysing fracture population, as it allows for the investigation of the spatial distribution of the set and the study of the scaling characteristics of fractures.
- ***Fill and associated thickness.*** The fill of a fracture, if any, is a useful tool for elucidating the origin and age of a fracture system. In the case of the Burren, vein thickness data could not be obtained from aerial photographs and can rarely be observed on the ground due to erosion. On the ground, chemical weathering erodes fill.
- ***Asperities/Roughness***. Natural fractures do not have smooth walls. The irregularities on the fracture surface are termed asperities. In the Burren, any fractures observed have undergone chemical weathering and been widened so that the original wall structure has been lost.
- ***Aperture.*** The aperture is the distance between the fracture walls. Due to the weathering of the fractures in the Burren, the original aperture is not preserved, and the present aperture is an artefact of weathering.
- ***Intersections and Terminations.*** Fractures may terminate as isolated tips in the rock matrix (blind terminations), they may cross fractures to create a cross-connected geometry (cross-termination) or they may terminate by abutting against a fracture (abutment termination) in a H pattern or in a Y pattern (Hancock 1985). In a natural system, connectivity is achieved through a combination of the fracture intersection, fracture abutment, and blind termination.

Fracturing occurs once the tensile strength (T_o) of a material is exceeded. The tensile strength (MPa) is the nominal stress at which a round block of material, loaded in tension, will fracture. When a

rock mass experiences high stresses, the tensile strength of a material is exceeded, and it fractures. The tensile strength of Carboniferous limestone from Colwyn Bay along the north coast of Wales is 13.72 MPa (Snowdon *et al.* 1982, in Gillespie *et al.* 2001). Tensile strength is typically 10 to 100 times less than the compressive strength of a material. The mechanisms for creating such high stresses are lithostatic pressure due to burial or uplift, high fluid pressure, and tectonic effects. Extension fractures are tensile features that form perpendicular to the minimum principle stress (σ_3) and parallel to the maximum stress (σ_1). Experimental work by early researchers such as Inglis (1913) and Griffith (1921) showed that samples of glass fractured at stress levels much lower than the theoretical tensile strength of the glass. These workers attributed this as the result of the presence of microscopic flaws within the material. Stress concentrations at the tip of these flaws cause the flaws to propagate and the medium to exceed its tensile strength and fracture.

A fracture is initiated at a flaw in a medium and propagates away from the flaw. The stress field around the fracture tip controls the propagation of the fracture. For Mode I extension fractures, the tensile stress is largest in the plane of the fracture (σ_1) (Lawn & Wilshaw 1975). The magnitude of the stress field at the crack tip is defined in a linear elastic medium by the stress intensity factor K, which is a function of the applied load, geometry, and length of the crack (Atkinson 1987, Gross 1993) and is defined by the following equation:

$$K = -Y\sigma^r \sqrt{\pi c} \qquad \text{Equation 3.1}$$

Where,

K = stress intensity factor at the fracture tip

σ^r = remote tensile stress

c = half length of the initial crack

Y = a unitless geometric modification factor, related to the crack geometry, loading conditions and edge effects. It is commonly taken as 1 for a plate of infinite width (Gross 1993, Becker & Gross 1996).

Taking Y = 1, Equation 3.1 can be rewritten as:

$$\sigma^r = K / \sqrt{\pi c} \qquad \text{Equation 3.2}$$

Linear elastic fracture mechanics suggests that a fracture will propagate once the Mode I stress intensity factor, K, reaches a critical value K_{1c}. From Equation 3.1 and 3.2, it can be shown that the remote tensile stress needed for fracture propagation is strongly influenced by the initial flaw size (c). Figure 3.2 is a graph of half length of the initial crack size versus remote tensile stress based on Equation 3.2. The critical stress intensity factor for a particular material is a unique and defines its fracture toughness. Fracture toughness (MPa $m^{1/2}$) is a measure of the resistance of a material to the propagation of a crack. An estimate of K_{1c}=1.8MPa $m^{1/2}$ for a limestone-mudstone sequence was

obtained from Gross (1993) (after Senseny & Pfeifle 1984, Atkinson & Meredith 1987 in Gross 1993, values from 1.4 to 2.0 for limestone are mentioned in Atkinson & Meredith (1984)). The modification factor Y was taken to be 1 for elliptically shaped cracks in an infinite medium (Gross 1993, Becker & Gross 1996). The graph shows that for larger crack lengths or flaw lengths, a lower remote tensile stress is required in order for a fracture to propagate from that crack. As the initial crack size decreases, the amount of remote tensile stress required for fracture propagation increases.

The randomly distributed points throughout the layer where fractures initiate are known as flaws. Commonly fossils, they can be any heterogeneities in a rock mass.

Initiation of Mode I fractures in a rock depends not only on the principal stresses and the tensile strength of the rock, but also on the granular nature of the rock, the internal structure of the grains, and the presence of flaws with in the rock (Gross 1993, Van de Steen *et al.* 2002). Van de Steen *et al.* (2002) show that, in samples of Belgian concoidial limestone, the low grain size samples have a higher tensile stress (-17.89 MPa) than the high grain size samples (-12.98 MPa). As the number of flaws in a rock increases the resistance against Mode I failure of the rock decreases, with the flaws acting as points of fracture initiation.

The fractures in the Burren occur in a series of limestone beds that range from massive, fine-grained limestones, the Aillwee Member, to medium-grained crinoidal limestones, the Ballyelly Member. The presence of a large number of flaws in the limestone acts to facilitate Mode I fracturing, with the flaws acting as sites of fracture nucleation. As can be seen in Figure 3.2, the larger the flaw size, the lower the remote tensile stress needed for fracture nucleation and propagation. Fractures initiate at the larger flaws, with the composition of the bed playing a part in dictating the resultant joint pattern.

The two principal sets of fracture patterns present in the study area have contrasting size and spatial characteristics. The veins are vertically persistent, filled fractures that have a consistent strike NNE throughout the Burren. The vein fill is predominantly sparry calcite but is host to a range of minerals (see Appendix 3.1).

3.3 General features of the fracture sets.

The joints in the Burren are sub-vertical Mode I strata-bound features, that form organised connected networks in plan view (Gillespie *et al.* 2001). The joints have been solutionally enlarged to form grikes, enabling them to be easily recognised on aerial photographs. A dominant systematic joint set can be identified throughout the Burren consisting of long horizontally persistent smooth joints that can have lengths in excess of 50m. The joints observed do not show evidence of displacement, in agreement with the observations from Gillespie *et al.* (2001). Shorter cross-joints abut the earlier systematic joints, serving to link adjacent joints. The cross-joints are either oblique to or perpendicular to the systematic joints, and vary in density and orientation. Systematic joints are

often observed to terminate by rotating into an earlier systematic joint, forming oblique systematic joints.

The joint pattern can be seen to vary between beds, reflecting the control of bed thickness in terms of density and spacing. The joints are constrained by bed thickness, which varies from 1.2m at Sheyshmore to 4.8m at Cappanawalla, and by the presence of the earlier N-S veins which act as mechanical layer boundaries, defining mechanical layer thicknesses. The orientation of the systematic joints is not consistent throughout the Burren.

The joints vary in terms of overall density and spacing between beds. At Cappanawalla, the joint geometry varies between upper and lower beds (bed A and bed B respectively). The orientation in both is predominantly NW-SE, but the joints on the lower bed show an increased number of oblique systematic joints. Both beds are similar lithological units, grainstone/packstone. The primary difference between the two beds is bed thickness: the lower bed is 4.8m thick and the upper bed 1.8m thick. The beds act as distinct mechanical layers confining joints to individual beds.

The systematic joints in Cappanawalla strike NW-SE. The systematic joints in Sheyshmore strike east-west. The orientation of the cross-joints is more variable locally. One of the field areas, Gleninagh lies 2.5km to the west of Cappanawalla. There, the systematic joint pattern strikes NW-SE. In the second field area, Cathair Comhain, which lies 4km directly east of Sheyshmore, the joints trend E-W. In the third area, Oughtdarra, in the Eastern Burren 3 km NE of Carran, the joint trend is NE-SW. When the twenty-five caves were analysed, the dominant , joint trend was NW-SE (see Section 6.2). The three areas in which the joints do not trend NE-SW, Sheyshmore, Cathair Comhain, and Oughtdarra, lie parallel to an initially E-W trending, but later NE-SW trending, synclinal axis.

The variation in orientation between the joint sets at Cappanawalla and Sheyshmore can be reconciled with work by Rives & Petit (1990), which shows that a slight rotation in joint sets occurs during the development of non-cylindrical folds in analogue models (Gillespie *et al.* 2001). The joints in the Burren postdate folding, which is Variscan in age. The progressive rotation of joint orientations may reflect the small changes in the local stress orientation arising from the uplift of weakly folded beds (Gillespie *et al.* 2001). Immediately to the south of Sheyshmore is the axis of a NE-SW trending fold.

The systematic joints terminate either via abutment against other joints or as isolated tips. Where the joints abut, they overlap with a curving geometry indicating that the joints formed in response to relatively low differential horizontal stress (Olson & Pollard 1989, Gillespie *et al.* 2001). The barren joints are younger than the mineralised veins, and in Cappanawalla the joints crosscut the veins. In Sheyshmore the veins act as mechanical layers confining the joints. The length distributions of the systematic joints are lognormal (Aarseth *et al.* 1997, Odling *et al.* 1999, Gillespie *et al.* 2001).

3.4 Relative Timing

The relative age of fracture sets in layers that include more than one fracture set determined by analysing fracture abutments, cross-cutting relationships, and curving geometries (Eyal *et al.* 2001). Younger fractures often terminate against pre-existing fractures in a variety of geometries, as described by Hancock (1985) and Eyal *et al.* (2001). In order to investigate the relative timing of fracture development in the Burren, three locations were examined: two at Cappanawalla on different beds (B1 and A7) and one location, SMF1, at Sheyshmore (Figures 3.3a-c).

Figure 3.3a shows a portion of the fracture pattern at B1. The different fracture sets have been colour coded to ease recognition. It can be seen that the NW-SE trending systematic joints cross-cut the NNE trending veins, indicating that the veins predate the joints. Gillespie *et al.* (2001) say that unimpeded joint propagation is to be expected, as the veins were calcite cemented prior to joint formation. In addition, the joints are barren, offering further evidence that they postdate the veins. The systematic joints can often be seen to terminate with curving overlaps into earlier systematic joints. It can be seen that the earlier NW-SE systematic joints have restricted the propagation of succeeding joints with cross-joints abutting against them. The spacing of the systematic joints controls the length and spacing of the cross-joints. The cross-joints either abut against pre-existing joints or terminate blindly in the bedrock. The orientation of these cross-joints is variable over tens of metres. At this location, the cross-joints are generally orientated E-W with a minor amount of NE-SW orientations. The fractures at location A7 (Figure 3.3b) are on a different bed to those at location B1. There are a number of systematic, oblique systematic, and cross-joint patterns present here in addition to the vein set. The cross-joints are principally composed of a series of parallel oblique NE-SW joints that curve into the pre-existing joints. The fractures at Sheyshmore (Figure 3.3c) consist of a series of regularly spaced E-W trending systematic joint set which in most cases cross cut the veins. In the remainder of cases the joints curve into the veins. In between the regularly spaced joints there are a series of cross-joints that are principally orientated NW-SE with a minor number trending N-S. These cross-joints consist of a series of sinusoidal joints that terminate at either end with a curving geometry. They terminate as either abutments against the EW joints and other contemporaneous joints or as blind terminations in the bedrock. The time frame of the fracture development is outlined in Table 3.1.

At Cappanawalla, the general pattern is as follows: The vein set was the first set formed. Later a NW-SE regularly spaced systematic joint set was created. Contemporaneous to the formation of this set, the fracture tips of other systematic joints were influenced by the stress shadow of the first set. This resulted in the joint tips curving in to terminate against the first set, as the stress intensity factor at the fracture tip was insufficient to propagate through the stress shadow of the first joints formed . After the development of the systematic set, a series of cross-joints developed that share the geometry and spatial characteristics of these being controlled by the systematic joints.

	Cappanawalla				Sheyshmore
B1	Orientation	A7	Orientation	SMF1	Orientation
1	NNE-veins	1	NNE-veins	1	NNE-veins
2	NW-SE systematic joints	2	NW-SE systematic joints	2	EW systematic joints
3	Oblique NW-SE systematic joints	3	Oblique NW-SE systematic joints	3	NW-SE cross-joints
4	E-W cross-joints	4	NE-SW cross-joints		N-S cross-joints
5	NE-SW cross-joints	5	E-W cross-joints		

Table 3.1: Timeframe of the fracture development.

3.5 Spacing

3.5.1 Background information

In layered rocks, joints are often confined to discrete horizons. Joints in layered rocks often display a regular spacing, and it has long been established that there is a first order linear correlation between fracture spacing and mechanical layer thickness (Bodgonov 1947, Novikova 1947, Krillova 1949, Laderia & Price 1981, Narr & Suppe 1991, Becker & Gross 1996, Eyal *et al.* 2001). This relationship between mechanical layer thickness and fracture spacing is typified by the equation:

$$\mu = kB \qquad \text{Equation 3.3}$$

where,

μ = spacing

k = a constant

B = bed thickness

Laderia & Price (1981) investigated this relationship and found it held in general, though they noted that very thick beds may deviate from this generalisation. In layered rock, lithological contacts or pre-existing fractures may serve as mechanical boundaries that act to confine fractures to individual layers separating the unit into a mechanical stratigraphy (Price 1966, McQuillan 1973, Laderia & Price 1981, Huang & Angelier 1989, Narr & Suppe 1991, Gross 1993, Becker & Gross 1996, Gross *et al.* 1997) (Figure 3.4). Fractures terminate at these mechanical layer boundaries, which act as free surfaces, preventing the transfer of stress across them and confining the fractures to specific layers (Gross 1993, Becker & Gross 1996).

The relationship between joint spacing and mechanical layer thickness can be quantified by using the Fracture Spacing Index (FSI) developed by Narr & Suppe (1991). The FSI refers to the slope of the

regression line on a graph of mechanical layer thickness versus median fracture spacing for a number of beds of varying thickness. Gross (1993) further refined this by developing the Fracture Spacing Ratio (FSR), which corresponds to the mean mechanical layer thickness divided by the median joint spacing. In the Burren, the joints are confined by mechanical layers in the form of bed thickness and the pre-existing vein sets. At Sheyshmore this is especially evident, as there, the veins define mechanical layers of different thicknesses, with the joints in each layer displaying different mean spacing. In order to quantify the relationship between joint spacing and mechanical layer thickness, the FSR was derived for each layer (Table 3.5) and plotted (Figure 3.10). The relationship between the FSR and the mechanical layer thickness is shown to be linear, although this breaks down beyond a specific mechanical layer thickness.

Hobbs (1967) and Gross (1995) both describe how stress perturbations occur in the vicinity of an open joint with the joint acting as a free surface and hence as a barrier to the transmission of tensile stress (Narr & Suppe 1984, Gross 1993, Becker & Gross 1996, Bai & Pollard 2000, Eyal *et al.* 2001). Tensile stress perpendicular to the fracture is greatly reduced to levels well below the tensile strength of the rock, and it increases with distance from the fracture. Fractures are inhibited from growing in the zone of low tensile stress perpendicular to the fracture plane. Bai & Pollard (2000) postulate that this zone of low tensile stress could be a zone of increased compressive stress, which would act to inhibit joint initiation and propagation. This zone of reduced stress is known as the stress reduction shadow (Figure 3.5), which equates with the interaction zone of Rives (1992). The dimensions of this stress shadow control the location of initiation of the next fracture. The likelihood of a fracture entering the stress reduction shadow of another fracture increases with the number of fractures. The dimensions of the stress shadow are controlled by the dimensions of the fracture, larger fractures having larger stress shadows.

The Hobbs (1967) model for joint spacing requires a change in elastic properties across mechanical layer boundaries. This model is appropriate for lithologically controlled mechanical layers, as there is often a change in elastic properties across bedding planes (Gross 1993). The Hobbs model would not be appropriate for fracture-controlled mechanical layers, as on a bedding plane surface there are no changes in elastic properties across the fracture-controlled mechanical layer boundaries (Gross 1993). Pollard & Segall (1987) presented a theoretical model for fracture spacing which assumes an infinite elastic medium and constant elastic properties for all layers. Rabinovitch & Bahat (1999) deem the Pollard and Segall model appropriate for fractures embedded within a homogeneous medium of uniform elastic properties. Pollard & Segall (1987) demonstrate that in the vicinity of a newly formed fracture, the stress field is highly heterogeneous, with large stress concentrations at the fracture tips and zones of low stress normal to the fracture plane. Pollard & Segall (1987) conclude that it is this stress perturbation that controls fracture spacing, as the magnitude of the stress normal to the fracture plane (σ_{11}) is a function of distance from the fracture plane (x_1). The magnitude of the local stress can be calculated using the following equation which produces the graph seen in Figure 3.6.

$$\sigma_{II}(x_1/T, x_2 = 0) = \sigma^r_{II}\, 8\, |x_1/T|^3\, [4(x_1/T)^2 + 1]^{-3/2} \qquad \text{Equation 3.4}$$

where

x_1 = distance from the fracture, T = layer thickness, σ_{II} = tensile stress

σ^r_{II} = remote tensile stress, x_2 = distance form the fracture on the symmetry plane

From Figure 3.6, it can be seen that tensile stress perpendicular to the fracture increases as a percentage of the remote tensile stress (σ^r_{II}) with increasing distance away from the fracture along the axis (x_1). The process of fracture propagation creates a stress reduction shadow around the newly formed fracture.

Gross (1993) proposed a model for sequential infilling, the process whereby new fractures form between two pre-existing fractures, to explain the relative timing of fracture propagation (as illustrated in Figure 3.7). In proposing his general infilling model, Gross (1993) made a number of assumptions:

1. Initial fracture propagation from a pre-existing flaw occurs in an infinite elastic medium (similar to model proposed by Pollard & Segall (1987) and shown in Equation 3.4), and is not influenced by free surfaces at mechanical layer boundaries.
2. Fractures propagate when local stresses reach approximately 90% of the remote crack-driving stress. This corresponds to a distance of $(x_1/T) = 1.85$ (Figure 3.6). Beyond this distance, a large increase in distance results in only a small change in the percentage of remote stress.
3. Reduction in stress at a point influenced by the two adjacent fractures is calculated using linear scaling. If the presence of one fracture reduces the local stress to $0.7\sigma^r_{II}$ at a given point and a second fracture creates a $0.8\sigma^r_{II}$ reduction, the local stress at that point is found by superposition: $(0.7\sigma^r_{II})(0.8\sigma^r_{II}) = (0.56\ \sigma^r_{II})$
4. As the stress across a fracture surface equals zero, the reduction of stress at any given point is influenced only by the two adjacent fractures.
5. Joints do not initiate in the vicinity of mechanical layer boundaries. In Sheyshmore, the E-W trending fractures curve into the earlier NNE trending veins. Gross (1993), described a similar pattern for cross-joints in the Monterey Formation of California, contending that this geometry implies that the fractures originated in the mid-region of the mechanical layer.

Applying this model to the Burren gives an indication of the stresses involved in the generation of the joint sets. Initially the tensile stress intensity is below the tensile strength of the rock. Gillespie *et al.* (2001) used an approximate value of $T_0 = 14$ MPa for the Burren limestone. Since the local stress at fracture propagation is assumed to be in the region of 90% of the remote tensile stress, fracturing will initiate once this value is reached. Due to variations in flaw size, the fractures do not initiate all at once. This results in fracture initiation being influenced by the stress shadows of other fractures in the layer. At this stage the minimum joint spacing possible is equivalent to $(x_1/T) = 2.4$.

This is due to the fact that at distances less than $(x_1/T) = 2.4$, the local tensile stress is assumed to be too low to initiate fracturing. The first generation of fractures will propagate at a remote stress of 15.96 MPa, which corresponds to $90\%\sigma^r_{II}$. The next generation of fractures will only propagate after a considerable increase in remote tensile stress. The midpoint between the fractures, point A, is located at $(x_1/T) = 1.2$ from either fracture. This point equals 78.1% of the remote tensile stress. In order for the crack-driving stress to reach –14 MPa at point A, the remote stress must increase to 26.16Mpa. Once this value is reached, a second generation of fractures will initiate in the mid-region between adjacent first generation fractures. To initiate a third generation of fractures in the mid-region of the second generation fractures, point B would require a remote tensile stress of 127.5 MPa. This represents a five fold increase in the stress required to initiate fracturing. Gross (1993) contends that it is rare to find a third fracture set, as the remote tensile stress required is extremely high.

In order for sequential infilling to proceed, the local crack normal tensile stress must increase to critical values (Becker & Gross 1996). This is due to linear elastic mechanics suggesting that a fracture will propagate only once the Mode I stress intensity factor at the tip of the flaw exceeds the critical value of fracture of the rock (Pollard & Segall 1989, NRC 1996, Becker & Gross 1996). Researchers in this field, notably and Pollard & Segall (1989), Rives *et al.* (1992) and Becker & Gross (1996) contend that two important conclusions arise from the relationship between fracture infilling and strain.

- Due to the superimposition of stress reduction shadows, the amount of strain required for each infilling phase increases with each phase of fracturing. This is further magnified by the fact that flaw size decreases during progressive fracturing events, as larger flaws are loci of fracture initiation at early stages due to their lower critical fracture stress. This results in smaller flaws being available for fracture initiation.
- The decrease in local tensile stress between adjacent fractures and the increase in critical fracture stress causes additional fracturing to occur only after an incremental threshold strain.

As the perpendicular distances between adjacent fractures decrease, their respective overlapping stress reduction shadows reduce the effective crack normal tensile stress between the fractures. This factor combined with the decreasing critical flaw sizes requires very large additions of strain in order for further fracturing to occur (Gross 1993, Becker & Gross 1996). Existing fractures will then continue to open to accommodate the applied strain (Bai & Pollard 2000).

Fracture spacing is measured in the field as the perpendicular distance between adjacent fractures using a line sample perpendicular to the orientation of the fracture. A measure for characterising spacing is the coefficient of variation (Cv). The coefficient of variation is defined as the ratio of the standard deviation (σ) to the mean spacing (x), and measures departure from an exponential distribution of spacing, for which Cv = 1 (Cox & Lewis 1966, McCaffrey & Johnston 1996). It

allows the clustering of 1-D fracture data sets to be quantified in terms of clustering and anti-clustering.

$$Cv = \sigma/x \qquad \text{Equation 3.5}$$

For a random point process, line spacing has a negative exponential distribution, and the mean and the standard deviation are equal, hence Cv = 1 (Huang & Angelier 1989, McCaffrey & Johnston 1996). If the fractures are clustered, then Cv >1; if the fractures are anti-clustered, Cv <1; and when the fractures are perfectly periodic, Cv = 0.

Cv values	Spacing
Cv >1	Clustered
Cv = 1	Random
Cv < 1	Regular / anti-clustered
Cv = 0	Perfectly periodic

Table 3.2: Coefficient of variation values.

3.5.2 Joints

The spacing of the joints was obtained for a series of line traverses perpendicular to the joint orientation. This was done for a total of eight sites on Cappanawalla and nine on Sheyshmore. The orientation of the joints at Cappanawalla and Sheyshmore are different. The distribution of joints along a line traverse may be visualised using a plot of joint spacing versus distance (Gillespie *et al.* 1993). The results of the plots of spacing versus distance for a 200m "snap shot" of a selection of three traverses at Cappanawalla and three traverses at Sheyshmore can be seen in Figure 3.8. The plots graphically illustrate the regular spacing nature of the joint sets, confirmed by the coefficient of variation values and mean spacing results in tables 3.3 and 3.4. The plots clearly illustrate the difference in spacing of the joints between Cappanawalla and Sheyshmore. The joints at Sheyshmore are more closely spaced, confirming the impression given in the examination of the aerial photographs of both locations. The coefficient of variation values for Sheyshmore are more uniform than for Cappanawalla.

Name	N	L (m)	Mean (m)	SD (m)	Cv
CTP1NW	62	214.5	3.459	4.7	1.35
CTP2NW	61	141	2.311	1.37	0.59
CTP3NW	19	52.5	2.763	1.66	0.6
CTP4NW	28	102	3.643	1.82	0.5
CTP5NW	110	135.6	1.233	.844	0.68
CTP6NW	148	222	1.5	1.13	0.75
CTP6aNW	107	168	1.57	1.079	0.69
CTP7NW	96	139.5	1.453	1.08	0.75
ALL	627		1.73	1.41	0.815

Table 3.3: Spacing data of joints at Cappanawalla.

Name	N	L (m)	Mean (m)	SD (m)	Cv
ST11EW	100	240.6	2.41	2.87	1.19
ST12EW	90	201	2.23	1.03	0.46
ST13EW	62	157.8	2.54	1.03	0.41
ST14EW	55	113.4	2.06	0.92	0.44
STIEW	169	297	1.76	0.79	0.44
ST2EW	167	322.5	1.93	1.46	0.76
ST3EW	53	82.5	1.56	0.67	0.43
ST4EW	79	156.9	1.99	2.78	1.40
ST5EW	203	307.8	1.52	0.97	0.64
SM_all	978		1.92	1.39	0.72

Table 3.4: Spacing data of joints at Sheyshmore.

At Cappanawalla, the bed thickness defines the mechanical layer. At Sheyshmore, the regularly spaced systematic joints are influenced by two mechanically controlled layers, the bed thickness (1.2m), and the NNE veins that define a mechanical layer thickness. To investigate the influence of this mechanical layer thickness (MLT) on the spacing of the joints, a total of fifteen line traverses were done perpendicular to the joints in fifteen of these vein-controlled sections at Sheyshmore. The locations have a good geographical spread along the same geological unit at Sheyshmore. The spacing of the joints within these layers was recorded, and a number of parameters were calculated, including mean spacing, median spacing, coefficient of variation, and the mechanical layer thickness, which is equivalent to the vein spacing. When the mean spacing is plotted against the vein MLT, there is a crude linear correlation, with increasing MLT leading to increasing mean spacing (Figure 3.9). The relationship begins to break down for the larger vein MLT, presumably due to the influence of the bed controlled MLT. The relationship between joint spacing and mechanical layer

thickness can be quantified by using the Fracture Spacing Ratio (FSR) (Gross 1993). When the FSR for each layer is calculated and plotted against the mechanical layer thickness, there is a linear relationship between these variables (Figure 3.10). As the MLT increases, so does the FSR. This relationship seems to hold true up to a layer thickness of 30m; beyond this, it breaks down. The average spacing for the joints from the layers that obey this relationship is 1.77m, apparently indicating that the joints reach a saturation point at this mean spacing. This would relate to Figure 3.7c, where time = t2, the point beyond which the generation of further fractures would require an extremely large remote tensile stress.

The bed thickness of the lower unit at Cappanawalla is 4.8m. It hosts the fracture sets discussed in the analysis of locations A7 and B11. The upper unit, 1.8m thick, hosts the fracture sets discussed in the analysis of locations B9 and B1. The fractures from the thicker units at Cappanawalla display different characteristics to those found in the thinner units: they have a more sinusoidal shape and a larger number of oblique systematic joints.

MLT (m)	N	Mean (m)	FSR	Cv
12	40	1.875	8	0.49
16.5	36	1.6	11	0.47
21	44	2.18	14	0.36
22.5	33	1.36	15	0.25
22.5	45	1.47	15	0.23
22.5	50	1.62	15	0.35
24	37	1.62	16	0.32
24	16	2.14	16	0.44
25.5	39	2.19	17	0.44
27	45	1.83	18	0.42
31.5	34	2.74	10.5	0.44
33	36	2.06	22	0.4
36	39	2.46	15	0.49
54	44	2.22	25.7	0.34
58.5	19	2.815	19.5	038

Table 3.5: Mean and FSR for vein controlled MLTs from Sheyshmore.

3.5.3 Veins

The veins in the Burren are sub-vertical Mode I fractures. They have a consistent NNE strike throughout the Burren and form a series of parallel arrays (Gillespie *et al.* 2001). At Sheyshmore the veins have a less regular strike, from 350° to 010°. The veins have been solutionally enlarged,

making analysis of vein thickness and vein fill difficult. Vein fill is rarely preserved on the surface, It is preserved only under perched glacial erratics along the coast, such as at Black Head, and in cave passages, such as at Pollcahermann (section 6.5.10.1). Where vein fill is observed, it is typically blocky sparry white calcite, though there is a wide assortment of fill. Hydrothermal fluorite formed by fluids rising from the subterranean Galway Granite is a common fill, notably at Black Head, along with ores of Pb, Cu, Ag, Zn, and Bi (O'Raghallaigh *et al.* 1997). Appendix 3.1 contains information on 51 locations throughout the Burren where the veins are host to a variety of mineral assemblages in addition to giving information on the width and length of a number of veins. Where the veins have not been solutionally widened, they have a typical thickness of a few microns to 0.5m (Gillespie *et al.* 2001). There are a number of noticeable exceptions to this, such as at Murrooghtoohy, (grid reference 114700 210700), where a vein is recorded as being 14m wide and extends for over 1km. The veins occur in clusters, which have a large length.

Gillespie *et al.* (2001) state that the non-strata-bound veins must have formed at depths between 0.6km and 2.5km during N-S-directed compression of the Variscan orogeny, estimating the minimum burial depth to be circa 1.25km. The absolute age of the veins is uncertain. Gillespie *et al.* (2001) and Odling *et al.* (1999) contend that the veins either pre-date or are synchronous with Variscan folds, which implies that they are Upper Carboniferous to Permian in age. This is based on veins that occur within the limbs of a Variscan fold at Mullagh Mór, which indicate that the veins were formed during N-S-directed compression during the Variscan orogeny prior to folding. O'Connor *et al.* (1993), in a study on hydrothermal fluorite mineralisation, suggest a mid-Triassic age for the veins. This is based on the dating of a dolerite dyke that is cross-cut by filled veins at Costello Bay in Co. Galway, which yields an age of 231 ± 4Ma. This indicates that the age of formation of the veins or vein fill is coincident with continental rifting of the Atlantic margin. In a follow-up study of the fluorite veins of Co. Galway, Menuge *et al.* (1997) state that the age of 231 ± 4Ma is an upper limit for the age of mineralisation. A study by Meere (1995) of barren and filled veins in rocks of comparable age from the Allihies copper district on the western side of the Beara Peninsula in the southwest of Ireland suggests that the barren veins are Variscan structures, while the filled veins are hydrothermal in origin and postdate the main Variscan folding/faulting event. The clay concentrates from these structures were dated using K-Ar dating in the early 1980's by Halliday & Mitchell, yielding dates of between 307-331Ma for the barren structures and dates of circa 290Ma for the filled structures. In order to resolve this issue, a specific project needs to be undertaken, which would consist of the re-dating of any dykes cut by NNE-trending veins, detailed petrographic work, fluid inclusion work, the dating of hydrothermal fluorite veins, structural analysis of key areas, and other necessary work. This project falls outside the scope of this thesis.

In contrast to the strata-bound joints, the veins are vertically persistent, extending across bed surfaces. Vein clusters, which control cave passages in Aillwee at an altitude of 92m, are coincident with vein-controlled surface features 110m above. Vein clusters are responsible for the depth of Poll

na gCeim, the deepest cave in the Burren at a depth of 181m. This evidence suggests that individual vein sets have a vertical persistence in excess of 200m.

The spacing of the veins was obtained from a series of line traverses perpendicular to the vein direction. When the spacing of the veins along the line traverse is viewed on a plot of spacing versus distance, as in Figure 3.8, the clustered nature of the veins is very apparent. The results from the line traverse are shown in Table 3.6. The veins occur in discrete clusters with an increase in frequency towards the centre of these clusters and a corresponding decrease in vein spacing. The line spacing traverses at Cappanawalla are done perpendicular to the vein-controlled NNE-trending depression on the hilltop that is discussed in sections 7.5.3, 7.5.4, and 7.5.5. The fracture plots of the vein systems at Sheyshmore are different to those at Cappanawalla. There, the veins are more regularly spaced, particularly traverse ST1NNE, shown in Figure 3.8j. The Cappanawalla veins have a higher degree of clustering than the veins at Sheyshmore, as can be seen from the data in table 3.6. The Cv values for the sites at Cappanawalla are >1, while the sites at Sheyshmore have Cv values of just over and under 1. The main difference between the two areas is the wider spread of strike. The veins at Sheyshmore have a wider spread in orientation than elsewhere.

Location	Name	N	L (m)	Mean (m)	SD	Cv
Cappanawalla	CTP1NNE	57	208.5	3.658	7.8	2.13
	CTP2NNE	50	232.5	4.65	7.92	1.7
	CTP3NNE	23	123	5.35	11.46	2.14
	CTP4NNE	57	207	3.63	5.96	1.64
	CTP6NNE	47	253.5	5.4	8.78	1.69
Sheyshmore	S134T3NNE	39	189	4.85	3.94	0.81
	ST1NNE	80	316.5	3.95	3.5	0.88
	ST3NNE	67	250.5	3.74	3.03	0.81
	ST5NNE	22	211.5	9.61	11.36	1.18

Table 3.6: Spacing of veins from Cappanawalla and Sheyshmore.

The veins occur in long narrow zones and increase in frequency towards a large vein cluster. The clustering of the veins can be understood from a fracture mechanical perspective. The stress intensity at a crack tip is strongly controlled by the size of the crack, with longer cracks having higher stress intensities. As the flaw begins to propagate, the region in front of the flaw tip becomes a zone of elevated driving stress promoting the growth of smaller fractures at any flaws in front of the flaw tip (Olson 1993). As the longer fractures propagate faster than the smaller fractures, the smaller fractures enter the stress shadow of the longer fractures and their growth ceases; this is termed crack tip shielding (Weertman *et al.* 1983). This process will leave a series of smaller veins in the vicinity of a large vein.

3.5.4 Comparison between veins and joints

Both types of fractures are sub-vertical Mode I fractures. The difference between the two sets stems from the very different conditions under which they formed, visible from the different geometries of the sets. The veins are filled, non-strata-bound, clustered features with a consistent NNE trend. The joints are barren, strata-bound, regularly spaced fractures with a regionally variable trend. The joints formed in response to relatively low differential stress. As has been mentioned previously, the regionally variable orientation of the joints is not compatible with their formation under a high differential tectonic stress (Gillespie *et al.* 2001). The veins are estimated to have been formed during N-S-directed compression of the Variscan orogeny at a minimum burial depth of circa 1.25km. A summary of the principal differences between the two data sets is shown in table 3.7.

Veins	Joints
Non-stratabound	Strata-bound
Regionally uniform strike	Regionally variable strike
Filled	Barren
Clustered	Regularly spaced

Table 3.7: Comparison between the vein and joint systems of the Burren.

3.6 Conclusions

The Burren region hosts two types of Mode 1 fractures, joints and veins, each with different properties.

- The veins are non-strata-bound, strongly clustered features with a regionally consistent NNE trend. They formed in response to N-S-directed compression during the Variscan orogeny (Gillespie *et al.*2001). The vein fill is rarely preserved. Where is it preserved, it is predominately sparry calcite, though it often contains a variety of mineral assemblages (Appendix 3.1).
- The joints are strata-bound, regularly spaced features with a regionally variable strike. They formed in response to a low differential stress, possibly due to regional uplift.
- Joint spacing is controlled by mechanical layers which defines a layer thickness in which the joints can propagate. The mechanical layers act a free surfaces preventing the transfer of stress across layers. Bed layers and pre-existing vein sets act as these mechanical layers. The joint spacing indicates that joints have reached a saturation point beyond which the generation of further fractures would require extremely large remote tensile stress (Becker & Gross 1996). This point relates to the time interval t=2 in Figure 3.7 where the remote tensile stress is approximately –26MPa.

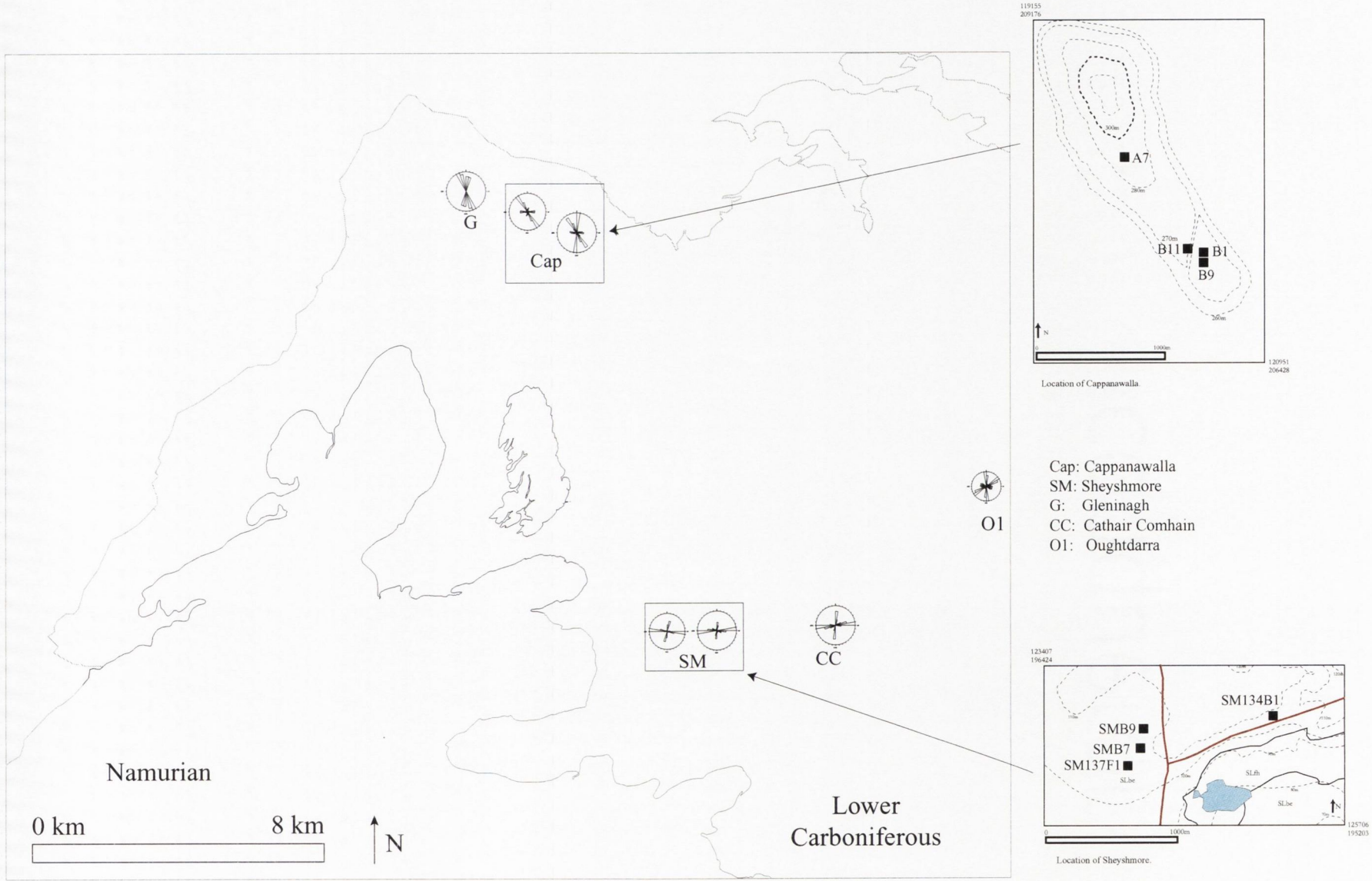

Figure: 3.1: Location map of all study areas. The rose diagrams display the dominant fracture pattern at each study area.

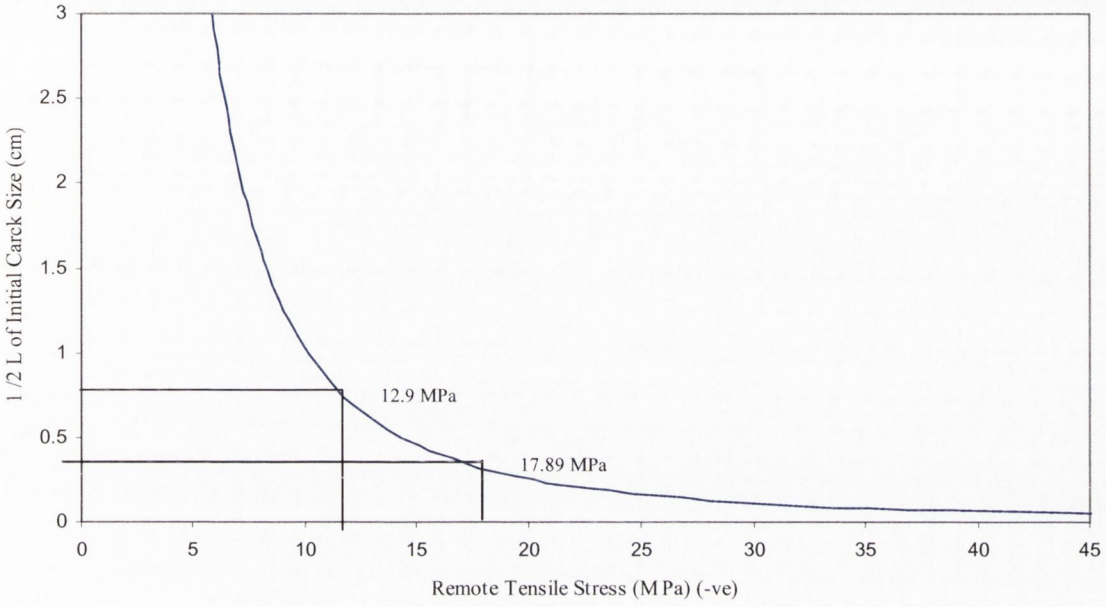

Figure 3.2 Graph of crack half length (c (cm)) and remote tensile stress (MPa) as calculated from Equation 3.2.

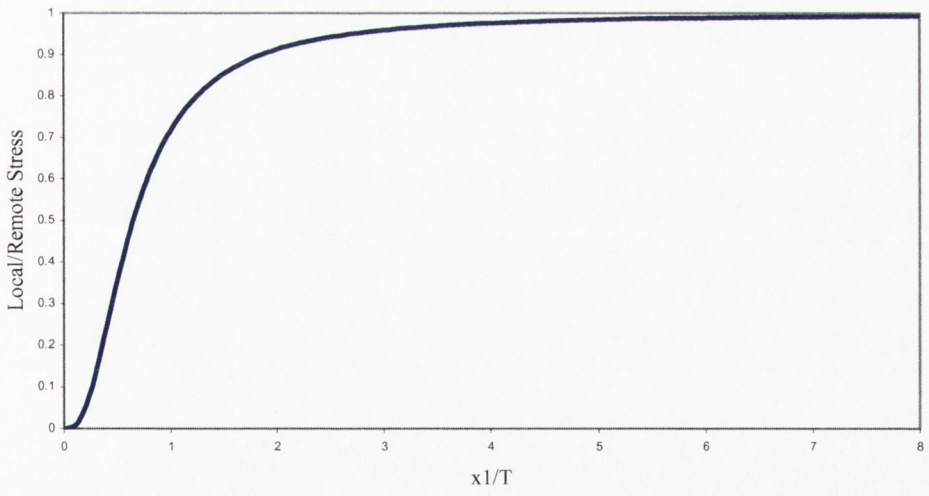

Figure 3.6: Plot of local stress / remote stress as a ratio of the function of distance from the fracture (x_1) and the mechanical layer thickness (T) based on Equation 3.4.

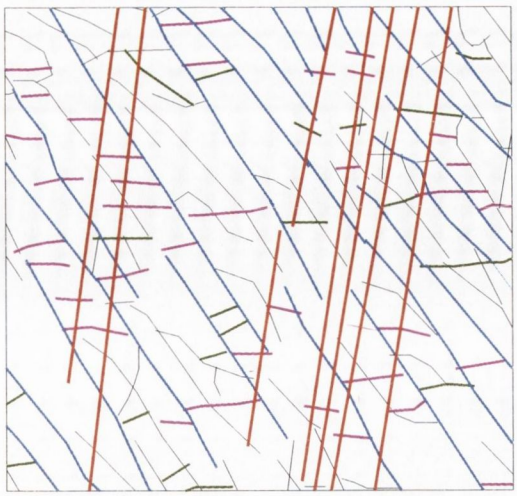

Relative timing of fractures:
1) NNE trending veins
2) NW-SE systematic joints
3) Oblique set of NW-SE joints
4) NE-SW cross joints
5) EW joints

a) Cappanawalla - B1

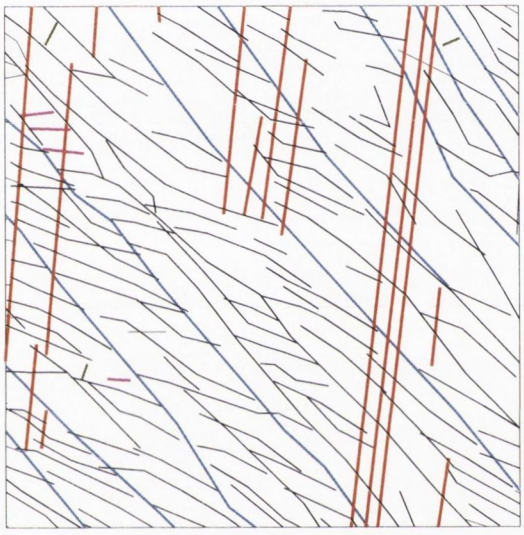

Relative timing of fractures:
1) NNE trending veins
2) NW-SE systematic joints
3) Oblique set of NW-SE joints
4) EW joints
5) NE-SW cross joints

b) Cappanawalla -A7

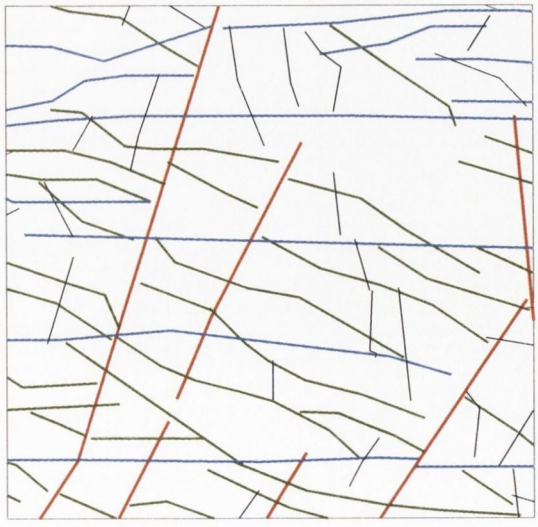

Relative timing of fractures:
1) NNE trending veins
2) EW systematic joints
3) NE-SW cross joints
4) minor NS cross joints

c) Sheyshmore - SMF1

Figure 3.3: Diagram illustrating the relative timing of the different fracture sets at three locations.

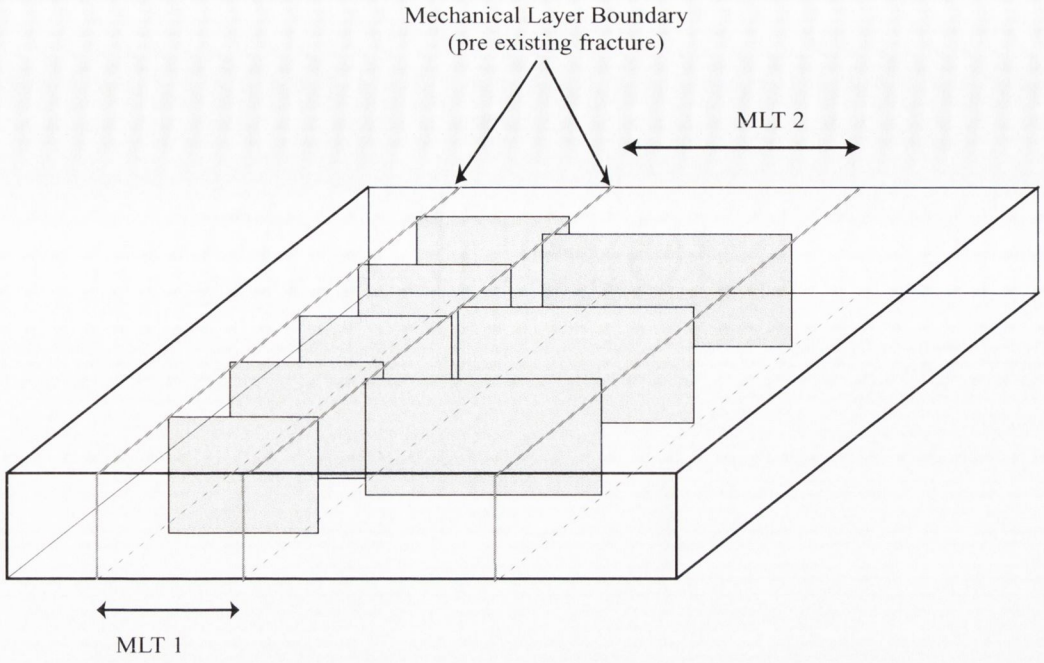

Figure 3.4: Illustration of mechanical layer boundaries defined by pre-existing fractures. Spacing of the fractures is proportional to the mechanical layer thickness (MLT). Diagram is illustrative only. Diagram modified from Gross (1993).

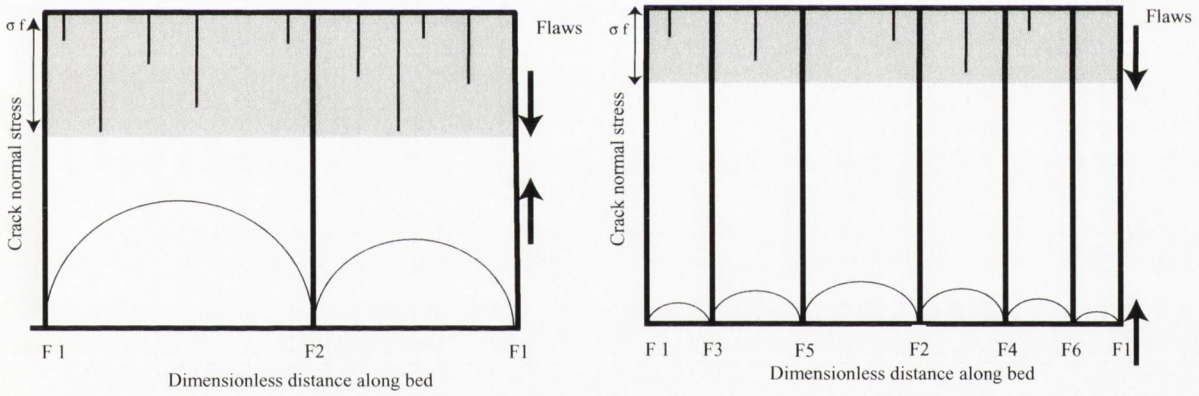

Figure 3.5: Effects of stress reduction shadows and critical flaw size on the process of sequential infilling.

a) Early stage of infilling, where the shaded area, to the top of the diagram depicts crack normal stress. The distances between the two bold arrows indicates the increase in local stress required to form the next fracture. There are flaws of varing length at the top of the diagram.

b) advanced stage of infilling. The fractures are closely spaced along with the decrease in critical flaw size means that large increases in local stress are required to form new fractures.

Diagram modified from Becker & Gross (1996).

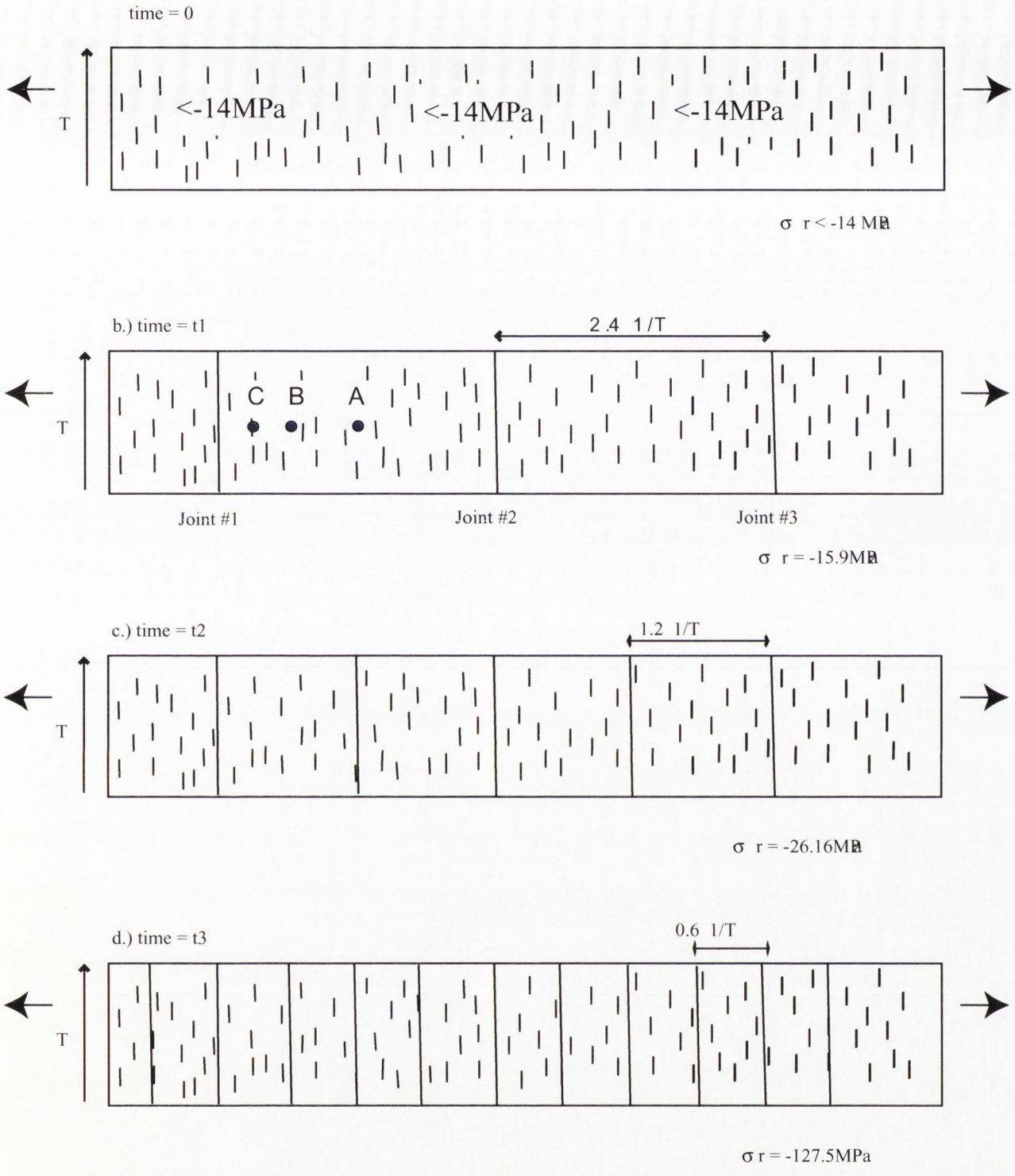

Figure 3.7: General model for sequential infilling in a mechanical layer containing abundant 0.5 cm flaws. Refer to text for more details. Diagram modified from Gross (1993).

Figure 3.8: a 200m "snap shot" of fracture logs of sample line, of veins and joints, through mapped areas at Cappanawalla and Sheyshmore (scale in metres). Refer to Tables 3.3,3.4 & 3.6 for more details on the spacing of the fracture sets.

a) Cappanawalla, CTP1NNE, vein-NNE orientation
Cv = 2.13, mean spacing: 3.66m

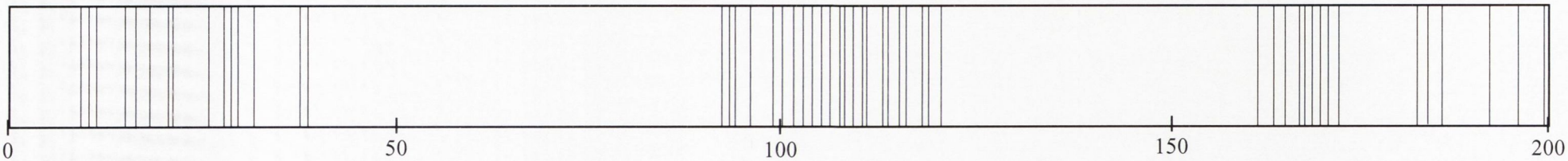

b) Cappanawalla, CTP1NW, joint-NW orientation
Cv = 1.35, mean spacing: 3.46

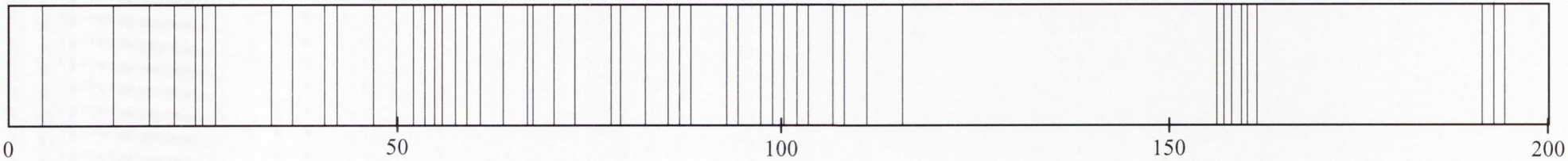

c) Cappanawalla, CTP4NNE, vein-NNE orientation
Cv = 1.64, mean spacing: 3.63m

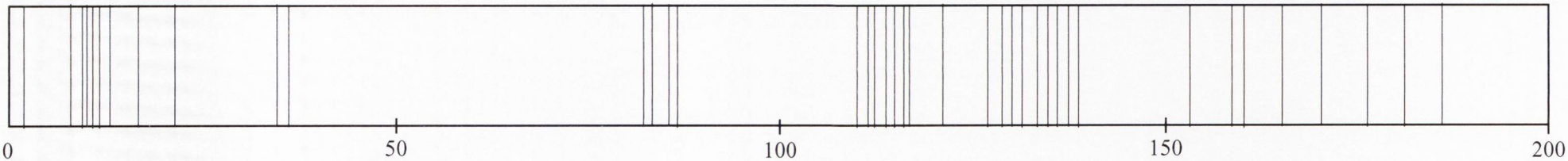

d) Cappanawalla, CTP4NW, joint-NW orientation
Cv = 0.5, mean spacing: 3.64m, L = 102m

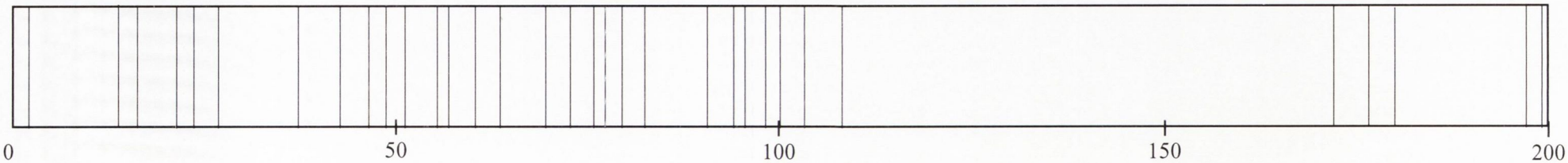

Figure 3.8: a 200m "snap shot" of fracture logs of sample line, of veins and joints, through mapped areas at Cappanawalla and Sheyshmore (scale in metres). Refer to Tables 3.3,3.4 & 3.6 for more details on the spacing of the fracture sets.

e) Cappanawalla, CTP6NNE, vein-NNE orientation
Cv = 1.69, mean spacing: 5.4m

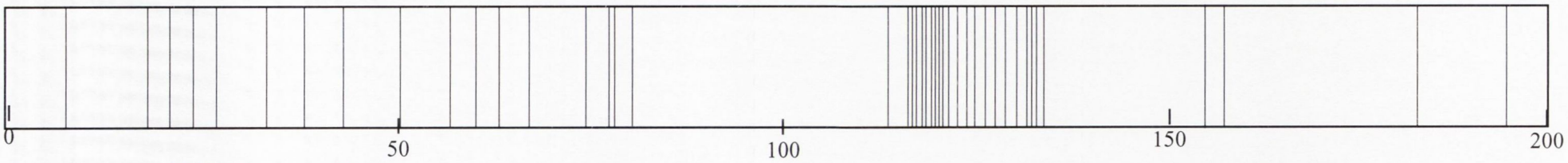

f) Cappanawalla, CTP6NW, joint-NW orientation
Cv = 0.75, mean spacing: 1.5m

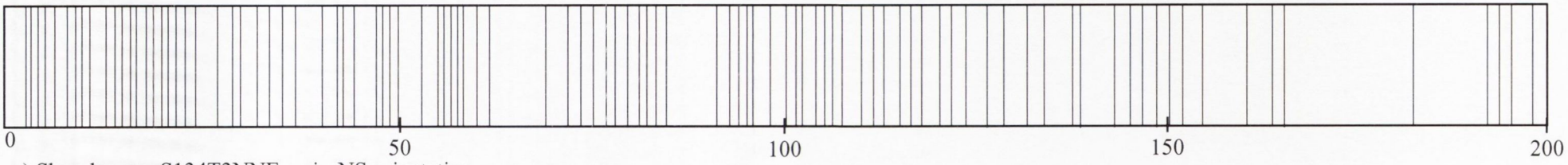

g) Sheyshmore, S134T3NNE, vein-NS orientation
Cv = 0.812, mean spacing: 4.85m

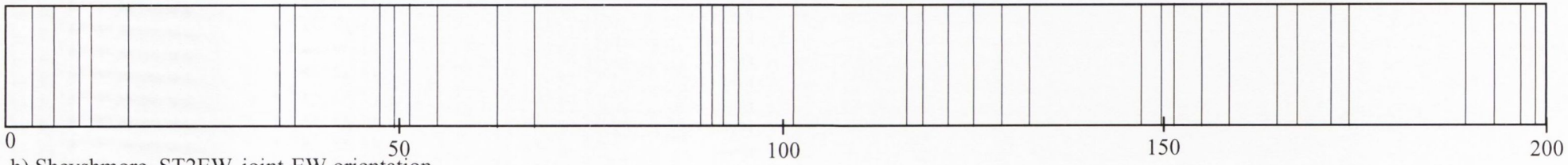

h) Sheyshmore, ST2EW, joint-EW orientation
Cv = 0.46, mean spacing: 1.93m

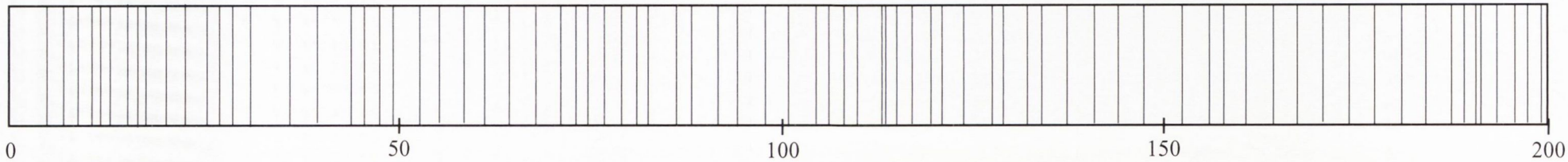

Figure 3.8: a 200m "snap shot" of fracture logs of sample line, of veins and joints, through mapped areas at Cappanawalla and Sheyshmore (scale in metres). Refer to Tables 3.3,3.4 & 3.6 for more details on the spacing of the fracture sets.

i) Sheyshmore, ST1NNE, vein-NNE orientation
Cv = 0.88, mean spacing: 3.95m

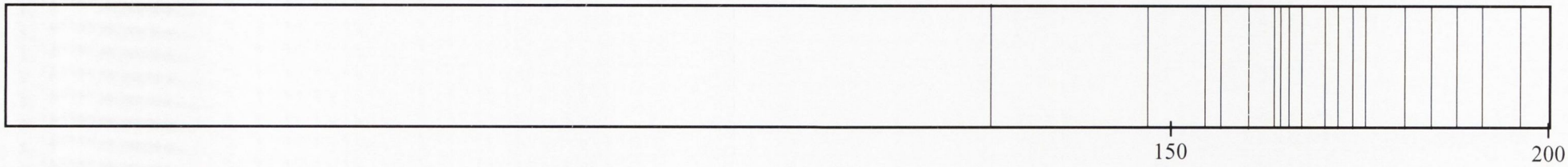

j) Sheyshmore, ST1EW, joint-EW orientation
Cv = 0.44, mean spacing: 1.76

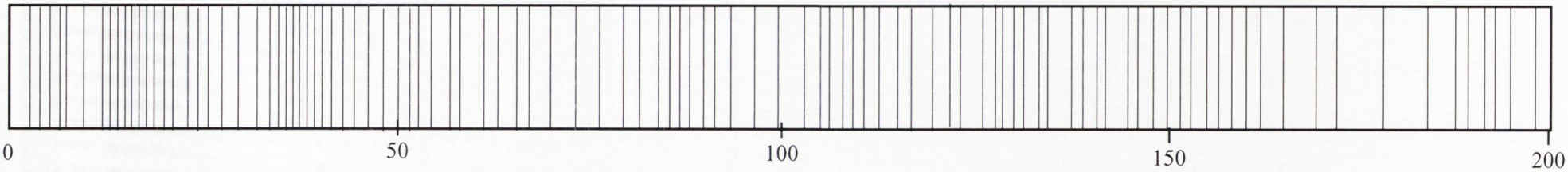

k) Sheyshmore, ST5NNE, vein-NNE orientation
Cv = 1.18, mean spacing: 9.61m

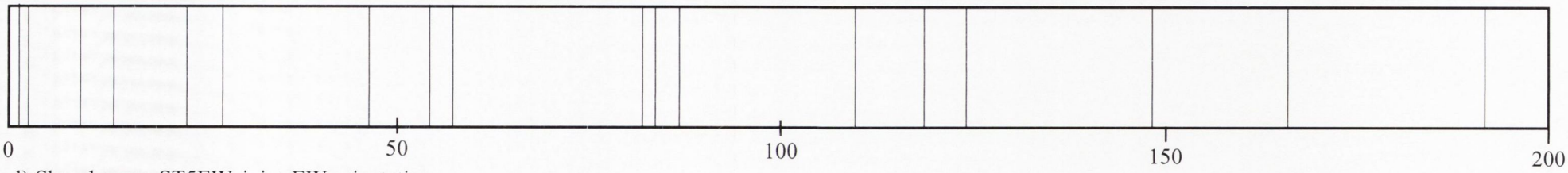

l) Sheyshmore, ST5EW, joint-EW orientation
Cv = 0.64, mean spacing: 1.52m,

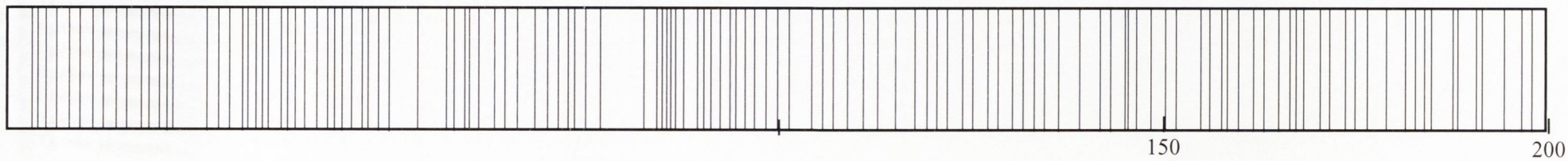

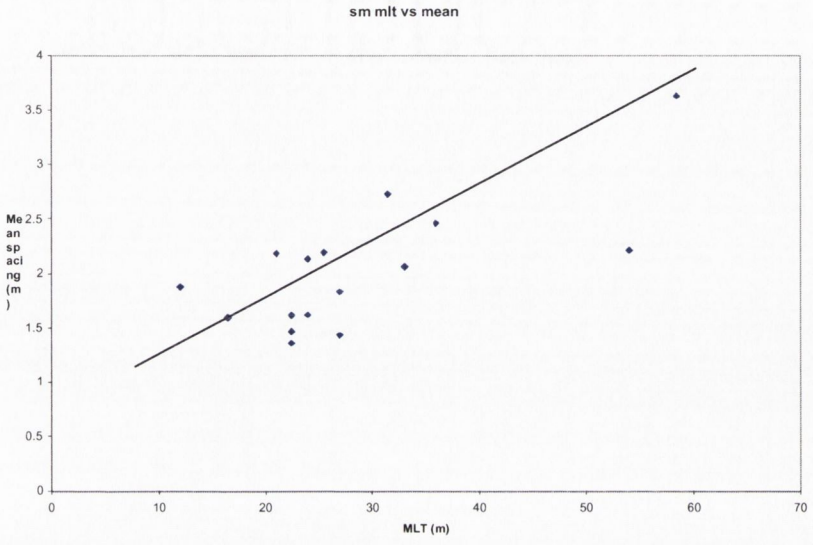

Figure 3.9: Mean vs. vein-controlled MLT at Sheyshmore.

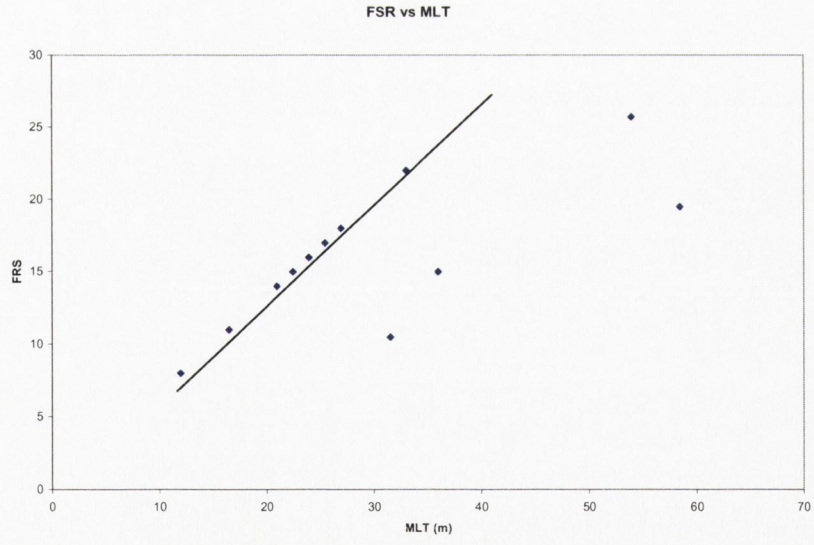

Figure 3.10: FSR vs. vein-controlled MLT.

CHAPTER 4: FRACTURE NETWORKS: CONNECTIVITY & PERCOLATION THEORY

4.1: Introduction

In regions such as the Burren where the rock matrix is impermeable, flow will be confined to the fracture network. In order for fluid to be transported by a fracture network, there must be a continuous path of connected fractures between the source and the output. Therefore the flow of fluids through a fractured rock mass is controlled by the properties of the fracture system: its orientation, length, aperture, density, and connectivity (e.g., Aarseth *et al.* 1997). Fracture connectivity has been investigated using percolation theory, a branch of physics that deals with flow through a system, and many of the basic concepts from this theory are relevant to fluid flow through fractured rock masses (Balberg *et al.* 1990, Berkowitz 1995, Odling *et al.* 1999).

In percolation theory, flow across a system will only occur once a cluster of fractures spans the entire region. This spanning cluster occurs when the percolation threshold of the system has been reached. The portion of the spanning cluster that lies on a direct flow path through the system is known as the backbone. The portions of the spanning cluster that are not on a direct flow path through the system are called dead ends. When the matrix is impermeable, flow will be confined to that part of the connected fracture system with no dead ends, the fracture backbone (Odling *et al.* 1999). An understanding of the processes that control fracture properties and fracture intersection in tandem with the application of percolation theory allows for a better understanding of flow and transport along a fracture system (Balberg 1986, Berkowitz & Balberg 1993, Stauffer & Aharony 1994, Cooke & Underwood 2001). The fracture networks at eleven locations throughout Cappanawalla and Sheyshmore have been examined, and the spanning cluster and backbone of each system has been derived. The connectivity of the system has also been investigated through analysis of the different fracture terminations that occur in the network. For each location, the backbone is compared with the fracture network in order to understand the role of the properties of the different fracture sets (joints and veins) in the control of flow in the region.

4.2 Connectivity

Fracture connectivity is the extent to which the individual fractures are linked, or interact, to form continuous pathways through the rock. A well-connected fracture system will provide many pathways for fluids through the rock. In systems composed of objects distributed in space, connectivity depends on how these objects interact. In this case, it concerns how one-dimensional fracture traces interact in two-dimensional space. Connectivity in a fracture system depends primarily on the fracture orientation, size distribution, and fracture density. Orientation plays a role due to the fact that fractures of the same orientation do not intersect each other; whereas fractures of different orientations, particularly those set at high angles to each other, have a greater likelihood of intersecting. Therefore a fracture system consisting primarily of one fracture set will tend to be

poorly connected relative to a system consisting of several fracture sets (Balberg *et al* 1991, Berkowitz & Balberg 1993, Aarseth *et al* 1997, Odling 1997).

The fractures studied in the Burren are perpendicular to the bedding, thus the connectivity in plan view is relevant to layer-parallel fluid flow (Odling 1997). In scenarios where cross-layer flow is inhibited, as is the case in many of the beds in the Burren, two-dimensional fracture patterns can be used to understand three-dimensional flow (Odling 1997). Odling *et al.* (1999) state that the connectivity of a fracture pattern can be defined quantitatively as the proportion of the total trace length of the largest cluster.

The proportion of the different types of fracture terminations in a system are of great importance in determining the connectivity of the system. Fracture tip terminations can be classified into one of three groups:

1. Blind terminations: fractures that terminate as isolated tips within the rock (b-nodes)
2. Abutments: fractures that terminate against another fracture as an abutment in the H or Y patterns of Hancock (1985) (a-nodes)
3. Cross-fracture terminations: fractures that cut across another fracture (x-nodes).

In a natural system, connectivity is achieved through a combination of fracture intersection (x nodes) and fracture abutment (a nodes).

Fractures that terminate as abutments are important in contributing to the connectivity of a fracture system (Derhowitz & Einstein 1988, Barton & Hsieh 1989, Odling 1993, Odling 1997), as they enhance the connectivity of a system by reducing the number of blind terminations or dead ends within the connected clusters.

The different termination styles of the fractures mapped from aerial photograph analysis and field mapping were classified into one of the three categories. The relative frequencies of the different node types were calculated, and the number of nodes of each classification was then calculated as a proportion of the total number of nodes. This data is presented in Appendix 4.1.

To calculate the density of a system with lines of different lengths, Manzocchi (2002) derived the following equation:

$$d = 1/4A \sum_{L\,\min}^{L\,\max} N_L L^2 \qquad \text{Equation 4.1}$$

Where, A = Area, N_L = number of lines of length L.

Furthermore,

$$P_A + P_B + P_X = 1 \qquad \text{Equation 4.2}$$

Where, P_A = the proportion of abutting termination, P_B = the proportion of blind termination, and P_X = the proportion of cross-terminations.

The connectivity (n) of a system in terms of particular proportions of blind and cross-terminations is therefore calculated using the following formula (Manzocchi 2002):

$$n = 4(1-P_B)/(1-P_X) \qquad \text{Equation 4.3}$$

Once the data from the fracture sites at Cappanawalla and Sheyshmore are plotted (see Appendix 4.1 for the data), it can be seen that there is a positive linear correlation between the proportion of cross-termination (Px) and connectivity (n) as can be seen in Figure 4.1. With an increasing proportion of cross-terminations, there is a corresponding increase in the connectivity of the system. There is a negative linear correlation between the proportion of blind terminations (Pb) and connectivity (n) as can be seen in Figure 4.2. With an increasing proportion of blind terminations, there is a corresponding decrease in the connectivity of the system.

The increase in cross-terminations reflects an increase in the degree of interaction of the fractures and leads to high values of connectivity. In the Burren, the NNE-trending clustered veins are cross-cut by the joints, creating a high proportion of cross-terminations causing the vein clusters to be zones of high connectivity. This aspect of the vein clusters has a strong influence on the sub-surface drainage and subsequent features of the Burren as well as on the surface topography. In the joint-dominated areas, where veins are absent or scarce, there is a higher proportion of blind terminations, which reflects a lower degree of connectivity in the system. More blind terminations relates to less interaction among the fractures. These blind terminations are dead ends from a flow perspective, as they do not contribute to flow through the system because they are not connected to other fractures.

Connectivity is dependent on the relative proportions of these terminations. Fractures that cross-cut other fractures enhance the connectivity of the system, as more of the fractures lie on a connected flow path through the system and act to connect otherwise separate clusters and increase the size of the largest connected cluster in the system. Conversely, as the proportion of blind terminations increases, the connectivity decreases as more fractures are isolated and do not lie on direct flow paths through the system.

4.3 Intersection Density

Intersection density is a measure of the number of fractures that a specific fracture or set of fractures intersects. It can be written as the number of intersections per fracture. As has been discussed in the previous section, connectivity is achieved through a combination of cross-terminations (x nodes or intersections) and abutment (a nodes), with there being a positive linear relationship between an increase in the proportion of cross-terminations and an increase in connectivity. Where there are multiple fracture orientations present in a fracture set, those fractures at a high angle to the others

will have a greater likelihood of intersecting. In the fracture sets analysed in the Burren, the veins are at a high angle to the joint sets. In addition, the veins are clustered. These clusters define discrete zones of intense intersections. The joints are regularly spaced, which prohibits zones of intense joint-on-joint intersection.

In order to ascertain the difference in the number of intersections, or interesection density, between the vein and joint sets, two locations at Cappanawalla were studied. For both locations, site A7 and site B1, the fractures were grouped into ten-degree bins and the number of fractures in each ten-degree interval intersected was counted, as was the number of fractures and the overall length of the fractures within each interval (table 4.1). The NNE-trending vein set and the NW-SE trending joint sets are presented in the table. It can be seen that in proportion to the number of veins present, there are a large number of intersections, whereas the joints have a lower density of intersections. The total length of each fracture type was calculated and divided by the total number of intersections in order to produce a value for the number of intersections per metre for each set. As can seen by the column on the right of Table 4.2, the veins have a significantly higher number of intersections per unit area than the joints.

Location	Orientation	N	ΣL (m)	Nint	Nint/ ΣL (m) (Int m^{-1})
A7	000-010 - Veins	19	108.87	121	1.11
	120-150 - Joints	217	1251.3	206	0.16
B1	000-010- Veins	58	183.34	442	2.41
	130-160 - Joints	375	2742.86	505	0.18

Table 4.1: Intersection values for locations A7 and B1.

N = Number of fractures

ΣL(m) = Sum of the length of the fractures within that orientation

Nint = Number of intersections

Nint/ΣL(m) = Number of intersections divided by the sum of the length of the fractures to give a value of intersections per metre for the main fracture sets.

The vein clusters define areas of high interesection density and, by association, high connectivity. The vein clusters create highly linked pathways through a system that are preferentially utilised by fluid flowing through a system. The joints have fewer intersections per unit area due to the regular spacing of the joints and the fact that a number of the joints terminate within the rock mass as blind terminations. The influence of joints on flow through a connected system is minimal

4.4 Percolation Theory

In physics, percolation is the process of finding an unbroken path across a lattice of randomly filled cells. The word percolation is derived from the Latin *colare*, to flow, and *per*, through. Thus percolation means 'to flow through.' In the field of statistical physics, a large volume of work has

been done on percolation theory, primarily by Stauffer (1985) and Stauffer & Aharony (1991, 1994). The concept of percolation theory is illustrated in Figures 4.3 and 4.4 and is discussed in the following paragraphs.

There are two types of percolation problems: bond percolation and site percolation. Consider a lattice in which the bonds, which represent the fractures, can be in one of two states, occupied (filled) or unoccupied (empty). The probability that any site or bond is occupied is given by p and the probability that it is vacant is 1-p. In bond percolation, two nodes are connected if there exists at least one path between them consisting solely of occupied, or filled, bonds (fractures) (Sahimi 1997). A set of connected bonds bounded by vacant bonds is called a cluster (Figure 4.3b). A procedure to study percolation is to generate a random number for each cell of the lattice and say a bond is vacant if the random number is less then p, where $0 \leq p \leq 1$. When $p = 0$, all the bonds are vacant (Figure 4.3a), and when $p = 1$, the system is completely connected, as all bonds are occupied (Figure 4.3d). If p is small, only small isolated clusters will be present. As p increases towards 1, most of the bonds will be occupied, and a single large cluster will extend from one end of the lattice to the other (fig 4.3c). These are called spanning clusters. There is a critical value of p, the percolation threshold pc, below which spanning clusters do not arise. This has been empirically determined as 0.5 for a square lattice. At the critical point, a connected fluid pathway is established from one side of a system to the other, and fluid flow across a finite region becomes possible. The permeability of the fracture rock matrix close to the percolation threshold behaves as a "critical phenomenon", in that there are large changes in the permeability of the system for small changes in the fracture density (Figures 4.3 and 4.4) (Stauffer & Aharony 1994).

Once the percolation threshold is reached, the spanning cluster spans the entire region. The spanning cluster is characterised by two groupings of fractures, those that lie on a direct flow path through the fracture system (the backbone) and those that do not (dead ends) (Figure 4.3e). Flow is localised along the backbone, which is a connected system of line segments. The number of line segments is directly proportional to the number of intersections within the backbone. The fracture intersection density, which is based on the number of fractures that a particular fracture or fracture set intersects, is one factor that controls the length of line segments in the backbone. A fracture with a high fracture intersection density will intersect a large number of fractures, and as a result it will be represented in the backbone by a large number of small line segments. Conversely a fracture with a low fracture intersection density will be represented by a small number of relatively long line segments. Therefore the length profile of a backbone system can be useful in elucidating the fracture intersection density of particular fracture sets. Each link of the backbone has at least two independent routes that lead to the system boundaries (Bour & Davy 1997). Another important feature are "red links", which are fracture segments that, if removed, would disconnect the system. , h Hence all the flow passes through red links.

With increasing fracture density, the spanning cluster contains an increasing proportion of the total fracture trace length in two dimensions (Balberg & Binehaum 1993). Taking the critical percolation threshold value as 0.5 for a square, a system can be said to be well connected if more than 75% of the fracture traces contribute to the spanning cluster (Odling *et al* 1999) and poorly connected if the largest cluster does not span the entire sample area. As the fracture density increases, more fractures become connected and form large clusters.

Beyond the percolation threshold, the probability that a fracture belongs to the spanning cluster increases with fracture length. Therefore, the fracture length distribution of the spanning cluster and the backbone should be different from the length distribution of the whole network, with the difference being greater for the length distribution of the backbone (Bour &Davy 1997). It should be noted that a basic assumption of percolation theory is that the location of every site or fracture is random, a fact that is not borne out in nature where the fracture patterns are very well ordered. The location of each fracture is determined by a number of factors such as bed thickness and location of discontinuities.

4.5 Analysis of fracture data

The fracture pattern at eleven locations was mapped in detail through a combination of aerial photograph analysis and subsequent verification on the ground at eight locations, and by mapping in the field at the other three – Gleninagh, Cathair Comhain, and Oughtdarra. The eight locations that were mapped through aerial photography are evenly split between two locations, Cappanawalla and Sheyshmore. Of the four locations at Cappanawalla, two, A7 and B11, are on the lower 4.8m-thick unit of peloidal packstones, whilst the remaining locations, B9 and B1, are located on the upper 1.8m unit peloidal packstone, both of the upper Aillwee Member of the Burren Formation. First, the fracture network is identified and statistics such as the number of fractures, the total length of the system, the mean and median length of fractures, standard deviation, connectivity, and proportion of terminations are generated for it. From this network, the spanning cluster is created and statistics generated including a figure indicating the length of the system expressed as a percentage of the length of the fracture network. The spanning cluster is divided into a series of individual line segments; the segments that form the backbone are isolated, and dead ends are discarded. The orientation of the different systems is analysed using a rose diagram as are the lengths of the different networks in an attempt to investigate the control that fractures of certain orientations have on the different systems. The methodology for this study largely follows the concepts developed by Odling in analysing fracture systems, in particular Odling (1993, 1997) Odling & Roden (1997) and Odling *et al.* (1999). In this last study, it is stated that a fracture pattern can be considered well connected if more than 75% of the fracture traces contribute to continuous pathways through the system.

4.5.1: B9

The fracture pattern at location B9 (Figure 4.5) is located along the exposed limestone pavement of Cappanawalla. The bed is a 1.8 m thick unit of peloidal packstone of the upper Aillwee Member of the Burren Formation. The fracture pattern consists of a series of regularly spaced NW-SE-trending systematic joints, which are horizontally persistent, and a set of minor oblique cross-joints of varying density and orientation, though primarily trending EW. To the bottom left of the figure, a small number of NNE veins occur. From a visual inspection of the fractures at this location, it can be seen that the fractures here are well connected. Further analysis shows that 83% of the fractures contribute to the spanning cluster, which would classify this as well connected according to Odling *et al.* (1999). A high percentage (56%) of the terminations in the system are abutments. A quarter of all the terminations are blind, or dead ends, as they do not lie on a direct flow path through the system. The remaining terminations are cross-terminations.

From °	To °	Fracture Network	Spanning Cluster	Backbone
0	10	4.36	4.59	4.34
10	20	4.84	5.63	5.54
20	30	1.61	1.13	0.2
30	40	0.45	0.28	0.18
40	50	0.84	0.99	0.57
50	60	0.96	1.01	1.08
60	70	1.26	1.29	1.1
70	80	2.18	1.92	1.4
80	90	8.13	7.72	6.85
90	100	6.06	5.22	3.48
100	110	0.94	0.92	0.59
110	120	0.44	0.52	0.21
120	130	1.52	1.31	0.88
130	140	3.87	2.72	3.34
140	150	35.35	36.48	41.95
150	160	21.96	22.79	23.2
160	170	2.43	2.57	2.1
170	180	2.8	2.91	2.98

Table 4.2: % of Σl per ten-degree bin for B9.

The fracture network at B9 is dominated by the NW-SE-trending systematic joints, which account for >57% (Table 4.2) of the length of the system, with the E-W cross-joints accounting for >16% of the total length of the system. The proportion of the total length of NW-SE-trending systematic

joints is slightly greater in the spanning cluster than in the network as a whole, with the proportion of E-W joints decreasing accordingly. The lower proportion of cross-joints in the spanning cluster reflects the fact that many of the cross-joints terminate blindly or are not connected to the main fracture system. The backbone shows a continued decrease in the cross-joint proportion of the system and an increase in the proportion of NW-SE joints, which account for 65% of the length of the system. The backbone is principally composed and controlled by the NW-SE systematic joints, which are connected to each other through a combination of joints abutting against each other and by the cross-joints linking adjacent joints. The backbone contains 63% of the length of the original fracture network.

4.5.2: B1

The fracture pattern at location B1 (Figure 4.8) is located on the same bed to the north of location B9. Compared to the previous location, there are more of NNE-trending veins at this site, with a corresponding increase in the proportion of cross-terminations (Px) and therefore an increase in connectivity. The proportion of the length of the system that is composed of NNE-trending fractures increases from <5% for the fracture network to ~20% for the spanning cluster to 24% for the backbone (Table 4.3 and Figure 4.10). The system is well-connected.

From °	To °	Fracture Network	Spanning Cluster	Backbone
0	10	2.50	17.74	21.29
10	20	2.39	2.28	2.41
20	30	0.29	0.27	0.11
30	40	0.17	0.13	0.10
40	50	0.31	0.25	0.20
50	60	0.38	0.49	0.41
60	70	1.12	1.19	1.02
70	80	3.06	3.11	2.93
80	90	7.20	5.64	5.51
90	100	6.35	7.01	4.92
100	110	2.37	2.91	2.06
110	120	2.62	2.16	1.32
120	130	5.09	4.12	3.22
130	140	12.17	8.14	7.71
140	150	35.31	29.21	32.20
150	160	14.73	13.26	13.49
160	170	2.89	1.02	0.48
170	180	1.07	1.08	0.63

Table 4.3: % of Σl per ten-degree bin for B1

4.5.3: A7

The fracture pattern at location A7 (Figure 4.11) is located to the north of the previous sites on a different bed, a 4.8m-thick unit of peloidal packstone. The fracture pattern consists of a series of regularly spaced NW-SE-trending systematic joints which are horizontally persistent, a set of cross-joints that obliquely trend WNW-ESE into the NW-SE-trending systematic joints, and a set of clustered NE-trending veins. The proportion of the length of the system that is composed of NNE-trending fractures / line segments increases from the fracture network, where they account for >5% of the total length of the system, to the backbone, where they account for >15% of the length of the system, as can be seen from Table 4.4 and Figure 4.13. The proportion of NW-trending fractures decreases as the backbone is created. The backbone contains 70% of the original trace length.

From °	To °	Fracture Network	Spanning Cluster	Backbone
0	10	5.29		15.076522
10	20	0.67		0.7747343
20	30	0.16		0
30	40	0.25		0.252725
40	50	0.13		0.0889877
50	60	0.10		0.19438
60	70	0.17		0.2745463
70	80	0.33		0.3354448
80	90	0.42		0.3386948
90	100	3.38		1.821384
100	110	8.58		6.5680632
110	120	18.53		12.80633
120	130	14.70		12.42407
130	140	27.56		22.726984
140	150	18.46		24.152102
150	160	0.33		0.9996023
160	170	0.08		0
170	180	0.86		1.1654288

Table 4.4: % of Σl per ten-degree bin for A7.

4.5.4: B11

The fracture pattern at B11 is located in the same 4.8m thick unit as the fractures at location A7. The fracture pattern consists of a series of regularly spaced NW-SE-trending systematic joints that are horizontally persistent and a set of oblique cross-joints of varying density and orientation, though

primarily trending WNW-ESE. To the bottom right of the figure, a small number of NNE veins occur. The system has a low number of cross-terminations at <8% and a relatively high number of blind terminations at 36%, producing a correspondingly low connectivity value of 2.45. Unlike the previous two locations, which had a series of NNE-trending vein clusters, this location, like B9, has an insignificant number of veins. Unlike B9, the joints at this location are more sinuous and apparently poorly connected. The spanning cluster contains 69% of the total trace length, which according to Odling *et al.* (1999), would characterise it as poorly connected. A visual analysis of the backbone shows that a number of clusters to the right of the maps are connected to the remainder of the system by a small number of relatively isolated segments, which if deleted would leave the entire right side of the system disconnected. Of the four sites analysed at Cappanawalla, this is deemed to be the most poorly connected due to the relative absence of vein clusters and their associated cross-terminations, as well as the nature of the joint pattern at this location. The systematic joints here are sinuous, with a large number of oblique sets that often terminate blindly. The joints in the thinner beds have a more regular spacing and are better connected by shorter, predominately EW-trending cross-joints.

From °	To °	Fracture Network	Spanning Cluster	Backbone
0	10	1.30	2.15	2.07
10	20	6.78	8.35	8.44
20	30	0.55	0.91	0.71
30	40	0.40	0.19	0.07
40	50	0.01	0.38	0.51
50	60	0.15	0.15	0.20
60	70	0.25	0.30	0.07
70	80	0.23	0.31	0.23
80	90	1.32	2.53	2.88
90	100	10.35	9.73	8.51
100	110	23.25	22.74	19.03
110	120	22.94	23.67	23.85
120	130	15.90	15.57	10.29
130	140	10.31	1.06	9.87
140	150	2.58	3.46	3.66
150	160	2.74	7.04	8.02
160	170	0.74	1.10	1.23
170	180	0.19	0.35	0.36

Table 4.5: % of Σl per ten-degree bin for B11.

4.5.5: 134B1

The fracture pattern at location 134B1 (Figure 4.17) is located along the exposed limestone pavement at Sheyshmore. The bed is in a 1.2m-thick unit of peloidal packstone of Ballyelly Member of the Slievenaglasha Formation. The fracture consists of a series of regularly spaced E-W-trending systematic joints, a set of oblique cross-joints of varying density and orientation, though primarily trending WNW-ESE, and a set of N-S-trending veins. In contrast to the previous locations, the percentage of the total fracture length that each orientation accounts for is similar. The first red link connects the bottom of the system to the middle cluster, which is in turn connected by a red link, in the form of a NS trending vein segment, to the remainder of the system.

From °	To °	Fracture Network	Spanning Cluster	Backbone
0	10	8.74	8.36	7.65
10	20	4.30	4.57	3.01
20	30	0.33	0.35	0.27
30	40	0.00	0.00	0.00
40	50	0.71	0.76	1.09
50	60	0.00	0.00	0.00
60	70	0.00	0.00	0.00
70	80	0.00	0.00	0.69
80	90	53.96	56.23	55.34
90	100	12.00	11.55	16.02
100	110	0.72	0.76	1.58
110	120	8.03	8.15	8.38
120	130	1.85	1.00	1.10
130	140	1.84	1.95	0.98
140	150	0.36	0.00	0.91
150	160	2.76	2.04	0.83
160	170	1.17	1.24	0.56
170	180	2.79	2.66	1.59

Table 4.6: % of Σl per ten-degree bin for 134B1.

4.5.6: SMB7

The fracture pattern discussed at location SMB7 is on the same bed as the previous fracture set. It has a similar fracture pattern consisting of a series of regularly spaced E-W-trending systematic joints, a minor set of oblique cross-joints of varying density and orientation, and a set of N-S-trending veins. The principal difference in this site is that there are more N-S trending veins, which increases the proportion of cross-terminations and leads to an increased connectivity value of 4.17 compared to 3.96 at the previous location. As at the previous site, the percentage of the total fracture length that each of the three orientations accounts for varies little.

From °	To °	Fracture Network	Spanning Cluster	Backbone
0	10	6.17	6.98	7.24
10	20	11.61	11.10	11.01
20	30	0.00	0.00	0.00
30	40	0.00	0.00	0.00
40	50	0.00	0.15	0.00
50	60	0.00	0.00	0.00
60	70	0.00	0.00	0.00
70	80	0.00	0.00	0.00
80	90	2.55	6.06	6.46
90	100	59.25	52.41	51.60
100	110	16.50	18.43	19.53
110	120	2.64	3.50	3.17
120	130	0.00	0.00	0.00
130	140	0.00	0.00	0.00
140	150	0.20	0.17	0.00
150	160	0.26	0.22	0.25
160	170	0.00	0.00	0.00
170	180	0.81	0.84	0.75

Table 4.7: % of Σl per ten-degree bin for SMB7.

4.5.7: SMB9

The fracture set consists of a series of regularly spaced E-W-trending systematic joints, a set of WNW-ESE oblique joints that curve into the pre-existing E-W-trending joints, and minor N-S cross-joints. It lies on the same bed as the two previous examples from Sheyshmore. As with the other sites, it is a well-connected network, with each orientation accounting for approximately the same percentage of the total fracture length although the E-W-trending joint set contributes a slightly smaller proportion of the total length. The site is connected from top to bottom only by the presence of a red link along the line segment of an oblique NW-SE-trending cross-joint found at the bottom left-hand corner of the Figure 4.23.

From °	To °	Fracture Network	Spanning Cluster	Backbone
0	10	5.12	4.67	3.39
10	20	4.56	5.09	4.89
20	30	1.37	1.86	2.03
30	40	1.02	1.34	1.65
40	50	1.46	0.16	0.17
50	60	0.00	0.42	0.28
60	70	0.78	1.25	1.23
70	80	2.52	1.57	1.90
80	90	7.39	10.55	11.02
90	100	24.16	27.02	25.45
100	110	36.84	28.63	30.76
110	120	7.24	10.55	9.48
120	130	0.84	1.31	1.70
130	140	0.79	0.83	0.00
140	150	0.29	0.73	2.38
150	160	2.39	1.24	1.47
160	170	1.26	0.93	0.82
170	180	1.97	1.77	1.39

Table 4.8: % of Σl per ten-degree bin for SMB9.

4.5.8: SMF1

The fractures at this location consist of a series of regularly spaced E-W-trending systematic joints with a set of WNW-ESE oblique joints that curve into these joints along with a set of broadly N-S-trending veins. The site lies on the same bed as the three previous examples from Sheyshmore. Like the other sites, it is a well-connected network with the three orientations each accounting for a similar proportion of the total fracture length, except for a slightly higher proportion of E-W-trending joints. The presence of the veins increases the connectivity of the system through the increased number of cross-terminations that they create.

From °	To °	Fracture Network	Spanning Cluster	Backbone
0	10	2.70	3.74	3.15
10	20	4.83	4.95	5.37
20	30	4.33	2.77	2.58
30	40	3.33	3.98	4.27
40	50	0.91	1.48	1.09
50	60	0.66	0.47	0.38
60	70	1.63	1.68	1.26
70	80	2.04	1.96	1.88
80	90	11.24	10.80	11.44
90	100	24.80	26.36	28.97
100	110	18.43	16.30	14.89
110	120	13.18	13.85	13.76
120	130	3.72	3.42	3.42
130	140	1.58	1.31	1.15
140	150	0.50	1.23	0.88
150	160	1.15	1.20	1.03
160	170	2.02	1.22	0.98
170	180	2.94	3.22	3.49

Table 4.9: % of Σl per ten-degree bin for SMF1.

4.5.9: Cathair Comhain

The fracture pattern at location Cathair Comhain (Figure 4.29) is located along the exposed limestone pavement at Cathair Comhain, to the south of a NE-SW trending syncline approximately 4.2 km to the east of Sheyshmore. The scale of the fracture pattern is smaller than the previous examples, being 6m wide and 10m long. The bed is part of the Ballyelly Member of the Slievenaglasha Formation. The fracture pattern consists of a series of regularly spaced E-W-trending systematic joints, N-S veins, and a set of minor NE-SE trending oblique joints that curve into the pre-existing E-W-trending joints. The fractures at this location, as well as at the following two locations, Gleninagh and Oughtdarra, were mapped in the field using a chalked out $1m^2$ grid.

From °	To °	Fracture Network	Spanning Cluster	Backbone
0	10	2.70	3.74	3.15
10	20	4.83	4.95	5.37
20	30	4.33	2.77	2.58
30	40	3.33	3.98	4.27
40	50	0.91	1.48	1.09
50	60	0.66	0.47	0.38
60	70	1.63	1.68	1.26
70	80	2.04	1.96	1.88
80	90	11.24	10.80	11.44
90	100	24.80	26.36	28.97
100	110	18.43	16.30	14.89
110	120	13.18	13.85	13.76
120	130	3.72	3.42	3.42
130	140	1.58	1.31	1.15
140	150	0.50	1.23	0.88
150	160	1.15	1.20	1.03
160	170	2.02	1.22	0.98
170	180	2.94	3.22	3.49

Table 4.10: % of Σl per ten-degree bin of Cathair Comhain.

4.5.10: Gleninagh

The fracture pattern at location Gleninagh (Figure 4.32) is located along the exposed limestone pavement at Gleniagh Hill 3km to the west of Cappawalla at an elevation of 280m. The bed is a member of the upper Aillwee Member of the Burren Limestone Formation. The fracture pattern consists of a series of regularly spaced NW-SE-trending joints which cross-cut NNE-trending clustered veins. The system has a high proportion of cross-termination, 38.6%, due to the presence of the veins. The system has a connectivity of 4.2. The spanning cluster of Gleninagh contains 94.16% of the total trace length and would, according the criteria of Odling *et al.* (1999), be deemed very well connected. The backbone for the system contains 89.75% of the total trace length. The system is well connected horizontally.

From °	To °	Fracture Network	Spanning Cluster	Backbone
0	10	1.14	12.63	0.69
10	20	27.92	2.61	46.51
20	30	26.44	41.02	12.62
30	40	0.00	12.45	0.60
40	50	0.00	0.00	0.00
50	60	0.00	0.00	0.00
60	70	0.00	0.00	0.00
70	80	0.00	0.00	0.00
80	90	0.00	0.00	0.00
90	100	0.00	0.00	0.00
100	110	0.00	0.00	0.00
110	120	0.00	0.00	0.00
120	130	0.00	0.00	0.00
130	140	0.00	0.00	0.00
140	150	0.00	0.00	0.00
150	160	3.40	0.00	0.46
160	170	27.74	0.93	30.50
170	180	13.37	30.04	8.99

Table 4.11: % of Σl per ten-degree bin of Gleninagh.

4.5.11: Oughtdarra 1

The fracture pattern at location Oughtdarra 1 (O1) (Figure 4.35) is at Oughtdarra, 4km to the northeast of Carran on Goratclare Mountain. The bed is a member of the upper Aillwee Member of the Burren Limestone Formation. The fracture pattern consists of a series of regularly spaced NE-SW-trending joints which cross-cut NNE-trending clustered veins.

The system has a high proportion of blind terminations, 47%, which reduce the overall connectivity of the system, which is 2.5. The system also has a high percentage of abutment terminations, 36.84%. Cross-terminations are confined to the NNE veins. The spanning cluster of O1 contains 98.4% of the total trace length and, would according the criteria of Odling *et al.* (1999), be deemed very well connected. The backbone for the system contains 90.1% of the total trace length. The system is well connected horizontally.

From °	To °	Fracture Network	Spanning Cluster	Backbone
0	10	4.78	9.48	8.69
10	20	3.03	0.00	0.00
20	30	0.00	1.71	2.00
30	40	1.81	3.60	3.16
40	50	2.15	0.58	0.79
50	60	13.50	13.72	18.66
60	70	9.54	8.54	7.42
70	80	0.00	2.17	0.00
80	90	9.90	7.10	7.52
90	100	2.33	6.75	6.88
100	110	8.32	1.37	1.02
110	120	4.19	8.26	7.26
120	130	0.00	1.74	1.84
130	140	0.00	0.12	0.00
140	150	0.00	0.00	0.00
150	160	0.00	0.00	0.00
160	170	1.29	0.00	1.31
170	180	39.16	34.86	33.45

Table 4.12: % of Σl per ten-degree bin of Oughtdarra.

4.6: Conclusion:

Where veins occur, they define discrete zones of high connectivity. The veins are cross-cut by the joints, creating a high proportion of cross-terminations, which leads the vein clusters to be zones of

high connectivity. It can be seen in Figure 4.1 that there is a positive linear correlation between an increase in the proportion of cross terminations and an increase in connectivity. In the joint-dominated areas, where the veins are absent or scarce, there is a higher degree of blind terminations in the system, which reflects a lower degree of connectivity. Due to the clustered nature of the veins, these zones of high connectivity are narrow discrete zones. The veins have a higher number of intersections per unit area, or a higher intersection density, than the joints (Table 4.1). The increased connectivity and high intersection density illustrate that the vein sets are highly connected. When the fracture network is analysed and the backbone derived from it, can be seen that, where they occur, veins account for a large percentage of the overall length of the backbone. The vein-dominated backbones can have different directional characteristics than the fracture networks that are dominated by joints. The veins exert a strong control on the fracture pathways that fluid uses to flow through the region. Where veins occur, they form a narrow zone of elevated connectivity, providing a direct flow path across the system.

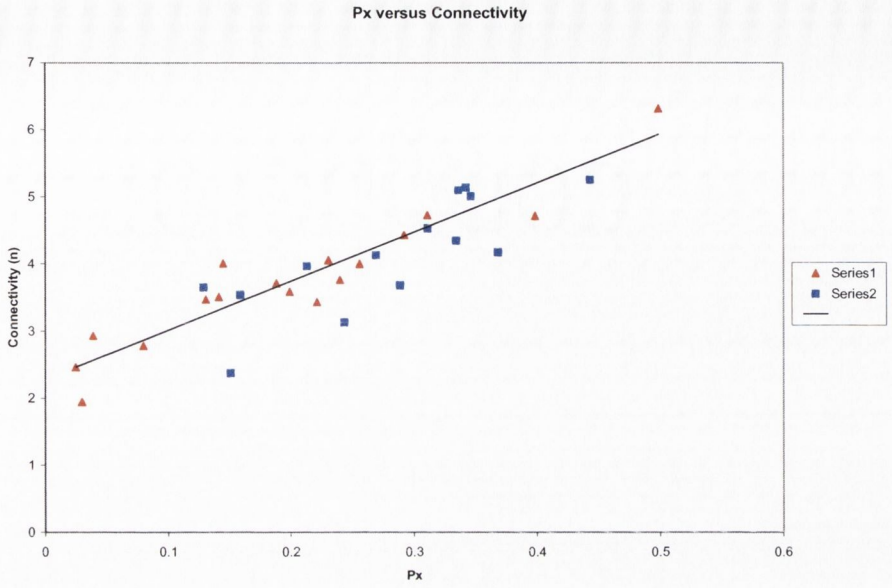

Figure 4.1: Px vs. connectivity (n), for 29 locations on Sheyshmore (squares) and Cappanawalla (triangles).

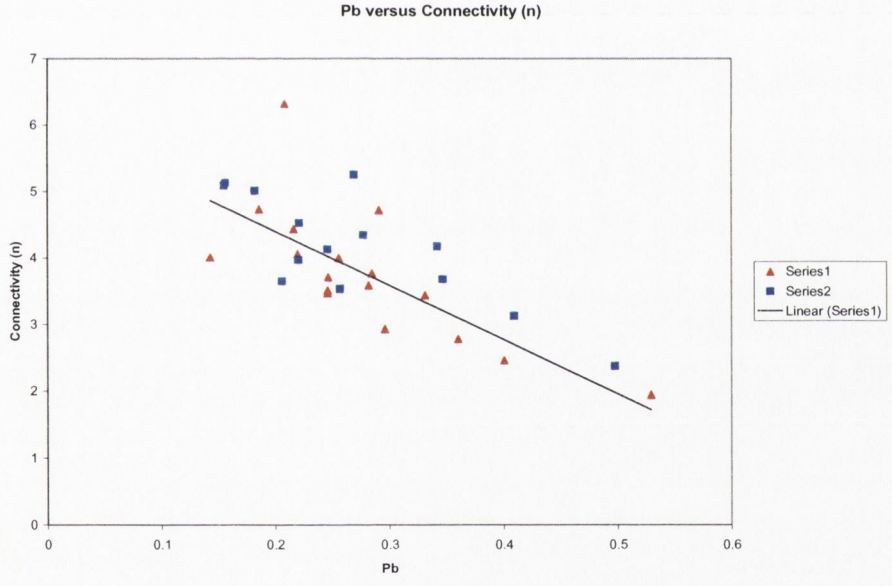

Figure 4.2: Pb vs. connectivity (n) for 29 locations on Sheyshmore (squares) and Cappanawalla (triangles).

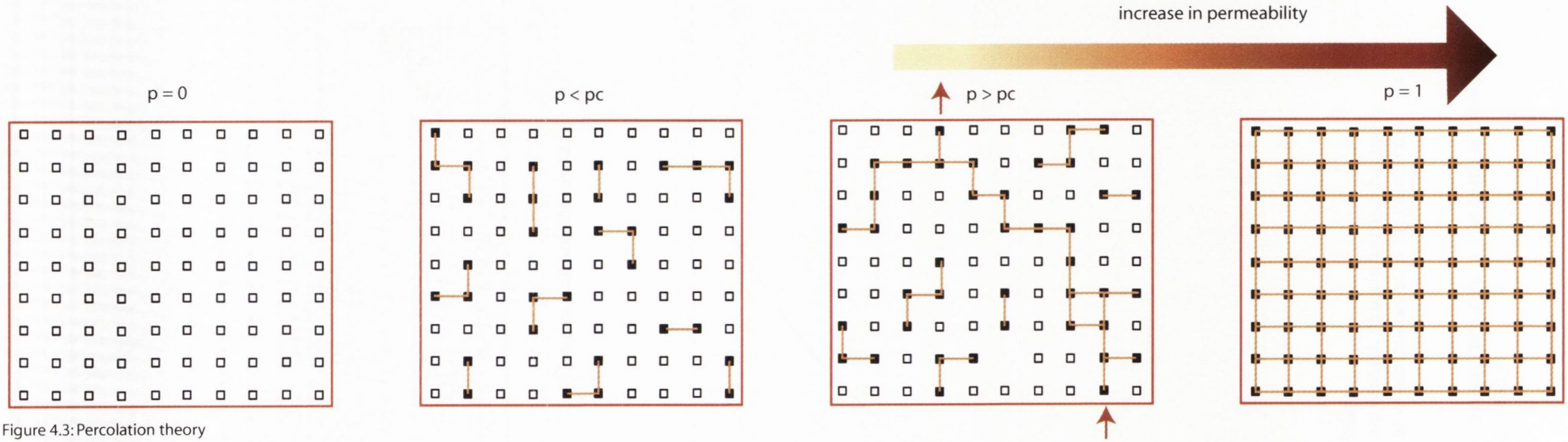

Figure 4.3: Percolation theory

a) no cells occupied, no sites connected.

b) small finite clusters which are internally connected but do not percolate.

c) development of a spanning cluster creating a connected fluid pathway through the system - percolation established.

d) all cells are filled, all sites are connected.

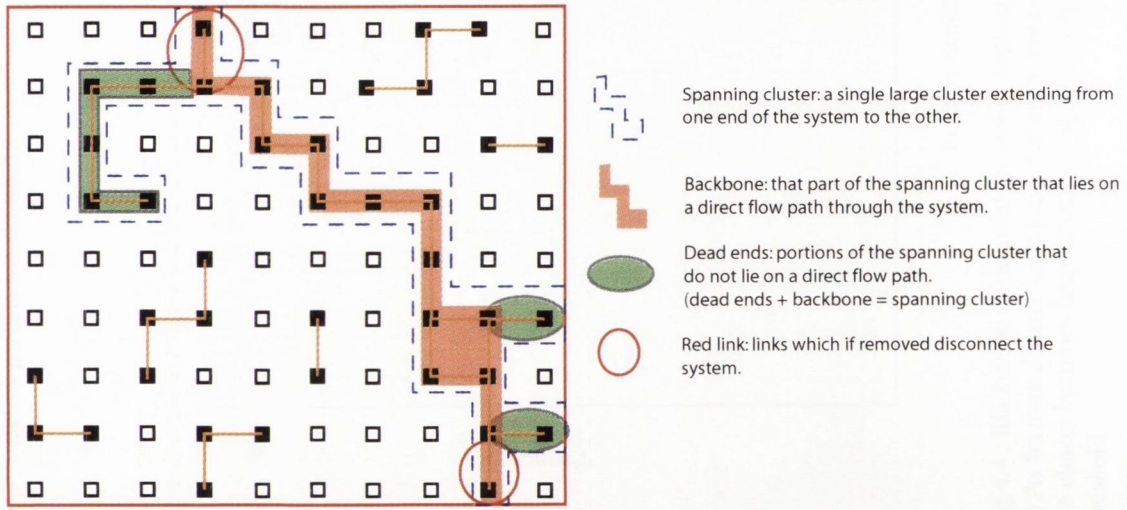

e) "anatomy" of a spanning cluster.

A: Below percolation threshold

Above percolation threshold

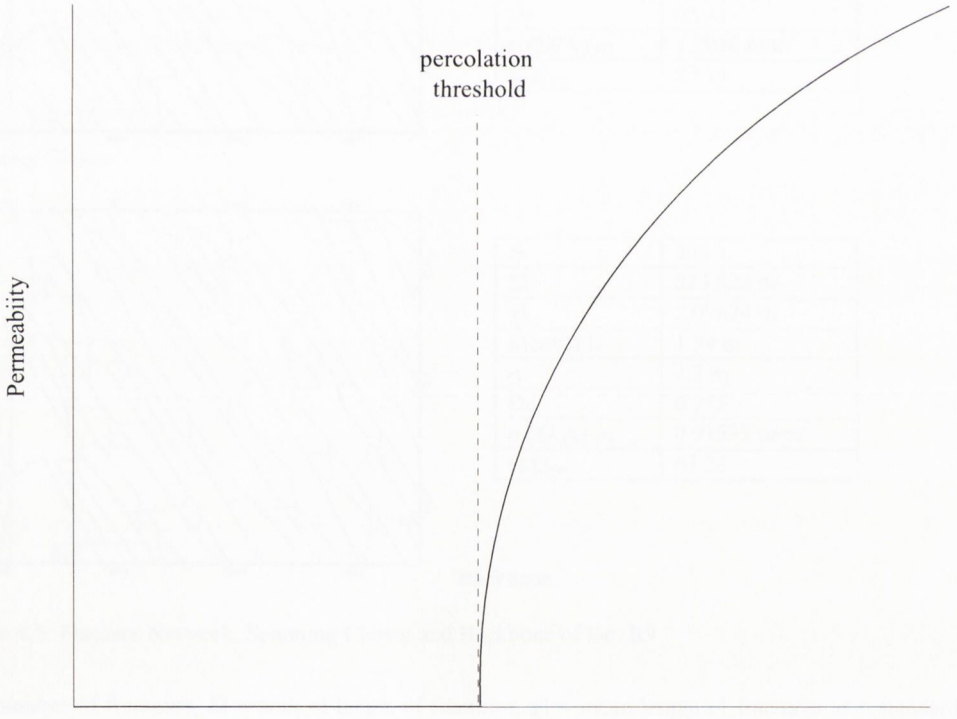

B: Fracture density

Fig 4.4 : Illustration of percolation theory applied to a fracture system.
A) As fracture density increases, clusters of connected fractures are formed. With increasing density one cluster becomes large enough to span the region. The point at which this occurs is the percolation threshold.

B) The threshold corresponds to that point at which permeability becomes non-zero. Close to the threshold rapid changes in permebaility occur for small changes in fracture density.

Diagram modified from Aarseth et al (1997).

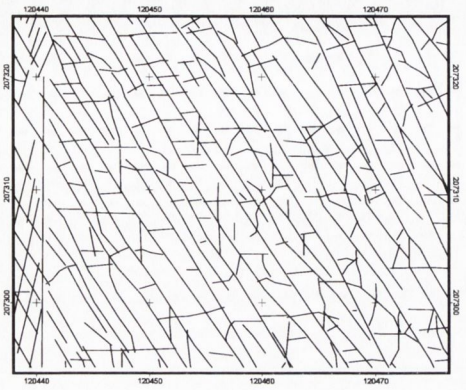

N	283
Σl	1302.594 m
χl	4.602 m
Median L	2.480 m
σ	5.874 m
Dc	3.2764
ρ (Σl/A) m	1.08 m/m^2

Fracture Network

Pa: 0.565, Pb: 0.247, Px:: 0.188, n = 3.71

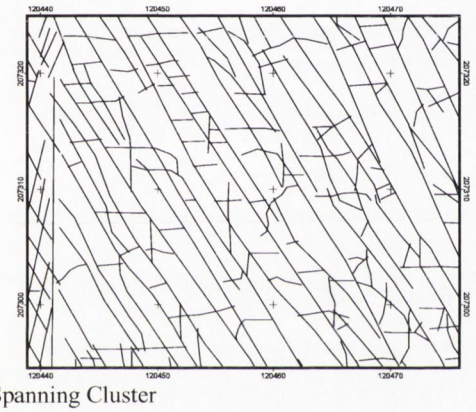

N	574
Σl	1083.272 m
χl	1.887 m
Median L	1.386 m
σ	2.078 m
Dc	0.941
ρ (Σl/A) m	1.2036 m/m^2
$\%\Sigma l_{FN}$	83.16

Spanning Cluster

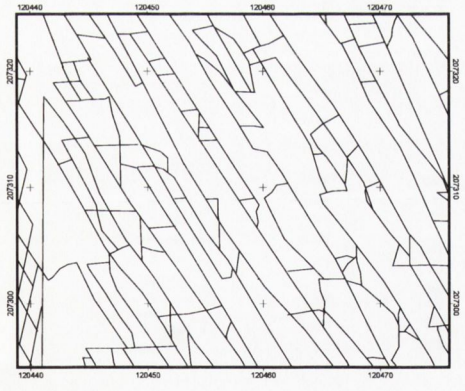

N	393
Σl	823.823 m
χl	2.09624 m
Median L	1.54 m
σ	2.2 m
Dc	0.755
ρ (Σl/A) m	0.91533 m/m^2
$\%\Sigma l_{FN}$	63.24

Backbone

Figure 4.5: Fracture Network, Spanning Cluster and Backbone of loc. B9

N = number of fractures, Σl = sum of length of fractures, χl = mean length of fractures, σ = standard deviation, Dc = critical density, n = connectivity, ρ (Σl/A) = density, $\%\Sigma l_{FN}$ = length of system expressed as a percentage of the fracture network. Pa/b/c = proportion of abutment/blind/cross termination.

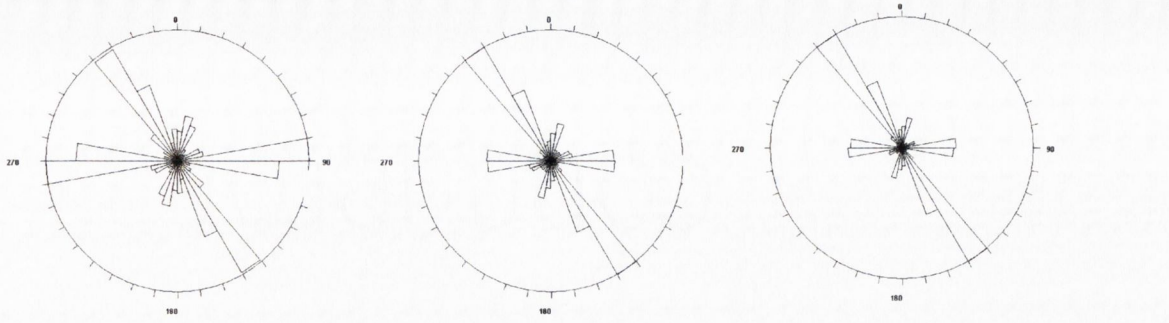

a) Rose diagram of the orientation of the fracture network of loc: B9.

b) Rose diagram of the orientation of the spanning cluster of loc: B9.

c) Rose diagram of the orientation of the fracture backbone of loc: B9.

Fig 4.6: Rose diagrams illustrating the frequency of the different orientations.

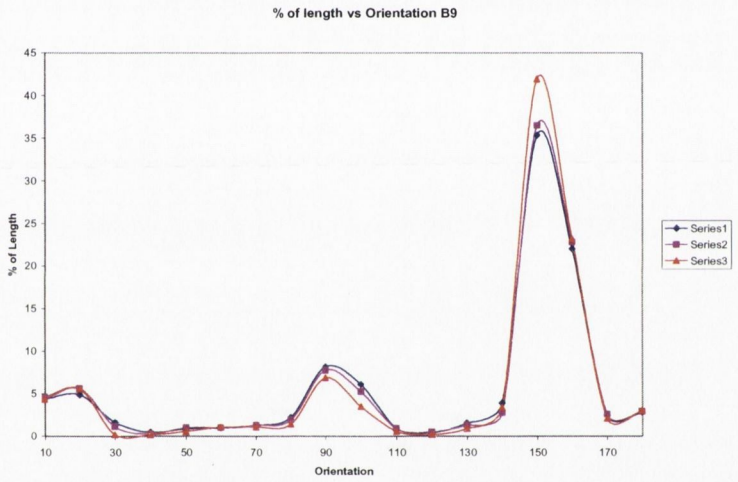

Fig: 4.7 Comparison of % of total length versus orientation for the fracture network (series 1), the spanning cluster (series 2) and the backbone (series 3)v

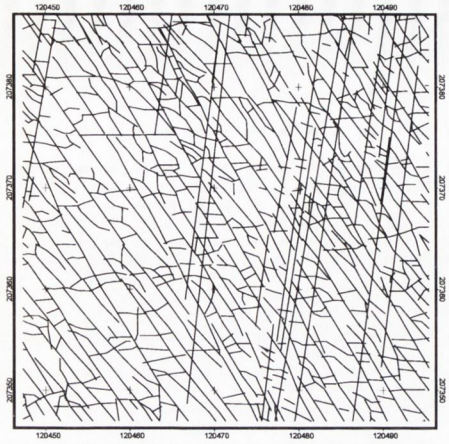

N	576
Σl	2610.298 m
χl	4.531 m
Median L	2.437 m
σ	5.27 m
Dc	4.43
ρ (Σl/A) m	1.6314 m/m^2

Fracture Network

Pa: 0.488, Pb: 0.255, Px: 0.255 n = 4

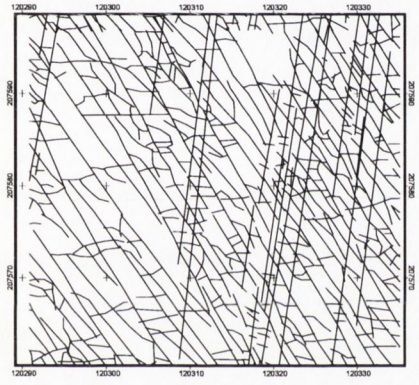

N	1763
Σl	2122.954 m
χl	1.20417 m
Median L	.935 m
σ	1.154 m
Dc	0.766
ρ (Σl/A) m	1.327 m/m^2
%Σl_{FN}	81

Spanning Cluster

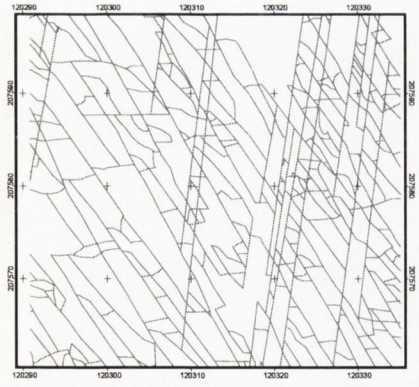

N	1193
Σl	1587.378 m
χl	1.33058 m
Median L	1.042 m
σ	1.001 m
Dc	0.602
ρ (Σl/A) m	0.992 m/m^2
%Σl_{FN}	60

Backbone

Figure 4.8: Fracture Network, Spanning Cluster and Backbone of loc. B1

N = number of fractures, Σl = sum of length of fractures, χl = mean length of fractures, σ = standard deviation, Dc = critical density, n = connectivity, ρ (Σl/A) = density, %Σl_{FN} = length of system expressed as a percentage of the fracture network. Pa/b/c = proportion of abutment/blind/cross termination.

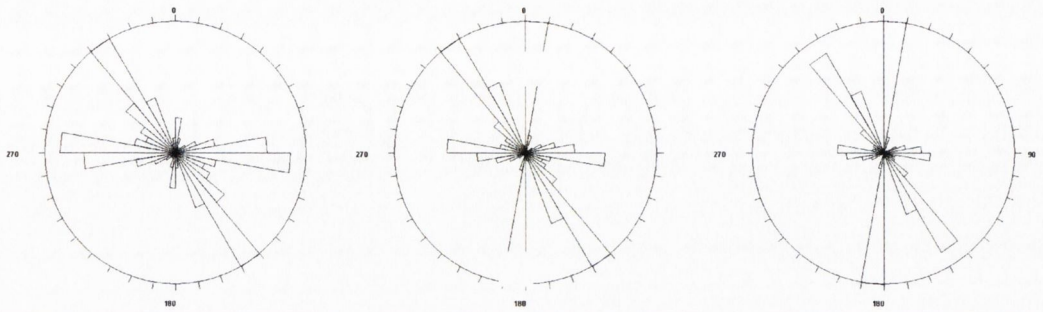

a) Rose diagram of the orientation of the fracture network of loc: B1.

b) Rose diagram of the orientation of the spanning cluster of loc: B1

c) Rose diagram of the orientation of the fracture backbone of loc: B1

Fig 4.9: Rose diagrams illustrating the frequency of the different orientations

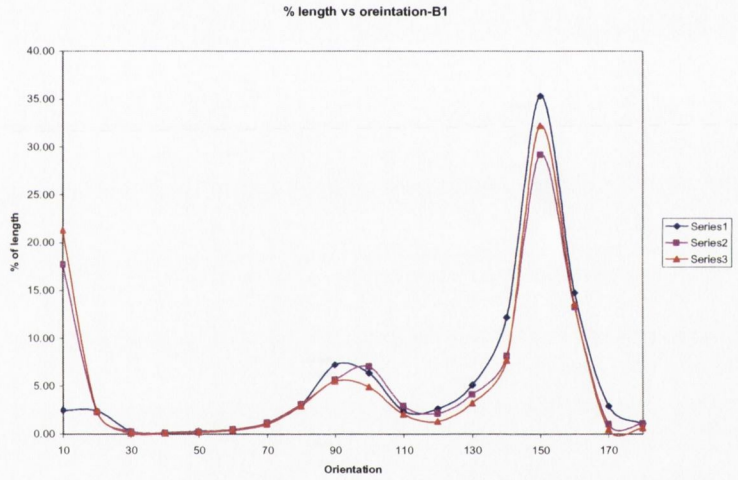

Fig: 4.10 Comparison of % of total length versus orientation for the fracture network (series 1), the spanning cluster (series 2) and the backbone (series 3)

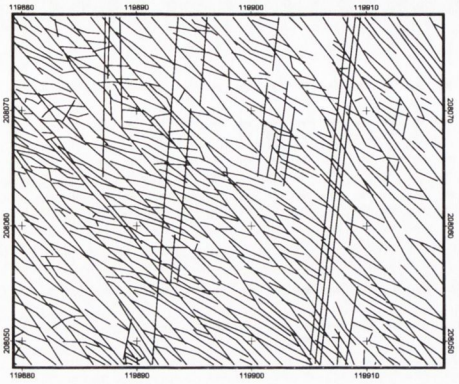

N	395
Σl	2059 m
χl	5.212 m
Median L	1.77 2m
σ	5.683 m
Dc	4.8866
ρ (Σl/A) m	1.715 m/m^2

Fracture Network

Pa:0.5495, Pb: 0.2198, Px: 0.2306, n = 4.056

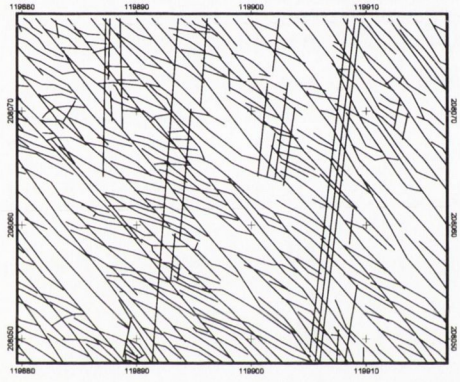

N	310
Σl	1844.66 m
χl	5.95 m
Median L	3.98 m
σ	6.16 m
Dc	4.73
ρ (Σl/A) m	2.05 m/m^2
$\%\Sigma l_{FN}$	89.589

Spanning Cluster

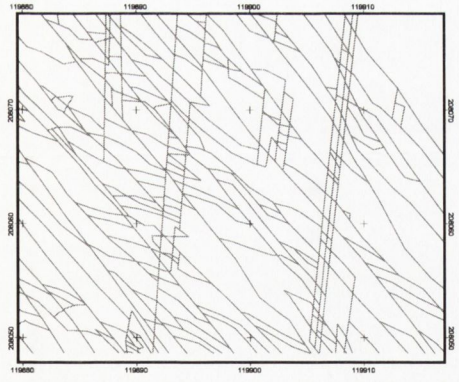

N	779
Σl	1291.814m
χl	1.6583m
Median L	1.141m
σ	1.738m
Dc	0.936
ρ (Σl/A) m	1.435 m/m^2
$\%\Sigma l_{FN}$	70.03

Backbone

Figure 4.11: Fracture Network, Spanning Cluster and Backbone of loc. A7

N = number of fractures, Σl = sum of length of fractures, χl = mean length of fractures, σ = standard deviation, Dc = critical density, n = connectivity, ρ (Σl/A) = density, $\%\Sigma l_{FN}$ = length of system expressed as a percentage of the fracture network. Pa/b/c = proportion of abutment/blind/cross termination.

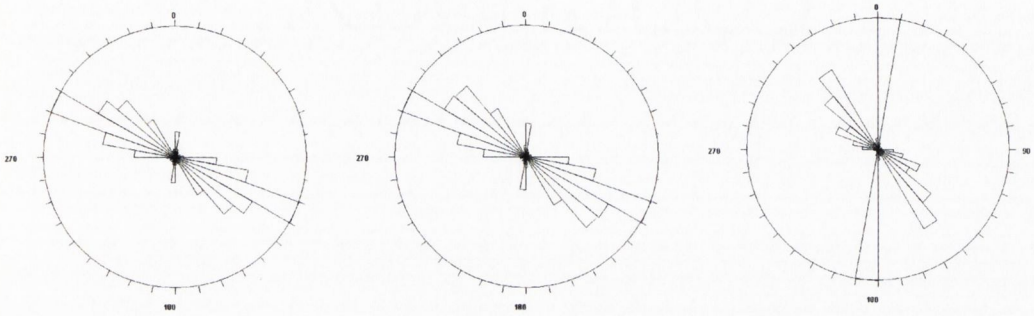

a) Rose diagram of the orientation of the fracture network of loc: A7.

b) Rose diagram of the orientation of the spanning cluster of loc: A7.

c) Rose diagram of the orientation of the fracture backbone of loc: A7.

Fig 4.12: Rose diagrams illustrating the frequency of the different orientation

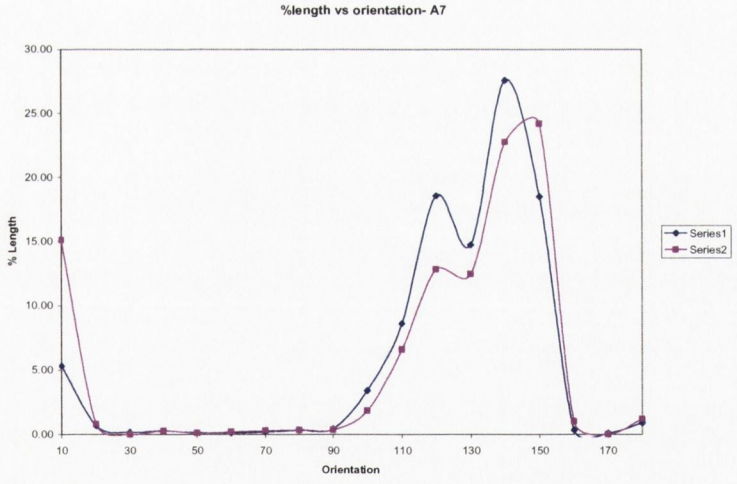

Fig: 4.13 Comparison of % of total length versus orientation for the fracture network (series 1), the spanning cluster (series 2) and the backbone (series 3)

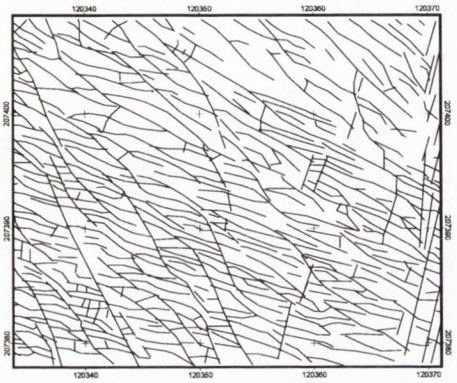

N	468
Σl	1772.425 m
χl	3.787 m
Median L	2.796 m
σ	3.25 m
Dc	2.4262
ρ (Σl/A) m	1.47 m/m^2

Fracture network

Pa: 0.5596, Pb: 0.3604, Px: 0.0799 n = 2.458

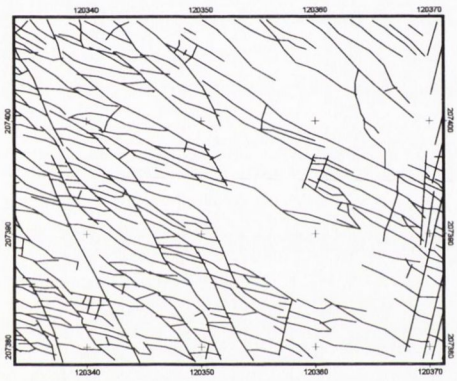

N	802
Σl	1233.083 m
χl	1.53751 m
Median L	0.993 m
σ	1.673 m
Dc	0.862
ρ (Σl/A) m	1.37 m/m^2
$\%\Sigma l_{FN}$	69.57

Spanning Cluster

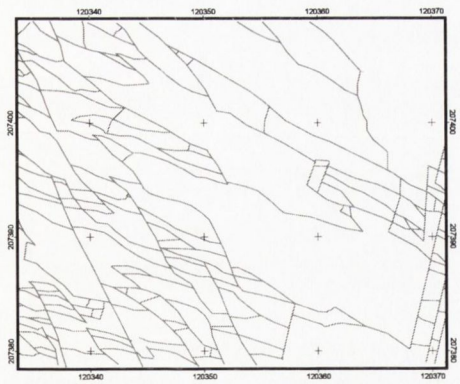

N	514
Σl	868.845 m
χl	1.69 m
Median L	1.211 m
σ	1.534 m
D	0.557
ρ (Σl/A) m	0.9653 m/m^2
$\%\Sigma l_{FN}$	49.02

Backbone

Figure 4.14: Fracture Network, Spanning Cluster and Backbone of loc. B11

N = number of fractures, Σl = sum of length of fractures, χl = mean length of fractures, σ = standard deviation, Dc = critical density, n = connectivity, ρ (Σl/A) = density, $\%\Sigma l_{FN}$ = length of system expressed as a percentage of the fracture network. Pa/b/c = proportion of abutment/blind/cross termination.

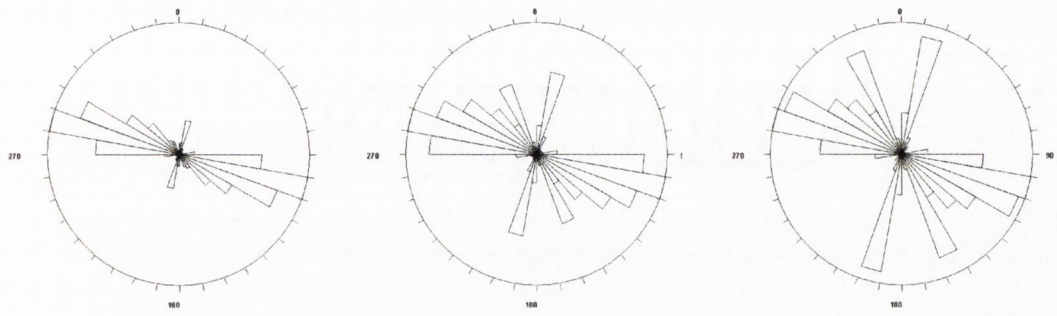

a) Rose diagram of the orientation of the fracture network of loc: B11.

b) Rose diagram of the orientation of the spanning cluster of loc: B11

c) Rose diagram of the orientation of the fracture backbone of loc: B11.

Fig 4.15 Rose diagrams illustrating the frequency of the different orientations.

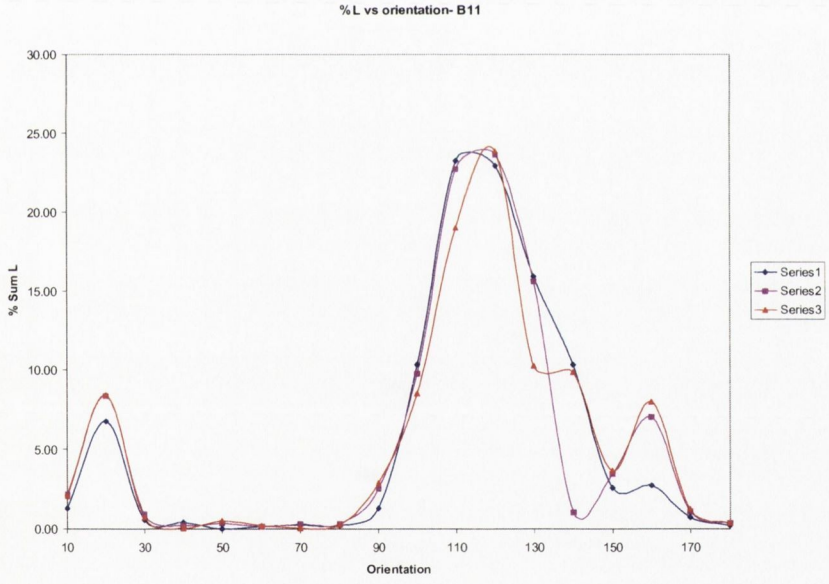

Fig: 4.16 Comparison of % of total length versus orientation for the fracture network (series 1), the spanning cluster (series 2) and the backbone (series 3)

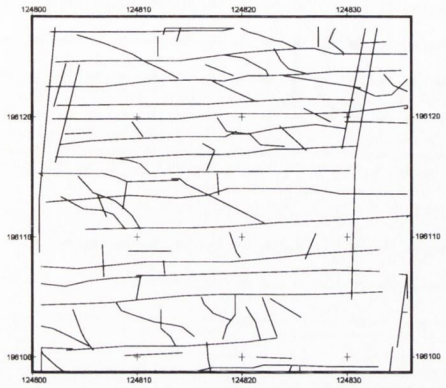

N	101
Σl	679.144 m
χl	6.724198 m
Median L	3.2085 m
σ	8.2636 m
Dc	3.1542
ρ (Σl/A) m	0.755 m/m^2

Fracture network

Pa: 0.56 Pb:0.22:Px: 0.22 n = 3.96

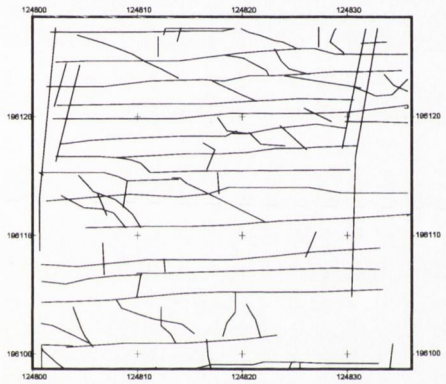

N	85
Σl	639.342 m
χl	7.52 m
Median L	3.676 m
σ	3.76 m
Dc	3.12
ρ (Σl/A) m	0.71 m/m^2
%Σl_{FN}	94.14

Spanning Cluster

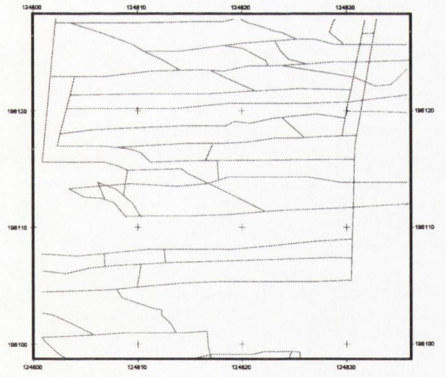

N	145
Σl	518.762 m
χl	3.577 m
Median L	2.265 m
σ	3.823
Dc	1.1
ρ (Σl/A) m	0.576 m/m^2
%Σl_{FN}	76.38

Backbone

Figure 4.17 Fracture Network, Spanning Cluster and Backbone of loc. SM134B1

N = number of fractures, Σl = sum of length of fractures, χl = mean length of fractures, σ = standard deviation, Dc = critical density, n = connectivity, ρ (Σl/A) = density, %Σl_{FN} = length of system expressed as a percentage of the fracture network. Pa/b/c = proportion of abutment/blind/cross termination.

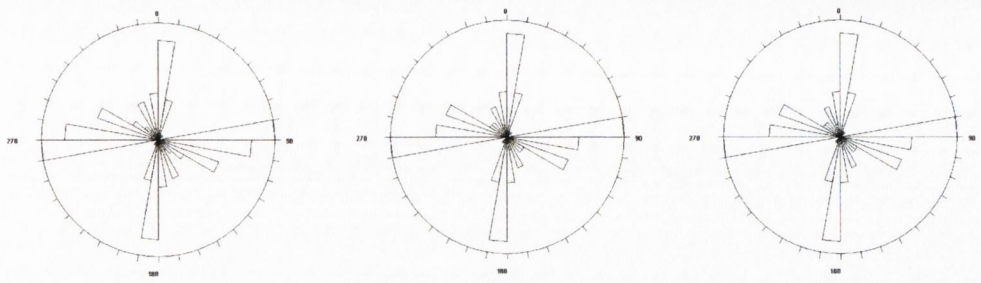

a) Rose diagram of the orientation of the fracture network of loc: sm134b1

b) Rose diagram of the orientation of the spanning cluster of loc: sm134b1

c) Rose diagram of the orientation of the fracture backbone of loc: sm134b1

Fig 4.18: Rose diagrams illustrating the frequency of the different orientations.

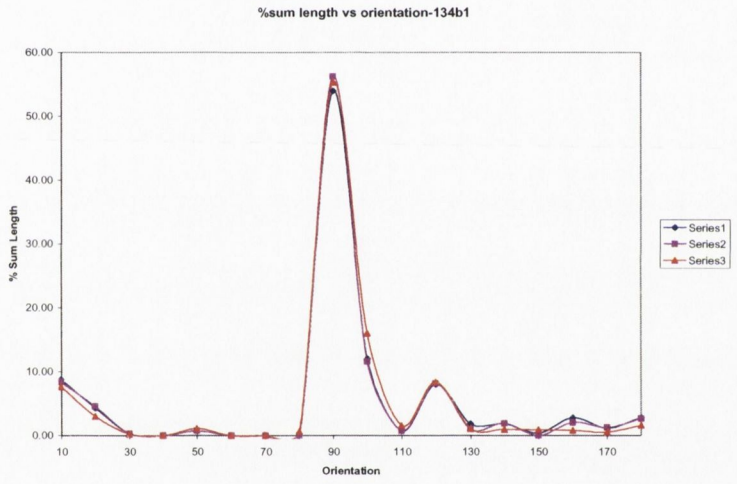

Fig: 4.19 Comparison of % of total length versus orientation for the fracture network (series 1), the spanning cluster (series 2) and the backbone (series 3)

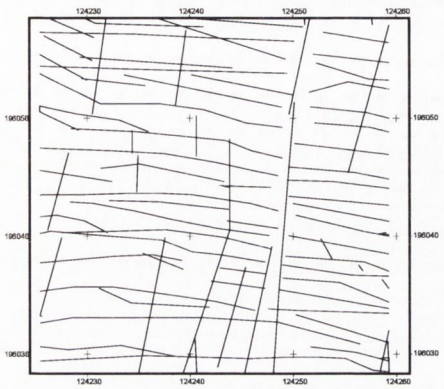

Fracture Network

N	96
Σl	783.175 m
χl	8.158 m
Median L	6.788 m
σ	6.630 m
Dc	2.937
ρ ($\Sigma l/A$) m	0.871 m/m^2

Pa:0.29: Pb: 0.34 Px: 0.37 N=4.166

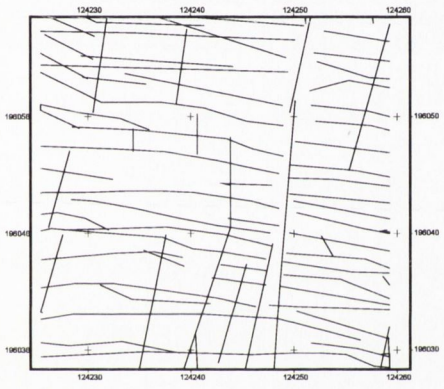

Spanning Cluster

N	91
Σl	749.716 m
χl	8.23 m
Median L	6.788 m
σ	6.73 m
Dc	2.85
ρ ($\Sigma l/A$) m	0.833 m/m^2
$\%\Sigma l_{FN}$	95.72

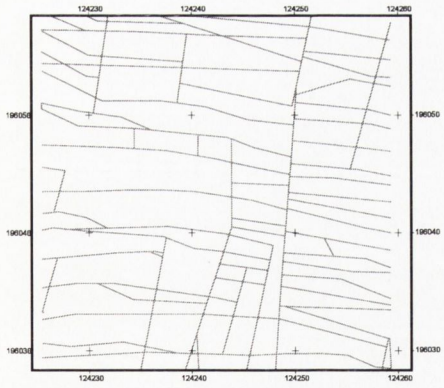

Backbone

N	200
Σl	679.757 m
χl	3.398 m
Median L	2.211 m
σ	3.024 m
Dc	1.147
ρ ($\Sigma l/A$) m	0.755 m/m^2
$\%\Sigma l_{FN}$	86.795

Figure 4.20: Fracture Network, Spanning Cluster and Backbone of loc. SMB7

N = number of fractures, Σl = sum of length of fractures, χl = mean length of fractures, σ = standard deviation, Dc = critical density, n = connectivity, ρ ($\Sigma l/A$) = density, $\%\Sigma l_{FN}$ = length of system expressed as a percentage of the fracture network. Pa/b/c = proportion of abutment/blind/cross termination.

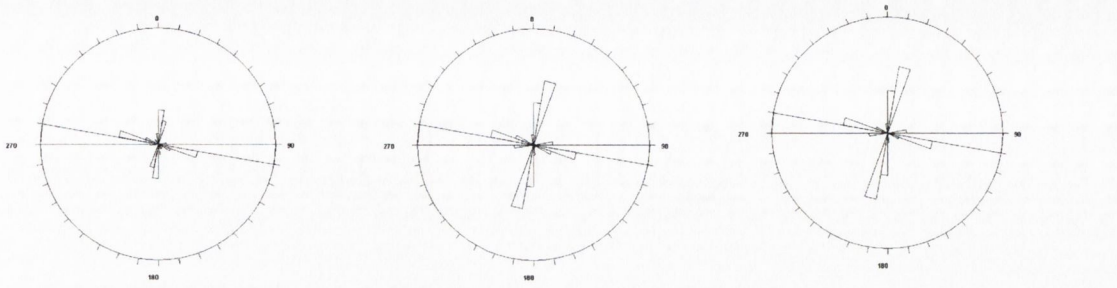

a) Rose diagram of the orientation of the fracture network of loc: smb7

b) Rose diagram of the orientation of the spanning cluster of loc: smb7

c) Rose diagram of the orientation of the fracture backbone of loc: smb7

Fig 4.21: Rose diagrams illustrating the frequency of the different orientations.

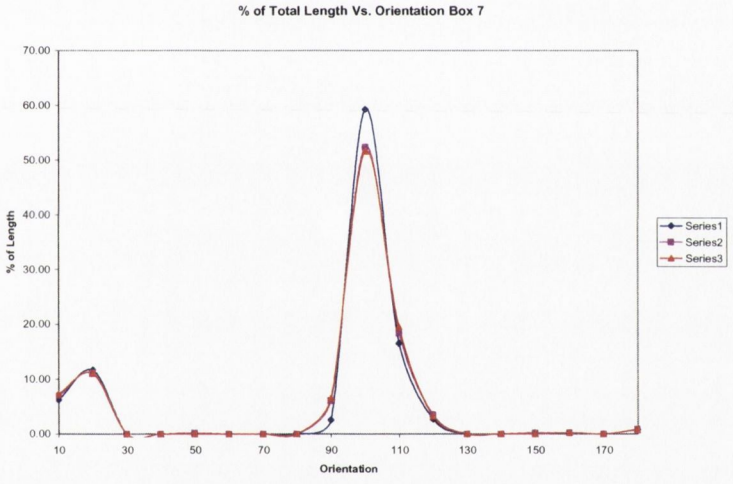

Fig: 4.22 Comparison of % of total length versus orientation for the fracture network (series 1), the spanning cluster (series 2) and the backbone (series 3)

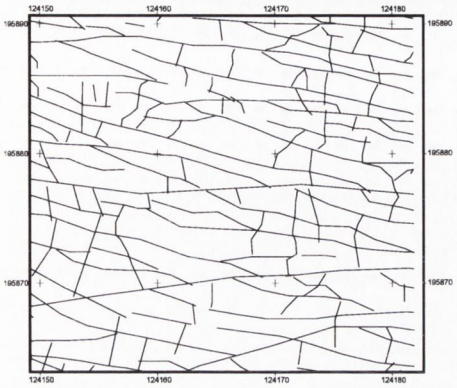

Fracture Network

N	156
Σl	832.31 m
χl	5.33 m
Median L	2.984 m
σ	6.119 m
Dc	2.845
ρ ($\Sigma l/A$) m	0.925 m / m^2

Pa: 0.665 Pb: 0.205 Px::0.13 N= 3.645

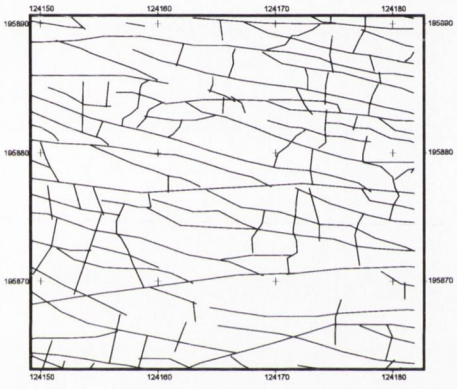

Spanning cluster

N	125
Σl	761.209 m
χl	6.089 m
Median L	3.737 m
σ	6.52 m
Dc	1.201
ρ ($\Sigma l/A$) m	0.846 m / m^2
$\%\Sigma l_{FN}$	92.14

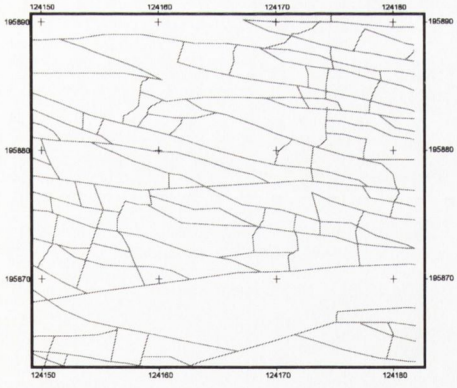

Backbone

N	236
Σl	614.97 m
χl	2.6058 m
Median L	1.850 m
σ	2.350 m
Dc	.806
ρ ($\Sigma l/A$) m	0.6833 m / m^2
$\%\Sigma l_{FN}$	73.88

Figure 4.23: Fracture Network, Spanning Cluster and Backbone of loc. SMB9

N = number of fractures, Σl = sum of length of fractures, χl = mean length of fractures, σ = standard deviation, Dc = critical density, n = connectivity, ρ ($\Sigma l/A$) = density, $\%\Sigma l_{FN}$ = length of system expressed as a percentage of the fracture network. Pa/b/c = proportion of abutment/blind/cross termination.

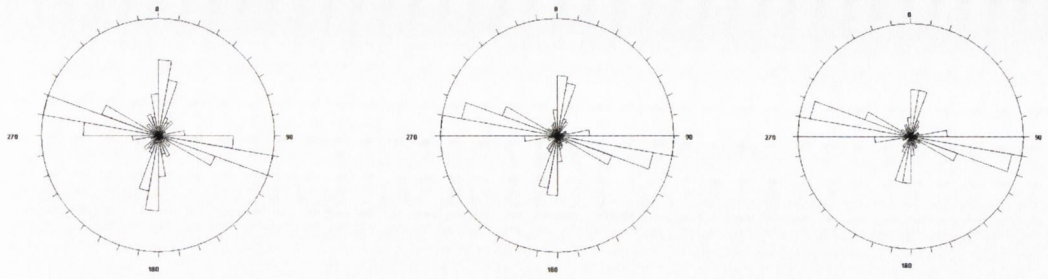

a) Rose diagram of the orientation of the fracture network of loc: smb9

b) Rose diagram of the orientation of the spanning cluster of loc: smb9

c) Rose diagram of the orientation of the fracture backbone of loc: smb9

Fig 4.24: Rose diagrams illustrating the frequency of the different orientations.

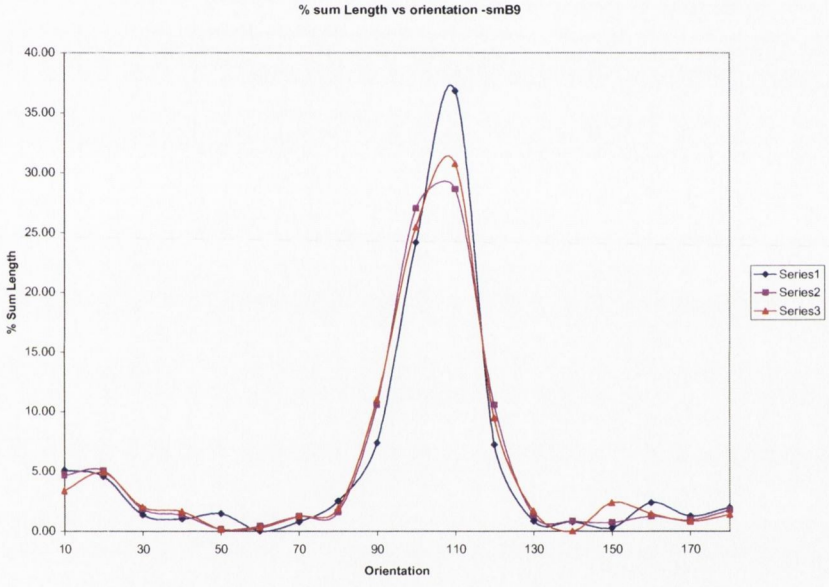

Fig: 4.25 Comparison of % of total length versus orientation for the fracture network (series 1), the spanning cluster (series 2) and the backbone (series 3)

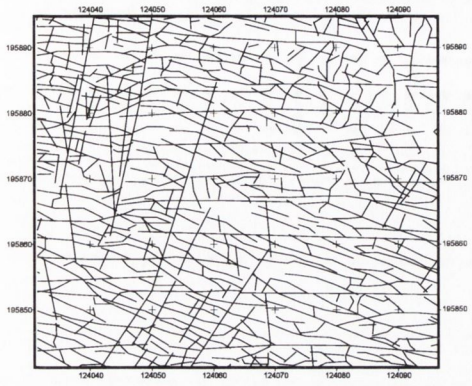

N	570
Σl	3535.386 m
χl	6.202 m
Median L	4.184 m
σ	6.715 m
Dc	3.3047 m
ρ (Σl/A) m	0.982 m / m^2

Fracture Network Pa: 0.4712, Pb: 0.1852, Px: 0.3464 n = 5

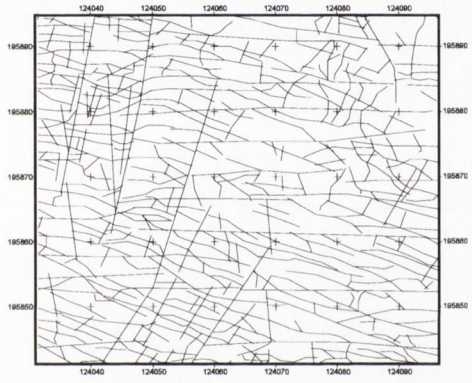

N	450
Σl	3216.941 m
χl	7.1487 m
Median L	4.917 m
σ	7.1912 m
Dc	3.21
ρ (Σl/A) m	0.8935 m / m^2
$\%\Sigma l_{FN}$	90.99

Spanning Cluster

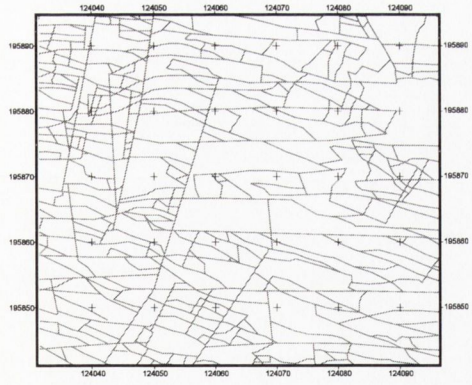

N	1098
Σl	2602.383 m
χl	2.3701 m
Median L	1.742 m
σ	2.267 m
Dc	0.82
ρ (Σl/A) m	0.7228 m / m^2
$\%\Sigma l_{FN}$	73.609

Backbone

Figure 4.26: Fracture Network, Spanning Cluster and Backbone of loc. SMF1

N = number of fractures, Σl = sum of length of fractures, χl = mean length of fractures, σ = standard deviation, Dc = critical density, n = connectivity, ρ (Σl/A) = density, $\%\Sigma l_{FN}$ = length of system expressed as a percentage of the fracture network. Pa/b/c = proportion of abutment/blind/cross termination.

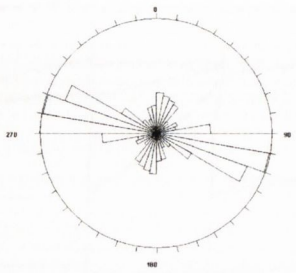

a) Rose diagram of the orientation of the fracture network of loc: smfrac1

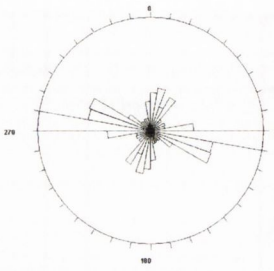

b) Rose diagram of the orientation of the spanning cluster of loc: smfeac1

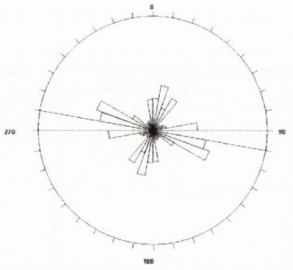

c) Rose diagram of the orientation of the fracture backbone of loc: smfrac1

Fig 4.27: Rose diagrams illustrating the frequency of the different orientations.

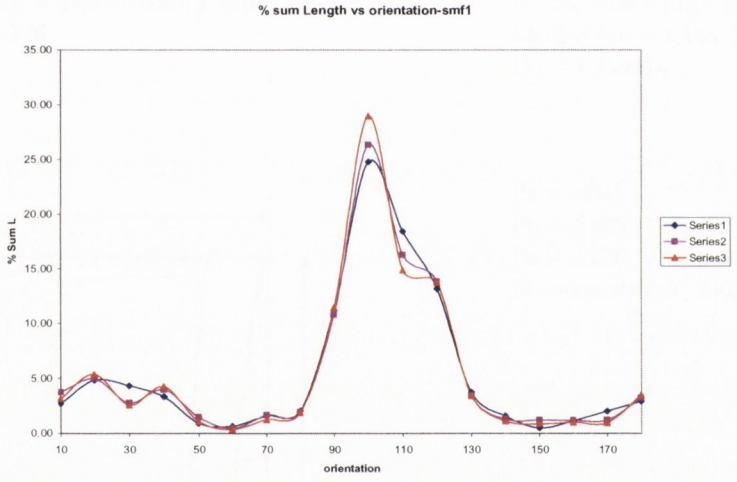

Fig: 4.28 Comparison of % of total length versus orientation for the fracture network (series 1), the spanning cluster (series 2) and the backbone (series 3)

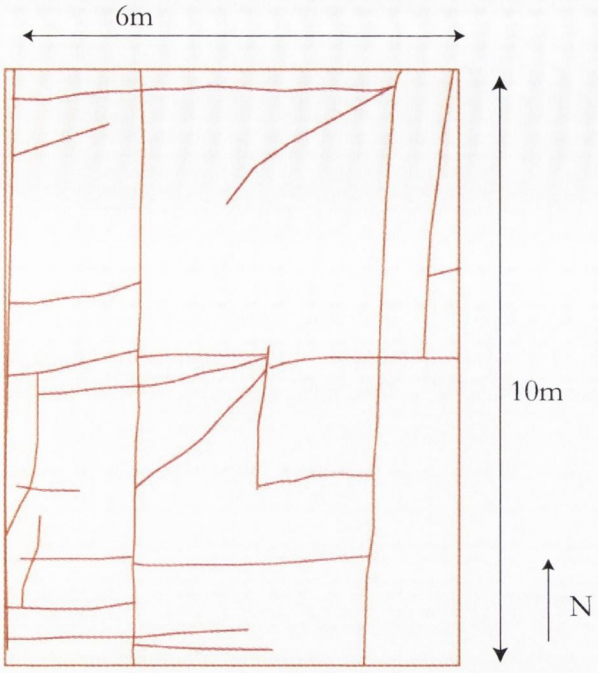

Cathair Comhain Fracture Pattern
n= 23, Sum L (m) = 84.645 Mean L (m)= 3.68
Median (m) = 2.278
Dc = 1.759314

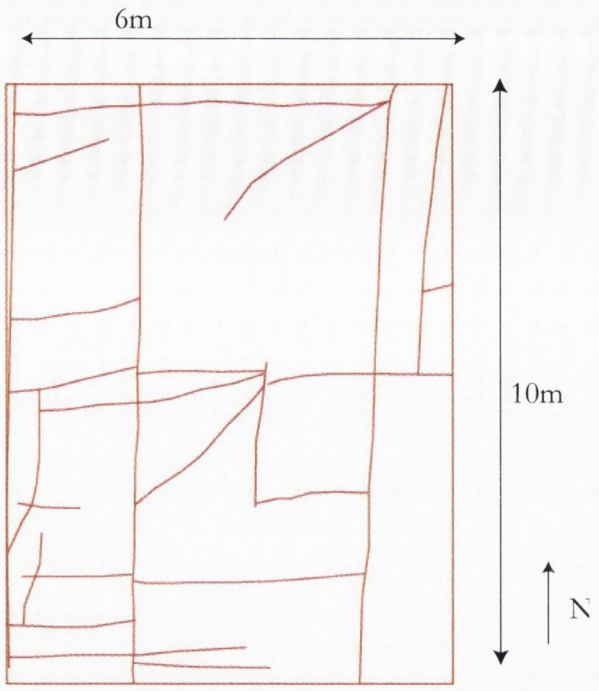

Cathair Comhain Spanning Cluster
n= 65, Sum L (m)= 84.639 Mean L (m)= 1.3021
Median (m) = 1.156, ΣL= 99.99%
Dc = 1.759314

Pa = .4893
Pb = .3829
Px = .1276
N connectivity = 2.829

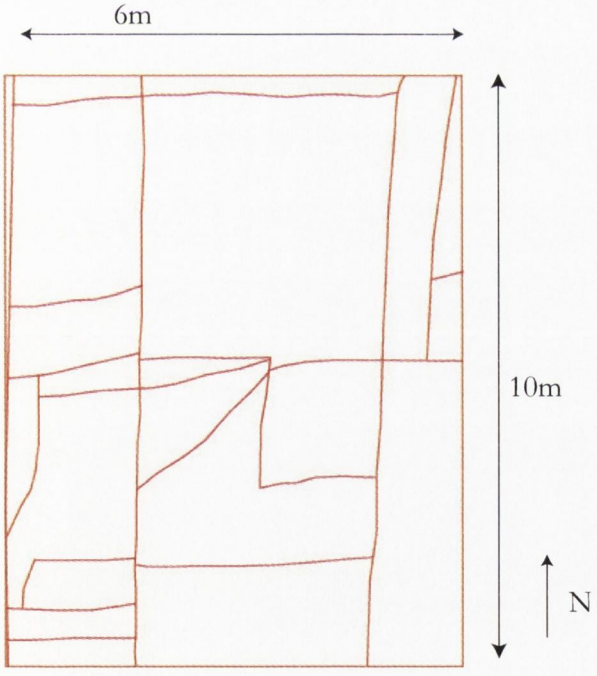

Cathair Comhain Backbone
n= 54, Sum L (m) = 73.791 Mean L (m)= 1.3665
Median (m)= 1.172, ΣL= 87.18%
Dc = 0.5777

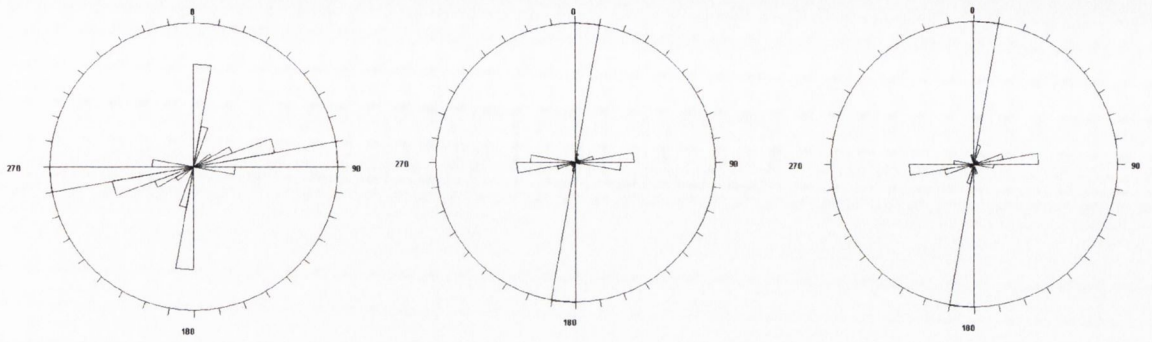

a) Rose diagram of the orientation of the fracture network of loc: CC.

b) Rose diagram of the orientation of the spanning cluster of loc: CC

c) Rose diagram of the orientation of the fracture backbone of loc: CC

Fig 4.30 Rose diagrams illustrating the frequency of the different orientations.

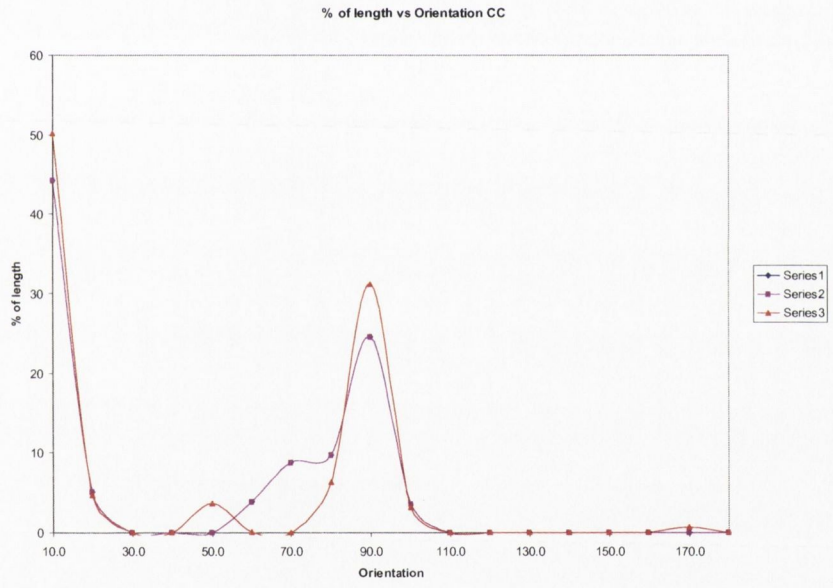

Fig: 4.31 Comparison of % of total length versus orientation for the fracture network (series 1), the spanning cluster (series 2) and the backbone (series 3)

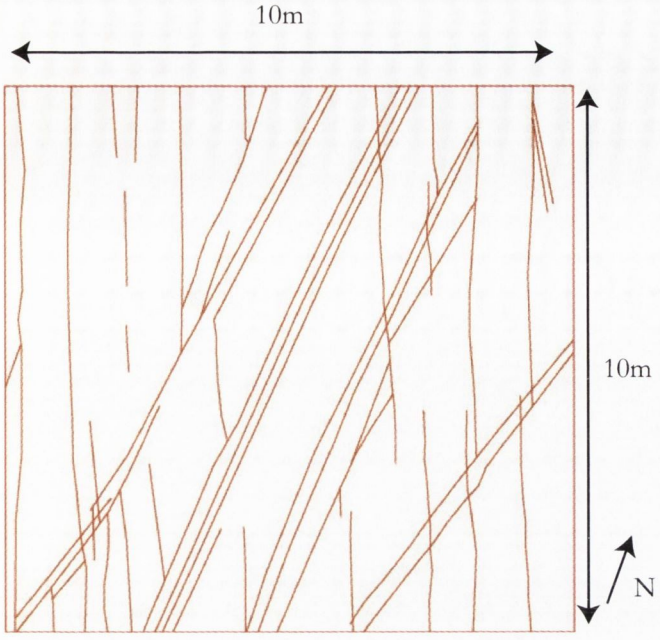

Gleninagh Fracture Pattern
n= 47, Sum L (m) = 198.802 Mean L (m)= 4.23
Median (m) = 2.573
Dc = 3.355

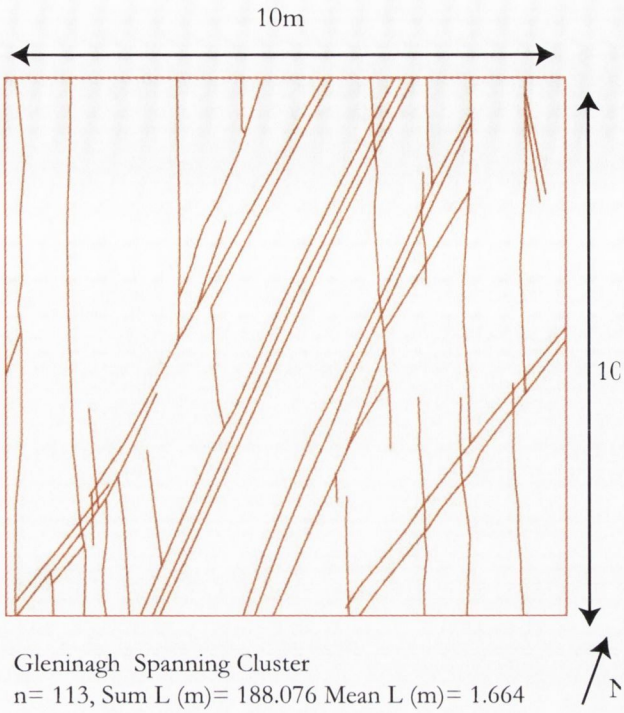

Gleninagh Spanning Cluster
n= 113, Sum L (m)= 188.076 Mean L (m)= 1.664
Median (m) = 1.013 ΣL= 94.6%
Dc = 1.8069

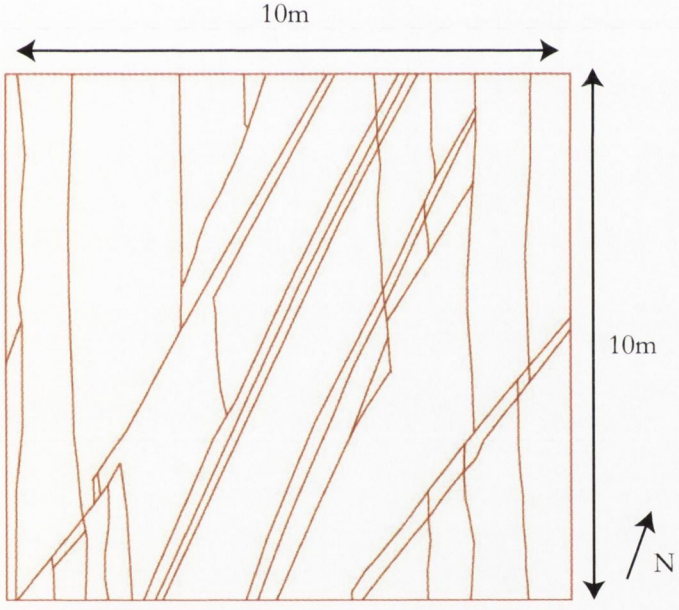

Area 100m2
Pa = .2666
Pb = .3466
Px = .3866
N connectivity = 2.419

Gleninagh Backbone
n= 94, Sum L (m) = 168.805 Mean L (m)= 1.795
Median (m)= 1.013 ΣL= 89.75%
Dc = 1.7335

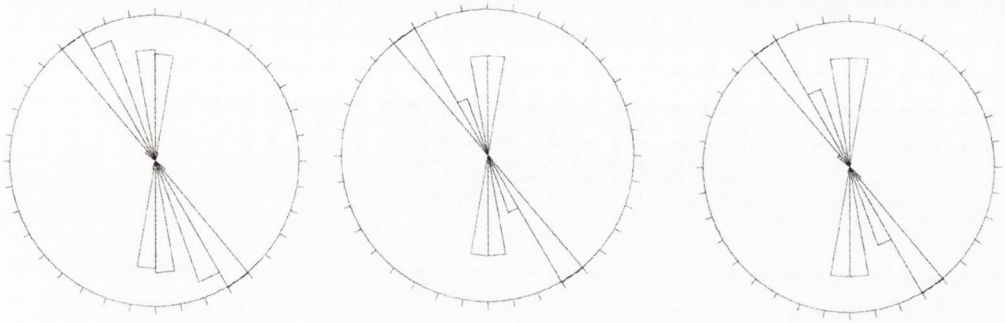

a) Rose diagram of the orientation of the fracture network of loc: Gleninagh

b) Rose diagram of the orientation of the spanning cluster of loc: Gleninagh

c) Rose diagram of the orientation of the fracture backbone of loc: Gleninagh

Fig: 4.33 Rose diagrams illustrating the frequency of the different orientations.

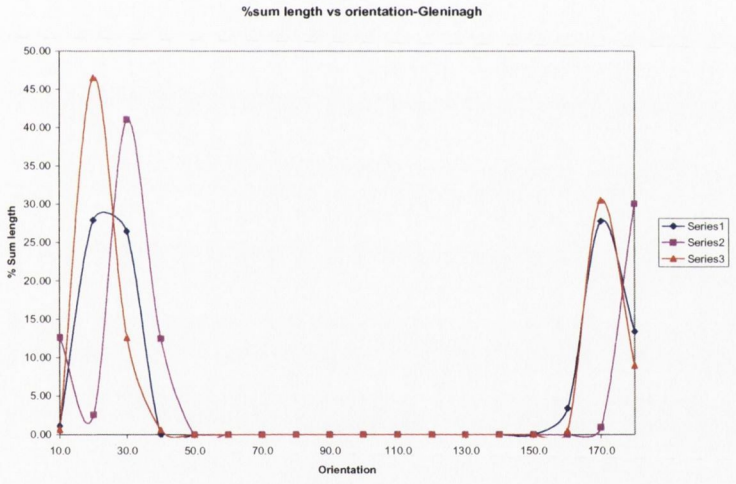

Fig: 4.34 Comparison of % of total length versus orientation for the fracture network (series 1), the spanning cluster (series 2) and the backbone (series 3)

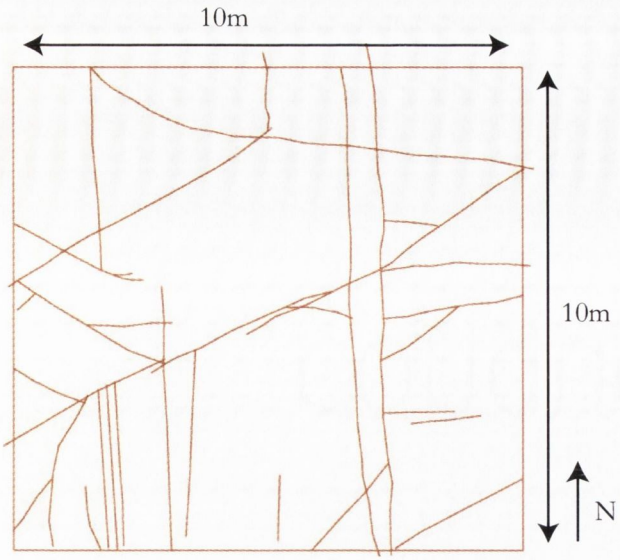

Oughtdarra1 Fracture Pattern
n= 33, Sum L (m) = 111.333 Mean L (m)= 3.373
Median (m) = 2.878
Dc = 1.465

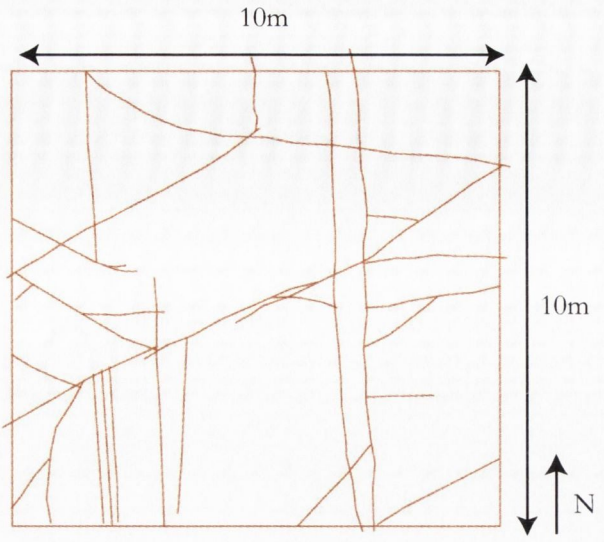

Oughtdarra1 Spanning Cluster
n= 83, Sum L (m)= 109.518 Mean L (m)= 1.319
Median (m) = 1.084 ΣL= 98.4%
Dc = 0.5987

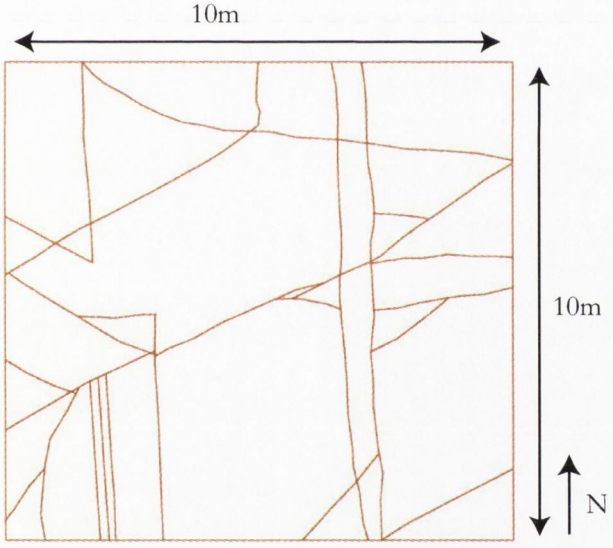

Area 100m2
Pa = .3684
Pb = .4736
Px = .1578
N connectivity = 2.5

Oughtdarra1 Backbone
n= 70, Sum L (m) = 98.685 Mean L (m)= 1.4097
Median (m)= 1.150ΣL= 90.1%
Dc = 0.5436

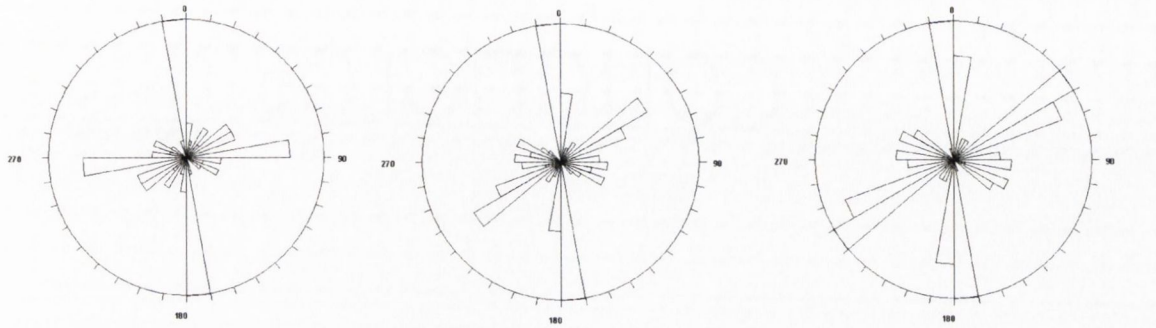

a) Rose diagram of the orientation of the fracture network of loc: Ought1

b) Rose diagram of the orientation of the spanning cluster of loc: Ought1

c) Rose diagram of the orientation of the fracture backbone of loc: Ought1

Fig 4.36: Rose diagrams illustrating the frequency of the different orientations.

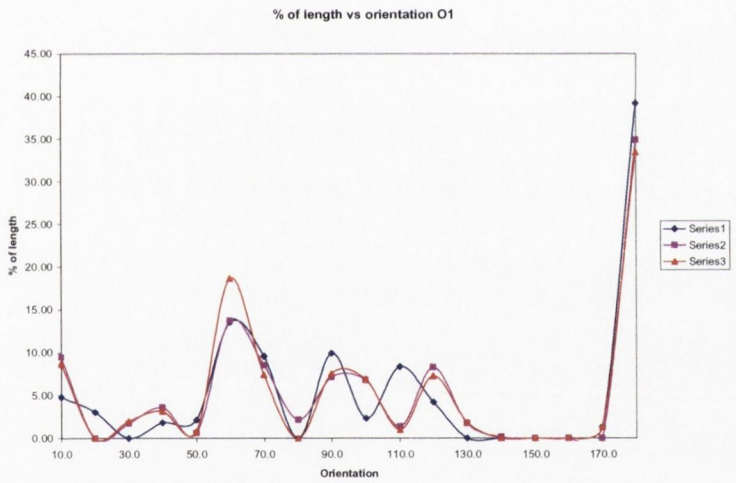

Fig: 4.37 comparison of % of total length versus orientation for the fracture network (series 1), the spanning cluster (series 2) and the backbone (series 3)

CHAPTER 5 REMOTE SENSING

5.1 Introduction to Remote Sensing

Remote sensing is the science and technique of gathering data and obtaining information about an object, area or phenomena with out being in direct contact with that object, area or phenomena by detecting and measuring the electromagnetic spectrum. Remote sensing detects and measures the phenomena with instruments sensitive to the electromagnetic spectrum such as visible light –cameras and scanners, infra red-thermal scanners and radio waves-radar

5.2 Imagery

The main sections of this chapter are concerned with the analysis of

- SAR imagery
- Aerial Photographs at a scale of 1:48,000 and 1:3,000

5.2.1 SAR

Synthetic Aperture Radar (SAR) is a radar system in which the antenna is aligned parallel to the motion of the satellite projecting radiation at right angles to the flight path and detects the backscattered radar reflections from the ground surface in order to produce a radar image of the ground. SAR is an active sensor in that it provides its own source of illumination in the form of radar signals, as result of this imagery can be obtained during the day or during the night. Due to the longer wavelength of Radar (RAdio Detection And Ranging) than visible light, it is relatively undistorted by cloud coverage, SAR and other Radar based remote sending devices such as Side Looking Airborne Radar (SLAR) are used to obtain imagery from cloud covered areas. A SAR device hosted by European Remote Sensing Satellite 1 (ERS-1) operated by the European Space Agency (ESA) collected the images that were analysed. The ERS-1 was launched on the 7th of July 1991; it has been superseded by ERS-2 launched on the 21st of April 1995. The ERS-1 was launched into an 800km at a 98° inclination orbit. The European Remote Sensing satellite Synthetic Aperture Radar uses C Band 5.66cm radar wavelength to compile their images. Radar can be divided into several different categories according to the wavelength of the radar -the different bands are L, S, C, X, K. (Figure 5.1 shows the location of Band C in the electromagnetic spectrum). Below is a brief description of each radar band.

- **L band radars** operate on a wavelength of 15-30cm and a frequency of 1-2GHz.
- **S band radars** operate on a wavelength of 8-15cm and a frequency of 2-4GHz. Due to the wavelength and frequency, S band radars are not easily attenuated. S band radar devices require a large antenna dish and a large motor to power it.
- **C band radars** operate on a wavelength of 4-8cm and a frequency of 4-8GHz. Due to the wavelength and frequency, the dish size does not need to be very large, an important feature in terms of the design and cost of a satellite system. The signal is more easily attenuated than an S or

L band radar device. The frequency allows C band radars to create a smaller beam width using a smaller dish.

- **X band radars** operate on a wavelength of 2.5-4cm and a frequency of 8-12GHz. Due to the smaller wavelength, the X band radar is more sensitive and can detect smaller particles; as a result X band radars are used for studies on cloud development because they can detect the tiny water particles. X band radars are easily attenuated.

- **K band radars** operate on a wavelength of .75-1.2cm or 1.7-2.5cm and a corresponding frequency of 27-40GHz and 12-18GHz. Due to the high degree of sensitivity of K band radar they are commonly used to record speed by law enforcement agencies.

Band C is commonly used by Remote sensing devices due to it economical size and the high quality of data produced. Synthetic aperture refers to the distance the satellite travels while synthesising the data, this system utilises the motion of the satellite to simulate a larger antenna, the ESR-1 satellite travels approximately 4 kilometres while an object is "within sight" of the radar, allowing the 10 metre by 1 metre antenna to act as a 4 kilometre long stationary antenna. The larger the antenna the more information that can be obtained about a particular object.

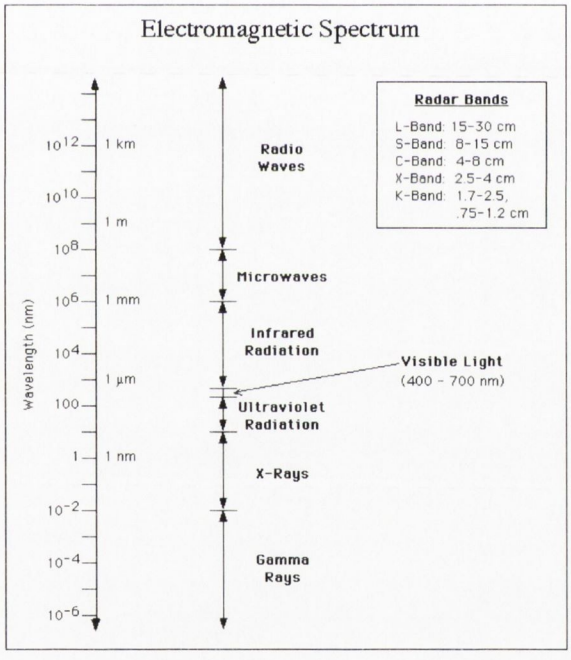

Figure 5.1 The Electromagnetic Spectrum.

The SAR images used for this study were taken of the South Galway-North Clare region on four occasions over am period of five months from November 1st 1994 to the 30th of March 1995 under a project co-ordinated by the Office of Public Works entitled "An investigation of the flooding in the Gort-Adrahan Area of South Galway". The four images used are listed below and the location and extent of the images are shown in Figure.5.2

Image	Date
ERS 527	1/11/94
ERS 522	8/12/94
ERS 532	14/1/95
ERS 524	30/3/95

Table 5.1 SAR images used.

5.2.2 Aerial Photography

Aerial Photography is the oldest form of remote sensing dating back to 1858 when Gaspard-Felix Tournachon took photographs of Paris from a rising balloon. Since that time aerial photography has expanded to become an invaluable tool for remote sensing. A specialised camera mounted onto an aircraft or satellite takes aerial photographs. The photographs are taken in "runs" in the direction of flight of the aircraft in such a way that there is approximately 60% overlap, in order to enable stereoscopic vision, between adjacent photographs. The aerial photographs examined are vertical photos, in that the airborne camera was pointing vertically downwards. While maps and aerial photographs both present a vertical representative section of the surface of the Earth it should be noted that a map is an orthogonal representation of the Earths surface, while aerial photographs display radial distortion, with the edges distorted to a degree with only the central section truly representative of the surface. This factor needs to be taken into account when analysing aerial photographs, until the distortion of the photograph is corrected measurements taken from aerial photographs are not accurate.

The advantages of aerial photographs over field-based surveys, are many, the main factors are listed below

- They offer an improved vantage point
- Provides data from locations that my be inaccessible or difficult to access e.g. islands
- Provide a current pictorial view of the ground, facilitating comparison with previous or future images of the same area.
- They are a permanent recording.
- They are both a time and cost effective way of studying a large area. An aerial photograph interpreter can record a wide range of information from the photographs in a short period of time.
- They are useful in identifying key target areas for field study.
- Broadened spectral sensitivity

While there are many advantages, there are a number of factors one must realise prior to using aerial photographs many of which are easily rectifiable

- The scale of the image needs to be calculated
- In their basic form aerial photographs need some form of geometrical correction due to radial distortion

- As with all remote sensing data there is a need to ground truth – or reference features to those on the ground- the aerial photographs to ensure your data is of the highest quality and that features you have interpreted exist in the real world and are not an artefact of processing or a cultural feature that resembles a geological feature e.g. in lineament analysis depending on scale a fence, road/ trail or railway may appear as a lineament.

In this study two separate sets of aerial photographs were studied (see Figure 5.3 for location map). The first set were a series of 28 photographs consisting of three west to east runs

- 1) 6591-6584
- 2) 2326-2335
- 3) 6473-6480

These photographs are vertical black and white aerial photographs taken on 24th of June 1995 for runs 1 and 3 and on the 13th of June 1995 for run 2, at a scale of approximately 148,300 using a shutter speed of between 1/200 and 1/140 with an aperture of f/4.

The second set of aerial photographs consisted of sets of detailed vertical aerial photographs of two study areas in the Burren, Cappanawalla and Sheyshmore. The aerial photographs are black and white vertical aerial photographs at a scale of 1:3,000 taken from a height of 760m by BKS Surveys Ltd on the 11th of June 1994.

The Cappanawalla set consist of seven photographs taken in a NW-SE trending run

- Cap 19 088 to 19 094 –with 19 088 being the furthest north-west, Figure 5.4

The Sheyshmore set consist of seven photographs taken in a NW-SE trending run

- SM 19 133 to 19 139 –with 19 139 being the furthest west, Figure 5.4

These photographs were taken of areas of extensive exposure of limestone pavement where chemical solution has enhanced the visual signature of the fractures present.

5.3 Techniques

5.3.1 Rose Diagrams

Rose diagrams were used to display the orientation of the lineaments in the study areas. Rose diagrams are relative frequency circular histogram which display the orientation of the lineaments in 10 degree bins over 360°.

5.3.2 Relative Entropy (RE)

The degree of preferred orientation of a lineament data set can be quantified by a measure of its non randomness (Relative Entropy) (Dolan 1984). Relative Entropy is derived as follows.

$$RE\% = \left(\frac{-100 \sum_{i=1}^{k} [n_i - \log(n_i)]}{\log(K)} \right) \qquad \text{Equation 5.1}$$

Where

n_i = frequency of samples in each class

K = number of classes = 180°/ class interval

If RE = 100, the lineaments exhibit a perfectly uniform distribution of data in all class intervals, therefore as RE tends towards 100 the data has a greater random distribution. Changes in Relative Entropy can be related to the development of fracture patterns associated with among others fracture networks, faults, shear zones and folding.

5.3.3 Fracture Density

Fracture density is derived by calculating the sum of the fracture intersections divided by the area of the cell. A high fracture density corresponds to a large number of fracture intersections, and by implication multiple fracture sets with differing orientations, as fracture sets with differing orientations, particularly those set at a high angle to each other have a greater likelihood of intersection. This can give a measure of the connectivity of a system as has been previously discussed in Chapter 4.

5.4 Lineament Analysis

5.4.1 Lineaments

Lineaments are naturally occurring alignments of soil tones, topography, stream channels, vegetation or combinations of these features that are visible on remotely sensed imagery and aerial photography. The main assumption inherent in performing any lineament analysis is that these alignments represent fracture zones or other discontinuities (faults, geological contacts), lineaments are considered to be surface (two dimensional) expressions of three dimension structures (Mollard 1957, Mabee 1995). It is presumed that the geomorphology observed on the imagery is due to differential weathering with the fracture zones and discontinuities being more susceptible to weathering than un-fractured rock (Mollard 1962). Structural lineaments such as fracture zones and faults may leave subtle topographic features visible as a lineament on remotely sensed imagery. In addition these structural lineaments may act as conduits for the movement of fluids and as a result can be detected on imagery by vegetation patterns. Remotely sensed images have the potential to contain non-structural lineaments such as cultural lineaments, i.e. fences, roads, railway lines, canals. The extent to which these cultural lineaments can influence subsequent lineament fracture maps and

the ease, which they can be identified, depends on the scale and resolution of the image being analysed. For example in the 1:3,000 scale aerial photographs being studied, fences and stone walls (cultural lineaments) occur as linear features which are easily identifiable given the high quality of the image and would not be included in a subsequent fracture map of the region. For the 1:48,000 aerial photographs cultural lineaments take the form of roads, electricity pylons and fences. The roads, field boundaries and pylons are readily identifiable when the image is compared to a map of the region, fences are more difficult to identify and remove from the subsequent lineament map. Cross checking with detailed six inch to the mile maps helps in identifying field boundaries and other cultural artefacts which have remained quite similar since 1923 when these detailed maps were last updated. The percentage of cultural lineaments in a lineament map can be function of the skill of the analyst and familiarity with the area under investigation, as well as the characteristics of cultural lineaments, transport links (roads and railway tracks) have a tendency to change direction, increase or decrease in size all of which act as indicators of their true nature. For the SAR images the resolution is not refined enough to pick out fences so roads, rivers and railway lines appear as cultural lineaments, again cross reference with a 1:50,000 scale Discovery series map from the Ordnance Survey of Ireland helps identify the location of these features and enables them to be deleted from the subsequent lineament map. The lineament maps are strongly controlled by the resolution of the images, the 1:3,000 aerial photographs are of a high resolution and minor joints are readily identifiable, with the 1:48,000 aerial photographs the resolution is not high enough identify the joints, for the SAR images individual fractures are difficult to identify and lineaments tend to consist of a zone of fractures rather than one individual entity.

A lineament data set consists of an array of spatially distributed lines each of which has the following characteristics orientation, length and position (Mabee 1995).

5.4.2 Methodology

The identification of lineaments is a subjective process, with the identification of lineaments from images being the product of the analyst recognising linear features from the image, which is down to the resolution of the image and the skill and experience of the analyst (Mabee 1995). In general a linear feature can show up on an image as a feature that is a) darker in the middle and lighter on both sides or b) is lighter on one side and darker on the other side. Processing of the image allows for algorithms to identify linear features in an effort to reduce the subjective nature of lineament capture.

The stages involved in the production of lineament maps from the data sources being studied can be depicted in the form of a generic flow chart involving 4 main steps.

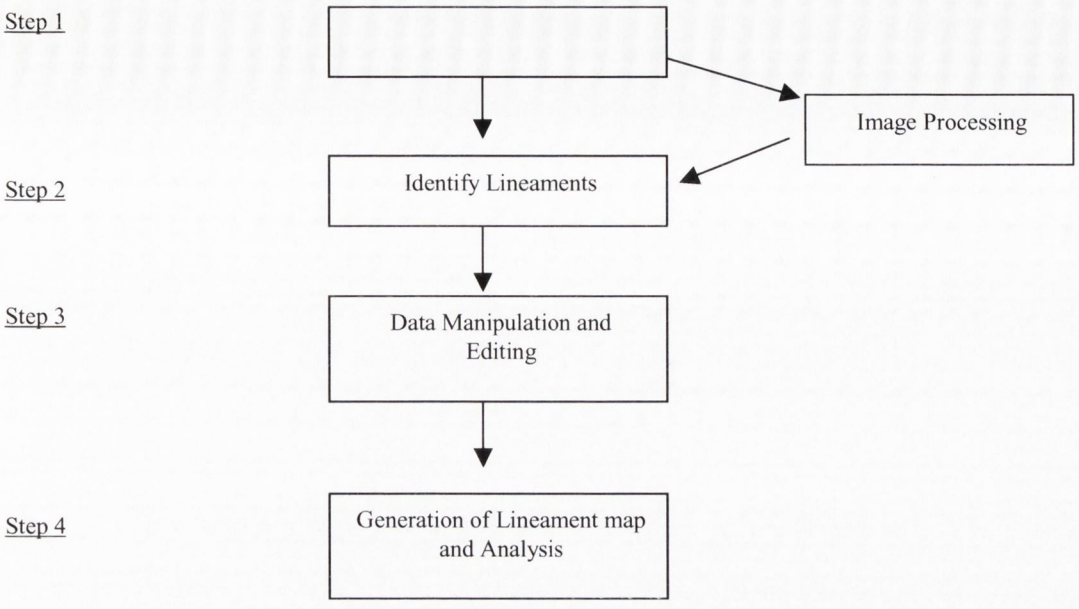

Figure 5.6 Flow chart for Lineament Analysis.

Step 1 Data Capture

The first step involves sourcing the data and processing the data in order to highlight any potential lineaments. In the case of the aerial photographs it involved scanning the photographs at a high resolution and then using ARC/INFO to geo-reference and correct the photographs for radial distortion to allow them to be viewed in their true coordinate system in a GIS package such as Arc View.

Step 2 Identify Lineaments

Chemical weathering, in the form of solution, of the limestone in the region is greatly enhanced along fractures producing grykes, which act to enhance the visual signature of the veins and joints in the region. For the 1:3,000 scale aerial photographs the fractures are easily identifiable due to the excellent exposure of the limestone pavement and the solution of the fractures. This enables detailed fracture maps with a ground resolution of about 5cm (Gillespie *et al* 2001) to be produced. For the 1:48,000 scale aerial photographs, there are a number of areas of good exposure in which the larger fractures have been enhanced due to chemical weathering and are readily apparent, else where in the images where the exposure is reduced it is possible to recognise lineaments based on topographic expressions and tonal differences in the photographs. It was necessary to visit these locations and ground truth the results in order to test the results obtained. For the 1:48,000 scale aerial photographs the lineaments were first delineated onto acetate overlays and the lineaments were digitised using the ARC INFO GIS package. With the SAR images, lineaments were identified through a combination of tonal differences in the images and through processing the images to enhance any linear features.

Step 3 Data Manipulation and Editing

Once the lineaments had been identified they were entered into a GIS (Arc View and Arc Info) in order that all the lineaments at different locations and scales can be compared to each other. Once the lineaments had been digitised it was necessary to perform a number of functions in order to assign topology to the

lineaments. Once inputted into a GIS package the lineaments were edited in ARC INFO using the build and clean commands. After the data had been edited it is available for presentation or for further data manipulation such as measuring Relative Entropy, Intersection Density (density of interesection of fractures) creation of rose diagrams and highlighting orientations coincident with regional and local scale topography,

Step 4 Generation of Lineament map and Analysis

Once that data has been edited it is now available for presentation and further analysis. The orientation of lineaments can be compared to that of fracture from the same location, similar to the process of domain overlap analysis described by Mabee *et al* (1994) which is equivalent of the ground truthing practice of visiting specific field locations to describe the local fracture pattern and lineament patterns can be compared to know fracture orientations.

5.4.3 Data validation / Ground truthing

Ground truth data collection is a vital part of any remote sensing effort as it acts as a validation of the remotely sensed lineaments. From the aerial photographs a map of the exposure in the region was created this in turn was cross-referenced with a series of field sheets of the region from the Geological Survey of Ireland (GSI). The purpose of this was to identify a series of locations where lineaments identified from the aerial photographs analysis would be exposed. A total of 6 locations were identified, 4 in relation to the 1:48,000 aerial photographs, 3 on the Gort Lowlands and 1 on the Burren, and 2 in relation to the 1:3,000 scale aerial photographs (Figure 5.7). The locations were selected in order to confirm the presence of specific fracture sets as outlined in Table 5.2

Location	Reason
Kinvarra,	WNW-ESE lineament set identified to be at this location, coincident with a series of karstic features. Fractures of this orientation predicted from the termination of the Fergus Shear Zone.
Lough Coole,	Multiple lineaments sets identified at this location. Located within the mapped extent of the Fergus shear Zone
Lough Bunny	Multiple lineaments sets identified at this location. Located within the mapped extent of the Fergus shear Zone
Slieve Carran	Outside the mapped extent of the Fergus Shear Zone on the Burren plateau. NS orientated lineaments identified at this location and in adjacent areas.
Cappanawalla	NNE clustered fractures and regularly spaced NW-SE joints identified. Site visited to investigate the interactions between the fractures.
Sheyshmore	NNE clustered fractures and regularly spaced EW joints identified. Site visited to investigate the interactions between the fractures.

Table 5.2: Locations, and rational for visiting, for ground truthing

The first 4 sites were visited in spring and summer 1997 with the latter 2 sites being visited in autumn 1999. At each location the local fracture pattern was mapped and subsequently compared to the remotely sensed derived lineament pattern of the area. The result of the field visits was to validate the orientation of the lineaments derived from the analysis of the aerial photographs, thereby giving confidence in the subsequent analysis of the lineament patterns.

5.5 Analysis

The northern extent of the Fergus Shear Zone was examined using a series of remotely sensed images Synthetic Aperture Radar (SAR) images and Aerial photographs. Lineaments identified from the SAR (Figure 5.8) and Aerial Photographs (Figure 5.9) show the Fergus Shear Zone as a region with a complex fracture pattern. Both images overlap onto the Burren where the fracture pattern is more ordered; the NNE trending veins are the dominant feature observed. The lineaments derived from analysis of the SAR image show that the area that corresponds to the Fergus Shear Zone/Gort Lowlands is a zone of lineaments with a more variable orientation, to the west in the area that corresponds to the Burren the lineament pattern appears to have a more consistent orientation. The primary use of the SAR images in this study was to identify the low-lying land that was subjected to the flooding events that were mentioned in the Introduction. This data was used to generate the depression/Turlough coverage seen on Figure 2. 7. The analysis of lineaments was a secondary aspect to the images. The lineaments derived from the aerial photographs show, in agreement with the SAR images a zone of high fracture density and multiple orientations in the Fergus Shear Zone region. The principal advantage to the use and analysis of this image type over the SAR images is that they can be "ground truthed". The aerial photographs cover the eastern part of the Burren and the regionally dominant NNE trending vein set can be see along the eastern margin of the Burren. In addition to the NNE fracture set present a set of NE-SE fractures are visible towards the middle left and bottom left. This area corresponds to the Oughtdarra (4.5.11) area, which was described in Chapter 4. These NE-SE fractures parallel the axis of folds in the region. A visual inspection of the Gort Lowlands part of Figure 5.9, middle right, and shows a number of fracture sets of variable orientation. The fractures derived from the aerial photographs were divided into 2km grids and a series of ten degree bin rose diagrams were created- using 1km overlapping grids (Figure 5.10). The rose diagrams show that there are a number of fracture patterns present, with the area corresponding to the Fergus Shear Zone displaying the largest variety on orientation. The rose diagrams corresponding to the Burren region show the regionally dominant NS veins, are the dominant set, with NW-SE- corresponding to the joint set seen at the sites at Cappanawalla and Gleninagh. Analysis of the rose diagrams from the aerial photographs reveals 4 principal fracture sets as outlined in Table 5.3.

Degree	
030-050°	NE-SW
110-130°	WNW-ESE
140-170°	NW-SE
170-190°	NS

Table 5.3 Principal orientations of fracture in the Fergus Shear Zone

When the relative entropy (RE) of the system calculated, Figure 5.11, it is apparent that the system has higher relative entropy within the shear zone and lower relative entropy in the "more ordered" regions on the peripheries of the shear zone. This corresponds to an increase in the number of fracture orientations present in the centre of the shear zone. Correspondingly there is a higher fracture density, Figure 5.12, in the centre,

with the system having a higher connectivity. It will be shown in Chapters 6 and 7 that where a fracture system has increased connectivity it corresponds to a topographic feature.

5.5.1 Comparison between SAR and Aerial photograph derived lineaments

SAR images are subject to geometrical distortion, which can introduce bias in the form of

1. Fore shortening: slopes angled towards the sensor will appear to be compressed versus slopes angled away from the sensor. The image of the fore slopes will therefore appear to be brighter than other features on the same image. In the case of the examined images the NW trending fold controlled slopes along the south-eastern margin of the Burren are subject to fore shortening, being brighter than other features, thereby introducing a bias into the imagery.
2. Pseudo-shadowing: the back slope of the hills appear to be expanded.
3. Shadowing: objects may block radar from hitting objects behind them. The radar shadow masks down range features, so slopes facing away from the radar antenna will return a weak signal if any.
4. Layover: is the effect where the image of an object appears to lean towards the radar antenna. It is an extreme case of foreshortening when the top of the object is detected before the bottom of the object.

The two lineament maps (Figures 5.7 & 5.8) are derived from two different images, which cover the same areas, the Gort Lowlands. In addition to the biases outlined above the SAR images were of a lower resolution than the aerial photographs. Both data sets show similar general attributes the Fergus Shear Zone is shown as an area of anomalous fracturing, a zone showing a density of multiple lineament orientations. The SAR images give a good indication of the overall regional picture but in terms of elucidating the fracture patterns of the Gort Lowlands and the Burren they are not sufficiently detailed and have too many inherent biases to accurately describe the fractures at specific locations. The aerial photographs are an ideal data set to use to obtain this information for the reasons outlined in Section 5.2.2, notably clarity of images and the fact that specific locations can be readily identifiable on the ground giving an increased level of confidence in the lineaments derived from these images.

The SAR images identify a number of the regional fracture patterns particularly the fold axes that swing into and out of the Fergus Shear Zone. The SAR images pick these up by highlighting the fold controlled scarps along the southern extent of the Burren, in this instance the bias of fore shortening is an advantage in highlighting these features. In regards to identifying the NNE trending vein sets of the Burren the SAR images only give an indication as to their presence but are only able to highlight the larger features. The 1:3,000 aerial photographs and field mapping of the region show that they are regionally dominant and persistent. The 1:48,000 scale aerial photographs are able to identify this regional set but are unable to identify the different joint sets. The aerial photographs are able to identify the NNE vein set clearly. Both remotely sensed images give an indication as to the regional fracture pattern but the biases and limitation of both sets need to be recognised and incorporated into any prediction as the regional fracture pattern.

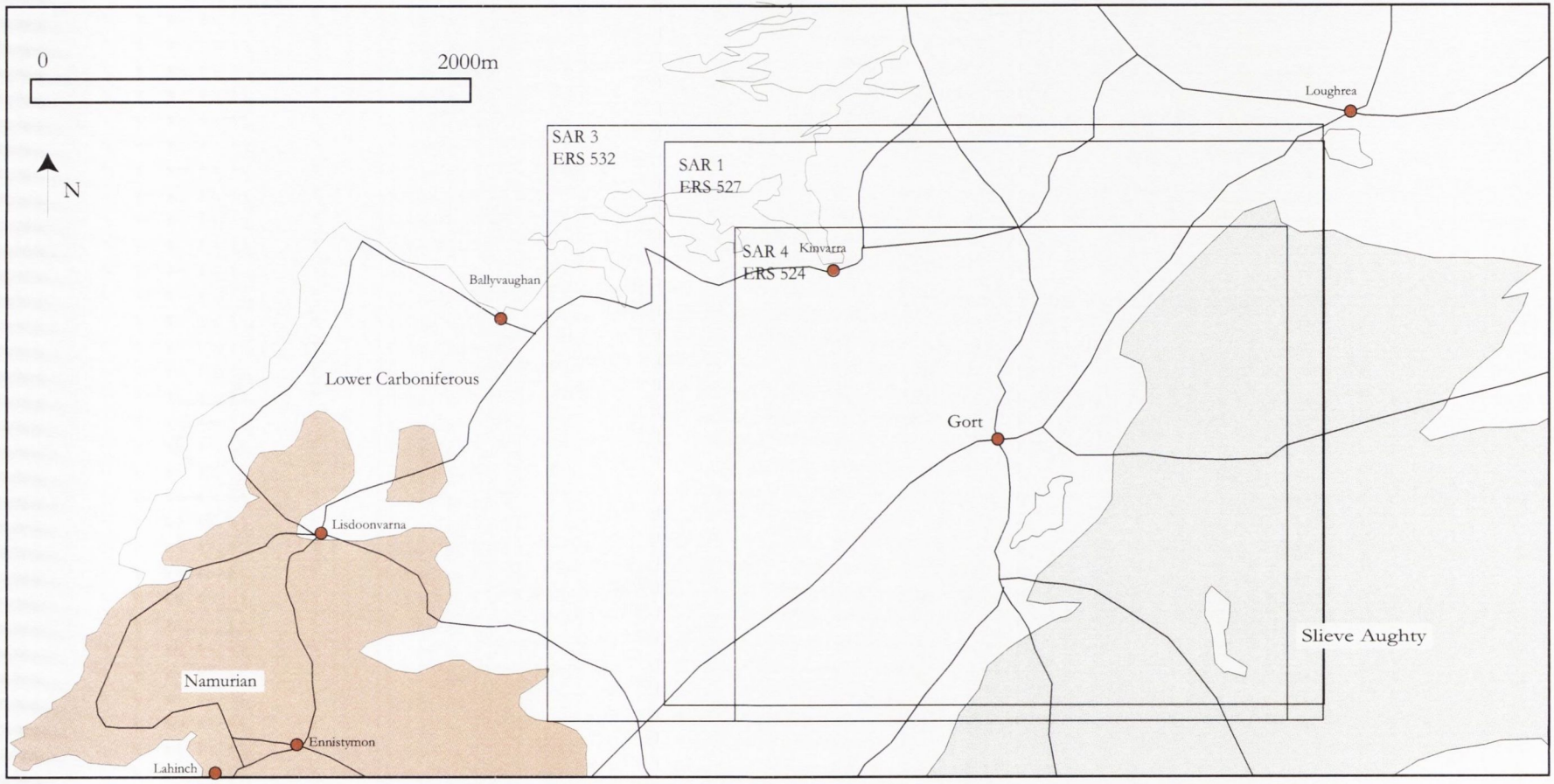

Figure 5.2: Location of SAR images.

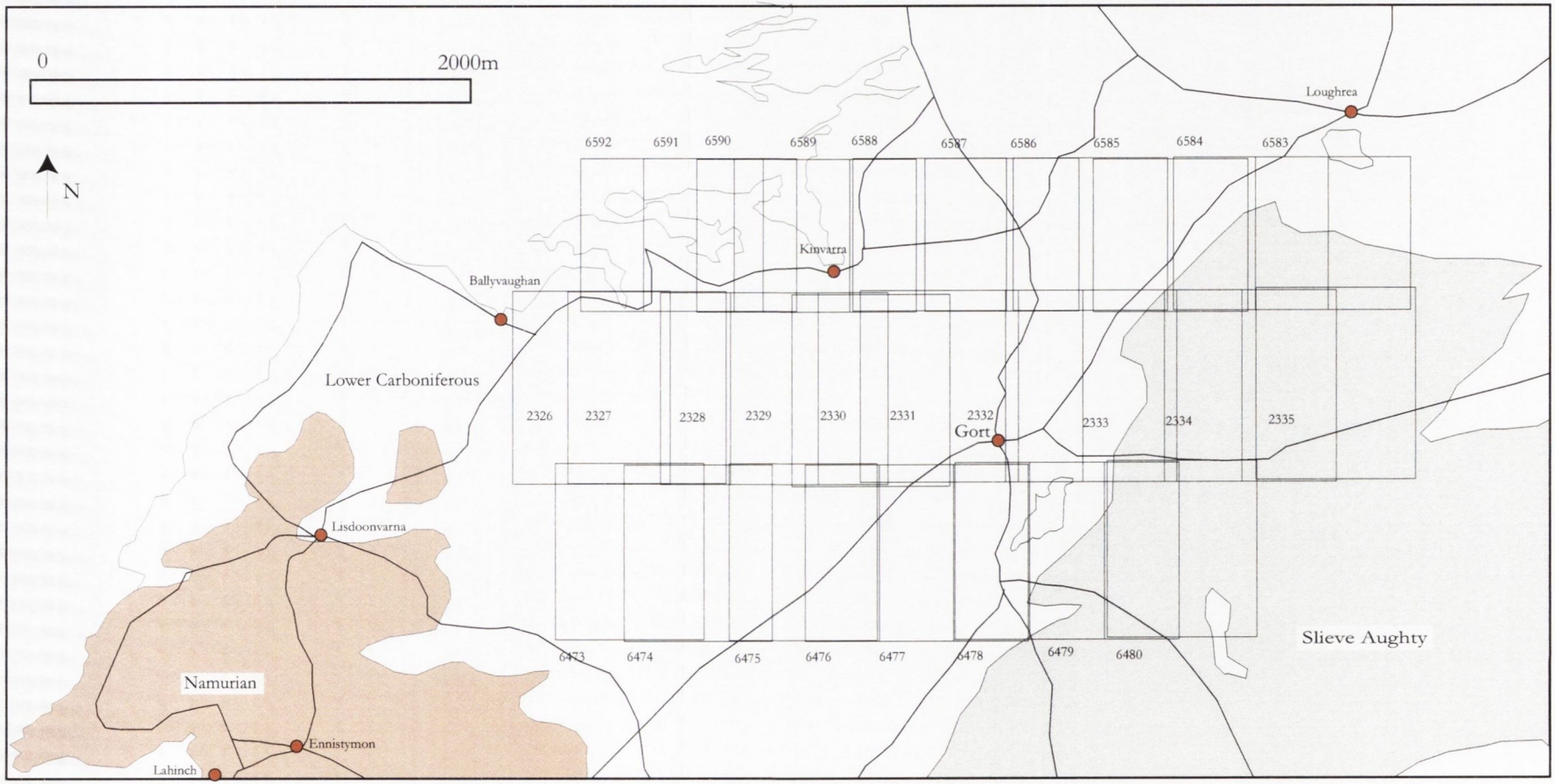

Figure 5.3: Location map of 1:48,000 Aerial Photographs.

119155
209176

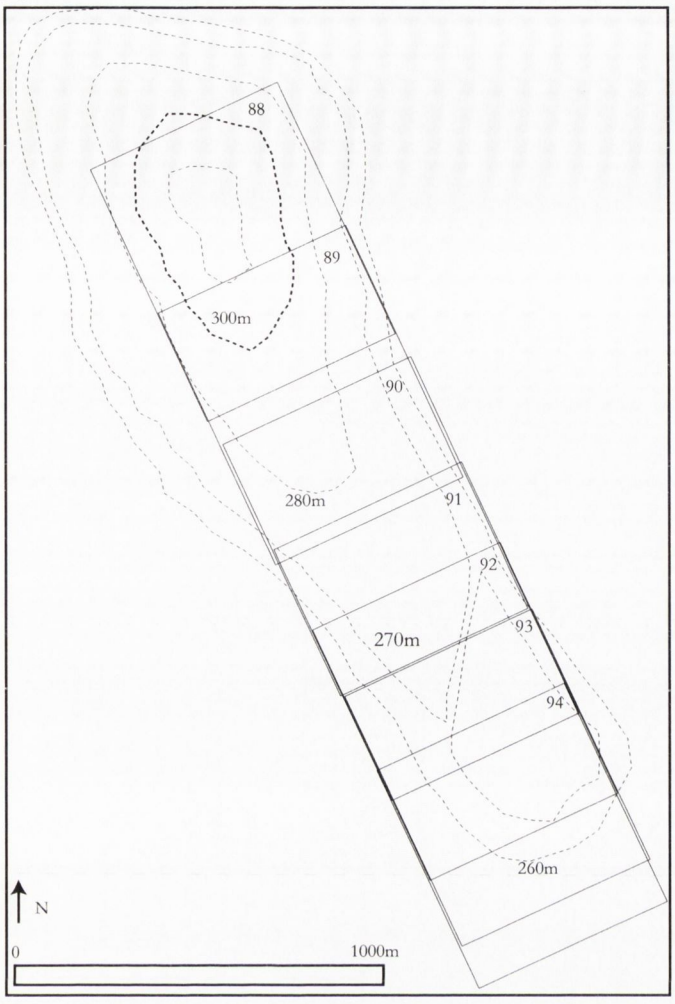

120951
206428

Figure 5.4: Location of 1:3,000 scale Aerial photographs on Cappanawalla.

123407
196424

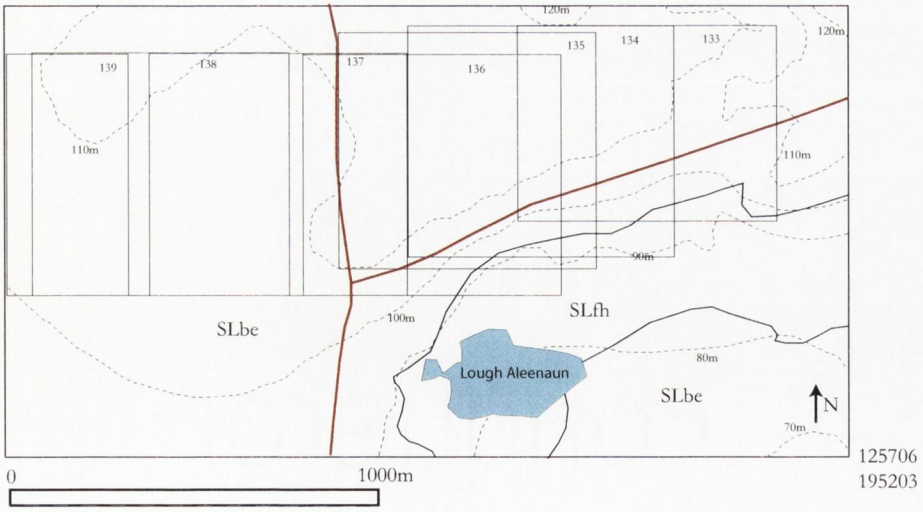

125706
195203

Figure 5.5: Location of 1:3,000 scale Aerial photographs on Sheyshmore.

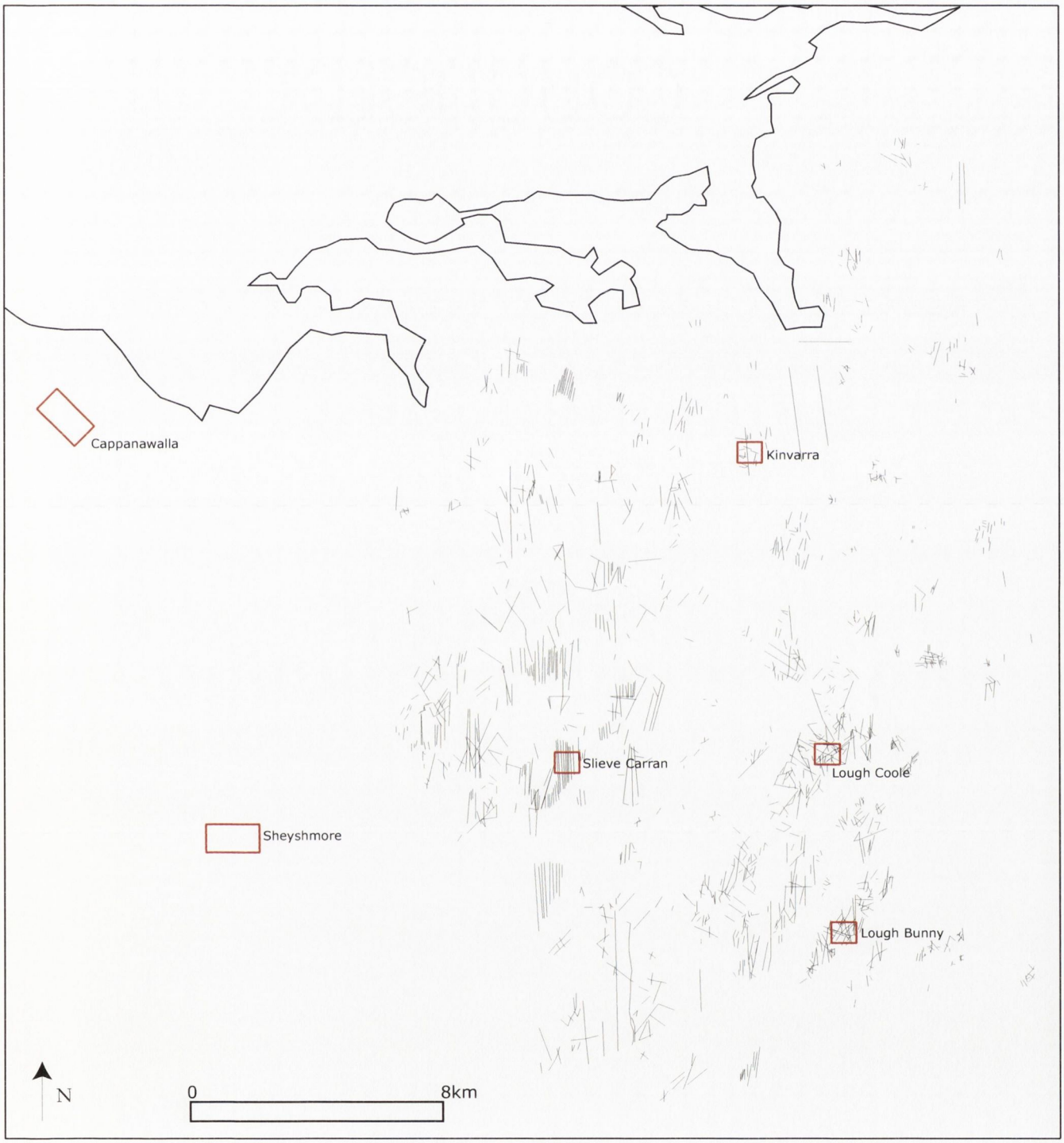

Figure 5.7: Location of field visits to "ground truth" remotely sensed lineament data. 4 locations were visited to investigate the lineaments derived from the 1:48,000 aerial photographs (3 on the Gort Lowlands and 1 on the Burren). The sites visited corresponded to regions where specific lineament patterns existed and the aim of the visits was to "groundtruth" these patterns and check the local fracture pattern. The 2 sites that had 1:3,000 aerial photograph coverage were visited and mapped.

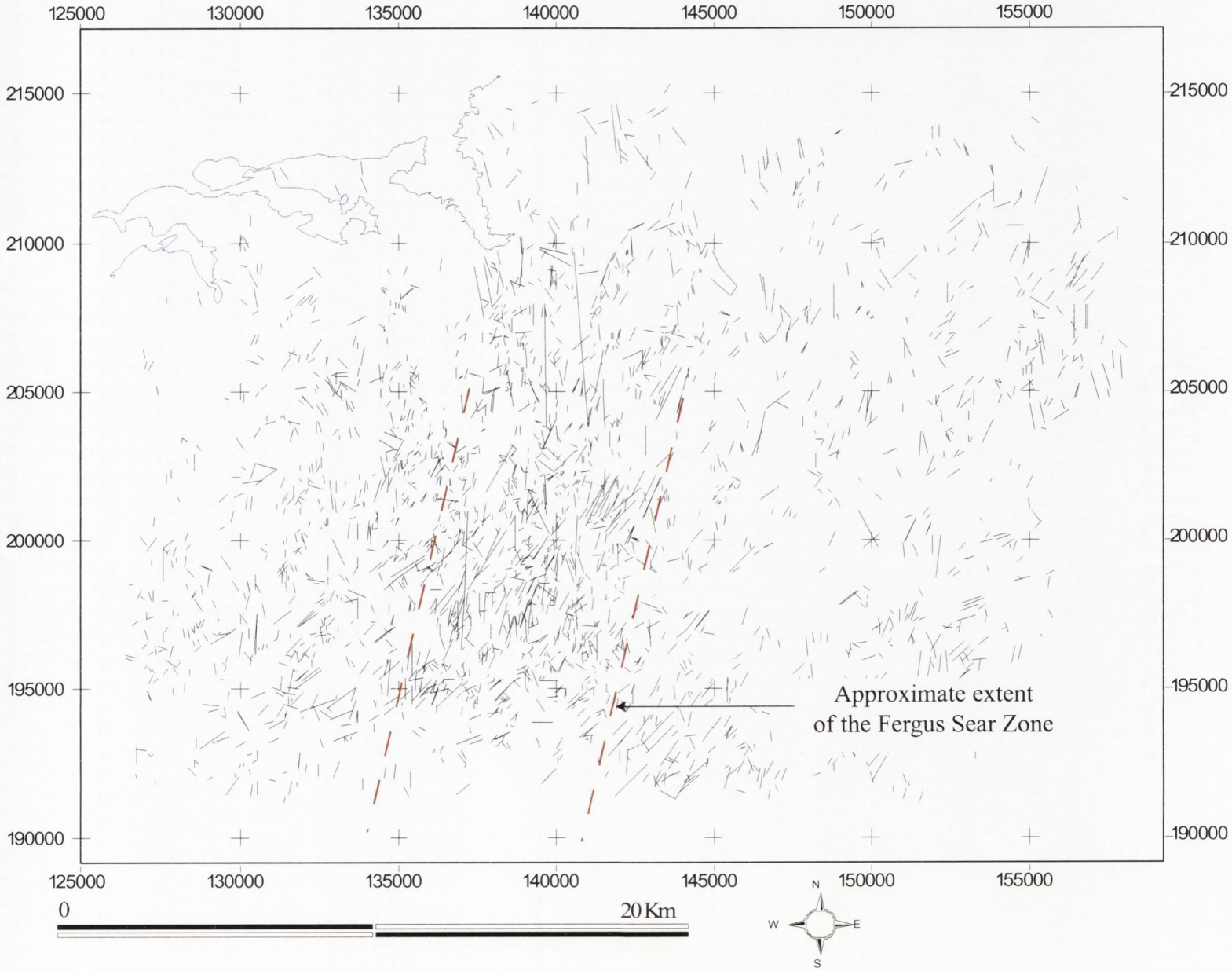

Figure 5.8: Lineament map derived from SAR imags.

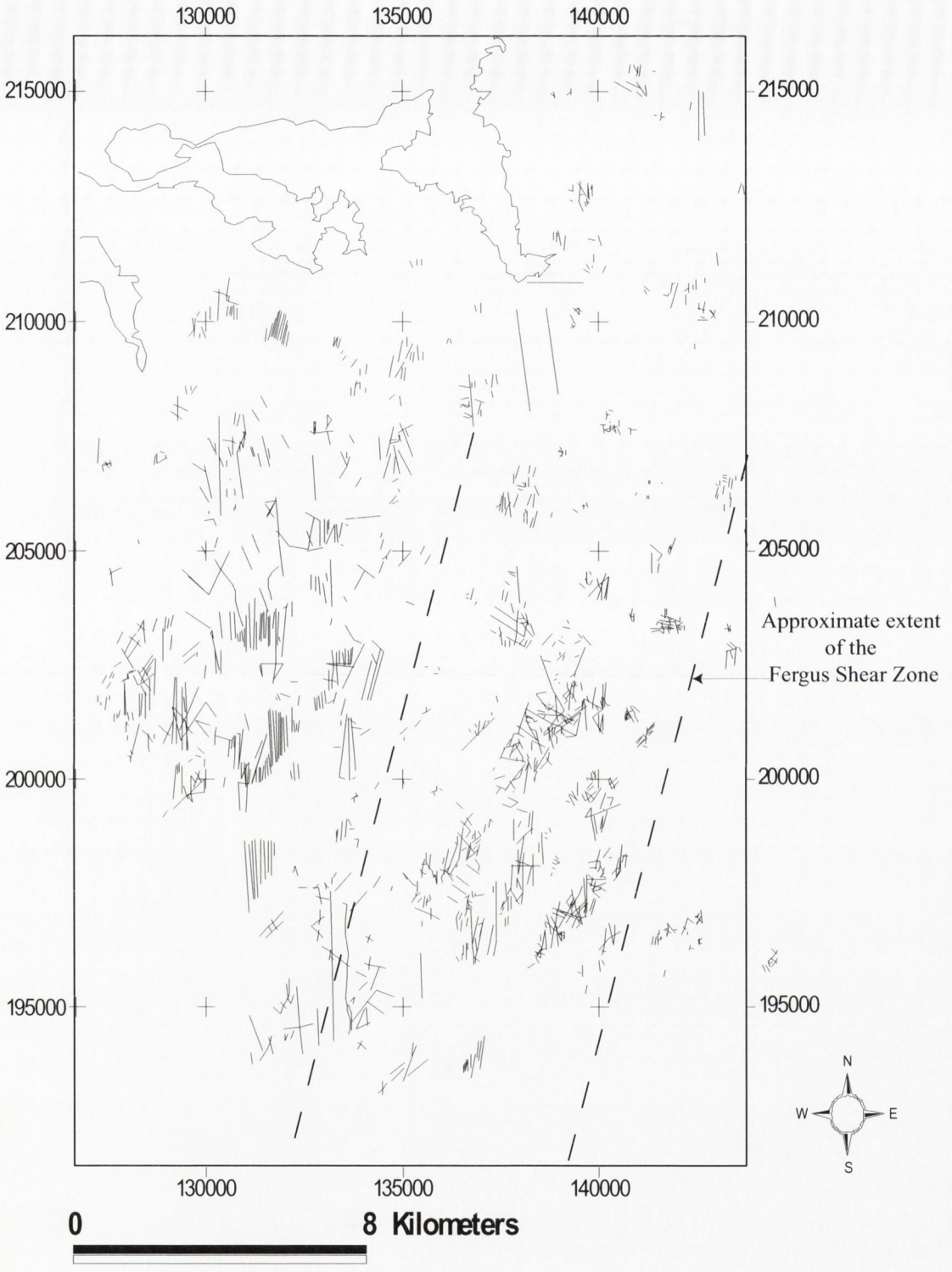

Figure 5.9: Lineament map derived from aerial photograph interpretation.

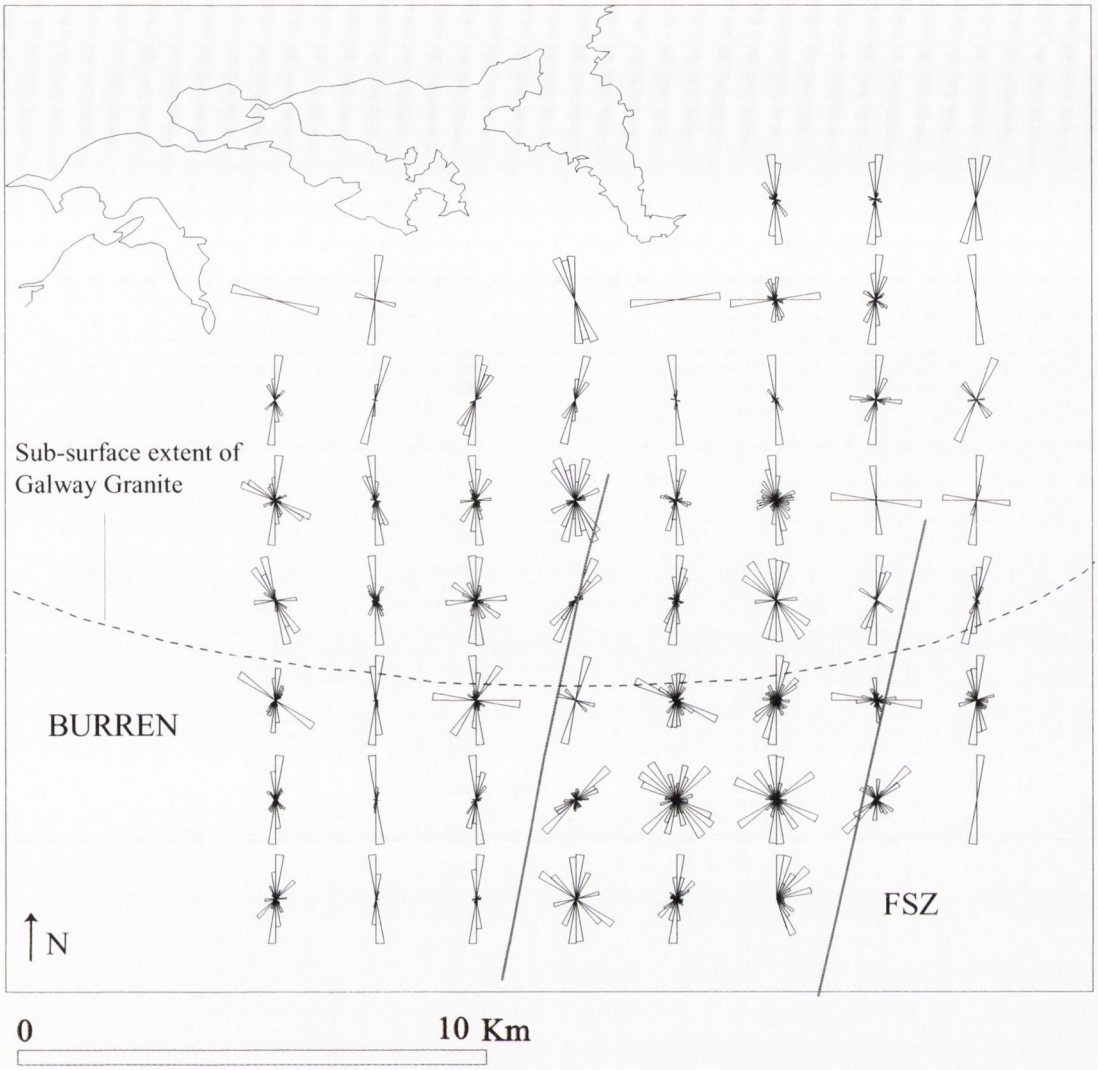

Figure 5.10: Rose diagram of aerial photograph lineaments (fig 2.8). The rose diagrams display the increase in number of frature patterns in the centre of the Fergus Shear Zone compared to the fracture pattern of the Burren to the west.

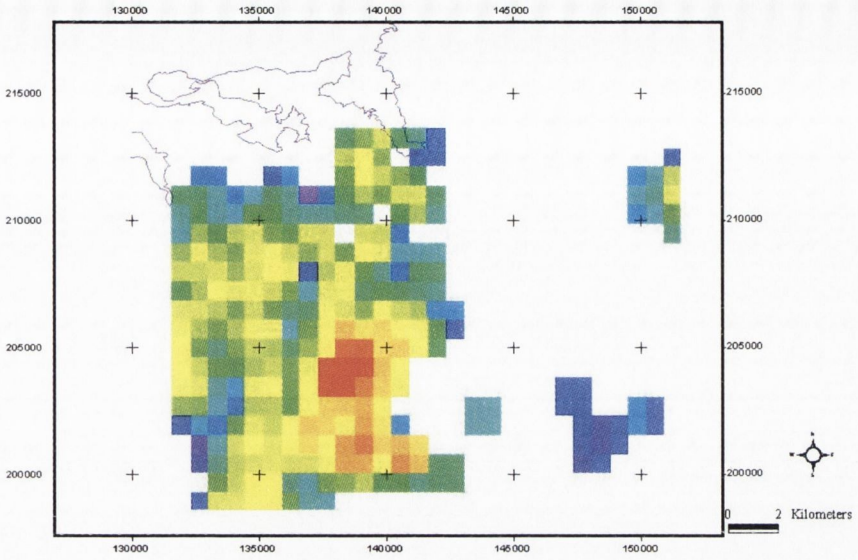

Figure 5.11: Relative Entropy (RE) of the fracture pattern in the Gort Lowlands. Red corresponds to high RE, blue to low RE. The Fergus Shear Zone is marked by a zone of high RE.

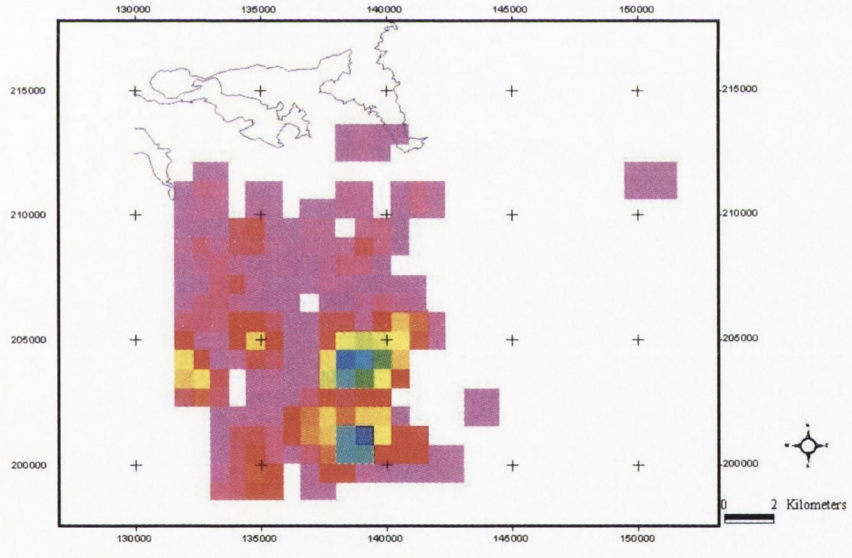

Figure 5.12: Intersection Density of the fracture pattern in the Gort Lowlands. Red corresponds to high Intersection density, blue to low levels of intersection density. The Fergus Shear Zone is marked by a zone of high Intersection Density

CHAPTER 6: CAVES

6.1: Introduction:

Karstic areas have a unique drainage pattern due to the movement of most of the surface water into the sub-surface with a resultant absence of surface drainage. For a description of karstification, see Section 7.1. In the Burren, the boundary between the Namurian strata and the Lower Carboniferous limestone is dominated by active karstification in the form of sinkholes. The surface drainage coming off the Namurian, which is an impermeable catchment rock, flows on to the limestone where it is transferred into sub-surface drainage through the formation of sink holes. Once the flow is into the sub-surface, underground solution conduits known as caves form. A cave is defined by the *International Union de Speleologies* as a natural underground opening in rock large enough for human entry. Ford & Williams (1989) define a karst cave as a solutional opening that is greater than 5-15mm in diameter. Caves have an input point, a sinkhole/swallow hole, and an output point, known as a rising. Where a solution conduit extends continuously between these two points it constitutes an integrated cave system. The science which studies cave systems is known as speleology from the Greek *spelaion* (cave) and *logos* (study).

The essential requirements for speleogenesis - that set of processes, which create caves- to begin, are

1. Carbonate rocks which contain discontinuities, fractures, as they enable carbon dioxide enriched meteoric waters to penetrate the rock mass and act as preferential flow routes through the system.
2. Water containing dissolved carbon dioxide; carbonate rocks dissolves in a weak carbonic acid (H_2CO_3) produced by the reaction of water (H_2O) and carbon dioxide (CO_2) (Equation 7.1, see Section 7.4. for more information on the process of chemical weathering). In addition to the above reaction the presence of additional strong acids enhances the corrosive power of the fluid, giving rise to so-called "hyper karstic phenomena" (Stoch 2002). Strong acids may be present in the external environment, through industrial pollution, but they are commonly found within the rocks themselves, e.g. H_2SO_4 is linked to the reaction of oxidation of pyrite (FeS_2) as are found in the Clare Shale Formation.
3. Difference in altitude, permitting the movement of water.

In the Burren the caves are for the most part horizontal cave systems confined to the same lithological unit, which they follow down dip, with only a few deep vertical passages. The caves are strongly controlled by the fracture pattern particularly the NNE – SSW trending vein system. The carbon dioxide enriched meteoric waters dissolve the calcite filled veins preferentially and utilise the characteristics of the veins – clustered, vertical persistent, high proportion of cross and abutment terminations and a resulting high value of connectivity- to create long passages.

Cave passages can develop both above the water table, in the vadose zone, or below it, in the phreatic or permanently saturated zone. A vadose cave has a passage occupied by a stream with air above it, while in a phreatic cave passage the entire passage is water filled. The two hydrological situations produce different passage shapes that are of use in determining the origin of cave passages. In the vadose zone, water flows only in the lower part of the passage and always downhill resembling a surface stream, creating vadose

canyons by cutting into the floor of the cave or creating a vadose shaft where the stream descends vertically down a fracture. Below the water Table in the phreatic zone all cavities are filled with water, which chemically reacts with the limestone in all directions forming passages that are circular or elliptical in form, known as phreatic tubes. Water flow in phreatic cave passages follows the line of least resistance, even flowing uphill providing there is sufficient hydraulic head.

The location of all published sinkholes and caves was compiled from literature (Tratman 1968, Self 1981, Drew 1973, Drew 1988, Boycott *et al* 1996) and plotted on a geological map of the Burren, Figure 6.1. Of the 195 features located in the Burren, 153, (78%), were located in the Namurian dominated Western Burren, 61, (31%), occurred within the Namurian outcrop. Of the 134 swallow holes that are located on Visean rocks, 83 out of the 134, (42.5%), were located within 50m of the Namurian boundary; with 93 of the total, (47%), being located within between 50m and 100m of the Namurian boundary.

Formation	N	%
Namurian	61	31
Slievenaglasha Fm.	93	48
Burren Limestone Fm.	41	21

Table 6.1: Number of caves / swallow holes per geological formation: n =195

The largest proportion of cave features occurs in the Slievenaglasha Formation and the lowest proportion in the Burren Limestone Formation, the site of many of the oldest fossil caves in the region, such as Aillwee cave. The hydrologically active cave systems are confined to the zone adjacent to the Namurian / Limestone boundary. The surface streams coming off the Namurian strata are transferred into the sub-surface via swallow holes and remain close to the surface for their entire length, bar a few notable exceptions such as Poll na gCéim and Faunarooska. These are exceptions as these caves have a greater vertical extent that other caves in the region, 181m and 94m respectively, and have cut through the clay, shale and chert layers which are interbedded with the limestone (of the Slievenaglasha Formation) and act as barriers to vertical percolation and encourage sub-lateral, horizontal propagation of the cave passages flow along bedding planes. The majority of cave systems mapped in the Burren have a vertical extent under 60m remaining perched above chert beds at the base of the Ballyelly Member of the Slievenaglasha Formation, known as the Upper Faunal Zone. A few cave systems cut below this chert unit into the Fahee North Member, and fewer still penetrate the cherts at the base of this unit, the Lower Faunal Zone (Drew 1988). The caves of the Burren, especially those near the Namurian boundary, are for the most part post-glacial in age. Tratman (1969) cites the closeness of the cave passages to the surface, the scarcity of abandoned passages, and the close match of surface features to the caves as evidence of this. The caves often follow the lines of surface dry valleys, which pre-date the caves. As these valleys contain no glacial drift they are interpreted to be post-glacial in age (Tratman 1969). There are a number of notable exceptions, caves from the High Burren (see Section 7.3) are classified as being fossil caves with calcite precipitates dated from Aillwee Cave yielding a minimum age of 550,000 yrs BP, the cave is believed to be over one million years old (pers. comm. Drew 2003).

6.2 Influence of Fractures on Cave Passages.

The Upper Faunal Zone at the base of the Ballyelly Member has a strong controlling influence on the vertical extent of the cave systems. The caves of the Burren are vertically constrained by bed thickness, (strata-bound), and are horizontally persistent with the fluid that is creating them being forced to flow down dip in the one layer. Where cross layer flow is inhibited, as is the case here, two dimensional fracture patterns can be used to understand three-dimensional flow (Odling 1997). Flow through a karst aquifer is strongly dependent on fractures enlarged by chemical solution, which provide preferential flowpaths (Kaufmann 2003). As the caves are features created by flow, the caves are confined to these fracture backbones; therefore the cave systems are the mapped portion of the backbone of the fracture network. Percolation theory provides a means of analysing flow and transport along fracture systems (Berkowitz & Balberg 1993). Analysis of the caves will show which fractures are important for the make up of the backbone, and therefore important for the control of flow. Backbones consist of a series of interconnected line segments of varying size and orientation that link one side of an area to the other. The makeup of the backbone is dependent of the orientation, size, density, spatial distribution and degree of connectivity of the fracture network. Fluid will utilise line segments of varying size and orientation to cross the system.

Two dimensional fracture patterns were examined at two locations, Cappanawalla and Sheyshmore, with a view to determining the spatial relationships of the fracture patterns in each area and how the fractures are linked to each other. In both areas the joints are strata-bound features with the base of the units inhibiting cross layer flow, only the NNE trending veins are non strata- bound and cut through bed interfaces. The fracture backbone is representative of the overall geometry of the fracture network but is biased towards those fractures that have a high intersection density. In areas where the joints are dominant the backbone consists of long line segments that are only connected to adjacent joints by abutment or by minor cross-joints intersecting or abutting against adjacent joints. The joints have finite lengths and terminate by abutting against another joint, so that a joint system from afar may appear to be of great length but is composed of a number of connected fractures all of similar orientation, except for their terminations where the curve into other joints. The joints act to link the clustered NNE trending veins, at Sheyshmore the joint length is a function of the spacing of the vein clusters, at Cappanawalla the joints anastamose into long linear features that connect adjacent clusters. A cave formed in a joint dominated region will be horizontally persistent along the joint orientation, a cave formed in a vein dominated areas will be narrow and elongate and have an overall NNE trend but will consist of a number of small NNE trending passages connected to adjacent NNE passages by joint controlled passages. The vein controlled regions are highly connected zone of line segments, as the NNE veins have a high intersection density the resulting veins will consist of a large number of small line segments connected by joints.

The hydrology of the Burren has been discussed in Section 2.5; Figure 6.2 shows a synopsis of the flow pathway of the caves that are being discussed along with geographic extent of the caves themselves. The aim of analysing the cave systems from a fracture perspective is to understand the fractures that control individual cave passages.

6.3 Methodology:

A literature review of cave systems in the study area was conducted with the aim of compiling a series of surveyed maps and associated reports of the caves. This initial search of the available literature was further refined by the following requirements.

- The cave systems had to be surveyed to a high standard in order to produce a useable map.
- The associated cave description should contain information on the cave morphology and, ideally, additional information on its hydrological setting/history, geology, description of any fractures present and association with any other caves or surface features.
- The cave systems selected should have a geographical spread throughout the study area.

The principal source of information on cave systems in the north Clare/south Galway region is the University of Bristol Spelaeological Society (UBSS) and its associated publications, its annually published journal *Proceedings* and the seminal work on speleology in this region "*The caves of North West County Clare, Ireland*" first edited by Tratman in 1969 and the revised edition edited by Mullan and Drew in 2003. Secondary sources of information and cave maps included *Irish Speleology*, the UBSS published *"The Caves of Co Clare"* Self (1981) and communication with speleologist's familiar with the region. These sources yielded a number of high quality surveyed maps of cave passages in addition to description of the caves and their setting within a hydrological and geomorphological context. The reports that accompany the maps have been written by a number of individuals from a variety of backgrounds some scientific others not, which necessitates a degree of a caution being used when examining the interpretation of geological and geomorphological aspects of the caves contained within the reports. The cave maps represent the total explored length of the cave at the time of the survey, cave passages can terminate for a number of reasons, the principal reason being an obstruction in the form of a mud filled section which necessitates excavation of the mud, and pumping of any additional water, this is a labour, and financial, intensive procedure and can be carried on over a number of years, leading to revised maps and cave length. In addition as a number of caves are hydrologically active the accessibility of passages can change after heavy floods. A total of 26 sites fulfilled the criteria outlined above.

The maps were scanned at a high resolution (600 dpi) and were geographically rectified, using co-ordinate information obtained from the maps and the reports, through the processes of geo-registering and geo-rectifying within the Arc Info GIS platform. This process projects the cave maps into their correct spatial setting. The line work outlining the cave passages was digitised within the Arc View GIS platform. The cave maps varied between depicting the cave passages as a single line or showing both sides of the cave passages, as was the case in a small number of caves which had a limited geographical extent- in these cases a central line equidistant from each passage wall was used. The cave passages were digitised and subsequently edited; this edited data contained the length and azimuth of the individual line segments or vertices that make up the cave passages. The input of the cave systems into a GIS enabled the data to be spatially queried and establish relationships between the caves and other geographic information such as geological lithologies (from the GIS geological map of the region), surface features (obtained from a Digital

Terrain Model (DTM) of the region), location of swallow holes (obtained from literature review), groundwater flow tracer studies (obtained from literature review) and adjacent cave systems.

Using the length and azimuth of the individual vertices that make up the cave passages a number of parameters were calculated such as dispersion statistics (mean, median, range, standard deviation) and sinuosity. The data was grouped into ten-degree bins and rose diagrams and bar charts were generated. The mean is the arithmetic average of a set of *N* numbers/values, defined as the sum of the numbers/values divided by *N*. The median is the middle number/value in a series of numbers/values. The range is calculated by taking the difference between the maximum and minimum number/value in the dataset. The standard deviation is a measure of the dispersion of the data. Sinuosity is defined as the length of a line object versus a straight line distance between the beginning and end points. It is a measure of the overall length of a line object and is compared to the straight line distance between the points and a ratio is formed between the two lines. The closer this value is to 1 the less sinuous the line is.

6.4 Distribution of caves:

The caves that were chosen to be studied can be divided into belonging to one of 13 geographic areas (Figure 6.3). Througout the Burren sub-terraean flow appears to mimic previous surface flow.

6.4.1 The Doolin/Aille Valley system parallels the Namurian/Lower Carboniferous in this region as well as the course of the Aille River, and is located within the Fisherstreet catchment. The Doolin River/Fisherstreet cave system is the largest cave system in the area, over 10km long. It is a horizontal, active, vadose; down dip flow – to the southwest - cave system. The Aille River rises on the Knockavoarheen ridge to the east of Doolin and slowly looses water along its length (Drew1990). Karstification of the drainage (Aille River) is only partial and subterranean flow routes parallel those of the surface drainage (Drew 1990). The inputs to this area are along the shale margin and the Aille River and discharges to the sea immediately off shore from Doolin. The cave system consists of a series of narrow low sinuosity passages, which trend NNE, connected by a series of passages with substantial lateral development which trend NE-SW.

6.4.2 Western Knockauns & Oughtdarra, Poulnagree is the major conduit system in the present day drainage system in this area, which along with the smaller cave systems of Moonmilk, Through & Through and Robbers Cave are discussed later on in this chapter. The inputs are located along the shale margin and flow from the Poulsallagh catchment resurges at large offshore springs to the southwest. Poulnagree is a long, over 4500m, horizontal cave system initially to the southwest. Moonmilk, Through & Through and Robbers Cave are short, horizontal caves located adjacent to each other on NNE trending gullies that indent the northern edge of a large cliff at Oughtdarra on the south-western flanks of Knockauns Mountain. The caves are located in the Fahee Member of the Slievenaglasha Formation, presumably perched above one of the chert bands that serve as aquitards, at the base of this member.

6.4.3 Northwestern side of Slieve Elva. Caves within this region drain the sub-surface within this area from inputs along the shale margin to off shore springs to the west and north. Two of the deepest caves in the Burren are located within this region Poll Na gCéim and Faunarooska, which along with Hawthorn and

Pollballyiny cave are discussed later on. The NNE trending Poll na gCéim is a active, narrow elongate vertical extensive cave, the second deepest cave in Ireland at 181m deep, and lies directly below the NNE trending Ballyiny Depression and flows to the north, up dip, mirroring the behaviour of a phreatic cave system where flow can flow up dip provided the hydraulic head is sufficient. It has a number of phreatic sections and is described by Judd & Mullan (1989) as a vadose invasion cave with para-phreatic sections. Faunarooska is a deep, active, vadose cave system draining to the west to resurge at a submarine spring 300m off the coast (Irish National Grid co-ordinates of 111965 205610 at a depth of 10m). Hawthorn Cave lies 67m to the south of Faunarooska and immediately to the north east of Pollballyiny, it is a active, horizontal cave flowing close to the surface for its entire length, resurging to the south-east in Pollballyiny. Pollballyiny is a >1500m long, active, horizontal cave. Flow is to the southwest where it appears to resurge at the same submarine spring as water from Faunarooska.

6.4.4 Coolagh Valley. The only cave system studied in this region is Pol an Ionain that lies within the Poulsallagh catchment. The cave lies in the upper units of the Slievenaglasha Formation and drains to the southwest. The cave terminates in a large 18.3m high chamber that houses a 12.8m long freestanding stalactite. The cave has both vadose and phreatic sections with the large main chamber being described as a phreatic feature by Tratman (1969). There are a number of other caves systems within in this location that mimics previous surface flow (Drew 1990). Drainage in the Coolagh valley is subterranean with the exception of the headwater streams with water resurging from the submarine and intertidal springs at Poulsallagh (Drew 1990).

6.4.5 Eastern side of Slieve Elva. The surface of this area is cut by a series of dry valley features that follow the fracture set with the sub surface being dissected by a series of long cave passages that resemble tributary streams. The three caves that are studied in this area are Poulnagollum, Pollcragreagh, and Pollcahercloggaun. The St Brendan's/Killeany catchment drains the region along the western edge of Poulacapple and the eastern edge of Slieve Elva where a large number of swallow holes and cave systems exist. Poulnagollum is a horizontal, long (>12km) vadose cave that flows to the southeast. Dating of stalagmites in the main chamber of Poulnagollum yield an age of >70,000 BP. Waters first resurges at the internal spring of Killeany where they sink before reappearing again at St Brendan's Well 3km down dip to the southwest. Mullan & Drew (2003) describe Poulnagollum as a series of tributary [subterranean] streamways, which drain the shale margin along the east side of Slieve Elva. Pollcragreagh is located midway between Poulnagollum to the north and Pollcahercloggaun to the south, both Pollcragreagh and Pollcahercloggaun exhibit similar characteristics to Poulnagollum in that they flow to the south east, though Pollcahercloggaun drains primarily to St Brendan's Well.

6.4.6 Western Poulacapple. The caves in this area, Cullaun 1 & Cullaun 3, run almost parallel to each other draining the edge of Poulacapple to Killeany and St Brendan's spring respectively to the southwest. Both caves are horizontal, active vadose systems that are perched above the cherty base of the Ballyelly Member of the Slievenaglasha Formation.

6.4.7 Eastern Poulacapple. A series of caves, Doonyvardan, Gragan, and Green Streams, run parallel to each other in a series of overlapping, but independent, conduits. The caves are at the same altitude are only tens of

metres apart, indicating that there must be a series of parallel systems present. The caves occur within the Fergus River/Elmvale catchment with flow from these caves resurfacing at the Fergus River spring some 10km to the southeast. The three caves are active, horizontal, vadose, down dip caves that drain to the southeast.

6.4.8 Southern Poulacapple. Cullaun 5 is the principal cave system in this area. Inputs are from flow off the Namurian capped Poulacapple hilltop, with the cave draining the southern edge of Poulacapple to the south east, to the Fergus River spring though on occasion it drains to west to St Brendan's Spring (Drew 1988) due to the lack of clear distinction between surface and sub-surface hydrological systems in karstic areas (Coxon & Drew 2000). The cave is an active, horizontal, vadose, down dip system that trends strongly to the south southwest yet drain to the southeast.

6.4.9 North of Kilfenora, The caves in this area, Pollcahermaan and Poulawillin, are linear stream ways along the Knockavoarheen Ridge and are located in the Fergus River / Elmvale catchment. Pollcahermaan is a >900m long, elongate, narrow, horizontal, NNE-SSW trending cave that follows a series of calcite veins, which can be followed to the end of the cave (Mullan & Drew 2003). It lies immediately to the south of Cullaun 5 and similar to this cave it trends strongly to the south south west yet drains to the south east.

6.4.10 North Central Burren, The principal cave system in this area is Aillwee Cave. Input is from a series of discrete sources such as of swallow holes and ephemeral streams at the summit of Aillwee hill as well as from the sinkings of the Rathborney river and Berneens stream in addition to diffuse inputs via rainfall over the exposed limestone pavement that makes up a large portion of this region. Flow is primarily south to north up dip to the intertidal springs directly off shore Ballyvaughan. Aillwee Cave (Figure 6.2) is a 915m long horizontal, relict, phreatic, fracture controlled cave system located in the Aillwee Member of the Burren Limestone Formation. Aillwee cave can be divided into two sections based on its trend, the first section trends WNW-ESE along strike for 400m before changing orientation with the second section trending down dip to the south-south-west, coincident with the regional NNE/SSW trending vein clusters. It is the most extensive cave in the high Burren with its opening located 2m above a clay way board, which acts to retard vertical percolation (Drew & Cohen 1980). Unlike the active caves in the western Burren it shows extensive phreatic development under fast flowing water conditions (Drew & Cohen 1980) suggesting that Aillwee cave formed under different hydrological conditions that at the present. A calcite precipitate from one of the cave passages has been dated at > 500,000 BP (pers. comm. Drew 2003) with the cave passage it self being estimated to be at least 1 Ma, Early – Mid Pleistocene in age (pers. comm. Drew 2003).

6.4.11 South Central Burren, Kilcorney / Cave of the Wild Horses is the largest cave system in this area. Mullan & Drew (2003) contend that the cave formed in association with the Kilcorney Depression, which formed as a karst window during a time when the Namurian strata covered the region. The development of the depression/karst window was followed by a reversal in the drainage of the area from northward draining surface streams to southward draining sub-surface drainage towards the Fergus River spring under the influence of dip, with the depression serving as a focus for the drainage. The cave is a >520m long largely relict cave system. It was the first described in 1640 by Lucas in what is the first recorded cave exploration in Co. Clare (in Tratman 1969). The cave has had a complex hydrological history, a fact borne out by the

varied orientation of the cave passages. It consists of sections of vadose altered phreatic passages and more recent vadose passages. Stalagmites dated from the older phreatic tubes yield an age of 41,000 BP (pers. comm. Drew in Boycott *et al* 1983). The older sections of the cave are thought to predate the formation of the Kilcorney depression. The active sections of the cave are believed to resurge at the Fergus Springs 6.6-km to the south-southwest.

6.4.12 South Eastern Burren. The Seven Stream of Teeskagh is located along the southwestern side of Slieve Na Glasha; it is formed where several streams from the hilltop breach the chert layers of the Ballyelly Member of the Slievenaglasha Formation. It drains 4.3 km to the southwest to resurge at the Fergus River spring.

6.4.13 Upper Fergus River. The Fergus River Cave is a >1000m long horizontal resurgence cave and it is the resurgence for a 115km^2 catchment area including the Castletown River from the Carran Depression, over 6 km to the north-east (Drew 1988). It has a vertical extent of 50m (Wilkins *et al* 1980) of which there is a <30m drop from one horizontal chamber to another in the very north of the cave, the rest of the cave continues gently down dip. The cave is developed above the cherts of the Lower Faunal Zone (Drew 1988) at the base of the Fahee North Member of the Slievenaglasha Formation. The <30m drop to the north of the cave could be the result of the cave breaking through the cherts of the Upper Faunal Zone which mark the boundary between the Fahee North Member and the Ballyelly Member. A stalagmite from the Cave has been dated using U/Th dating techniques to >350,000 BP (Drew 1988).

6.5 Analysis of Caves:

Twenty-six cave systems were chosen including active and fossil caves and caves that occur in the Slievenaglasha Formation and the Burren Limestone Formation. Of the 26 caves the majority occur within 500m of the Namurian boundary. The location of the caves and their relationship to the Namurian boundary can be seen in Figures 6.1a, 6.1b and 6.1c. As is the case with backbone systems the cave is composed of a number of smaller line segments. In a backbone a fracture is divided into line segments of varying. The orientation of the cave passages is analysed using a rose diagram generated for the cave system as are the length of the individual line segments in an attempt to investigate any link between orientation and line segment length to see which orientation has a controlling influence on the length of the cave passages. The caves will be discussed according to geographic region. Grid references and elevations given refer to the entrance of the cave.

6.5.1 North Central Burren

6.5.1.1: Aillwee Cave - Grid reference: 123400 204870, Alt: 92m OD

Aillwee Cave (Figure 6.4) is a 915m long horizontal, relict, phreatic, fracture controlled cave system located in the Aillwee Member of the Burren Limestone Formation. The cave can be described as having an inverted L shape and can be divided into two sections based on the trend of the cave passages, from the entrance the first section trends WNW-ESE along strike for 400m before changing orientation to the second section which trends down dip to the south-south-west, coincident with the regional NNE/SSW trending vein clusters.

The first section is a series of cave passages that extend from the cave entrance for 400m in an overall WNW trend; coincident with the joint pattern observed at Cappanawalla 4km to the northwest. There is a degree of lateral variation of 60m along its length with a sinuosity value of 1.61. This section of cave is dominated by a series of WNW joint controlled passages connected by a series of NNE trending and EW trending shorter sections of cave passage. The WNW (100-130°) joint controlled passages account for 53% of the total length of the system, the remainder is made up of EW (11.5%) and a small percentage of NNE orientated passages (>4%), as can be seen in Figure 6.5. The range of the length of the cave passages is 35.2m with the mean length being 7.89m and a standard deviation of 6.65m. In cave morphology flow routes that acquire increasing amounts of discharge accelerate in growth while others languish with negligible growth (Palmer 1991). To rewrite this last sentence in percolation theory terminology (Section 3.3.3) the portions of the fracture pattern that do not lie on a direct flow path through the system are know as "dead ends", the part of the fracture pattern that does lie on a direct flow path through the system is known as the "backbone". Fluid flow for the cave as a whole is normal to the vein set with localised along the backbone, which implies that cave passages are equivalent to the percolation backbone. In this first section the cave is formed along the joint controlled percolation backbone. The cave passages that make up this section share similar characteristics to portions of the percolation backbone at location B11 on Cappanawalla (see Section 4.4); the joint controlled sections are horizontally persistent with a degree of lateral variation, they are intersected by a number of EW and NNE trending fractures, the joints tend to abut with a curving geometry produced a series of long slightly sinusoidal joints which resemble the cave passages seen in the joint controlled section of Aillwee Cave. The second section is a series of cave passages comprises of a narrow, elongate, linear set of cave passages that trend strongly NNE, coincident with the regional vein pattern as studied at Cappanawalla 4km to the north west, Sheyshmore to the south, Cathair Comhain to the south east and Oughtdarra to the east. There is a slight degree of lateral variation of 15m along its length of 170m with the cave system having a sinuosity value of 1.3. This section of cave is dominated by a series of NNE vein controlled passages interconnected by a series of NW-SE and EW joint controlled passages. The NNE vein controlled passages account for 76% of the total length of the system, as can be seen in Figure 6.6. The range of the length of the cave passages is 31.5m with the mean length being 8.87m and a standard deviation of 7.9m. The small amount of lateral variation is a function of the clustered nature of the vein population. The veins define a narrow zone of high fracture connectivity – due to the increased proportion of cross terminations- in which flow will be concentrated thereby creating the narrow nature of vein controlled passages. The NNE trending cave passages are geographically coincident with a series of depressions on the surface directly above the cave demonstrating that the vein cluster has a vertical extent in excess of 110m. Drew & Cohen (1980) noted that a number of small streams exist in this latter section and that after heavy rainfall large amounts of water quickly percolate from the surface to swell these streams, presumably utilising this long, over 6km, vertically extensive, highly connected NNE, >110m, trending vein system.

The two different fracture sets, joints and veins, create cave passages with different characteristics. The joint controlled sections are characterised by passages with wider lateral variation, higher degrees of sinuosity with a sinusoidal shape. The trend of the passages will reflect the trend of the local dominant joint pattern. As the joints are regularly spaced they will be laterally extensive and any abutments or cross linkages will exploit this laterally extensive aspect of a joint dominated percolation backbone. The vein-controlled

sections are characterised by passages that are narrow, with a low sinuosity, linear, elongate features that trend NNE-SSW. The passages will be dominated by NNE trending sections that are interconnected by shorter joint controlled sections. The veins are clustered, have a large proportion of cross terminations, a high fracture connectivity that control the characteristics of the cave passages.

	Total Cave	Joint Controlled Section	Vein Controlled Section
N	112	87	25
Σl (m)	916.5	694.5	221
Mean (m)	8.18	7.98	8.87
Median (m)	6.83	5.69	6.39
σ (m)	6.83	6.65	7.9
Range	35.2	35.2	31.5
Sinuosity	/	1.61	1.3

Σl (m) = Sum of the length, **σ (m) =** standard deviation

Table 6.2: statistics for Aillwee Cave

From °	To °	Joint Controlled Section % ΣL	Vein Controlled Section % ΣL
0	10	2.187	12.666
10	20	0	34.823
20	30	2.289	10.832
30	40	2.329	4.9783
40	50	3.537	7.4201
50	60	2.639	0
60	70	3.605	0
70	80	7.282	4.3745
80	90	4.498	0
90	100	10.35	0
100	110	15.97	0
110	120	23.78	1.4591
120	130	13.97	0
130	140	4.265	1.6154
140	150	0.887	2.7383
150	160	0.577	1.4113
160	170	0.325	0
170	180	1.509	17.726

Table 6.3: % of Σ l per ten-degree bin

6.5.2: The Doolin Valley

6.5.2.1: Doolin/Fisherstreet Cave: Grid reference: 109550 198330, Alt: 60m OD

Doolin Cave consists of a "series of narrow canyon type passageway with minor lateral development"- the vein controlled sections- "and sections of substantial lateral development"-joint controlled sections (Mullan & Drew 2003). A long, <1200m, NNE trending passage way the Aran Swallet joins the main system approximately two-thirds of the way from its entrance at St Catherine's to Doolin. The "Aran Swallet largely comprises of a single narrow canyon type passageway with minor lateral development [with low sinuosity value of 1.02]" (Mullan & Drew 2003). This description fits with a vein-controlled section of passageway; it has a lateral variation of fewer than 80m along its length.

	Total Cave
N	389
Σl (m)	8697.113
Mean (m)	22.35761697
Median (m)	16.9115
σ (m)	17.90365714
Range	171.485
Sinuosity	1.2

Σl (m) = Sum of the length, **σ (m) =** standard deviation

Table 6.4: statistics for Doolin Cave,

The cave system flows from St Catherine's to the south-west to Doolin and utilises any fractures of that orientation along its route as can be seen by the Rose Diagram and the graph in Figures 6.7 and 6.8. Flow is oblique to the vein set. The dominant trends are NNE –32% of the total length of the system, NW-SE (030-050°) –27% and EW with 19.5%.

From °	To °	% ΣL	From °	To °	% ΣL
0	10	11.733158	100	110	1.2391123
10	20	8.3300516	110	120	0.9446008
20	30	8.7427403	120	130	1.047911
30	40	7.5907948	130	140	1.4393282
40	50	9.8054147	140	150	1.0321126
50	60	10.394737	150	160	1.3698109
60	70	5.6256599	160	170	2.3074554
70	80	6.0168932	170	180	4.0886326
80	90	6.6722601			

Table 6.5: % of Σ l per ten-degree bin

6.5.3: Western Knockauns & Oughtdarra

There are four caves in this study area.

6.5.3.1: Poulnagree: Grid reference: 12200 203590, Alt 235m OD

6.5.3.2: Moonmilk Cave: Grid reference: 111186 202366, Alt: 140m OD

6.5.3.3: Robbers Den Cave: Grid reference: 110555 202377, Alt: 140m OD

6.5.3.4: Through & Through Cave: Grid reference: 111145 202364 Alt: 140m OD

Flow in this region is to the south and southwest. The map of Poulnagree shows a series of narrow elongate NNE trending vein controlled passages connected by a series of EW and NE-SW joint controlled passages. The NNE vein controlled passages account for 45% of the total length of the system, EW trending passages account for 12% with the NW-SE (030-050°) trending passages accounting for 8.5% of the total length of the system. Recent explorations have trebled the size of Poulnagree from 1309 to 4515m (Mullan 2000); no detailed map of this explored section was available at the time of this research. The recent discoveries occur to the west of the southerly section shown in Figure 6.9. It is composed of vadose passages with phreatic passages at its lower extent. The newly mapped sections to the west show the continued influence of the NNE trending set with NW-SE fractures beginning to exert a strong influence on the orientation of cave passages (Mullan 2000). Further along the newly mapped section NNE tending sections can be correlated with features along the northern cliff edge of Oughtdarra including the NNE veins in Moonmilk Cave (Section 6.5.3.2) (Mullan 2000). The cave sloped 30° along the first 160m after this for the remaining 4km of passage the average slope is caves 1° indicating an extremely strong control of flow along a single horizon (Mullan 2000). Groundwater flow in this cave is oblique to the vein set as can be seen by the shape of the cave in Figure 6.9, with vein controlled sections being linked by oblique fracture sets. The three Oughtdarra are strongly joint controlled (Self, Miller & Lloyd 1980). They are located adjacent to one another, Through & Through is 40m to the west and Robbers Den 130m to the west of Moonmilk Cave, they are spatially associated with NNE trending depressions which indent the northern cliff face of Oughtdarra. The NNE vein set are the dominant control on the caves sets with NW-SE and EW orientated joints having a secondary control. Flow in these caves is normal to the vein set.

	Poulnagree	Moonmilk	Robbers Den	Through & Through
N	76	96	62	37
Σl (m)	1309.119	273.236	147.321	47.782
Mean (m)	17.22525	2.8462083	2.3761452	1.2914054
Median (m)	12.850	1.649	1.316	0.7255
σ (m)	15.961535	3.0703495	2.8455291	0.9933773
Range	111.05	15.815	13.835	3.957
Sinuosity	1.42	2.14/1.11/1.11	2.28	1.15/1.23

Σl (m) = Sum of the length, **σ (m) =** standard deviation

Table 6.6: statistics for Western Knockauns & Oughtdarra caves

From °	To °	Poulnagree	Moonmilk	Robbers Den	Through & Through
0	10	25.04	6.57	4.34	1.43
10	20	20.32	10.75	5.25	0.81
20	30	3.13	4.19	24.48	15.99
30	40	4.49	8.54	5.73	2.04
40	50	4.04	1.05	3.28	3.59
50	60	5.16	8.53	3.55	1.38
60	70	12.23	4.67	3.22	10.92
70	80	3.90	6.45	0.00	2.93
80	90	2.69	5.97	7.61	9.79
90	100	8.09	10.80	2.28	2.59
100	110	4.16	9.35	14.39	4.79
110	120	1.10	2.73	9.84	14.92
120	130	1.51	5.93	11.73	18.40
130	140	0.00	4.66	1.77	9.43
140	150	0.00	3.36	1.69	2.27
150	160	0.42	1.91	0.76	1.98
160	170	0.79	2.78	0.00	0.78
170	180	2.92	1.77	0.00	0.00

Table 6.7: % of Σ l per ten-degree bin

6.5.4: Northwestern side of Slieve Elva.

There are four caves in this study area.

6.5.4.1: Poll Na gCéim: Grid reference: 112920 203340 Alt: 242m OD

6.5.4.2: Faunarooska: Grid reference: 224240 204500, Alt: 262m OD

6.5.4.3: Hawthorn: Grid reference: 114180 204440, Alt: 263m OD

6.5.4.4: Pollballyiny: Grid reference: 113950 204260, Alt: 253m OD

Flow is principally to the north in the case of Poll Na gCéim and to the southwest / west for the other three caves. As can be seen from the latter three cases the caves are strongly orientated southwesterly. Poll Na gCéim is a 1200m long, narrow, linear, low sinuosity, vertically persistent (181m deep) cave that trends to the NNE. The NNE vein controlled passages account for 82% of the total length of the system. The resulting rose diagram and graph of the % of total length per orientation all show the NNE trending bias. The cave mirrors the behaviour of vein clusters. Judd & Mullan (1989) in their description of the cave erroneously describe the cave as having formed along a fault plane. This author disagrees with this idea and instead suggests that the evidence indicates that an intense vein cluster controls the shape, depth and lateral extent of the cave. Vein clusters are well linked spatially through interaction with the joint pattern; they have a large proportion of cross terminations and a low proportion of blind terminations and a high intersection

density providing a fracture backbone with a high connectivity. The clustered nature of the veins confines these high connectivity zones to elongate narrow section, typically many times longer than they are wide. The cave, and the vein cluster it forms along, lies immediately below the Ballyiny Depression (Section 7.6.5) a closed, narrow, elongate depression. Flow in this cave is sub parallel to the vein set. Faunarooska has a unique shape among caves in the Burren being U shaped which accounts for its high sinuosity value. It consists of a series of NNE trending vein-controlled sections interconnected by a series of joint controlled passages. The joint controlled passages have a greater degree of lateral development. The orientations of the joint controlled passages are variable with NE-SW, EW and NW-SE joint sets being utilised. Hawthorn Cave has a general trend to the south west, along flow. The cave consists of a series of short NNE trending vein controlled sections interconnected by a series of joint controlled passages, in common to Faunarooska the orientation of these joints is variable with NE-SW, EW and NW-SE joint sets being utilises consist of a series of short joint controlled passage. The joint controlled passages consist of a series of short passages of variable orientation, which leads to the passages having a degree of lateral development. Both geometries of Faunarooska and Hawthorn cave indicate flow is normal to the vein set. Pollballyiny, similarly to Hawthorn Cave, trends NE-SW along flow, towards the end a series of NNE trending vein controlled passages occur which are coincident with the surface Ballyiny Depression.

It can be seen in these caves that the direction of flow, in this case south westwards, is a strong controlling influence of the shape of the cave. In this case as the joints of that orientation are minor the resulting caves passages consist of a series of short passages of variable orientation, with longer individual passages occurring where veins occur. Pollballyiny, Hawthorn and aspects of Faunarooska resemble the joint controlled passages of Poulnagree, which occurs 1km to the west, which has a similar flow regime.

	Poll na gCéim	Faunarooska	Hawthorn	Pollballyiny
N	72	191	73	86
Σl (m)	1201.545	1291.821	244.779	1567.3614
Mean (m)	16.688125	6.7634607	3.353137	18.225133
Median (m)	31.543	5.027	2.8935	13.737
σ (m)	17.18637685	5.7131442	1.8858419	14.495807
Range	98.887	36.212	11.684	103.3
Sinuosity	1.12	3.14	1.45	1.37

Σl (m) = Sum of the length, **σ (m) =** standard deviation

Table 6.8: statistics for Northwestern side of Slieve Elva caves

From °	To °	Poll na gCéim	Faunarooska	Hawthorn	Pollballyiny
0	10	19.76	12.26	5.83	9.18
10	20	38.40	8.17	10.05	3.17
20	30	23.73	4.62	10.89	4.17
30	40	0.24	8.79	4.19	15.46
40	50	0.00	11.02	6.70	9.23
50	60	1.44	11.99	12.70	12.49
60	70	0.55	6.04	7.08	7.64
70	80	0.67	4.37	9.27	14.38
80	90	1.97	3.50	5.12	10.58
90	100	0.00	4.37	4.22	4.24
100	110	0.40	2.40	5.16	1.92
110	120	0.00	1.55	4.48	1.08
120	130	4.05	2.93	6.21	2.26
130	140	0.71	2.17	1.24	0.60
140	150	0.09	6.22	0.00	0.79
150	160	2.57	1.95	3.30	0.87
160	170	0.98	2.68	1.73	1.02
170	180	1.94	4.97	1.83	0.94

Table 6.9: % of Σ l per ten-degree bin

6.5.5: Coolagh Valley

6.5.5.1: Pol an Ionain: Grid reference: 111187 202366, Alt: 72 m OD

Pol an Ionain consists of a series of NE-SW trending joint controlled region connecting adjacent NNE trending vein controlled passages. The main chamber appears to have been formed along a large vein cluster with an apparent increase in the frequency of veins towards the main chamber. The geometry of the cave indicates oblique flow to the vein set with a component of sub parallel flow along certain chambers.

	Pol an Ionain
N	141.00
Σl (m)	659.79
Mean (m)	4.68
Median (m)	3.00
σ (m)	5.19
Range	45.43
Sinuosity	1.64

Σl (m) = Sum of the length, **σ (m) =** standard deviation

Table 6.10: statistics for Pol an Ionain cave

From °	To °	Pol an Ionain	From °	To °		From °	To °	
0	10	7.95	60	70	6.03	120	130	0.54
10	20	12.39	70	80	4.05	130	140	0.62
20	30	8.31	80	90	3.09	140	150	1.64
30	40	6.43	90	100	2.97	150	160	0.82
40	50	16.74	100	110	4.11	160	170	4.71
50	60	6.09	110	120	5.01	170	180	8.50

Table 6.11: % of Σ l per ten-degree bin

6.5.6: Eastern side of Slieve Elva

6.5.6.1: Poulnagollum: Grid reference: 115625 204500, Alt: 262m OD

6.5.6.2: Pollcragreagh: Grid reference: 116050 202430, Alt: 183m OD

6.5.6.3: Pollcahercloggaun: Grid reference: 115640 202110, Alt: 179m OD

Flow in this region is to the southeast to Killeany and St Brendan's Well springs. Poulnagollum is a long horizontal cave system consisting of a series of long NW-SE orientated joint controlled passages connecting a series of NNE trending vein controlled sections. The cave reports (Tratman 1969, Self 1981, Mullan & Drew 2003) mention a number of NNE trending narrow canyon passages, some of which can be seen to "follow a calcite vein". The NNE trending passages account for 29% of the total length of the system. The NW-SE trending passages account for 26% of the total length of the system. Pollcragreagh consist of two narrow NNE trending vein controlled sections connected by a NW-SE trending joint controlled section with a larger amount of lateral development. The perpendicular distance between the veins is 140m; the veins can be followed along trend to coincide with vein-controlled passages in Poulnagollum to the north and in Pollcahercloggaun to the south. Pollcahercloggaun consist of a series of long NW-SE trending joint controlled passages which conned adjacent NNE trending vein controlled passages.

In this region NNE trending and NW-SE trending passages dominate, the NE-SW passages that were seen in the areas to the west (Western Knockauns, Western Slieve Elva) where the flow direction is to the south west and west, are rare in this area. The appearance of the caves are different, with the caves being longer, having a lower sinuosity value and the joint controlled passages appear to be longer. The geometries of the caves are strongly indicative of oblique flow of groundwater to the main vein set.

	Poulnagollum	Pollcragreagh	Pollcahercloggaun
N	412	51	36
Σl (m)	8221.38	426.98	1984.53
Mean (m)	19.95	8.37	55.13
Median (m)	14.84	5.61	41.30
σ (m)	17.78	9.96	38.02
Range	174.46	69.64	163.18
Sinuosity	1.16/1.28	1.22	1.04

Σl (m) = Sum of the length, **σ (m) =** standard deviation

Table 6.12: statistics for the Eastern side of Slieve Elva caves

From °	To °	Poulnagollum	Pollcragreagh	Pollcahercloggaun
0	10	12.29	15.90	34.28
10	20	6.37	22.41	17.96
20	30	2.78	8.87	1.74
30	40	3.42	4.40	0.00
40	50	1.50	1.36	1.57
50	60	0.67	6.16	0.00
60	70	0.46	0.00	0.00
70	80	0.46	0.00	0.00
80	90	2.21	0.00	0.00
90	100	1.98	5.69	0.00
100	110	2.70	3.95	0.00
110	120	5.19	0.00	0.00
120	130	6.79	0.00	0.52
130	140	10.94	11.16	7.32
140	150	8.66	8.57	2.08
150	160	12.19	3.11	10.14
160	170	9.24	5.11	12.75
170	180	11.02	3.32	11.65

Table 6.13: % of Σ l per ten-degree bin

6.5.7: Western Poulacapple

6.5.7.1: Cullaun 1: Grid reference: 118110 205400, Alt: 218m OD

6.5.7.2: Cullaun 3: Grid reference: 118490 201660, Alt: 210m OD

Flow is to the southwest to St Brendan's Spring. Cullaun 1 consists of two parallel vein controlled sections; the further west section is known as "Gaffers Gulch Old Streamway" and is located along an "eroded calcite vein" (Self 1981, Mullan & Drew 2003). The narrow vein controlled sections are connected via a NE-SW/EW joint controlled section with a substantial lateral development (108m over a length of 265m). The two caves run parallel to each other. Cullaun 3 is the longest cave in the area, consisting of a single passage just under 3km long. The cave consists of a series of narrow elongate vein controlled passages trending NNE that are interconnected by joint controlled passages of varying orientation, principally NE-SW, EW and NW-SE. Flow in these caves is oblique to the vein set.

	Cullaun 1	Cullaun 3
N	84	42
Σl (m)	2014.35	2812.57
Mean (m)	23.98	66.97
Median (m)	20.34	59.91
σ (m)	14.81	41.40
Range	77.85	192.13
Sinuosity	1.13/1.05	1.13

Σl (m) = Sum of the length, **σ (m) =** standard deviation

Table 6.14: statistics for the Western Poulacapple caves

From °	To °	Cullaun 1	Cullaun 3
0	10	26.34	22.20
10	20	7.79	16.42
20	30	13.77	15.92
30	40	6.90	9.11
40	50	9.95	5.34
50	60	5.77	6.26
60	70	4.60	0.00
70	80	1.55	4.21
80	90	1.38	0.00
90	100	5.34	2.33
100	110	0.00	0.00
110	120	0.00	0.81
120	130	0.00	0.00
130	140	0.47	2.19
140	150	0.60	1.17
150	160	1.30	4.68
160	170	3.13	2.23
170	180	1.15	3.95

Table 6.15: % of Σ l per ten-degree bin

In this region NNE trending dominate, the NE-SW passages that were seen in the areas to the west (Western Knockauns, Western Slieve Elva), where the flow direction is similar, make a return, the NW-SE joints which make up a large portion of the caves directly opposite the valley on the eastern side of Slieve Elva are less frequent in these two cave systems. The flow direction exerts a strong controlling influence on the joints sets that are utilised.

6.5.8: Eastern Poulacapple

6.5.8.1: Gragan: Grid reference: 119220 202400, Alt: 210m OD

6.5.8.2: Green Streams: Grid reference: 119171 202772, Alt: 235m OD

6.5.8.2: Doonyvardan: Grid reference: 119520 201665, Alt: 210m OD

Flow is to the southeast where the waters resurge at Fergus Springs. The caves are a series of overlapping conduits, which run parallel to each other. The caves show no indication of linking together so therefore there must be a number of parallel systems (Mullan & Drew 2003). The three caves are only tens of metres apart. Green Steams Cave is a single narrow canyon. Gragan Cave is overlapped to the north by Green Stream Cave and Doonyvardan Cave to the south though it is independent from both (Self 1981, Mullan & Drew 2003). Gragan Cave consists of a series of NNE trending passages connected by a series of linear NW-SE trending joint controlled sect. Green Streams Cave consists of three adjacent NNE trending sections connected by NW-SE orientated joint controlled passages. These two caves have very low sinuosity values, 1.09 and 1.04 respectively. Doonyvardan Cave has a higher sinuosity value of 1.38, which reflects the wider variation in the orientation of its cave passages. The NNE trending vein and NW-SE joints are the dominant control though minor amounts of NE-SW and EW trending cross-joints occur. AS with the previous region flow in these caves in oblique to the vein set

	Gragan	Green Streams	Doonyvardan
N	79	8	97
Σl (m)	2355.87	360.44	1927.74
Mean (m)	29.82	45.06	19.87
Median (m)	23.55	40.80	12.03
σ (m)	20.87	28.17	18.55
Range	110.19	74.02	109.13
Sinuosity	1.09	1.04	1.38

Σl (m) = Sum of the length, **σ (m) =** standard deviation

Table 6.16: statistics for the caves of Eastern Poulacapple.

The veins can be followed along trend to be seen to control cave passages in all three caves. In common with the caves along the Eastern side of Slieve Elva the NW-SE direction of flow has a strong control on the joints that are used to form the cave. In this area the NW-SE trending set that has been studied at Cappanawalla to the north, are utilised to create long parallel running adjacent cave systems that have a lower sinuosity value than the NE-SW trending cross joints which are commonly utilised by south westward flow are rare.

From °	To °	Gragan	Green Streams	Doonyvardan
0	10	18.80	24.57	7.01
10	20	6.97	0.00	8.54
20	30	5.54	0.00	1.02
30	40	5.31	0.00	2.39
40	50	0.86	0.00	0.95
50	60	0.49	0.00	1.55
60	70	1.63	0.00	0.00
70	80	1.33	0.00	1.78
80	90	0.00	0.00	0.00
90	100	0.00	0.00	0.29
100	110	3.01	0.00	1.55
110	120	7.91	0.00	0.86
120	130	1.70	0.00	8.22
130	140	9.19	0.00	13.76
140	150	5.43	35.43	9.59
150	160	5.97	4.03	8.34
160	170	8.52	23.24	18.55
170	180	17.33	12.78	15.59

Table 6.17: % of Σ l per ten-degree bin

6.5.9: Southern Poulacapple

6.5.9.1: Cullaun 5: Grid reference: 118560 201050, Alt: 190m OD

Flow is to the southeast, to the Fergus River spring though on occasion it drains to west to St Brendan's Spring (Drew 1988). The caves consists of a series of parallel NNE trending vein controlled low sinuosity passages interconnected by joint controlled sections.

	Cullaun 5
N	197
Σl (m)	3765.69
Mean (m)	19.12
Median (m)	14.67
σ (m)	14.00
Range	90.63
Sinuosity	1.19/1.05/1.26

Σl (m) = Sum of the length, **σ (m) =** standard deviation

Table 6.18: statistics for Cullaun 5.

The NW-SE trending joints are dominant due to the southeastward flow direction. There are a minor amount of NE-SW and EW joints in the system, presumably a function of the occasional flow to St Brendan's Spring

to the west. The veins can be followed along strike to the north to be seen to have an influence on the three caves that lie along the eastern edge of Poulacapple. The shape of the cave is consistent with flow being oblique to the vein set

From °	To °	Cullaun 5	From °	To °	
0	10	23.50	90	100	1.25
10	20	8.60	100	110	2.72
20	30	11.72	110	120	1.05
30	40	6.71	120	130	4.24
40	50	2.83	130	140	5.98
50	60	1.10	140	150	4.02
60	70	1.35	150	160	3.96
70	80	2.15	160	170	4.14
80	90	1.34	170	180	13.36

Table 6.19: % of Σ l per ten-degree bin

6.5.10: North of Kilfenora

6.5.10.1: Pollcahermaan: Grid reference: 118671 199427, Alt: 60m OD

6.5.10.2: Poulawillin: Grid reference: 119700 199460, Alt: 171m OD

Pollcahermaan is a narrow linear stream way cave that is strongly aligned NNE (flow being sub parallel to the vein set). It follows a series of calcite veins, which can be followed to the end of the cave (Mullan & Drew 2003), which are so prominent it has been described as "if someone painted a white line along the top of the cave passage" (Drew pers. comm 2002). The cave has a lateral variation of less than 12m over its length. The cave is parallel to vein dominated cave passages seen in other caves in this region. The vein cluster can be followed along strike to coincide with vein clusters in the caves along the eastern edge of Poulacapple. Poulawillin is a horizontal cave which consists of adjacent vein controlled passages being connected by EW and NE-SW trending joint controlled passages. These caves occur within the Fergus-Elmvale catchment and as such will follow the hydrological gradient and flow towards Fergus springs to the south west, though there will occasional flow to St Brendan's Spring to the west which would explain the utilisation of the EW trending cross joint set as seen in Poulawillin.

	Pollcahermaan	Poulawillin
N	51	63
Σl (m)	903.48	950.93
Mean (m)	17.72	15.09
Median (m)	14.13	11.93
σ (m)	10.28	10.69
Range	61.41	56.61
Sinuosity	1.05	1.28

Σl (m) = Sum of the length, **σ (m) =** standard deviation

Table 6.20: statistics for caves north of Kilfenora.

From °	To °	Pollcahermaan	Poulawillin	From °	To °	Pollcahermaan	Poulawillin
0	10	19.47	5.30	90	100	2.41	19.57
10	20	27.44	12.48	100	110	0.00	3.87
20	30	34.09	10.94	110	120	0.00	2.48
30	40	5.29	4.29	120	130	0.00	5.95
40	50	2.63	6.49	130	140	0.00	0.00
50	60	1.01	5.97	140	150	0.00	0.00
60	70	0.00	3.54	150	160	0.00	0.00
70	80	0.00	5.28	160	170	0.00	2.88
80	90	2.37	5.86	170	180	5.32	5.10

Table 6.21: % of Σ l per ten-degree bin

6.5.11: South Central Burren

6.5.11.1: Kilcorney: Grid reference: 114180 204440, Alt: 263m OD

Kilcorney Cave also known as the Cave of Wild Horses, is a 510m long largely relict cave system located in the High Burren on the southern edge of the Kilcorney Depression. The Depression it self is located along a large NNE trending vein cluster that controls the location of the cluster of enclosed depression along the western side of Aillwee Hill. The cave has had a complex hydrological history, a fact borne out by the varied orientation of the cave passages which show traces of flow oblique, normal and sub parallel to the vein set. It consists of sections of vadose altered phreatic passages and more recent vadose passages. Stalagmites dated from the older phreatic tubes yield an age of 41,000 BP (Drew pers comm. in Boycott *et al* 1983). The older sections of the cave are thought to predate the formation of the Kilcorney depression. The active sections of the cave are believed to resurge at the Fergus Springs 6.6km to the south-southwest. The vein-controlled passages are narrow elongate features NNE trending cave passages. The variability of the joint pattern as utilised by the cave passages illustrates the complex hydrological history of the cave, NW-SE, NE-SW and EW trending joints all have a similar contribution to the length of the cave system. The NW-SE trending sections exhibit different characteristics to the sections dominated by the NE-SW and EW sections, they are longer, less sinuous features, while the cross joint dominated sections consist of shorter, more sinuous passages with a more variable orientation manifesting the shorter nature of these cross joint sets. The NNE and NW-SE orientated sections mirror the orientation of the large Kilcorney Depression that has formed above the cave system (Section 7.7.1.3).

	Kilcorney
N	158
Σl (m)	512.30
Mean (m)	3.24
Median (m)	1.98
σ (m)	3.15
Range	18
Sinuosity	/

Σl (m) = Sum of the length, **σ (m) =** standard deviation

Table 6.22: statistics for Kilcorney Cave

From °	To °	Kilcorney	From °	To °	Kilcorney
0	10	22.96	90	100	8.79
10	20	3.17	100	110	3.15
20	30	2.87	110	120	4.81
30	40	3.43	120	130	4.75
40	50	6.63	130	140	10.00
50	60	3.87	140	150	4.35
60	70	8.79	150	160	3.17
70	80	2.53	160	170	2.30
80	90	3.23	170	180	1.21

Table 6.23: % of Σ l per ten-degree bin

6.5.12: South Eastern Burren

6.5.12.1: Seven Streams of Teeskagh: Grid reference: 128530 196120, Alt: 75m OD

The NE-SW trending cave passages are linked by a combination of NS and EW controlled sections of cave passages. The NW-SE fractures increase in frequency towards the end, southeast, of the cave. The NE-SW fractures are associated with a synclinal axis with the cave forming on or close to the fold axis (Bunce 1994). There are a number of NE-SW trending monocline features in this region; the Carran Depression to the northeast is controlled along a monocline as the valley that Lough Aleenaun Turlough occupies to the north-west (Drew 1988). The fractures that control the shape of the cave are similar to fracture patterns mapped on an equivalent unit at Sheyshmore 4km to the west. The fracture pattern at this location consists of EW systematic joints with cross joints of varying orientation and clustered NS veins, which have a spread of 10° either side of 000° with a series of NE-SW trending fractures increasing in frequency towards the fold axis that is present in the valley to the south-east occupied in part by Lough Aleenaun, which mirrors that seen in this cave system.

	Seven Streams
N	77
Σl (m)	80.28
Mean (m)	1.04
Median (m)	0.66
σ (m)	1.03
Range	5.04
Sinuosity	2.28

Σl (m) = Sum of the length, **σ (m) =** standard deviation

Table 6.24: statistics for the Seven Streams of Teeskagh Cave

The cave drains southwest to the Fergus River Cave (Section 6.3.8) possibly along the fold axis. The southerly section of the Fergus River Cave is formed along a fractures associated with a fold axis of the same

trend as the one that forms Seven Streams Cave. The cave shape is representative of flow oblique to the vein set.

From °	To °	Seven Streams	From °	To °	Seven Streams
0	10	2.520	90	100	12.772
10	20	3.460	100	110	3.984
20	30	4.320	110	120	11.775
30	40	26.354	120	130	0.872
40	50	2.823	130	140	4.695
50	60	2.230	140	150	0.397
60	70	6.348	150	160	5.741
70	80	0.681	160	170	2.135
80	90	2.836	170	180	6.055

Table 6.25: % of Σ l per ten-degree bin

6.5.13: Upper Fergus River

6.5.13.1: Fergus River Cave: Grid reference: 125200 192269, Alt: 45m OD

The Fergus River Cave is a horizontal, down dip, fracture controlled cave system draining to the south. It is the resurgence for an 115km^2 catchment area. Flow is sub parallel to the vein set with the resultant chambers beings highly developed along the vein network. The cave is dominated by a large cluster of NNE trending veins that create the large chamber of the cave; veins appear to increase in frequency towards the main cluster. Towards the south the cave passage is controlled by NE-SW fractures associated with regional monocline folds of the same trend (Drew 1988). At Sheyshmore it can bee seen that these fractures increase in frequency towards the fold axis. A large number of passages are controlled by EW jointing, reflecting similarities to the NNE vein and EW joint patterns observed on Sheyshmore in the Ballyelly Member 2.5km to the north. The southerly section of the Fergus River Cave is formed along a fractures associated with a fold axis of the same trend as the one that forms Seven Streams Cave.

	Fergus River Cave
N	306
Σl (m)	2688.09
Mean (m)	8.78
Median (m)	6.34
σ (m)	10.70
Range	53.29
Sinuosity	1.53

Table 6.26: statistics for Fergus River Cave

From °	To °	Fergus River Cave	From °	To °	Fergus River Cave
0	10	2.54	90	100	4.89
10	20	12.66	100	110	0.42
20	30	9.78	110	120	1.42
30	40	3.61	120	130	2.19
40	50	3.80	130	140	2.57
50	60	5.11	140	150	2.45
60	70	3.39	150	160	8.38
70	80	2.14	160	170	3.52
80	90	2.54	170	180	5.50

Table 6.27: % of Σ l per ten-degree bin

6.6 Conclusion.

- NNE trending vein controlled passages are the dominant control on the cave passages.
- The veins can be followed along strike to be seen to have an influence of other caves along strike.
- The NNE trending passages are narrow, long, parallel features
- Calcite filled veins are occasionally seen in caves
- There is a correlation between the NNE trending cave passages and surface features, the Ballyiny Depression is coincident with Poll Na gCéim, Aillwee Cave is coincident with a series of depressions on the surface.
- The direction of flow has a strong control on the orientation of the joints that are utilised to make up the cave system.
- South-westward flow utilises the NE-SW and EW cross joints, with the passages having a higher sinuosity, this is the case at Doolin, Western Knockauns, Coolagh Valley, North West Slieve Elva and Western Poulacapple
- Southeastward flow utilises the NW-SE joint set producing longer passages with a lower sinuosity, this is the case along the eastern side of Slieve Elva, eastern and southern side of Poulacapple.

6.7 Discussion

Caves in the Burren are non-randomly located; their location is controlled by the fracture pattern. The caves in the Burren are for the most part horizontal cave features being confined to the same geological unit for most of their length. The Upper Faunal Zone at the base of the Ballyelly Member and the Lower Faunal Zone at the base of the Fahee North Member of the Slievenaglasha Formation exert a strong controlling influence on the vertical extent of the cave systems acting as aquitards to prevent vertical propogation. Vertical propogation only occurs when NNE trending vein clusters break through these aquitards such as at Poll na gCéim. The caves are representative features of layer parallel flow being controlled by the fracture pattern of the bed they are confined to. They are effectively two dimensional flow features which can be modelled, described and understood by two dimensional fracture patterns.

In the Burren the limestone constitutes an impermeable matrix, confining flow to that part of the fracture network that consists of a series of interconnected line segments with no dead ends; the fracture backbone. The caves are localised along and define the fracture backbone, effectively mapping the fracture pattern of the beds they occur in. The makeup of the fracture backbone is dependent on the orientation, size, density, spatial distribution and degree to which the fractures interact; the connectivity, of the fracture network. The fracture pattern was mapped and analysed at two separate locations, Cappanawalla and Sheyshmore. The fracture pattern consisted of a series of NNE trending, clustered, non strata bound veins and a set of systematic regularly spaced, strata-bound joints, which have an NW-SE orientation at Cappanawalla and EW at Sheyshmore, with minor cross joints at a variety of orientations. The backbone of the two dimensional fracture networks was created and analysed from these fracture systems. It can be seen that section of the backbone are joint controlled and sections are vein controlled. The vein clusters, which define the vein controlled regions, through their interaction with the joints have a large proportion of cross termination (Px) and a low proportion of blind termination (Pb) as well as a high intersection density creating a narrow, high connectivity backbone. The joints have lower proportions of cross terminations and higher proportions of blind terminations and are not as well linked spatially defining lower connectivity backbones. The shape, length and orientation of the caves depends on the section of the backbone they occur in, cave passages in vein controlled backbones are elongate narrow features, with adjacent veins passages being connected by short joint controlled passages, they are typically many times longer than wider. Cave passages in joint controlled backbones typically have a greater lateral variation and serve to connect adjacent vein cluster controlled passages. Adjacent caves can be seen to be controlled by the same vein clusters; Hawthorn Cave and Faunarooska Cave have vein-controlled passages that can be attributed to the same vein cluster as do Pollcragreagh and Pollcahercloggaun caves. The vertical persistence of the vein clusters extends for over 110m in Aillwee cave where the vein controlled section lies immediately below a series of vein controlled surface depressions, and for over 180m in Poll Na gCéim, where the deepest cave in the Burren is formed along an intense non strata-bound vein cluster.

The vein fill is preferentially eroded compared to the surrounding bedrock. The vein fill is for the main part Calcite with minor amounts of Fluorite, Lead, Copper, Silver and Zinc (see Appendix 4.1 for more details on the vein fill). Vein fill is rarely seen on the surface except where it has been protected by rock pedestals, in these regions the fill can be seen, as you continue along strike the fill is seen to be eroded away, and the area the fill used to occupy is lower than the surrounding limestone. In caves veins are only rarely recorded, Pollcahermaan being a notable exception, in other caves the caving reports describe, "passage follows eroded calcite vein" (Mullan & Drew 2003) as at Cullaun 1. Preparing a block of both materials, measuring and weighing them accurately and placing them in a solution of weak carbonic acid to simulate the carbonation reaction that takes place could test the difference in the solubility between pure Calcite and the limestone's in the Burren. The blocks would be measured and weighed over a period of time in addition to the solution being tested for the proportion of Calcium and HCO^{-}_{3} contained in it, which are by products of the carbonation reaction between Limestone/ Calcite and the carbonic acid. This experiment repeated a number of times and over a number of time duration's should give a measure of the solubility of the two materials.

The local hydrological conditions, in the form of hydrological gradient, topography, location of resurgences and location of inputs, particularly localised sinking streams along the Namurian margin, exert a strong control on the shape of the cave systems in the form of the joint patterns utilised along the caves flow path. The caves discussed have formed under one or more of three different flow regimes, which result in different shapes of the cave systems as show in Figure 6.57.

1. Flow sub-parallel to the vein set
2. Flow oblique to the vein set
3. Flow normal to the vein set

Flow sub-parallel to the vein set (Figure 6.57b): These caves are strongly aligned along the vein sets with a low sinuosity and a direct flow path from input to output. Caves that are formed under this flow regime are dominated by the NNE trending vein sets with a minor amount of the cave passages being controlled by joints. The rose diagrams and length profiles of these caves reflect this fact. Examples of these caves are Poll Na gCéim, Pollcahermaan, the Fergus River cave and sections Aillwee and Cullaun caves. Where these caves are formed they are located along zones of intense clustering of veins and are often associated with surface topographic features, Ballyiny Depression and Aillwee depressions, and vertical propagation of the caves or flow in excess of 100m, Poll Na gCéim is 181m deep, in the vein controlled portion of Aillwee cave rainfall quickly percolates from the surface to swell the small streams in this section.

Flow oblique to the vein set (Figure 6.57c): Caves formed under this flow regime are typically located along the hydrologically active zone adjacent to the Namurian strata. The active caves are sourced from surface drainage off the Namurian areas of Poulacapple, Knockauns Mountain and Slieve Elva. The orientation of the caves is dependent on the relief and flow direction of the streams. Water draining to the west will utilise the NE-SW trending joints as they trend in the direction of flow producing NE-SW trending cave passages intersecting a number of vein clusters which the flow will utilise until it is captured by a joint controlled region. Water draining to the east will utilise the NW-SE trending joints as they trend in the direction of flow, producing long NW-SE trending cave passages intersecting vein clusters which the flow will utilise until it is captured by a joint controlled region.

Flow normal to the vein set (Figure 6.57d): Caves formed under this regime are indicative of a more complicated flow history frequently showing evidence of phreatic development of passages, Aillwee Cave, Cave of the Wild Horses and Faunarooska. These caves are all understood to be reflective of an older flow regime. The passages in these caves utilise a large number of fracture orientations as is reflected by the high degree of sinuosity of the caves and the associated rose diagrams.

When the location of the all the vein controlled passages is plotted, Figure 6.55, it can be seen that individual vein clusters have an effect on a number of cave systems. If the vein clusters are continued along their trend they can be seen to be coincident with a number of surface topographic features. The veins that control passages in Aillwee and Kilcorney can be see to be coincident with the cluster of NNE trending surface depression to the west of Aillwee. The vein clusters from Pollcahermaan and Cullaun 5 can be seen to influence Doonyvardan and Gragan caves as well as being coincident with the large gully on Cappanawalla.

The caves of the Burren are a useful tool in elucidating the fracture pattern of the region. An understanding of the geometry and interaction of fracture networks derived from analysis of mapped fractures at the outcrop scale and an understanding of the formation of fracture backbones can be applied to understanding the location, shape and orientation of the cave passages of the Burren, and in turn the regional fracture pattern. The properties understood and seen to be working at metre scale can be successfully applied to fracture systems, represented by the caves, at the kilometre scale.

Name	Area (m^2)	% Total Area	% Namurian	% Slievenaglasha
Ballyvaughan	44,136,336	12.25	0.62	13.45
Bellharbour	54,036,828	15	0	11.58
Caher	15,160,816	4.21	0	16.19
Corranoo	4,191,650	1.16	0	0
Derren-Trawee	16,386,045	4.55	6.612	22.96
Fergus-Elmvale	119,922,520	33.3	12.31	63.64
Fergus Lower	13,433,096	3.63	0	46
Fisherstreet	9,151,668	2.54	83	16
Killeaney	11,208,613	3.11	40.4	48
Kinvarra	26,391,312	6.33	0	14.5
Poulsallagh	18,232,602	5.06	44.65	28.8
St Brendan's	10,436,085	2.9	30.3	69.6

Table 6.28: Area of catchments and percentage cover of Namurian and Slievenaglasha Formations.

Geographic Region	Cave Name	1	2	3	4
Doolin Valley	Doolin	NNE	EW	NE-SW	
Western Knockauns	Poulnagree	NNE	EW	NE-SW	
	Robbers Den	NNE	NW-SE		
	Through & Through	NW-SE	NNE	NE-SW	
	Moonmilk	EW	NNE	NW-SW	NW-SE
NW side of Slieve Elva	Poll Na gCéim	NNE			
	Faunarooska	NNE	NE-SW	NW-SE	
	Hawthorn	NE-SW	NNE	EW	
	Pollballyiny	NE-SW	EW	NNE	
Coolagh Valley	Pol an Ionain	NE-SW	NNE	EW	
E. side of Slieve Elva	Poulnagollum	NNE	NW-SE		
	Pollcragreagh	NNE	NW-SE		
	Pollcahercloggaun	NNE	NW-SE		
W. Poulacapple	Cullaun 1	NNE	NE-SW		
	Cullaun 3	NNE	NE-SW	NW-SE	
E. Poulacapple	Gragan	NNE	NW-SE	NE-SW	
	Green Streams	NNE	NW-SE		
	Doonyvardan	NW-SE	NNE		
S. Poulacapple	Cullaun 5	NNE	NW-SE	NE-SW	
North of Kilfenora	Pollcahermaan	NNE			
	Poulawillin	EW	NNE	NE-SW	
North Central Burren	Aillwee- Joint	NW-SE			
	Aillwee- Vein	NNE			
South Central Burren	Kilcorney	NNE	NW-SE	EW	NE-SW
South Eastern Burren	Seven Streams	NE-SW	EW		
Upper Fergus River	Fergus River	NNE	NW-SE	NE-SW	

Table 6.29 Orientation of cave passages, ranked in order of percentage of fracture population.

The dominace of the NNE vein passages can be clearly seen in this compliation Table. The areas that have south-westward flow have NE-SW joints as the primary or secondary fracture set with the south-eastward flow regions having the NW-SE joints as the secondary set.

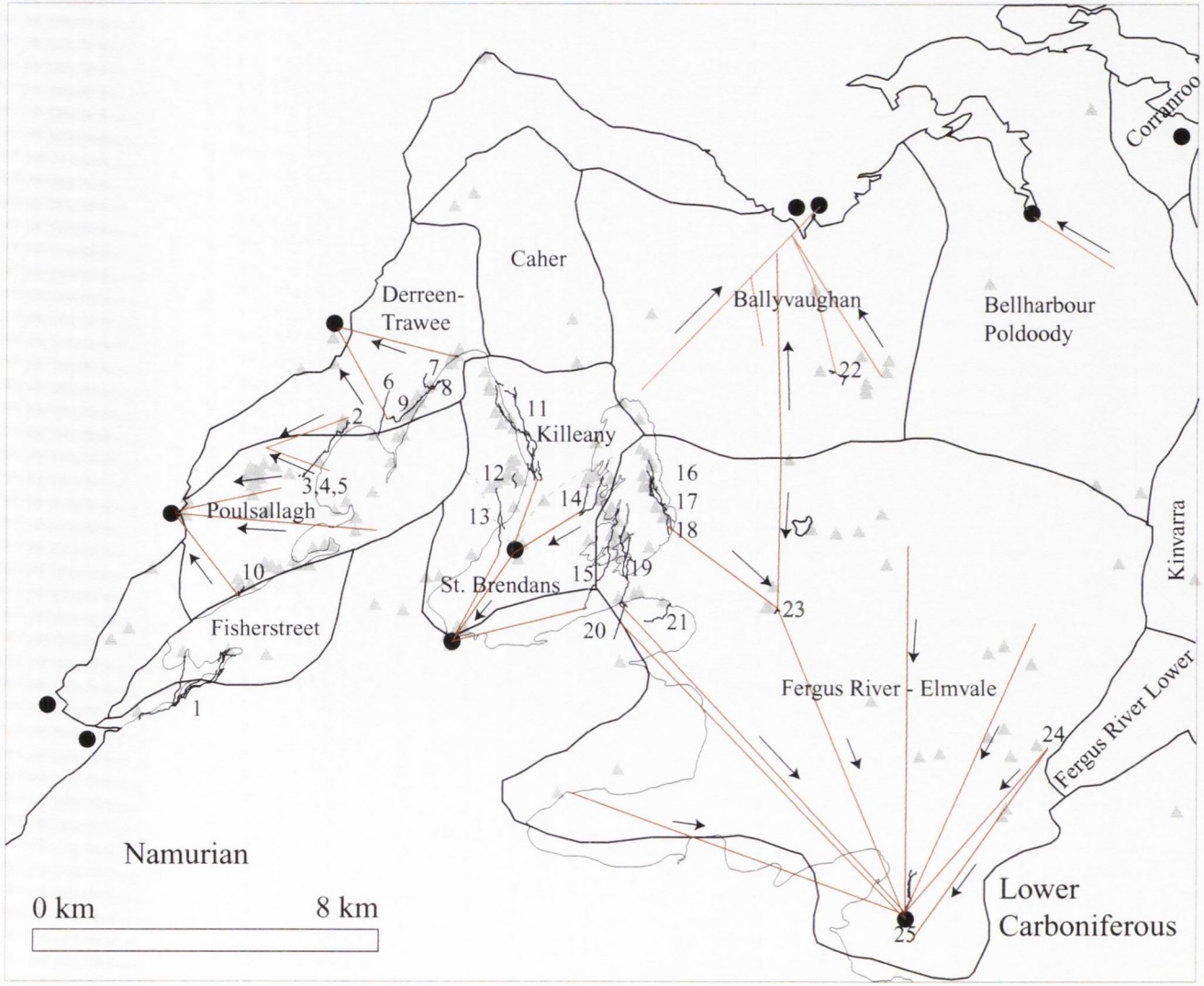

The Doolin Valley
1: Doolin cave

Western Knockauns& Oughtdarra
2: Poulnagree 3: Robbers Den
4: Through & Through 5: Moonmilk

Northwestern side of Slieve Elva
6: Poll na gCeim 7: Faunarooska
8: Hawthorm 9: Pollballyiny

Coolagh Valley
10: Pol an Ionain

Eastern Side of Slieve Elva
11: Poulnagollum 12: Pollcragreagh
13: Pollcahercloggaun

Western Poulacapple
14: Cullaun 1 15: Cullaun 3

Eastern Poulacapple
16: Gragan 17:Green Stream
18: Doonyvardan

Southern Poulacapple
19: Cullaun 5

North of Kilfenora
20: Pollcahermaan 21: Poulawillin

North Central Burren
22: Aillwee Cave

South Central Burren
23: Kilcorney

Southeastern Burren
24: Seven streams of Teeskagh

Upper Fergus River
25: Fergus River Cave

Figure 6.1: Location of the caves studied. The Namurian boundary is marked as a thick solid line, Catchments are marked as light solid lines. Catchments and springs are modified from Drew 1990. The dashed line between Killeany and St Brendans denotes that caves within the Killeany catchment drain internally initially before draining to St Brendans where they drain externally.●:Spring. ▲:Swallow hole. Flow direction's have been obtained from literature, Tratman (1969), Self (1981), Drew (1988), Drew (1990), Drew (2003).

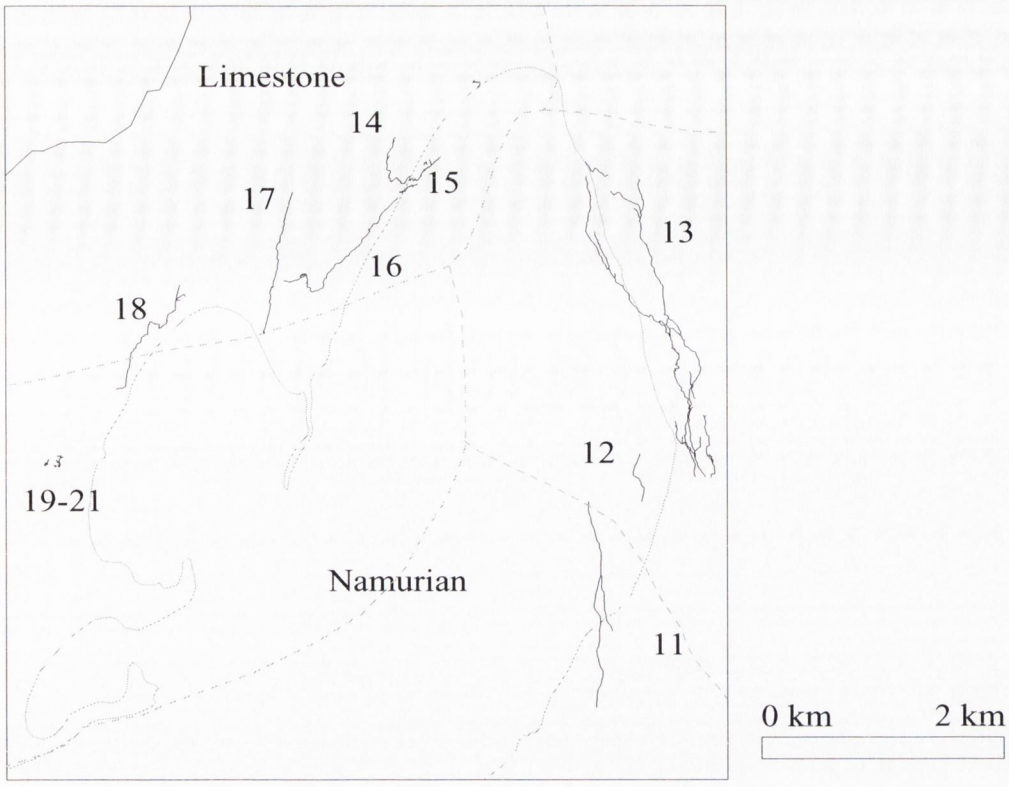

Fig 6.2: Diagram of the cave around Slieve Elva. The catchments are shown in a dashed line (see fig 6.56 for more information), the Namurian boundary in a solid line and the caves as dark solid lines.Cave numbers are the same as for Fig 6.53

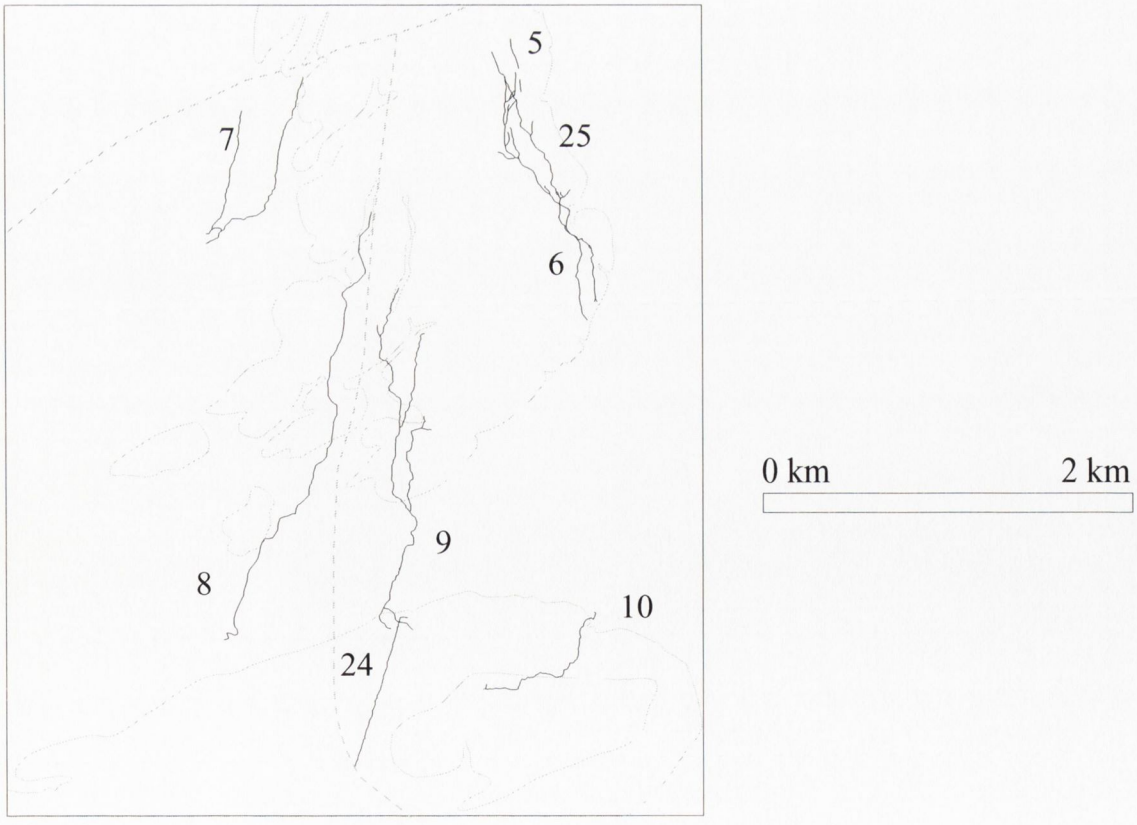

Fig 6.3: Diagram of the cave around Poulacapple.
The catchments are shown in a dashed line, the Namurian boundary in a solid line and the caves as dark solid lines.
Cave numbers are the same as for Fig 6.53

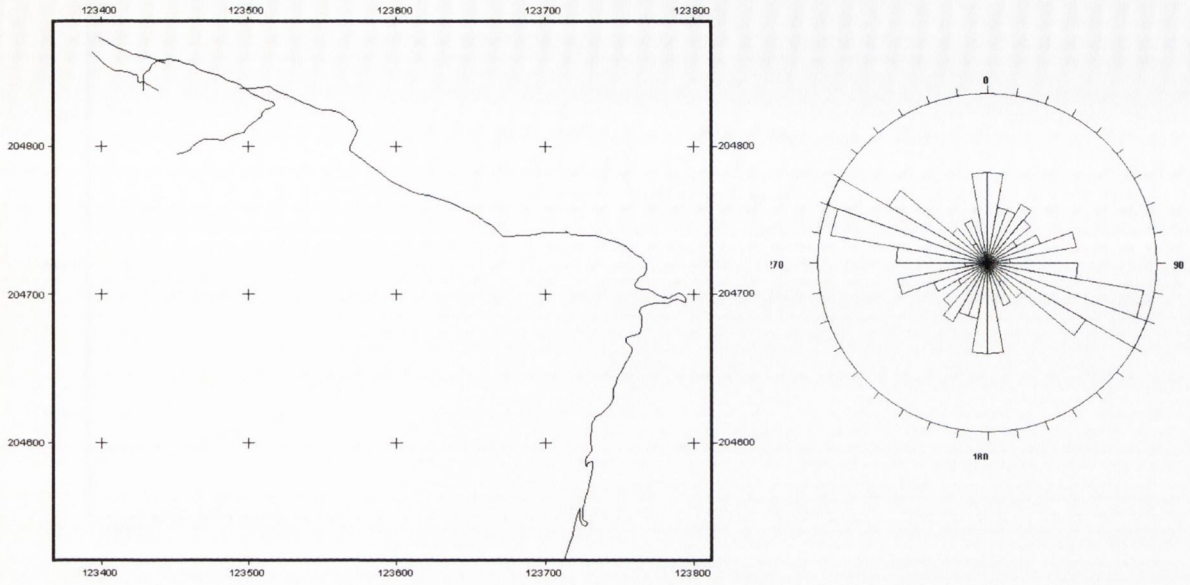

Figure 6.4: Map of cave passages in Aillwee Cave (6.5.1.1) with associated rose diagram.

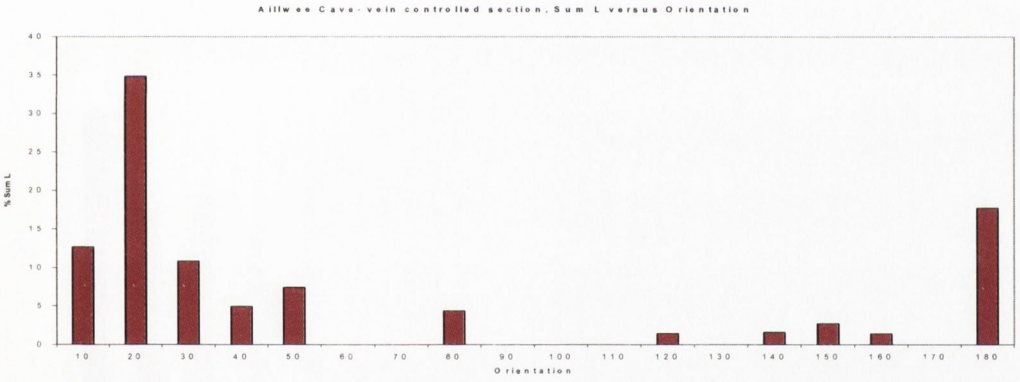

Figure 6.5: Sum Length per ten-degree bin expressed as a % for the joint controlled section.

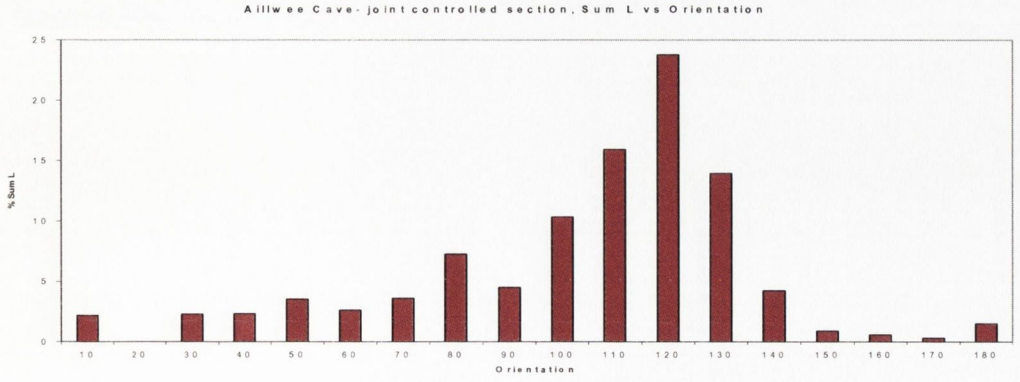

Figure 6.6 Sum Length per ten-degree bin expressed as a % for the vein controlled section.

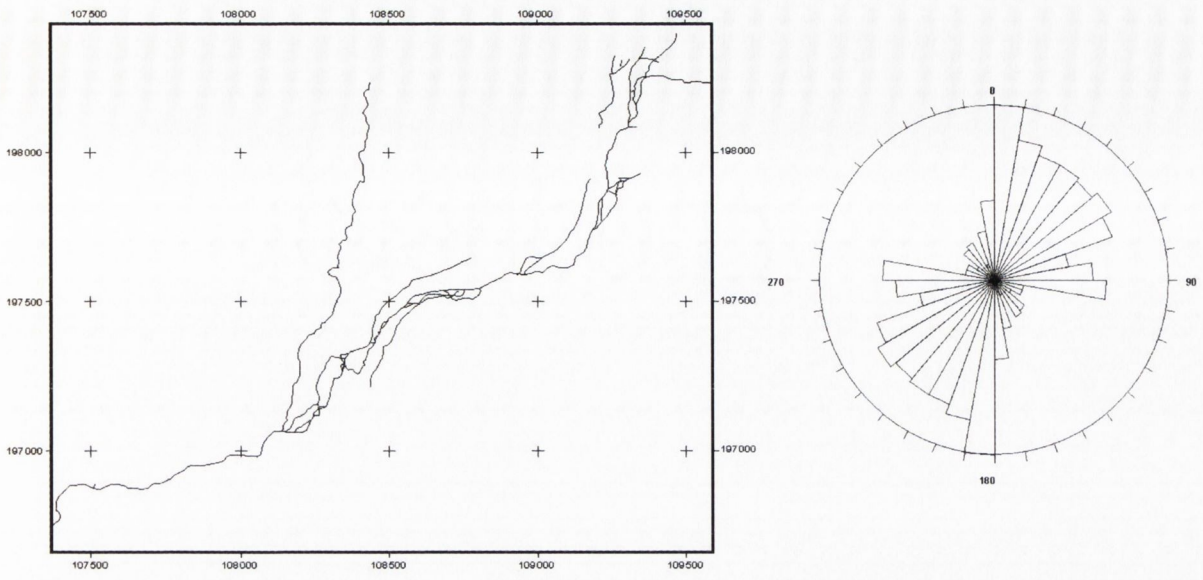

Figure 6.7: Map of cave passages in Doolin Cave (6.5.2.1) with associated rose diagram.

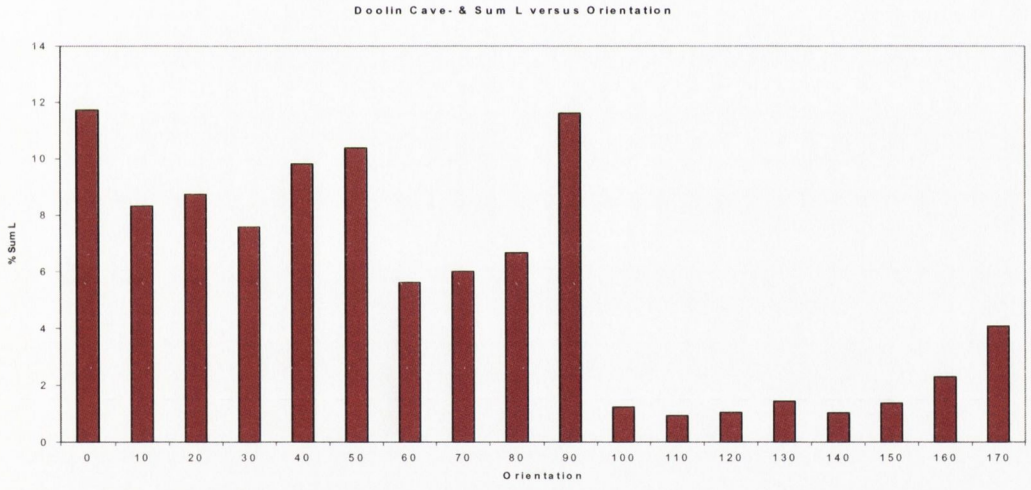

Figure 6.8: Sum Length per ten-degree bin expressed as a %.

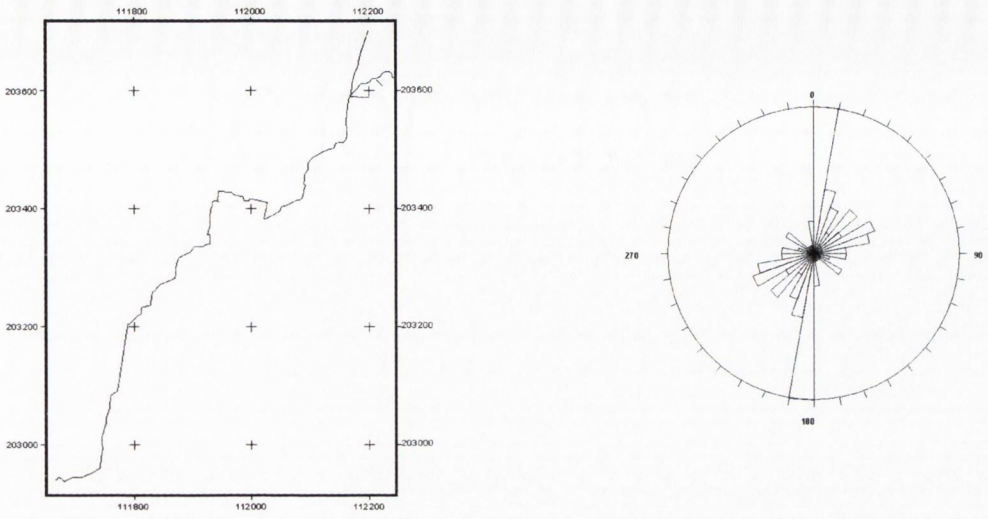

Figure 6.9: Map of cave passages in Poulnagree Cave (6.5.3.1) with associated rose diagram.

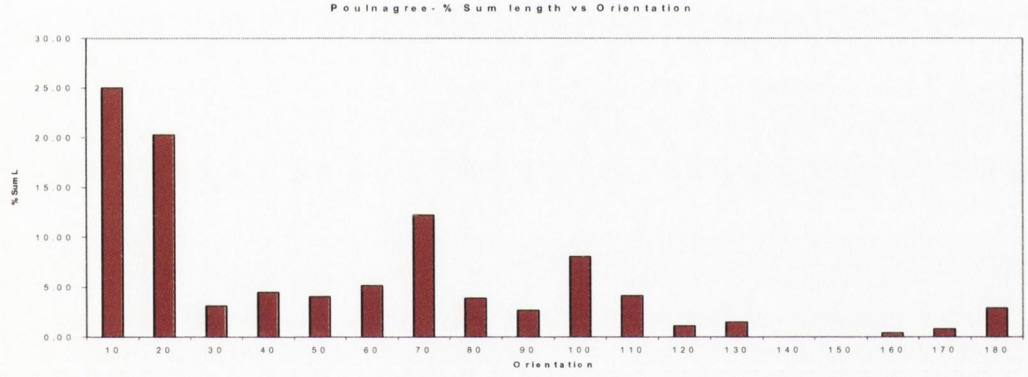

Figure 6.10: Sum Length per ten-degree bin expressed as a %.

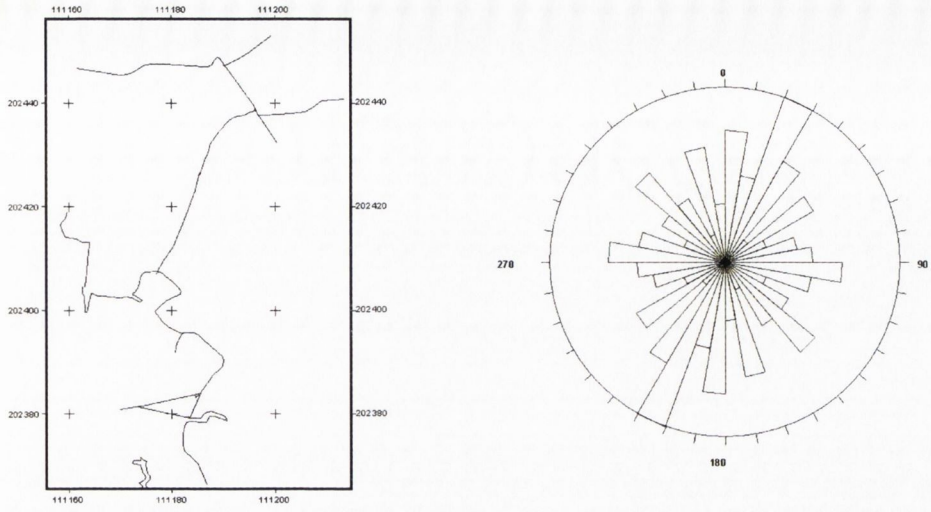

Figure 6.11: Map of cave passages in Moonmilk Cave (6.5.3.2) with associated rose diagram.

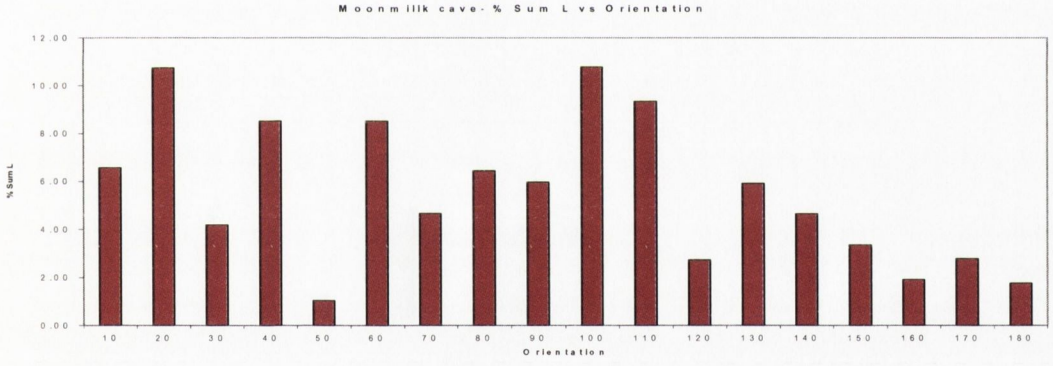

Figure 6.12: Sum Length per ten-degree bin expressed as a %.

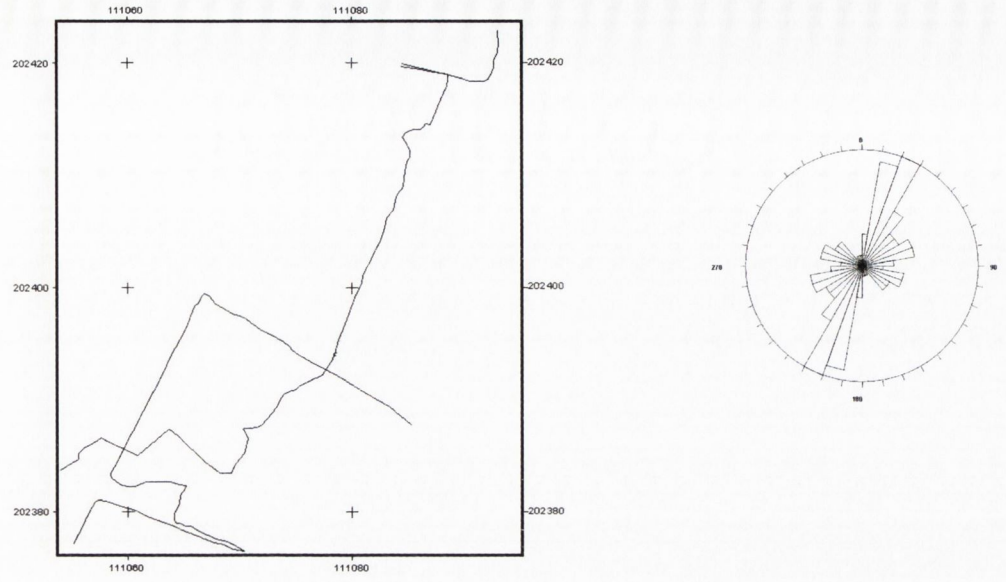

Figure 6.13: Map of cave passages in Robbers Den Cave (6.5.3.3) with associated rose diagram.

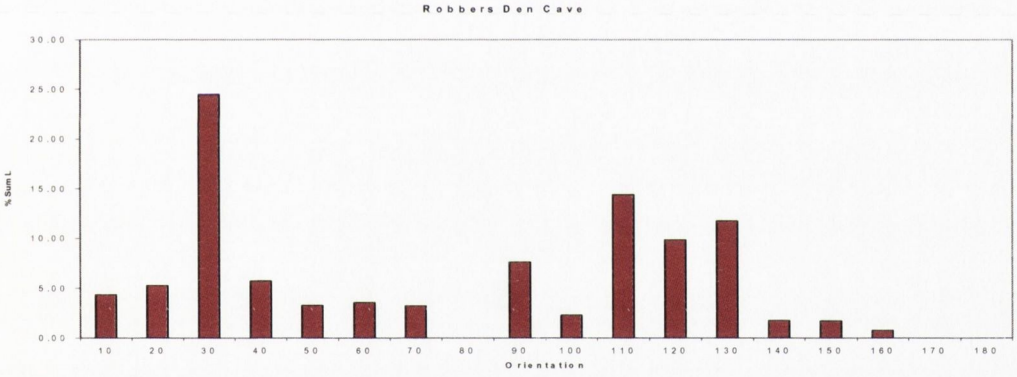

Figure 6.14: Sum Length per ten-degree bin expressed as a %.

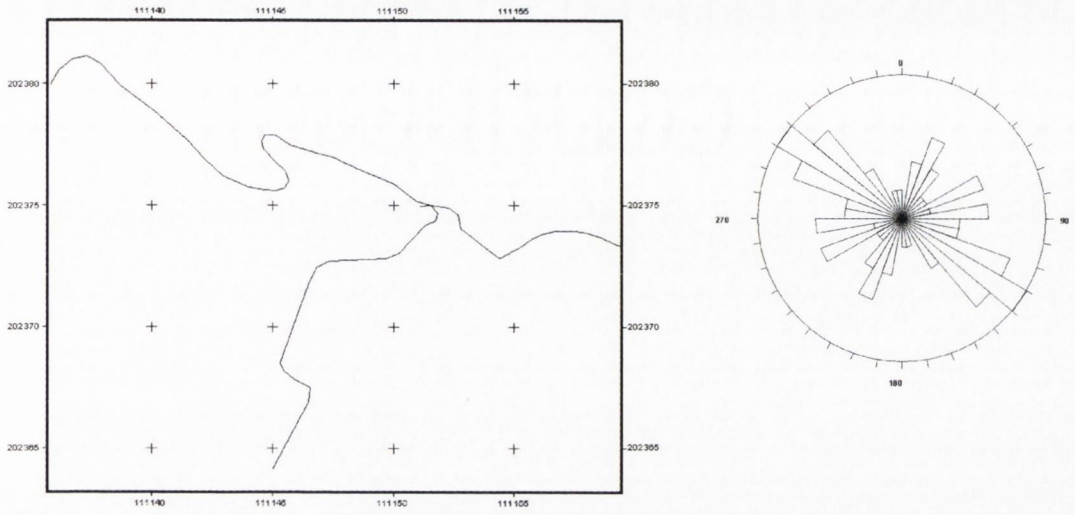

Figure 6.15: Map of cave passages in Through & Through (6.5.3.4) with associated rose diagram.

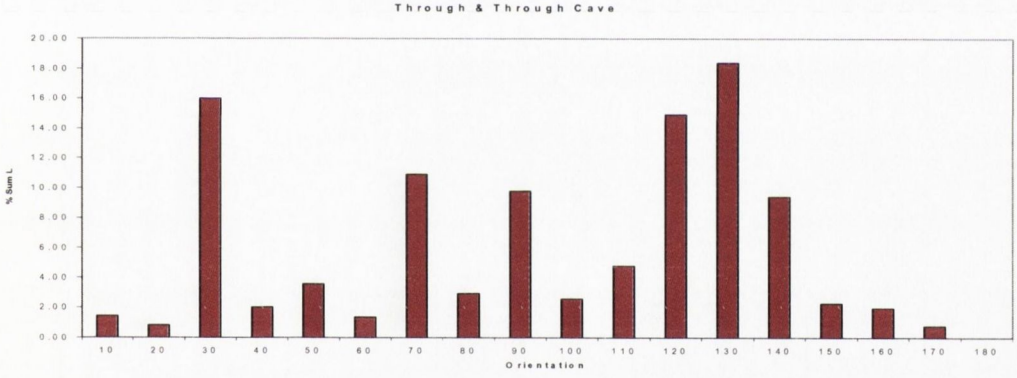

Figure 6.16: Sum Length per ten-degree bin expressed as a %.

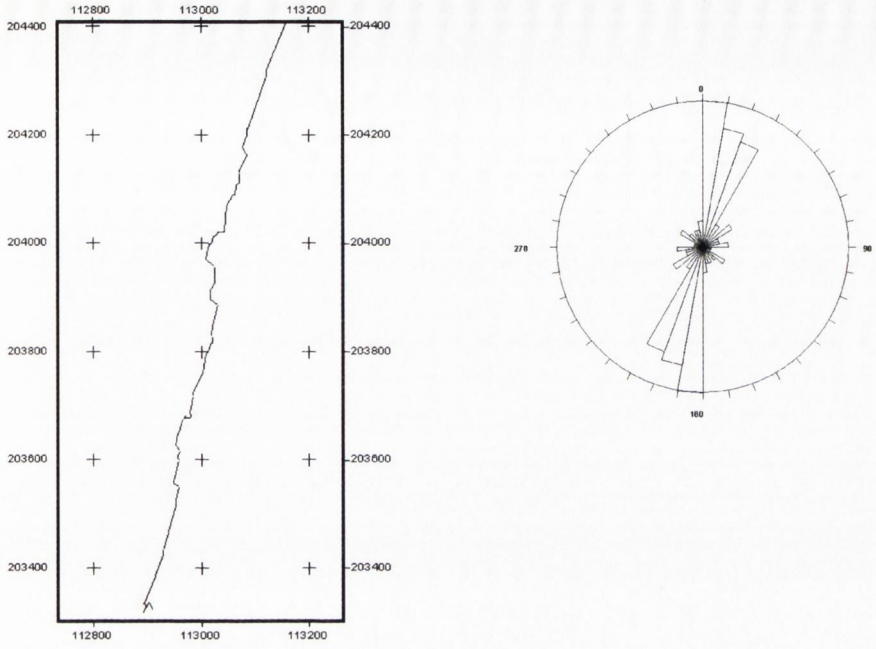

Figure 6.17: Map of cave passages in Poll Na gCéim (6.5.4.1) with associated rose diagram.

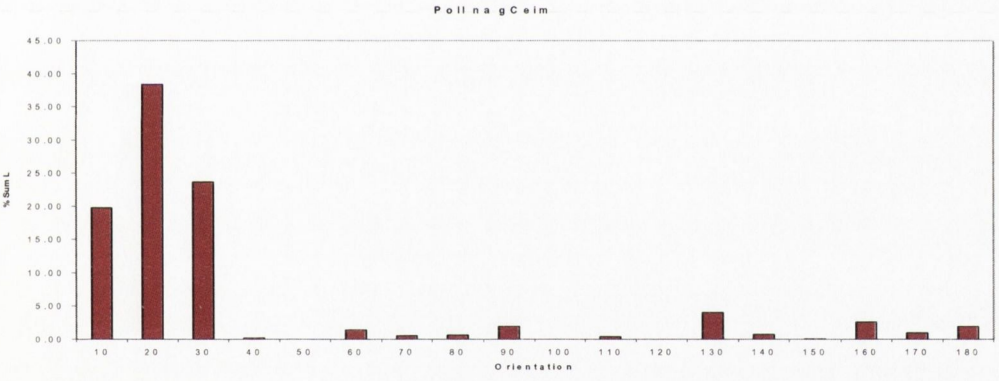

Figure 6.18 Sum Length per ten-degree bin expressed as a %.

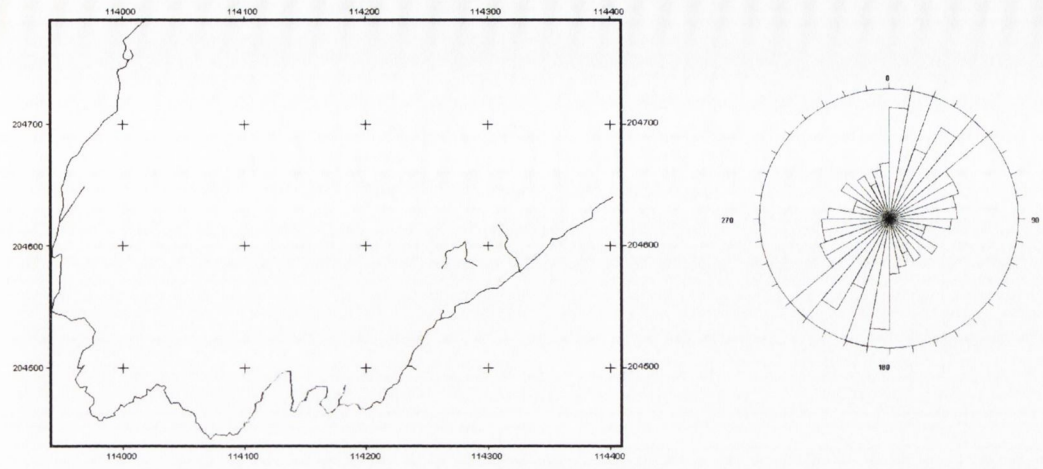

Figure 6.19: Map of cave passages in Faunarooska (6.5.4.2) with associated rose diagram.

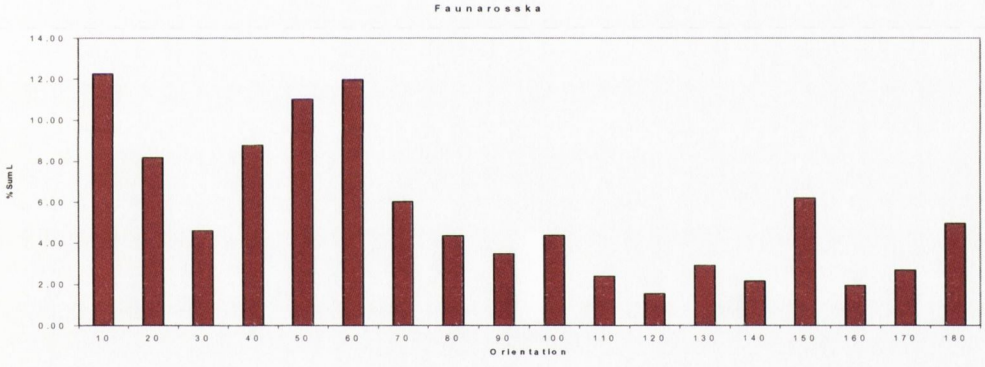

Figure 6.20: Sum Length per ten-degree bin expressed as a %.

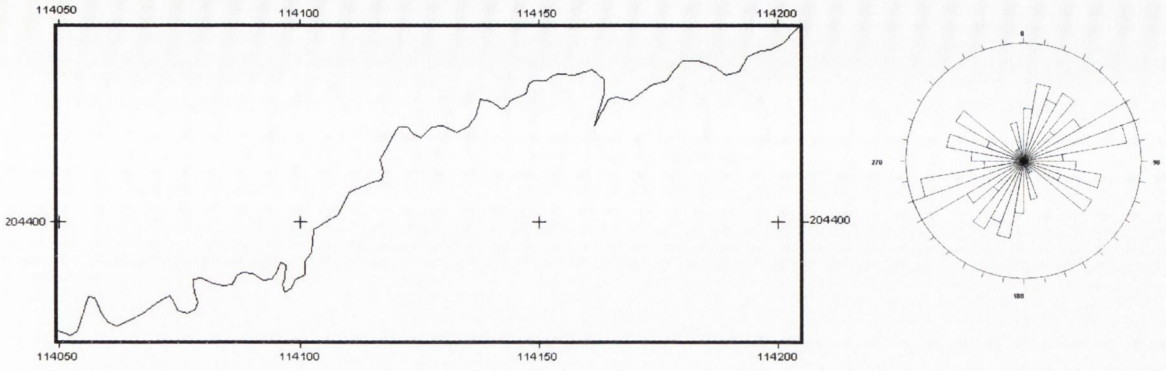

Figure 6.21: Map of cave passages in Hawthorn (6.5.4.3) with associated rose diagram.

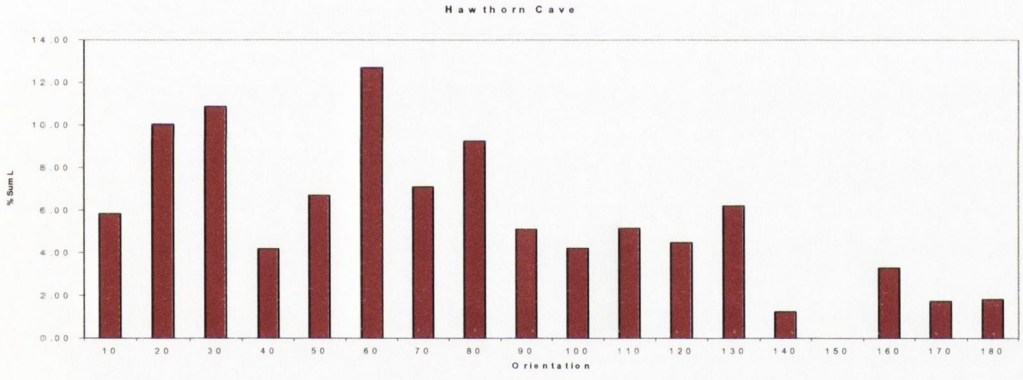

Figure 6.22: Sum Length per ten-degree bin expressed as a %.

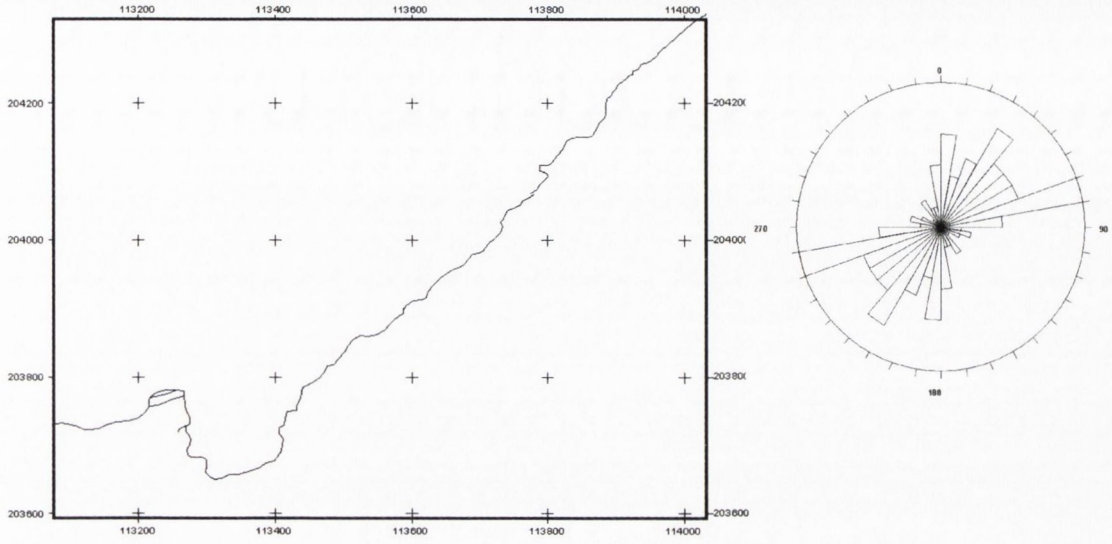

Figure 6.23: Map of cave passages in Pollballyiny (6.5.4.4) with associated rose diagram.

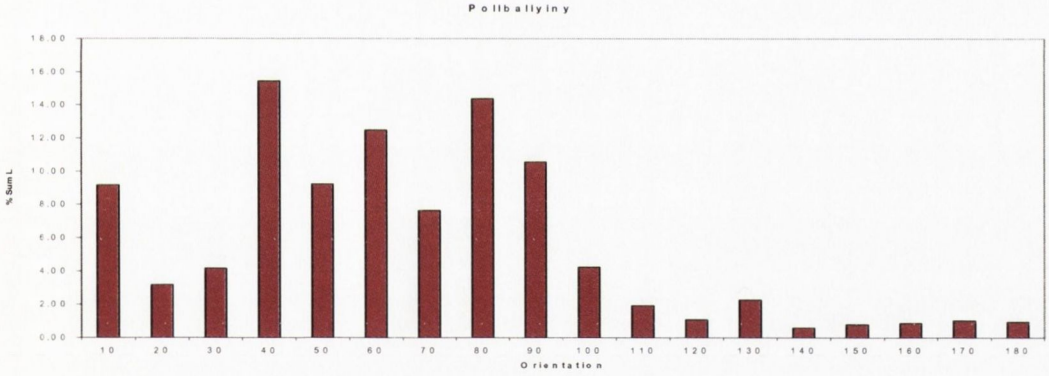

Figure 6.24: Sum Length per ten-degree bin expressed as a %.

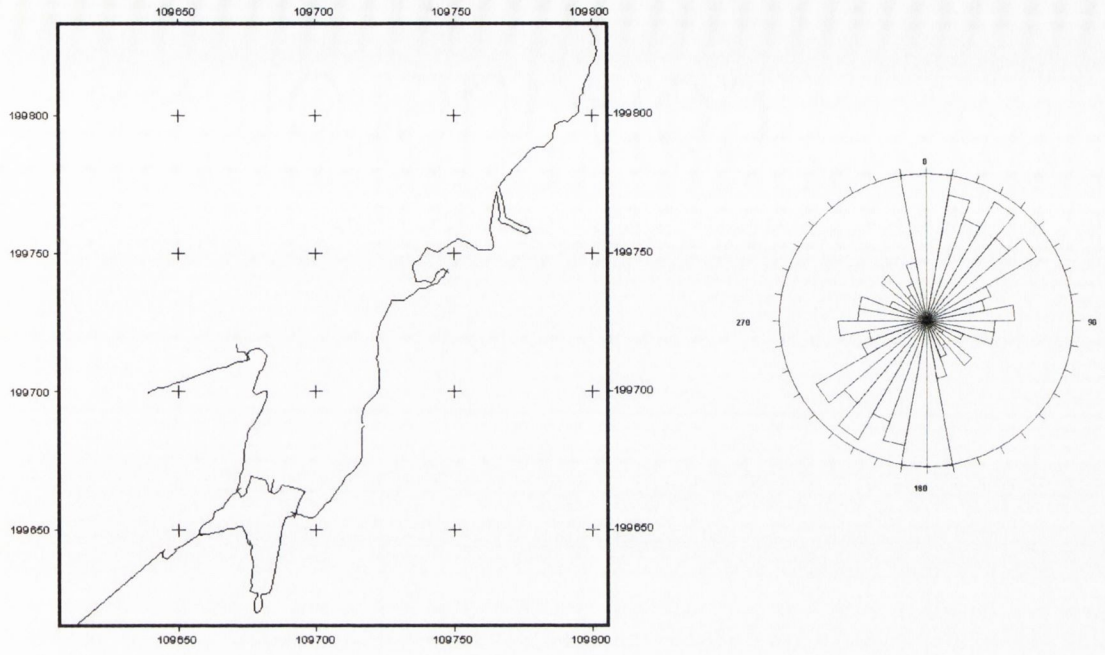

Figure 6.25: Map of cave passages in Poll an Ionain (6.5.5.1) with associated rose diagram.

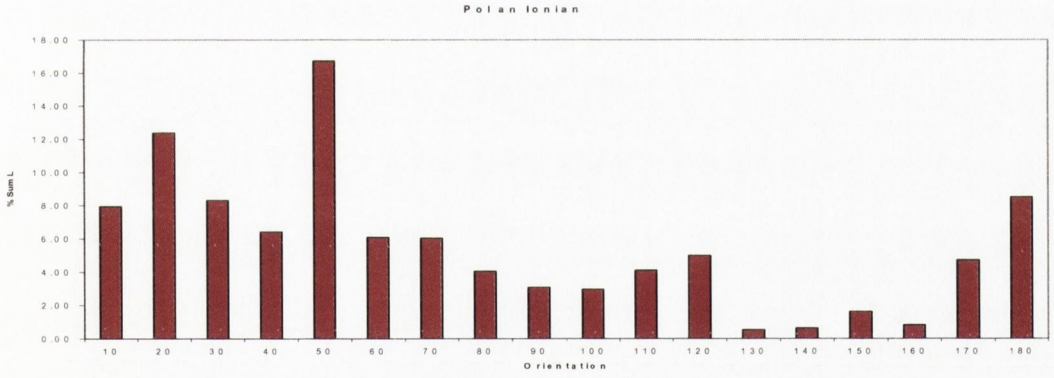

Figure 6.26: Sum Length per ten-degree bin expressed as a %.

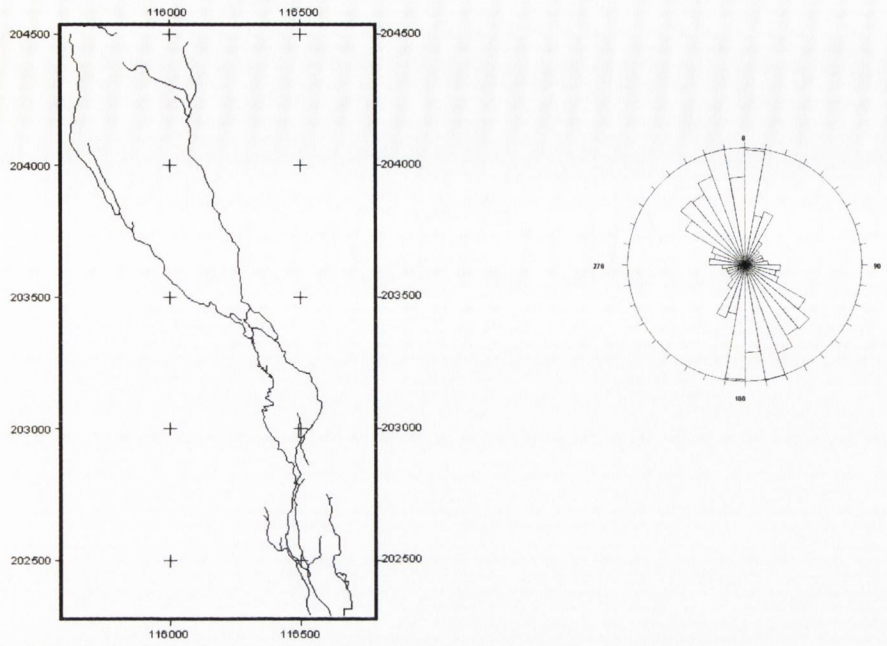

Figure 6.27: Map of cave passages in Poulnagollum (6.5.6.1) with associated rose diagram.

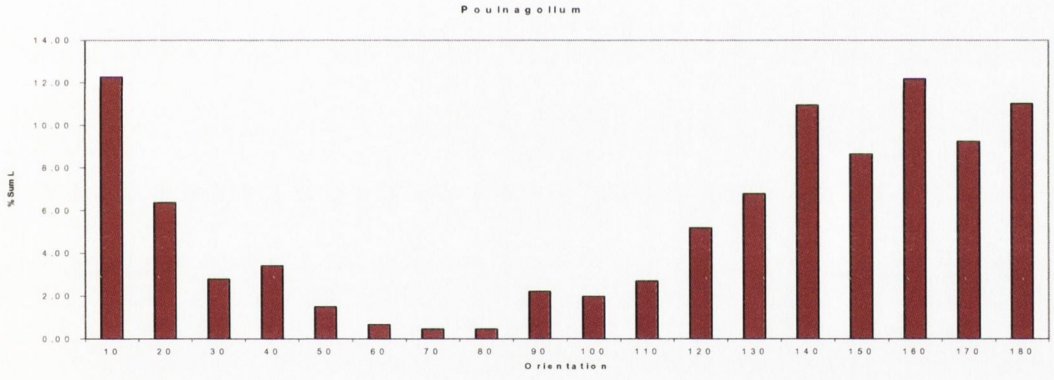

Figure 6.28: Sum Length per ten-degree bin expressed as a %.

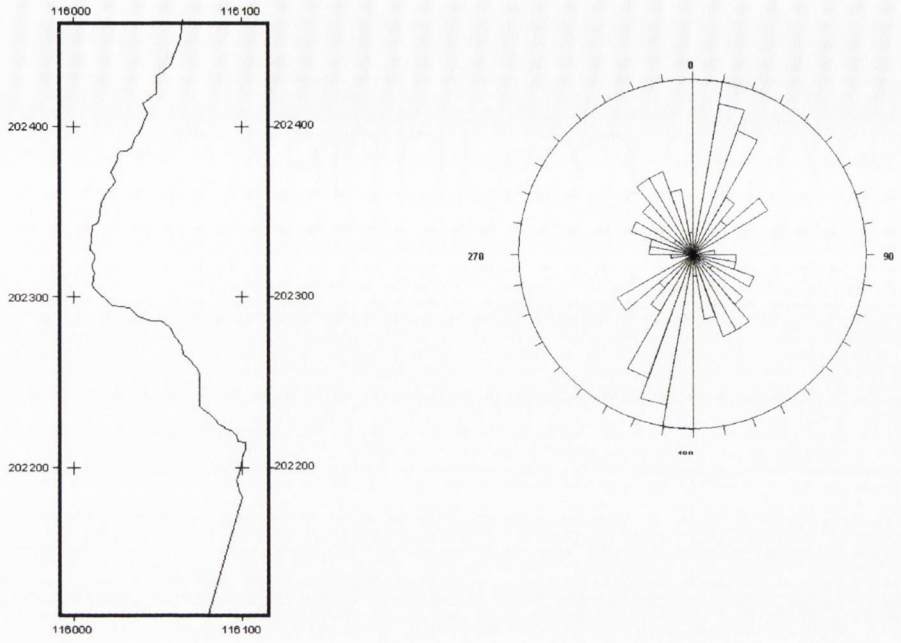

Figure 6.29: Map of cave passages in Pollcragreagh (6.5.6.2) with associated rose diagram.

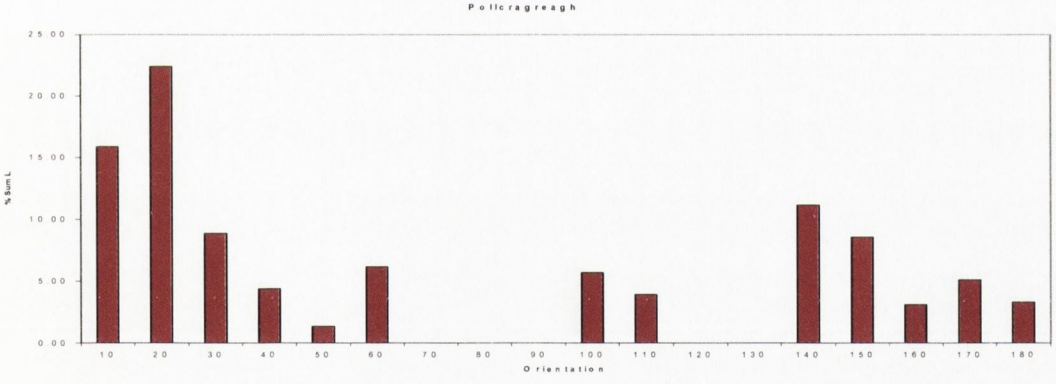

Figure 6.30: Sum Length per ten-degree bin expressed as a %.

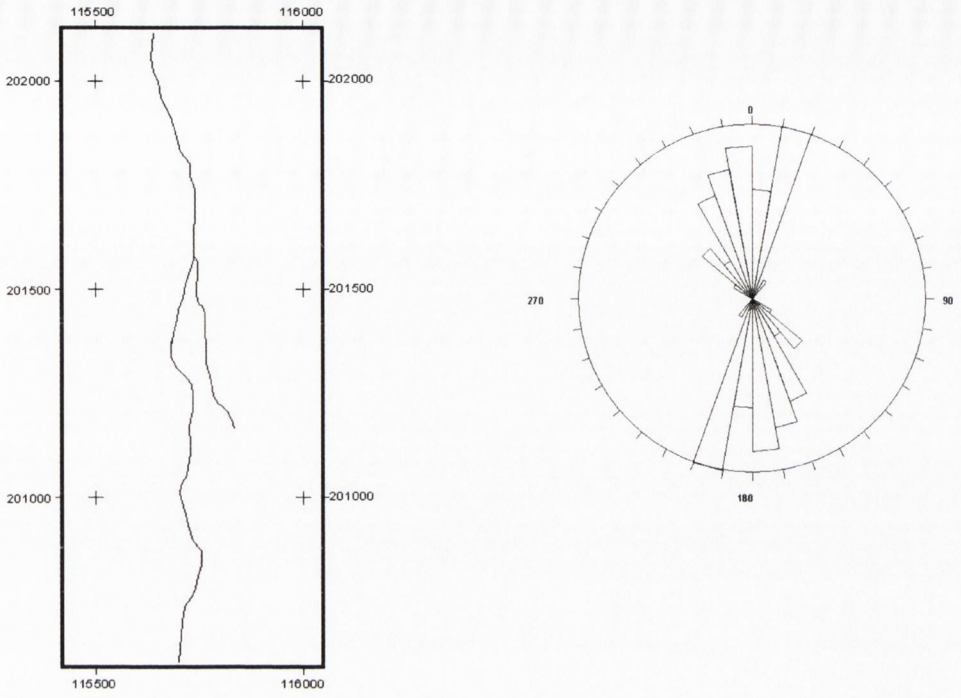

Figure 6.31: Map of cave passages in Pollcahercloggaun (6.5.6.3) with associated rose diagram.

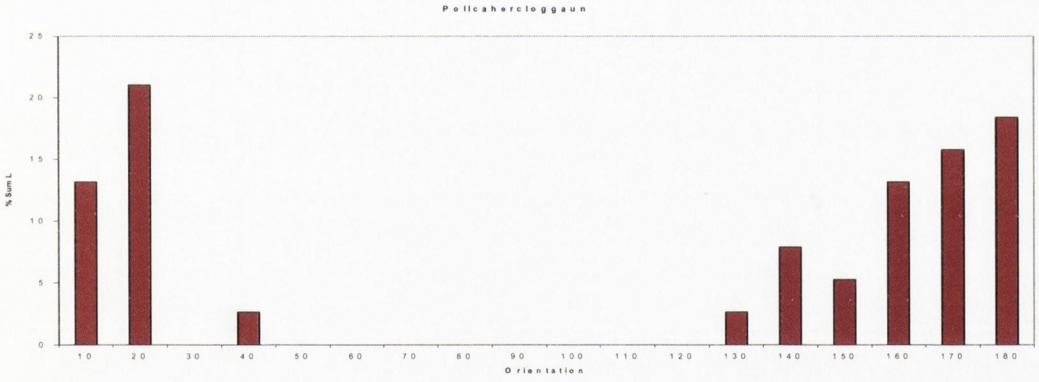

Figure 6.32: Sum Length per ten-degree bin expressed as a %.

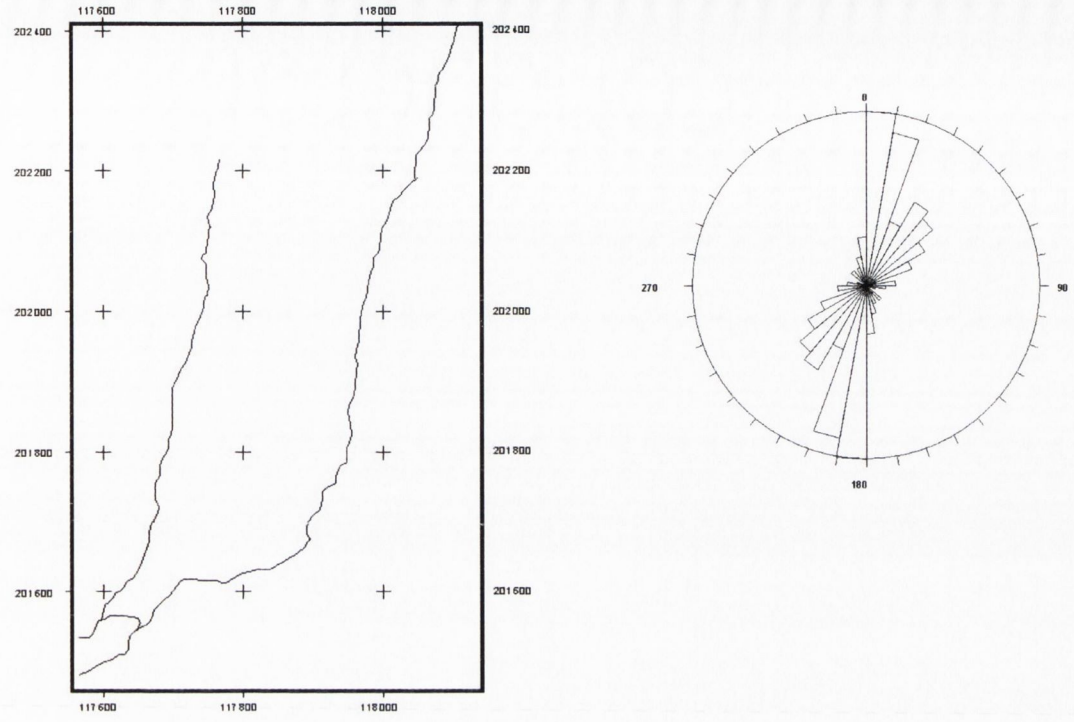

Figure 6.33: Map of cave passages in Cullaun 1 (6.5.7.1) with associated rose diagram.

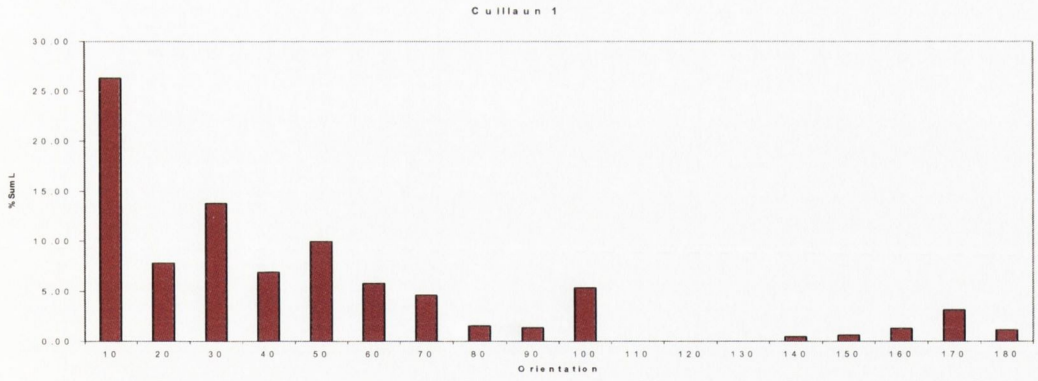

Figure 6.34: Sum Length per ten-degree bin expressed as a %.

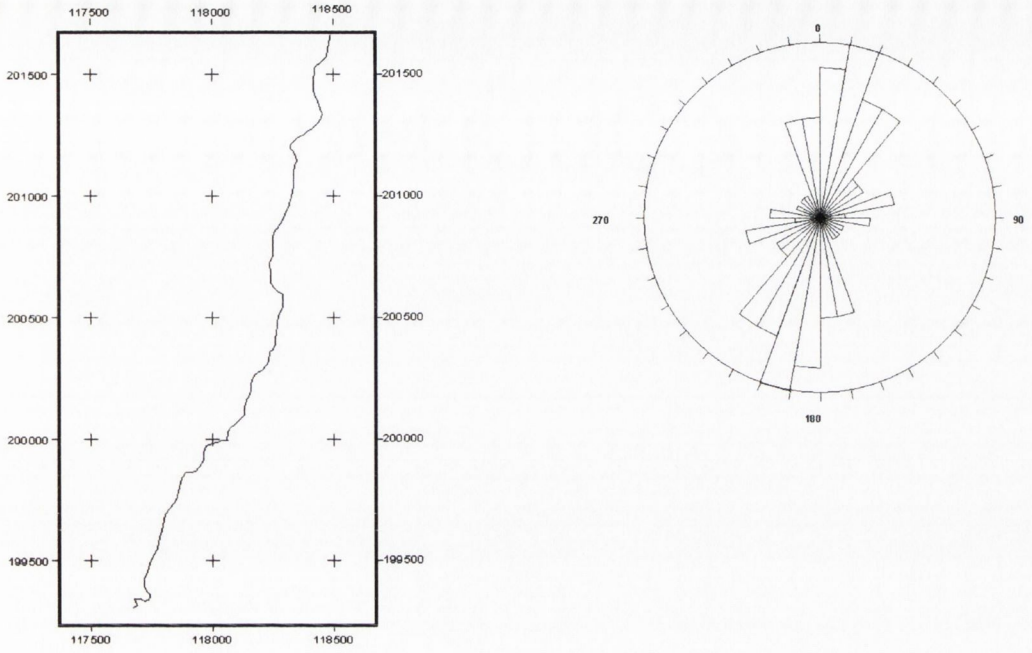

Figure 6.35: Map of cave passages in Cullaun 3 (6.5.7.2) with associated rose diagram.

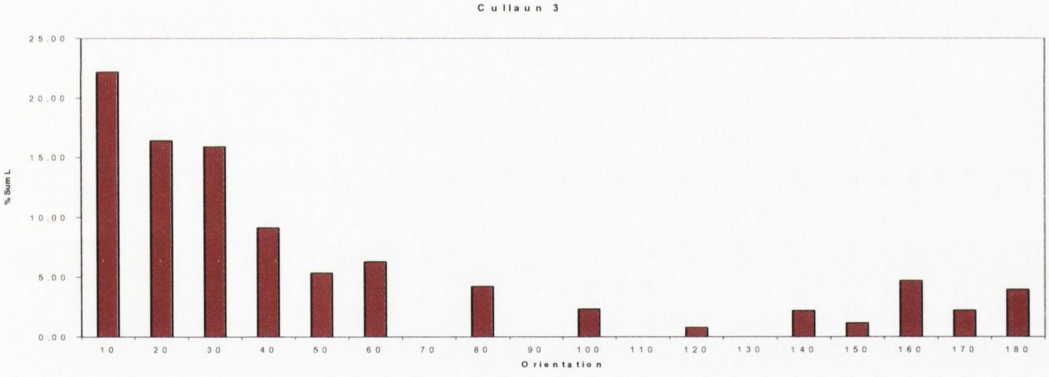

Figure 6.36: Sum Length per ten-degree bin expressed as a %.

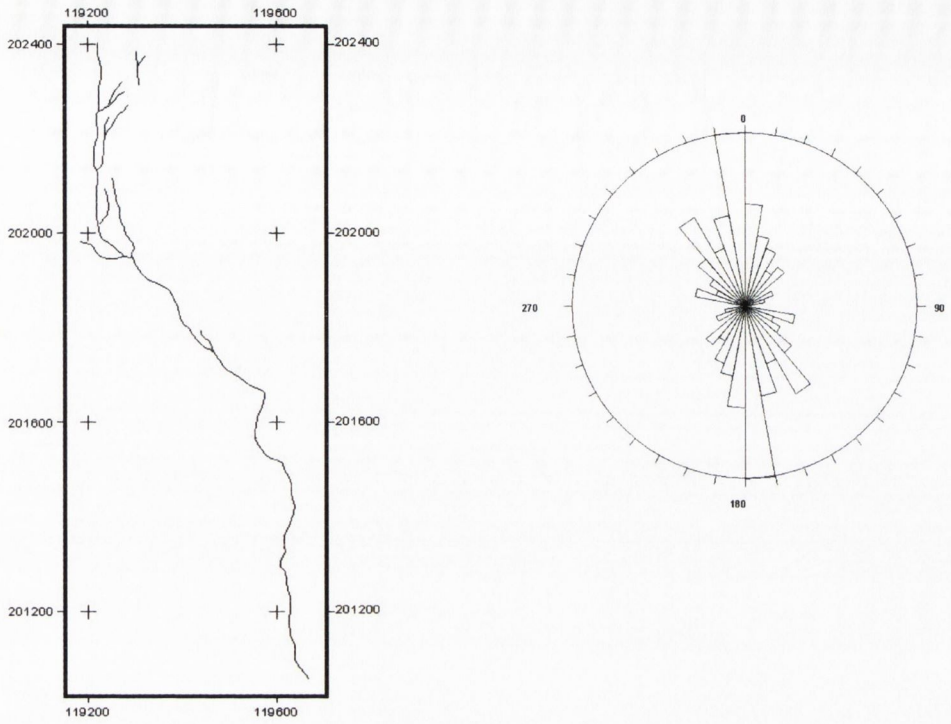

Figure 6.37: Map of cave passages in Gragan Cave (6.5.8.1) with associated rose diagram.

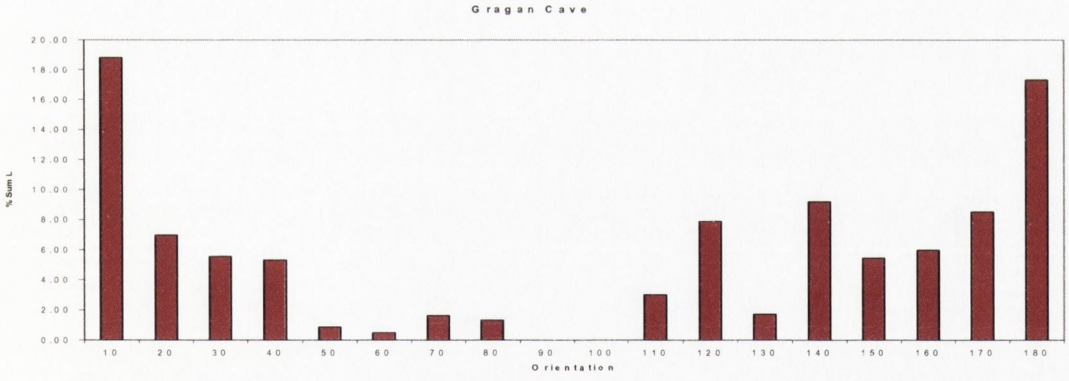

Figure 6.38: Sum Length per ten-degree bin expressed as a %.

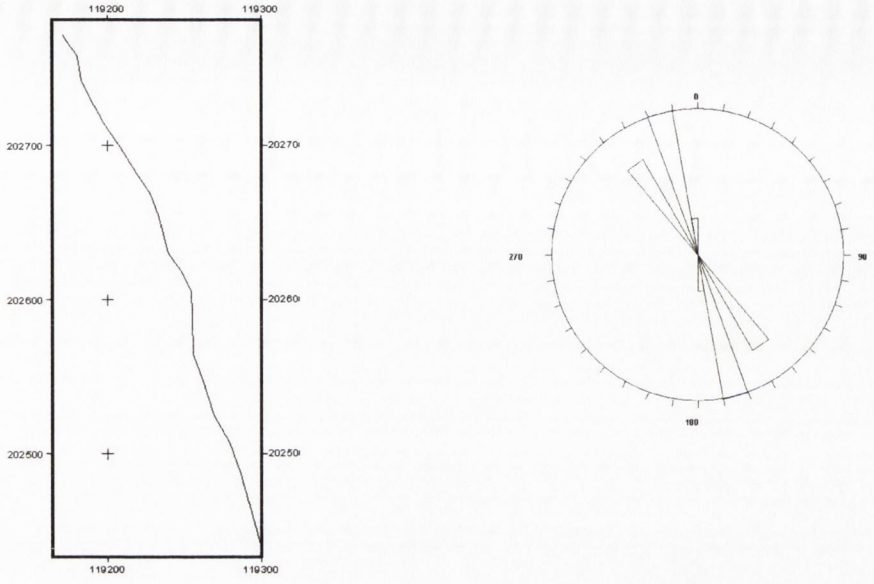

Figure 6.39: Map of cave passages in Green Streams Cave (6.5.8.2) with associated rose diagram.

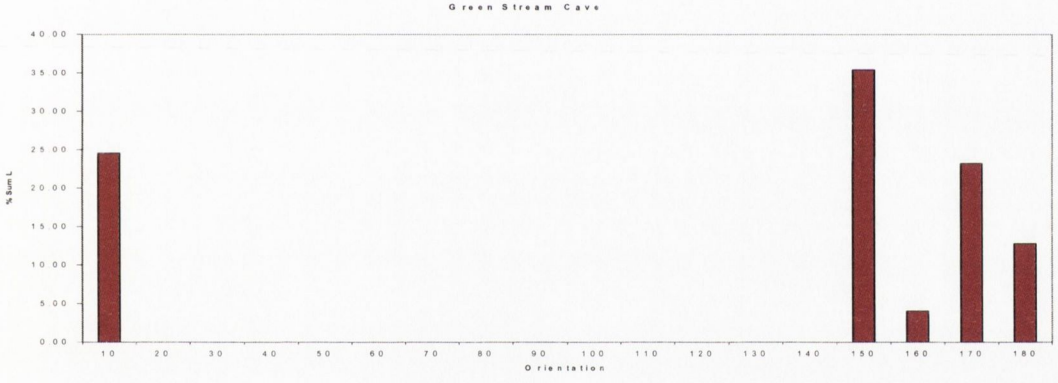

Figure 6.40: Sum Length per ten-degree bin expressed as a %.

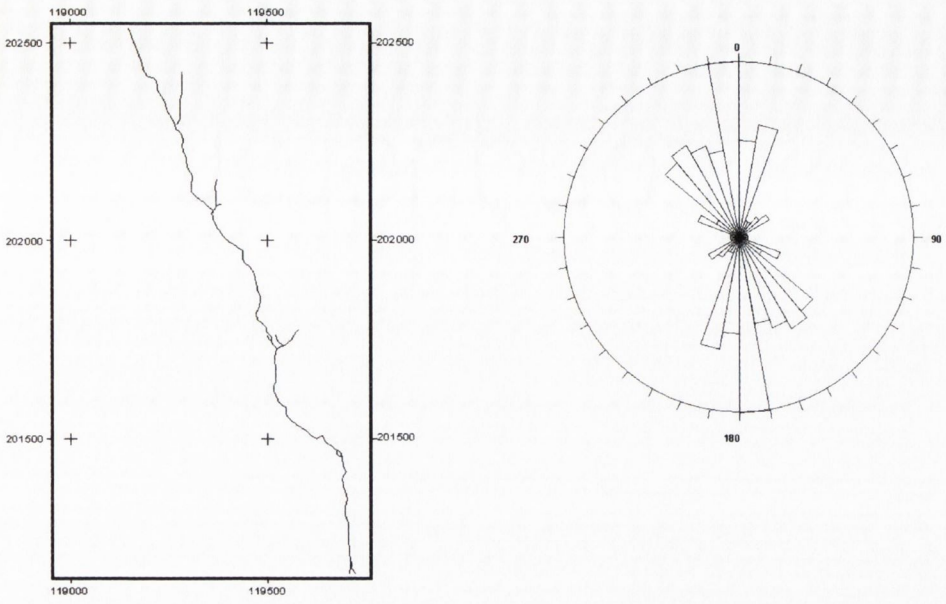

Figure 6.41: Map of cave passages in Doonyvardan Cave (6.5.8.3) with associated rose diagram.

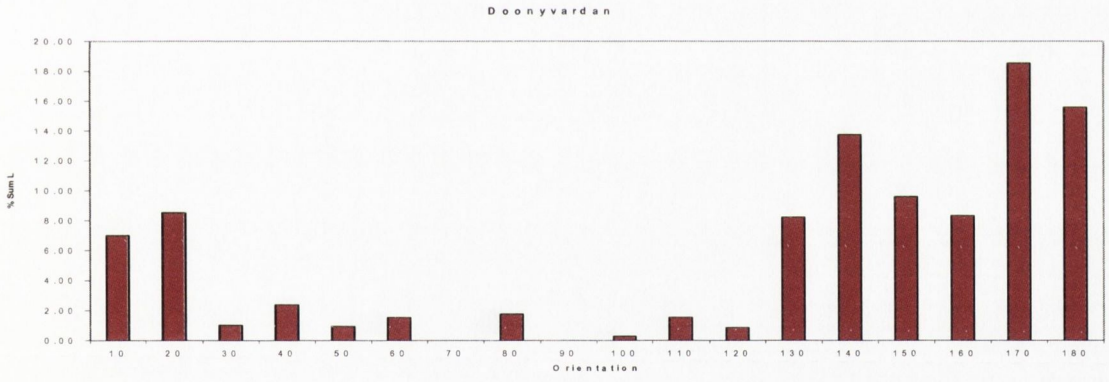

Figure 6.42: Sum Length per ten-degree bin expressed as a %.

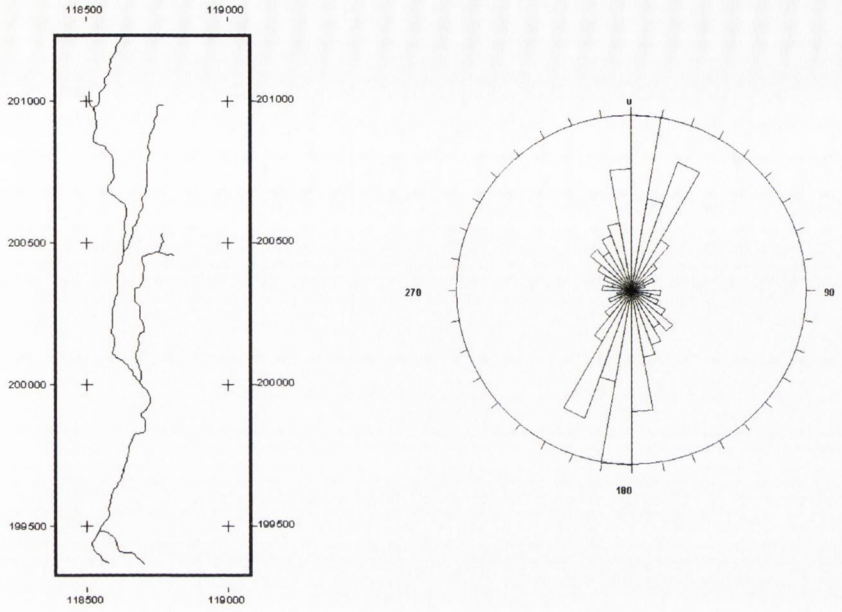

Figure 6.43: Map of cave passages in Cullaun 5 Cave (6.5.9.1) with associated rose diagram.

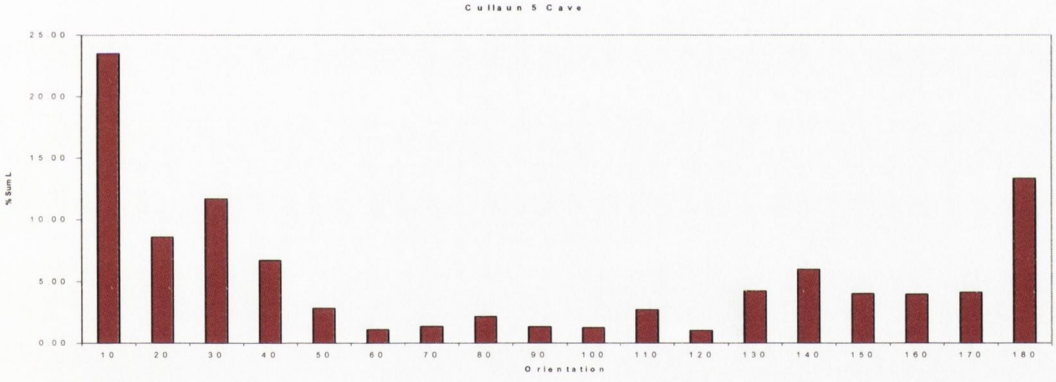

Figure 6.44: Sum Length per ten-degree bin expressed as a %.

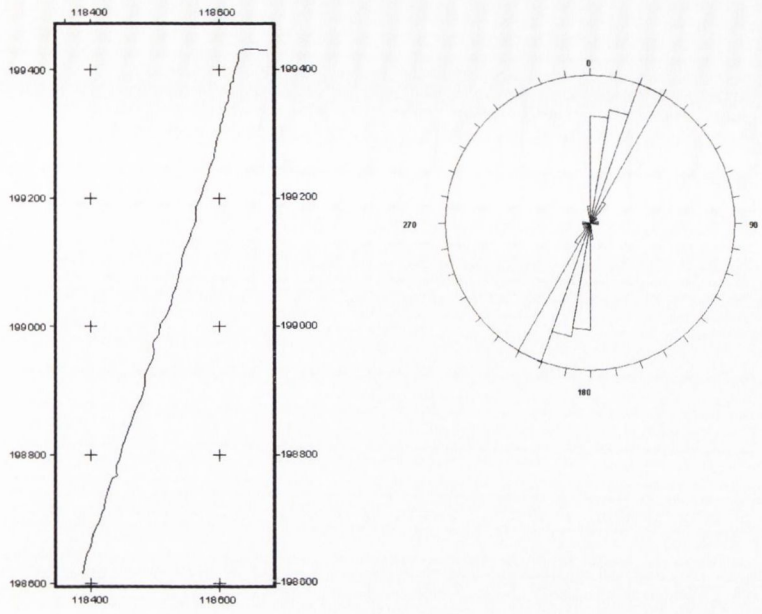

Figure 6.45: Map of cave passages in Pollcahermaan (6.5.10.1) with associated rose diagram.

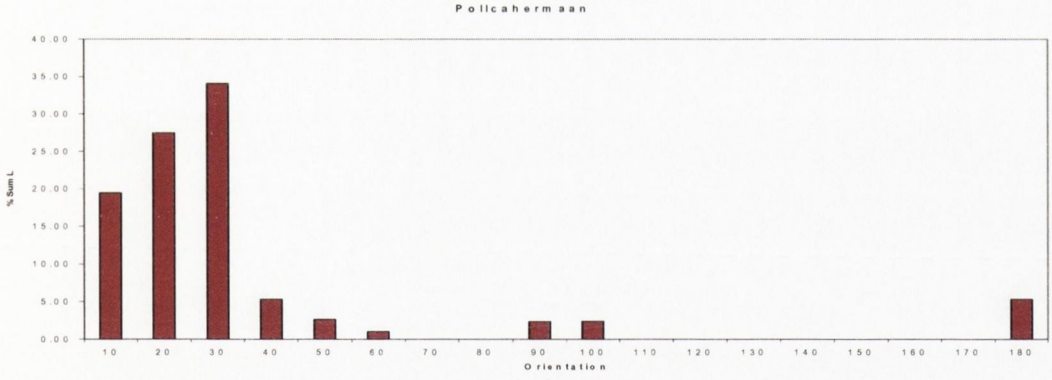

Figure 6.46: Sum Length per ten-degree bin expressed as a %.

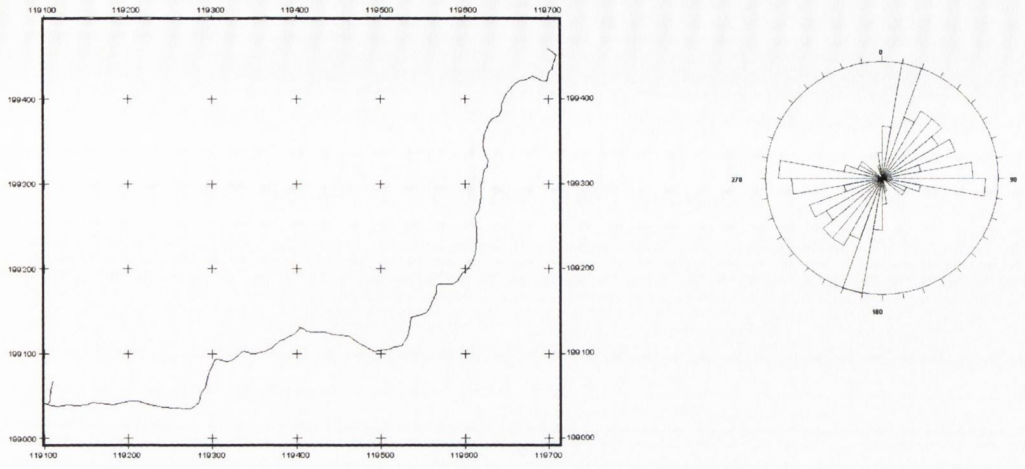

Figure 6.47: Map of cave passages in Poulawillin (6.5.10.2) with associated rose diagram.

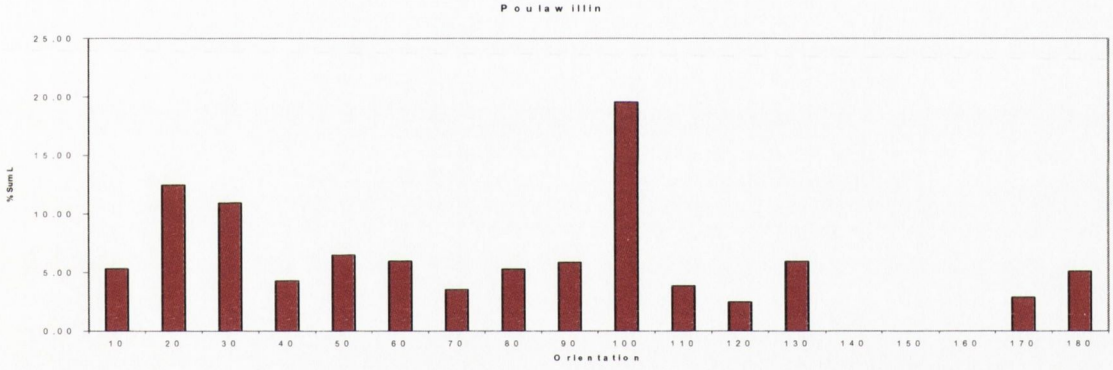

Figure 6.48: Sum Length per ten-degree bin expressed as a %.

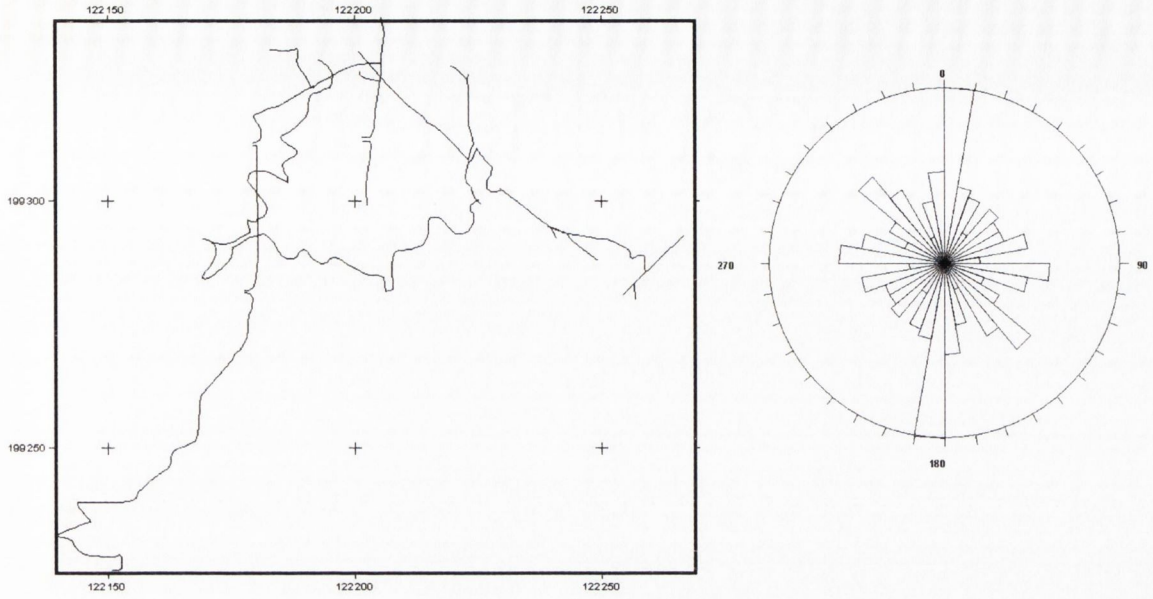

Figure 6.49: Map of cave passages in Kilcorney Cave (6.5.11.1) with associated rose diagram.

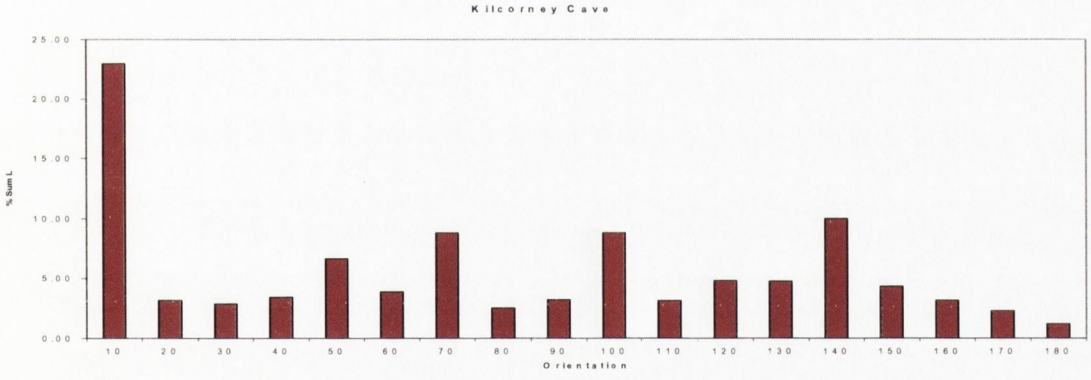

Figure 6.50: Sum Length per ten-degree bin expressed as a %.

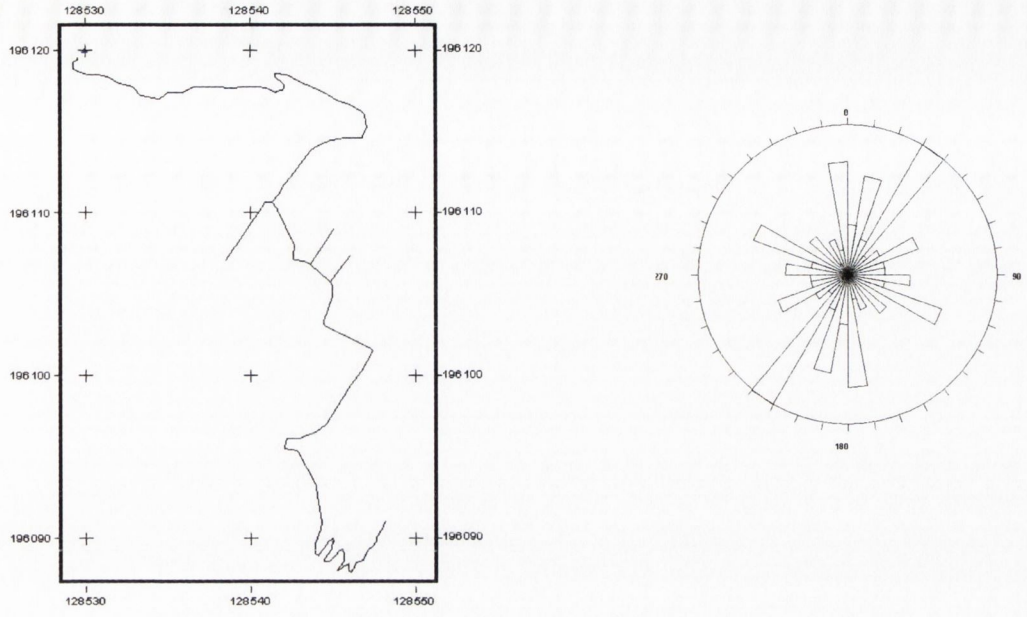

Figure 6.51: Map of cave passages in Seven Streams Cave (6.5.12.1) with associated rose diagram.

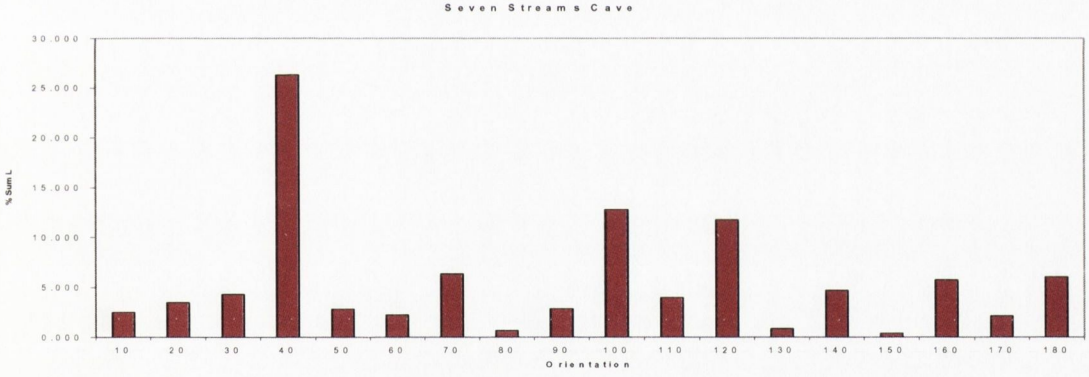

Figure 6.52: Sum Length per ten-degree bin expressed as a %.

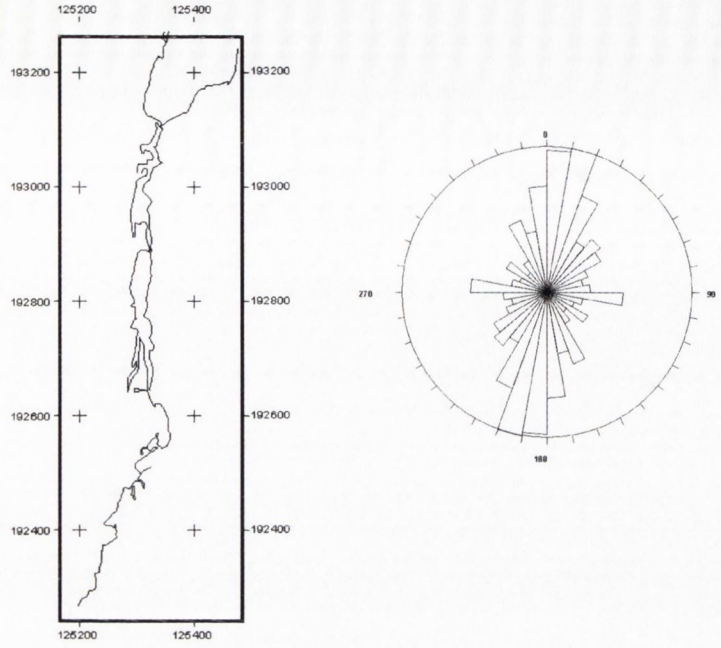

Figure 6.53: Map of cave passages in Fergus River Cave (6.5.13.1) with associated rose diagram.

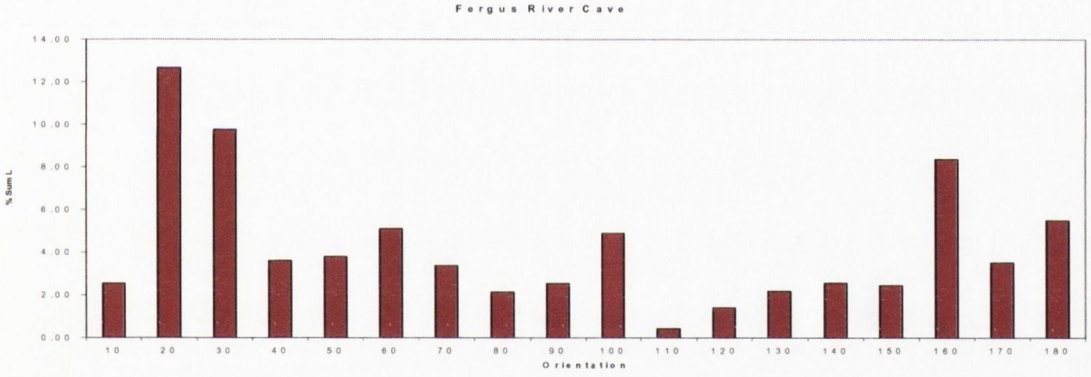

Figure 6.54: Sum Length per ten-degree bin expressed as a %.

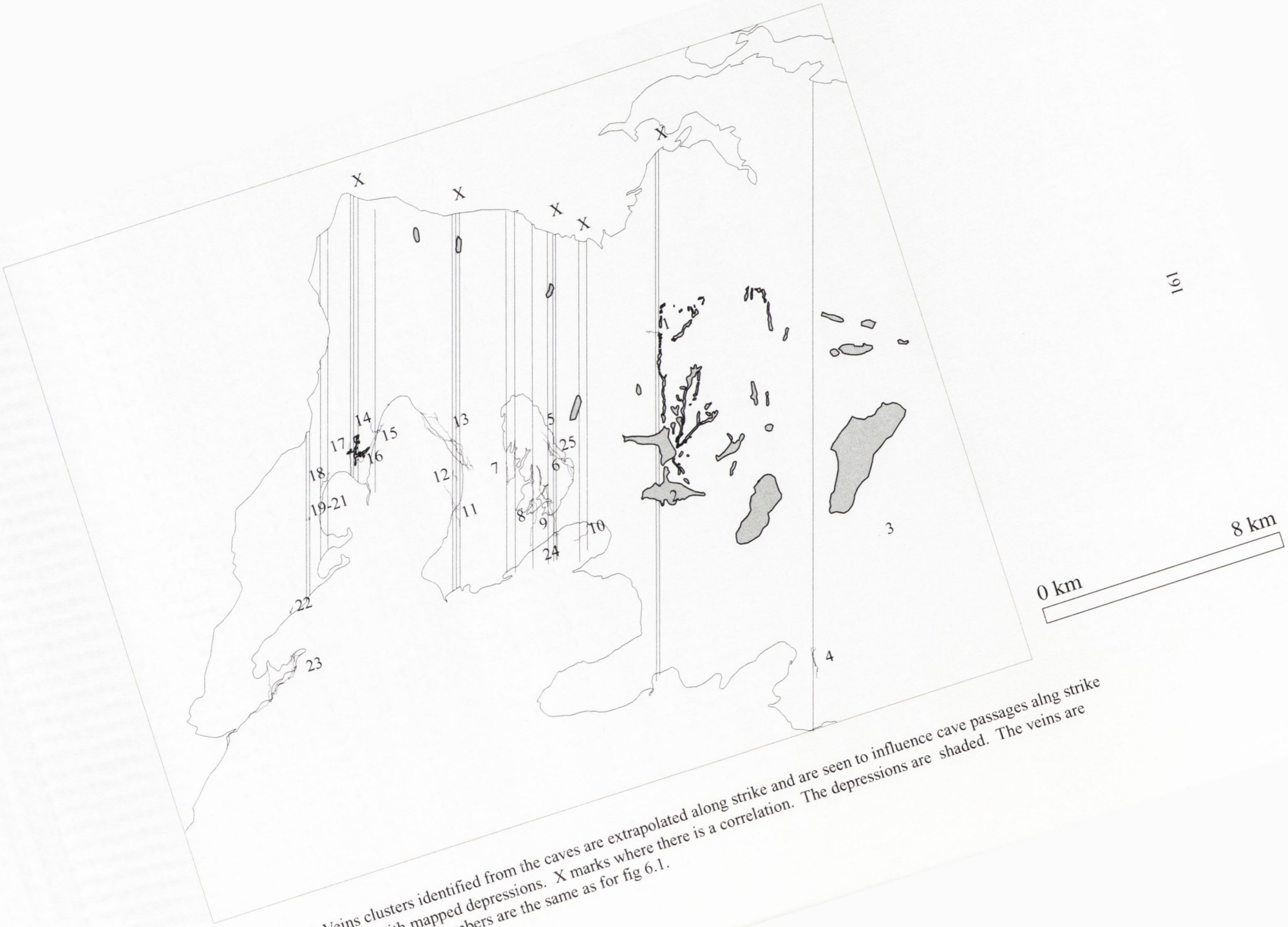

Figure 6.55: Veins clusters identified from the caves are extrapolated along strike and are seen to influence cave passages alng strike as well as coincide with mapped depressions. X marks where there is a correlation. The depressions are shaded. The veins are contiuous solid lines. Cave numbers are the same as for fig 6.1.

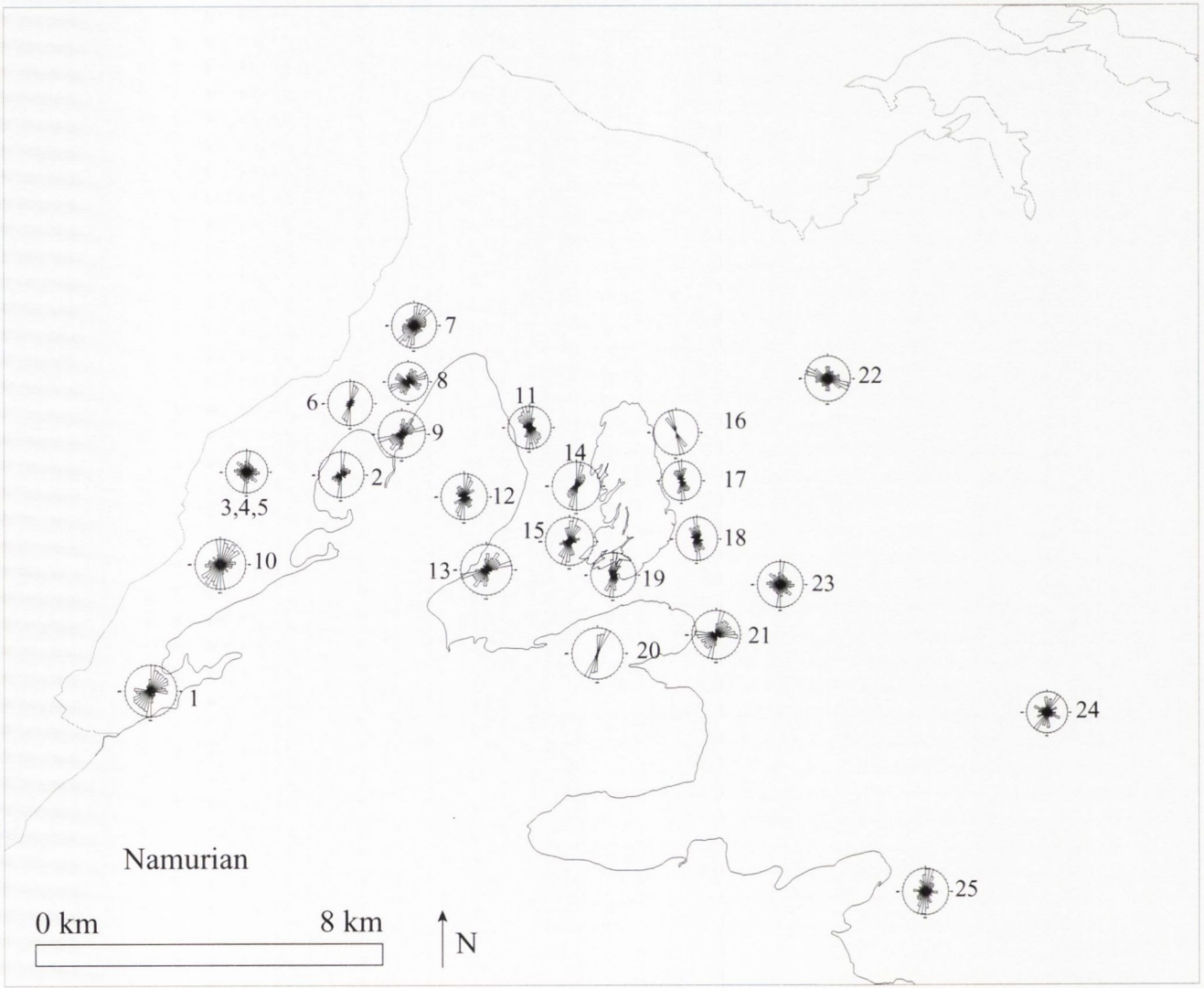

The Doolin Valley
1: Doolin cave

Western Knockauns& Oughtdarra
2: Poulnagree 3: Robbers Den
4: Through & Through 5: Moonmilk

Northwestern side of Slieve Elva
6: Poll na gCeim 7: Faunarooska
8: Hawthorm 9: Pollballyiny

Coolagh Valley
10: Pol an Ionain

Eastern Side of Slieve Elva
11: Poulnagollum 12: Pollcragreagh
13: Pollcahercloggaun

Western Poulacapple
14: Cullaun 1 15: Cullaun 3

Eastern Poulacapple
16: Gragan 17:Green Stream
18: Doonyvardan

Southern Poulacapple
19: Cullaun 5

North of Kilfenora
20: Pollcahermaan 21: Poulawillin

North Central Burren
22: Aillwee Cave

South Central Burren
23: Kilcorney

Southeastern Burren
24: Seven streams of Teeskagh

Upper Fergus River
25: Fergus River Cave

Figure: 6.56: Rose diagrams of the cave systems that have been studied.

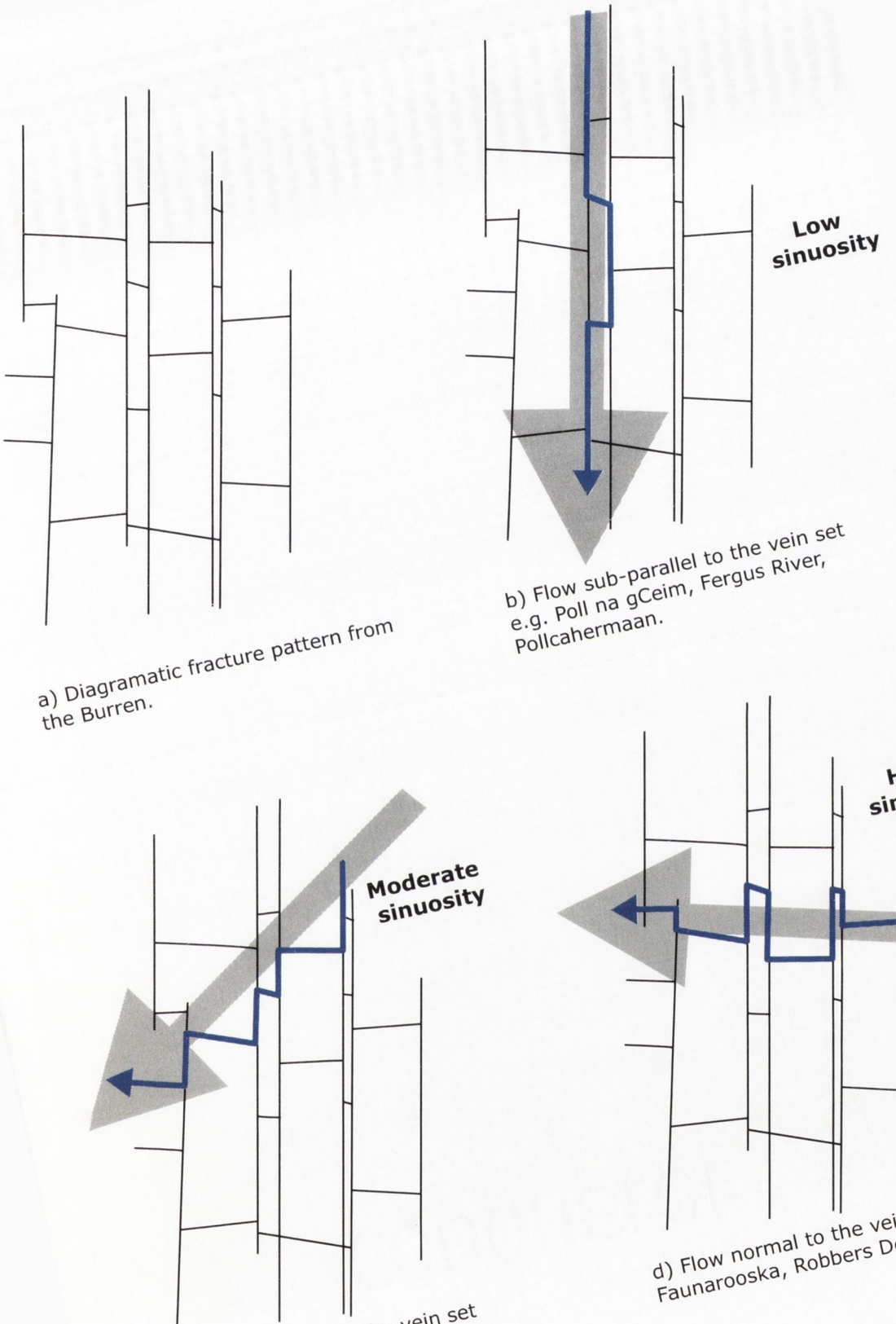

a) Diagramatic fracture pattern from the Burren.

b) Flow sub-parallel to the vein set e.g. Poll na gCeim, Fergus River, Pollcahermaan.

c) Flow oblique to the vein set e.g Doolin, Poulnagree, caves on the slopes of Slieve Elave & Poulnacapple.

d) Flow normal to the vein set e.g Aillwee, Faunarooska, Robbers Den, Moonmilk.

Figure 6.57 Diagrammatic view of the cave patterns formed under different flow conditions.

CHAPTER 7 GEOMORPHOLOGY

7.1: Introduction:

Karst is a term used worldwide to describe a terrain with distinctive hydrology and landforms arising from the dissolution of rock by carbon dioxide enriched water (Jennings 1985, Ford & Williams 1989, Kaufmann & Braun 1999). Karstic terrains develop on rock types that are readily dissolved by water. Worldwide limestone is the most common rock that shows karstic features. The etymology of the word karst is from the Slavic word *kras*, itself derived from palaeo-european linguistic origins in the form of the word *karra* meaning stone, the word *grast* was used in Slovene since 1177, *kras* has been in use in Croat since 1230. *Kras* means stony barren ground, similar to the meaning of the Irish word *boireann* (a stony place) from which the name Burren is derived from, as well as being the regional name for a district on the Slovenian/Italian border in the vicinity of the Gulf of Trieste (*Carso* in Italian). Earlier workers germanised the word kras to karst, when present-day Slovenia and Croatia were included into the Austro-Hungarian Empire. The type area for karst terrains remains the Kras region of Slovenia (Jennings 1971, Ford & Williams 1989). Karstified limestone covers approximately 10% of the land surface of the Earth, and Ford & Williams (1989) estimate that 25% of the world's population is supplied with water from karstic regions.

Karstic areas have a unique drainage pattern due to the movement of most of the surface water into the sub-surface with a resultant absence of surface drainage. In the case of fluvio-karst, the karst landforms are superimposed on a former fluvial landscape. It is a characteristic of karstic terrains that surface flow is replaced and captured by sub-surface drainage. Active karst systems are hydrologically active at the present, whereas relict karst is karst which formed under different conditions from those now active, but which is still exposed and open to modification by present day processes. The Burren is a combination of active and relict karst. Karstification is ongoing in the Burren at the present time particularly in the Western Burren. While the Eastern Burren is also undergoing karstification, it consists of landforms and subterranean features that were mainly formed during a previous period of karstification.

7.2 Landforms:

Karst areas are indicated by a general absence of permanent surface streams and the presence of swallow holes and enclosed depressions. The water is usually underground in solutionally enlarged channels. Karst landscapes are divided into two primary divisions, erosional and depositional zones. In the erosional zones there is a net removal of material via dissolution or via other processes triggered by dissolution, with minor re-deposition in the form of precipitates (Ford & Williams 1989). In the net deposition zone, which is principally offshore or in tidal flat areas the dissolved material is deposited. Solution produces a large number of surface features ranging from superficial micro-solutional features on the limestone, termed karren, to large kilometre-scale depressions known as poljes. There are three divisions in these landforms: micro, meso and macro.

7.2.1: Micro relief features (cm-m in scale)

- Karren

Karren is the generic name for a large number of micro-solutional features on the limestone surface. The most obvious features on a limestone pavement surface are clints and grikes (the etymology of both terms is derived from Yorkshire dialectical origins). Grikes are fractures that have been enlarged by solution, compartmentalising the limestone surface into blocks known as clints. Grikes are also known as kulftkarren; and clints as flachkarren. Clint size depends on the fracture, or grike spacing, with clint sizes in the Burren ranging from a few square centimetres to tens of square meters depending on the fracture patterns present. Solutional hollows known as kamenitzas may also develop on limestone surfaces. The flow of rainwater from the surface produces a series of runnels; with large runnels which are large elongated grooves known as rinnekarren and sharp-ridged grooves being known as rillenkarren in addition to rounded runnels which are formed beneath a soil cover which are known as rundkarren. Limestone pavements are some of the most widespread features in the Burren. Williams (1964) defines a limestone pavement as "a roughly horizontal exposure of limestone bedrock, the surface of which is a) approximately parallel to its bedding plane, and b) is divided in to a geometrical pattern of blocks [clints] by the intersection of widened fissures [grikes]". Williams attributes the extensive pavement in the Burren to a combination of the mechanical strength, massive bedding, purity of the Carboniferous Limestone, relationship of the beds to the regional dip and scouring action of glaciation. Pavements do not form in limestones that are not well bedded as in bank or reef facies, such as the Waulsortian limestone of the Clare-Galway district, which seldom has pavements (Williams 1964, 1966). The relationship of the dip of beds to the ground surface is an important factor in the development of pavements. The most favourable condition is found when both the strata and the land surface are approximately horizontal (Williams 1966), as is the case in most areas in the Burren. If the strata is inclined and the surface horizontal, a miniature scarp and vale topography is produced with pavements on the back-slopes as is common in the Gort Lowlands (Williams 1966). Action by glaciers, which have scoured away the surface debris of soil, stone and the topmost layer of solutionally weakened rock, is essential in pavement formation.

7.2.2: Meso-relief features (m-km in scale)

- Dolines
- Sink Holes / Swallow Holes

Enclosed depressions are regarded as diagnostic landforms of karst areas. Throughout the Burren there are a large number of enclosed depressions of varying size from a few metres to a few kilometres. Depressions of moderate dimension are termed dolines; those of larger dimensions are termed poljes.

Dolines: The term doline originates from the Slovene and Serbo-Croat word *dolina* meaning valley or plain. Cvijic in 1893 identified dolines as giving karst topography its particular character (Ford & Williams 1989). Dolines are usually circular depressions varying in diameter from a few metres to about one kilometre with no drainage outlet except underground. A distinction may be made between those formed mainly by direct

solution of the limestone surface zone, solution dolines, and those formed by collapse over a cave, collapse dolines. Many researchers believe that solution and collapse are the two end members of a system and that dolines rarely form exclusively by one method but have a tendency towards one of the end members (Jennings 1971, Bull 1980, Ford & Williams 1989). Localised surface lowering through focused solution of the limestone forms solution dolines. Solution is dominantly at the subsoil rock surface but may be sub-aerial (Waltham *et al* 1997). Collapse dolines are formed through a combination of three main mechanisms a) solution from above that weakens the span of a cave roof, b) collapse from below that widens and progressively weakens the span of a cave roof and c) removal of buoyant support by the water table (Ford & Williams 1989).

Sink holes: Sinkholes, also known as sinks, sluggas and swallets, are the point where a steam sinks and disappears below ground.

7.2.3: Macro relief features (>km)

- Poljes
- Dry Valleys
- Blind Valleys
- Caves

Polje: The term polje originates from the Slavic word for field. Poljes are large flat-floored depressions across which there may be an intermittent or perennial stream with sharply defined rock slopes. Poljes may be liable to flood and are often controlled by the structure of the region. The Carran Depression is the best-known polje in the Burren being circa 3.8km long 1.3km wide and 60m deep. The Carran depression lies along the axis of a NE-SW trending fold axis.

Dry Valley: A dry valley is a valley in a karst terrain without a surface flow of water. The thalweg of a dry valley may undulate with many closed depressions, and there may no longer be a distinct river channel. Dry valleys are a common feature in the Burren e.g. Gleninsheen on the southwestern flanks of Aillwee Hill. Many dry valleys in the British Isles were excavated or enlarged under periglacial conditions during cold stages of the Pleistocene Era (Waltham *et al* 1997).

Blind Valley: A blind valley is a valley that ends abruptly where a stream vanishes underground at its lowest point. This is usually marked by a sinkhole.

Caves: Caves are defined by the *International Union de Speleologies* as a natural underground opening in rock large enough for human entry. Ford & Williams (1989) define a karst cave as a solutional opening that is greater than 5-15mm in diameter. Caves have an input point, a sink hole/swallow hole, and an output point, known as a rising, where a conduit extends continuously between these two points it constitutes an integrated cave system. For more information on caves and the process of speleogenesis refer to Chapter 6.

7.3 The Burren:

The Burren plateau found in northwest Co. Clare is the finest example of karstic terrain in Ireland. The term Burren is an anglicised version of the Irish word *boireann* meaning stony place. The Burren consists of an approximately 360km^2 plateau of Lower Carboniferous Limestone and Upper Carboniferous Shales and Sandstones, gently dipping from 200-300m in the north to 100m in the south, following the regional dip to the south-south-west. The northern boundary is formed by Galway Bay with the Atlantic coast forming the boundary to the west. The southern boundary is taken to be the Aille and Fergus rivers. The eastern boundary is taken to be the scarp formed by the highlands from Abbey Hill in the north to Mullaghmore in the south; this boundary is the most difficult to define as the same geological units occur to the east and west of this boundary. This boundary also marks the western extent of the Gort Lowlands. In a geological and geomorphological sense, the Aran Islands are an extension of the Burren. The Burren is fretted along its northern and eastern flanks by a series of re-entrant valleys. The largest of these is the north-north-easterly trending Ballyvaughan Valley, which is separated from the adjacent Turlough Valley by a north-north-easterly ridge, which consists of Moneen Hill and Aillwee Hill. Turlough Valley is a composite structure comprising of three smaller embayments: Glenamanagh, Aughawiniaun and Oughtmama (Plunkett Dillon 1985). A number of the other valleys have degraded into large north-north-easterly trending depressions such as the Glencolmcille Depression (Sweeting 1955, Drew 1975, Plunkett Dillon 1985).

The Burren has been influenced by fluvial and glacial process in addition to karstification and is more accurately described as a fluvio-glacio-karst region. Traditionally a distinction is usually made between the High Burren, and Eastern Burren, east of a line from Corkscrew Hill to Noughval and the remainder of the Burren to the west (Drew 1977). The Western Burren is dominated by Namurian sequences with the limestone outcropping to the north and west, the depressions being restricted to the limestone areas. By contrast, the Eastern Burren is dominated by the Lower Carboniferous Limestone and large enclosed depressions and limestone pavements. As previously mentioned the Burren is a combination of active and relict karst with karstification ongoing in the Burren at the present time, the Eastern Burren consists of landforms and subterranean features that are relict and were formed during a previous period of karstification. This aspect of the Burren is manifested in the distribution and occurrence of the karstic landforms throughout the Burren. The boundary between the Namurian strata and the Lower Carboniferous Limestone, which is in the Western Burren, is dominated by active karstification in the form of sinkholes. As the surface drainage on the Namurian flows onto the limestones it is transferred into the sub-surface through the formation of sinkholes. The location of all published sinkholes and caves was compiled from literature (Tratman 1968, Self 1981, Drew 1973, Drew 1988, Boycott *et al* 1997) and plotted on a geological map of the Burren. Of the 195 features located in the Burren, 153, or 78%, were located in the Western Burren, 83, or 42.5%, were located within 50m of the Namurian boundary and 92, or 47%, were located within 100m of the Namurian boundary. The location and orientation of 1477 enclosed depression (Figure 7.21) were compiled from an unpublished MSc thesis from the Department of Geography in Trinity College Dublin by Yeates (1997) and incorporated in the GIS for spatial analysis. By contrast with the location of the sink holes, enclosed depressions which require longer periods to develop are concentrated away from the

Namurian boundary, just 2, or 0.13%, out of 1477 closed depressions recorded on the Burren occur within 50m of this boundary with only 14, or 0.95%, of the closed depressions located within 100m.

The largest depression in the Western Burren is the Ballyiny depression to the west of Slieve Elva, which is an 88,951 m^2, 970 m long narrow depression trending north-north-east. The other large enclosed depressions in the Western Burren are located on Gleninagh and Cappanawalla and are similar elongate narrow features trending approximately north-northeast. The Eastern Burren is dominated by a series of large enclosed depressions. Of the 1477 recorded depressions 1256, or 85%, occur in this region, the largest being the NW-SE trending Carran Depression, which is approximately 3.8km long, 1.3km wide and 60m deep. There is a large cluster of depressions on the western side of Aillwee Hill, which converge on the large closed depressions of Glensleade and Kilcorney. The largest cluster of these depressions trends north-northeast continues upslope and down the northern flank of the hill in an uninterrupted sequence and appears to be developed along one major fracture zone (Drew 1973).

7.4 Chemical weathering:

Karst landforms develop on limestone result predominantly from solution of the limestone. This is the chemical reaction of a mineral to acidic weathering agents. Limestone dissolves in a weak carbonic acid (H_2CO_3) produced by the reaction of water (H_2O) and carbon dioxide (CO_2) (Equation 7.1)

$$CO_{2\,(aq)} + H_2O_{\,(aq)} \leftrightarrow H_2CO_{3\,(aq)}$$
$$CaCO_{3(s)} + H_2CO_{3\,(aq)} \leftrightarrow Ca^{2+} + 2HCO^-_{3(aq)} \qquad \text{Equation 7.1}$$

The reaction is dependent on the amount of carbon dioxide available; adding carbon dioxide causes the formation of carbonic acid, which dissolves limestone; reducing the amount of carbon dioxide in the system causes the reverse reaction and the precipitation of limestone ($CaCO_3$). This is the reaction responsible for the formation of precipitates such as stalagmites and stalactites. The equilibrium shifts right or left according to pressure and temperature. The solubility of carbon dioxide depends on two factors: partial pressure (PP) and the temperature of solution (T). A linear relationship exists to show that as pressure increases the solubility of $CaCO_3$ also increases (Selby 1985). The PP of CO_2 in an aerated solution is 30Pa and the related solubility of $CaCO_3$ is 63mg/l. Under anaerobic conditions in a soil, the PP of CO_2 may increase to 30kPa (a thousand fold increase) resulting in an approximately tenfold increase of $CaCO_3$ in solution to 700mg/l. Rates of solution in karstic areas will differ depending on the supply and pressure of carbon dioxide (Selby 1985). In karstic areas with a soil cover carbon dioxide is produced by the decay of organic matter and by the respiration of plants. "Soil air" commonly has a carbon dioxide content of 0.25-4.5% in comparison to the atmosphere, which has a carbon dioxide concentration of 0.03% (Selby 1985). Therefore, limestone under a soil cover will be subject to increased rates of solution than the equivalent limestone exposed to the atmosphere. The rate of solution has been measured for a number of karstic terrains. In temperate northern karstic terrains such as the Burren and the Yorkshire Dales of England, this has been achieved through a combination of two principal techniques. The first is the examination of perched block, glacial erratics, and pedestals and the measurement of their height above the bedding surface. As the pedestals are due to the last glaciation their approximate age is available. Using the second technique

Williams (1964) analysed the discharge of the Fergus River to calculate the rate of solution for the Burren, he did this by repeated sampling of the Fergus River to calculate the mean quantity of limestone in the river and by calculating the river's discharge. It should be noted that the Fergus catchment consists of water derived from Lower Carboniferous limestone and Namurian areas. Williams input his collected data into the following formula (Equation 7.2) a variation of Corbels (1957) formula, to derive a figure of $55m^3a^{-1}km^{-2}$ or 55 Bubnoff (B) ($1B = 1mmka^{-1}$).

$$\left(\frac{ETn}{10D}\right) = X \qquad \text{Equation 7.2.}$$

Where,

E= River Discharge, (dm)

T= Total Hardness, (p.p.m.)

n = effective outcrop of limestone in area (%)

D= Density (kg m^3)

This rate of solution is similar to published rates of denudation by limestone solution for the British Isles.

Area	Reference	Rate (B*)
South Pennines, England	Pitty (1968)	75-83
Fergus Basin, Ireland	Williams (1964)	55
Mendip Hills, England	Drew (1974)	50-100
Burren, Ireland	Mitchell & Ryan (1997)	53
Yorkshire, England	Rice (1988)	49-50
Derbyshire. England	Rice (1988)	75-83

- 1 Bubnoff (B) = $1mmka^{-1}$. It is numerically equivalent to rates of removal of material expressed as $m^3a^{-1}km^{-2}$. Table modified from Clayton 1997.

Table 7.1: Denudation rates for limestone.

7.5 Topographic Profiles:

In order to investigate the correlation between fracture patterns and topography a series of topographic profiles were made at a number of locations and at a number of scales to compare the topography with fracture analysis done at the same locations. The topographic profiles ranged in length from 20m to 7,500m in length. Of these ten topographic profiles, five were the result of surveys in the field using an EDM surveying device, and five were the result of analysis of a digital terrain model (DTM) of the region. Two of the EDM profiles were carried out at Sheyshmore and three at Cappanawalla. The topographic profiles were carried out with the aim to investigate specific topographic features; with this in mind the profile is generally equidistant from the centre of the feature

For the five EDM surveyed profiles at Sheyshmore and Cappanawalla the fracture pattern along the profiles was obtained from analysis of a series of high quality back and white aerial photographs at a scale of 1:3,000 (see Section 5.2.3). The georectified images were incorporated into a GIS, Arc View, and the fractures, which have been solutionally enhanced, were delineated from them. The resolution of the images in Arc View allows for centimetre accurate delineation of the fractures, which reduces the introduction of artefacts into the fracture patterns generated. The quality of the images on the computer screen is significantly higher than what appears in the printed out diagrams, which are a function of the printer quality. In addition the fracture pattern areas that were surveyed was "ground truthed" during the course of the surveying.

7.5.1 Topographic profile 1: TP SM EW (Figure7.1).

A topographic profile was surveyed perpendicular to topographic features on the limestone pavement at Sheyshmore. The rationale for doing this was twofold: firstly, to investigate the magnitude of topographic depressions identified from stereoscopic analysis of a series of low-level aerial photographs of the region, and secondly, to investigate any correlation between the fracture patterns in the area and the topography. The topographic profile was 55m long orientated 095°. The fracture pattern of this area (Figure 7.1.b) consists of a set of clustered NS +/- 10° trending veins, a set of regularly spaced strata-bound systematic joints that trend approximately E-W and later joints of variable orientation which curve to meet the earlier systematic joints. The veins act as mechanical layer boundaries for the joints, and the area between adjacent vein clusters is a mechanical layer thickness.

A fracture backbone was derived for the fracture pattern (Figure 7.1.c) (for the theory behind this refer to Section 4.4 on Percolation Theory). The vein clusters have a high intersection density with a large number of cross termination (Px) and a low amount of blind termination (Pb). This leads to an area of high connectivity, as there is a linear relationship between increase in Px and an increase in connectivity. The vein clusters are an area of high connectivity with well-linked fractures.

The pavement areas form in the mechanical layer thickness between adjacent vein clusters, which have a lower overall connectivity. In the pavement areas there are a larger proportion of blind terminations, and the larger regularly spaced fractures have a low intersection density. The pavement areas represent a zone of poorly linked fractures with low connectivity. Long joints link each end of the system but are infrequently linked to nearby joints, thus reducing the overall connectivity of the system. When the topographic profile is analysed in conjunction to aerial photographs of the region, it can be seen that the topographic depressions highlighted on the aerial photograph as zones of dense vegetation (dark zones on Figure 7.1.a and shown on Figure 7.1.d) are confined to these zones of high connectivity caused by the vein clusters. The depressions observed along this topographic profile are minor narrow linear features elongated in the direction of the vein clusters, NS +/- 10°. The linear depression to the left of Figure 7.1.d can be traced for over 140m in this area while the other linear depression can be traced for over 200m. The maximum width of these features is 4m. In the areas between these depressions, the only features formed are clints and grikes and other karren features. The joints are enlarged by solution to form long, narrow grikes dividing the area into large blocks, or clints. When the block size along the traverse is analysed, it can be seen that the mean block size of the pavement shown in Figure 7.2a (the depressions divide the area into three separate areas) is 5.06m^2, the mean block size in the two areas with depressions is 0.97m^2. Figure 7.2.a shows the five divisions along the

traverse and the associated block size for each area. It can be seen that the depressions form in areas where the block size is greatly reduced.

From analysis of the topographic profile, block size and the fracture pattern, it can be seen that the location of the depressions is non random. The depressions only occur where certain parameters are met. Depressions are located at zones of high Px, low Pb, low mean block size, high connectivity, well-linked, clustered fractures with high intersection density and high fracture density. The pavement areas on the other hand occur in areas of high Pb, low Px, low connectivity, fractures of low intersection density, regularly spaced fractures and large mean block size. D1 has a fracture density of 4.64m/m^2 with D2 having a fracture density of 3.85m/m^2. The pavements have an average density of 1.34m/m^2, with P2 having a density of 2.03m/m^2 and P3 having a density of 1.69m/m^2. The depressions have a larger number of fractures, or line segments, per unit area and a correspondingly higher surface area. These zones of high connectivity are zones of elevated weathering by solution. The depressions are confined to, and shaped by, the vein clusters. The depressions do not occur outside the high connectivity regions.

7.5.2 Topographic profile 2: TP SM NS (Figure 7.3).

A topographic profile was surveyed perpendicular to the dominant joint pattern in the region on the limestone pavement at Sheyshmore. This topographic profile is perpendicular to the previous topographic profile, Figure 7.1. The topographic profile is 60m long and orientated 010° parallel to the vein pattern in the immediate area. From stereoscopic analysis of the area, the major topographic features were identified as trending 010° with few if any topographic features orientated in other directions. The fracture pattern along this profile (Figure 7.3.b) is dominated by the regularly spaced, approximately EW trending strata-bound systematic joints. Bed dip is, 002°, to the south. The clusters of NS trending veins lie on either side of the profile, and the profile is located in a mechanical layer thickness defined by the clustered veins. A fracture backbone was derived from the fracture pattern (Figure 7.3.c) dominated by the systematic joints. The backbone is composed of a large number of abutment terminations with few cross terminations. Those few cross terminations are the result of a number of NNE trending veins in the bottom right corner of the figure. The systematic joints link either side of the mechanical layer thickness, or pavement, but have little interaction with adjacent joints, which reduces the overall connectivity of the system. In addition, the joints have a low fracture intersection density, illustrating their lack of interaction with other fractures. When the topographic profile is examined, the result is a horizontal surface with little vertical variation. The dominant topography produced is limestone pavement with its characteristic narrow grikes and flat clints. When the block size along this profile is examined the average block size is 6.41m^2, comparable with the figure derived from the pavements along the previous profile.

There are few topographic depressions located along this profile. The fracture system is low in connectivity due to the large number of blind terminations. There is a linear relationship between increase in blind terminations and decrease in connectivity. The joints are not connected to a sufficient extent to enable depressions to form. Any depressions formed along this profile will be orientated along the joints and will be very narrow, in the order of cm due to its lack of interaction with other joints. The pavement is vertically constrained by the strata-bound nature of the joint pattern, and its horizontal extent is limited by the fact that

the vein clusters act as mechanical layer boundaries controlling the length of the joints. The only feature possible to develop under these conditions is the one dominant feature already present: grikes that separate large blocks with minor karren features on their surfaces such as kamenitzas.

7.5.3 Topographic profile 3: TP Cap 3-7 (Figure 7.4).

A topographic profile was surveyed perpendicular to the dominant topographic features on the top of Cappanawalla. Cappanawalla is a NW-SE trending hill on the north coast of Co. Clare that reaches a maximum height of 312m. There is a large expanse of limestone pavement on the hilltop from an altitude of 270m. A number of large NNE trending gullies cut across the pavement on the southeast part of Cappanawalla. This topographic profile was done perpendicular to one of these large gullies on the southeastern end of a limestone pavement on the hilltop. The topographic profile is 153m long and orientated at 104°. The fracture pattern of this area consists of a set of non strata-bound clustered veins trending NNE; strata-bound systematic joints trending NW-SE that are exposed on two different beds each having different geometric properties; and a set of minor oblique cross joints of variable orientation. The NNE veins increase in density towards the centre of the major depression in the area, and as a result, the NNE trending veins closer to the depression dominate the backbone of the system. In areas further away from the depression the systematic joints have a large influence on the backbone. In these areas, the joints divide the area into large blocks, which are part of the pavement on the hilltop. Due to the minor amount of veins in these areas the joint terminations are dominated by abutments and blind termination with little if any cross termination. As the proportion of blind terminations increases connectivity decreases resulting in these areas having low connectivity. As with similar areas on the previous profiles, horizontally persistent joints dominate these areas, which are poorly linked with adjacent joints leading to a poorly connected system. There are no depressions in these areas. When vein clusters are present, the fractures present a well-connected system. The veins have a high intersection density and are well linked to the joints, the joints are at a high angle to the veins and each vein is cross cut by a large number of joints leading to an increase in the proportion of cross termination (Px) which lead to an increase connectivity and a low amount of blind terminations (Pb). The veins are in turn well connected to adjacent veins due to the closely spaced nature of the veins and the fact that they are cross cut by the joints. The vein clusters increase in frequency towards the centre of the depression, creating an increasing number of high connectivity zones as you move towards the depression. When the topographic profile is analysed and compared to the fracture pattern along it, it is apparent that when the veins are absent the topographic profile has little vertical variation, once the vein cluster start to appear they cause the topographic profile to have an increased vertical variation which increases towards the centre of the depression. It can be seen that there is a clear correlation between the presence of vein clusters and the presence of depressions. When the depressions are analysed they are for the most part long narrow linear features elongated in the direction of the vein clusters, NNE. The major gully in the area is orientated 010° and can be clearly traced for over 360m, before it moves down the hill side, even form a distance of a few kilometres it is readily seen that this feature is a pronounced topographic feature along both sides of the hill, at its widest the depression is 30m and has a vertical relief of over 6m along the profile. Smaller depressions, with a horizontal extent in the region of tens of metres occur along the edges of the depression. The number of depressions increases towards the gully, Figures 7.4 to 7.6. In areas where there are no veins the landscape consists of horizontally persistent narrow, cm, vertically constrained grikes

the result of solution acting on the joints. These grikes divide the area into large blocks, clints, which have minor karren features on their surfaces such as kamenitzas.

Conclusion: The depressions are non-randomly located they occur only where veins clusters are located. The depressions are narrow linear features orientated in the same direction as the veins, in areas, which have a small amount, or no veins the topography is dominated by limestone pavement and its characteristic karren features. The depressions form at these specific locations due to a combination of the following factors, the zones of vein clusters are zones of high intersection density with a high proportion of cross fracture terminations and correspondingly low proportion of blind terminations which leads to a zone of high connectivity, the fractures in these zones are well linked spatially and are not vertically confine to the individual beds like joints and pavement are. These zones have a large fracture length per unit area and a correspondingly large surface area for solution to be localised on. The block size in these zones is dramatically reduced from an average on the pavements of $4.52m^2$ to $1.57m^2$ (Figure 7.2.b). From the topographic profile it can be seen that the vein cluster have large impact on the topography along the profile.

7.5.4 Topographic profile 4: TP CAP4z (Figure.7.5).

A topographic profile was surveyed perpendicular to the dominant topographic features on the top of Cappanawalla. The topographic profile is 23m long and orientated 103°. This topographic profile is a smaller scale that the previous one. It was done perpendicular to a series of minor depressions on the pavement on the east side of the large gully. The depressions are long narrow features, the longest being 20m with a width in the region of 1m. There are two dominant fracture sets along the profile, a series of regularly spaced NW-SE trending strata-bound systematic joints which are horizontally persistent and a set of clustered non strata-bound NNE trending veins. There is a minor set of oblique cross-joints of variable orientation. The joints are poorly linked spatially with a higher amount of blind terminations (Pb) and a low number of cross termination (Pa). Where the vein clusters occur they are zone of well connected fractures with a high proportion of cross terminations (Px) and a low number of blind terminations (Pb) as well as having a high intersection density causing theses zone to be zones of high connectivity. When the topographic profile is analysed the depression are located only along the vein clusters. The depressions are long narrow, shallow features, extending for a maximum of 20m with a width less than 1m and a depth under 1m.

Conclusion: The depressions measured along this profile are located at very specific sites that coincide with vein clusters. The magnitude of the depressions and the vein clusters is in the order of metres with the individual depression being less than 1m wide. At this small scale it can be scene that the depressions form where the vein clusters create a zone of elevated connectivity, elevated surface area and fracture density and a zone of reduced block size, all of which combine to enable a depression to form. In those areas where the depressions do not occur they correspond to zones of lower connectivity, lower fracture density and larger block sizes, all of which combine to retard the development of depressions. In these regions the only topographic feature possible to form are limestone pavements with its associated clints and grikes and minor karren features.

7.5.5 Topographic profile 5: TP CAP4-5-6 (Figure 7.6).

Topographic profile CAP 4-5-6 was carried out perpendicular to the major gully on Cappanawalla. The profile is 177m long and orientated 104° and is located 20m south of topographic profile Cap3-7. The profile crosses the main gully and continues along the pavement to the east of the gully cutting across a number of clusters of NNE trending veins with associated minor topographic depressions. The fracture pattern along this profile has already been described in the description of topographic profile Cap3-7, with the main points being NE-WS trending systematic veins which are poorly connected spatially and a set of NNE trending veins which have a high intersection density and a create a zone of high connectivity.

The joint dominated regions consist of horizontal limestone pavement with the joints being enlarged to horizontally persistent grikes and dividing the bed into a series of blocks or clints. The NNE trending veins occur in clusters and increase in frequency towards the main gully accounting for the increase in frequency of minor depressions towards the gully; in addition there are a number of small vein clusters along the pavement, which are represented on the topographic profile by minor depressions. The pavement areas have an average block size of $4.52m^2$ (Figure 7.2.b) compared to an average block size of $1.57m^2$ for the areas along the depression, with a fracture density of $1.11m/m^2$ for the pavement areas and a density of $1.69m/m^2$ for the depression areas.

Conclusion: As has been found along TP CAP 3-7 the depressions are non-randomly located occurring only where veins clusters are located. The depressions are narrow linear features orientated in the same direction as the veins, in those areas dominated by the joints the topography consist of limestone pavement. The depressions form at these specific locations due to a combination of the following factors, the zones of vein clusters are zones of high intersection density with a high proportion of cross fracture terminations and correspondingly low proportion of blind terminations which leads to a zone of high connectivity, the fractures in these zones are well linked spatially and are not vertically confine to the individual beds like joints and pavement are. These zones have a large fracture length per unit area and a correspondingly large surface area for solution to be localised on.

7.5.6 Summary:

A series of detailed topographic profiles were carried out at two separate locations. The profiles varied in length from 20m up to 177m. They were done perpendicular to the dominant topographic features and fractures in the two regions. The profiles complemented fracture analysis work on the same location. The topographic profiles combined with detailed analysis of the fractures at these locations allowed fro the investigation of the factors controlling the location of the depression, the randomness of depression location, and any correlation between fracture patterns and topography.

The depressions are non-randomly located; the location of the depressions is controlled by the presence of NNE trending vein clusters. The depressions have similar geometrical properties to the vein clusters, they are long narrow linear features and in the case of the large gully on Cappanawalla the depression is non strata-bound and on Cappanawalla when vein clusters begin to increase in frequency towards the large gully

the depression exhibit similar behaviour. The depressions are confined to the clusters and do not form outside the vein clusters. The depression form along the vein clusters due to a combination of the following parameters, the vein clusters are well linked spatially through interaction with the joint pattern, they have a large proportion of cross terminations and a low proportion of blind terminations and a high intersection density providing a fracture backbone with a high connectivity, the length of fractures per unit area is large creating a large surface area for solution to act on and correspondingly the bed is mechanically weakened by the block size being dramatically reduced compared to the surrounding pavement. The pavements form in joint dominated areas where the joints are poorly liked spatially with a higher proportion of blind terminations and a lower proportion of cross terminations leading to a zone of lower connectivity. The location of the vein clusters is clearly recorded from the topographic profiles by the location of depression. The depressions are caused by and highlight the vein clusters. Depressions in this area are controlled by the fracture pattern.

7.6 Topographic profiles at a larger scale:

As has been previously stated the central area along the western flanks of Aillwee Hill is the location of a large cluster of depression. The largest cluster of these depressions trends north north east and continues upslope and down the northern flank of the hill in an uninterrupted sequence and appear to be developed along one major fracture zone (Drew 1973). A map of all known depression was complied through a combination of the depressions mapped by Drew 1973 and analysis of aerial photographs of the eastern part of Aillwee Hill and Turlough Valley. This map was overlain onto a geological map of the region and onto a digital terrain model (DTM) of the Burren region. From the DTM it is possible to extract topographic profiles across the Burren. A series of profiles were done across and along a series of topographic features. The first profile was done longitudinally along the main axis of depression in the Aillwee area, two profiles were done perpendicular to this cluster of depressions, a fourth profile was done perpendicular to the NW-SE trending Glen of Clab to the east of Turlough Valley and a fifth profile was done perpendicular to the Ballyiny Depression located on the west coast of the Burren.

7.6.1 Topographic profile 1: Aillwee TP1 (Figure 7.7).

A topographic profile was done parallel to the largest cluster of depressions in this region, which is co-incident with the orientation of veins in the Burren. The profile is orientated 014° and is 7237m long and moves along dip across the Burren Limestone and Slievnaglasha Formations. The location of depressions was marked along the profile as were the location of any caves along with lithological contacts. The profile begins at the northern end of Aillwee Hill at an elevation of 90m before rising to an elevation of 230m before descending over several kilometres along dip to 150m. From the profile and the relationship of the topography, lithological contacts and bed dip the most obvious feature is that the depressions continue up the slope, against dip, and down the northern flank of the hill in an uninterrupted sequence, Drew (1973) postulates that these depressions developed along one major fracture zone. The different members of the two Formations present appear to have little influence on the creation of depressions, as depressions occur n all seven lithological members present, with the large depressions crossed Ballyallaba depression 8, Glensleade and Kilcorney Depression cutting through bed boundaries.

Conclusions: The depressions are all aligned NNE and are not strata-bound, which are similar geometric properties as the NNE trending veins. A number of the larger depressions appear to be elongated perpendicular to the profile, being orientated, or having a portion of the depression orientated NW-SE. There are a number of cave systems along this topographic profile, which have significant NNE trending vein controlled cave passages, Aillwee Cave (Section 6.5.1.1) and Kilcorney Cave (Section 6.5.11.1).

7.6.2 Topographic profile 2: Aillwee TP2 (Figure 7.8).

Topographic profile TP2 was done perpendicular to the largest cluster of depressions in the region; it is 7951m long and orientated 105°. It begins on the easterly slopes of Aillwee Hill/Turlough valley and continues across Aillwee hill to Ballyvaughan valley. It crosses a number of observed depressions. The depressions crossed are narrow elongate features trending NNE similar to the depressions observed on Cappanawalla and Sheyshmore, which have been correlated to vein clusters. The depressions observed are tens of metres wide and extend of hundreds of metres. The depressions highlighted from the topographic profile can be correlated with the mapped depressions from the region.

Conclusion: At the kilometre scale narrow elongate depression trending NNE, coincident with vein geometries, are observed along the topographic profile. From the profiles carried out at smaller scale it can be seen that depression location is a non-random event and is strongly linked to the location of NNE trending vein clusters.

7.6.3 Topographic profile 3: Aillwee TP3 (Figure 7.9).

Topographic profile TP3 was done perpendicular to the largest cluster of depressions in the region; it is 6066m long and orientated 106°. It begins on the easterly slopes of in Turlough valley and continues across Aillwee hill to Ballyvaughan valley. It is located 2 km to the north of the previous profile, TP2. A number of depressions are picked out form the topographic profile. Starting form the east of the profile the NNE trending arrow elongate Deelin Beg Depression is apparent as the profile moves westwards two NNE trending depressions located at Deelin More are apparent, these depressions can be confirmed from analysis of aerial photographs of the region. They are narrow zones of depressions elongated to the NNE. The top of Aillwee Hill is dominated by a series of minor depressions, which lead to a large depression at approximately 3900m along the depression. There is an apparent increase in depressions towards this feature, reminiscent of the increase in frequency of depressions towards the gully on Cappanawalla. This depression is part of the Aillwee dry valley network on the summit of Aillwee Hill. The depressions occur in a number of lithologies.

Conclusion: As with the previous topographic profile it can be seen at the kilometre scale narrow elongate depression trending NNE, postulated to be coincident with vein geometries, are observed along the topographic profile. As the topography along Aillwee Hill is analysed it can be seen that these narrow elongate depressions are persistent Deelin More depression 1 continues along the same trend as the Poulaphuca depression from TP2. On the eastern side of Aillwee Hill Ballycahill depression 6 is a continuation of the Berneens depression 2 observed on TP2.

7.6.4 Topographic profile 4: Glen of Clab TPG1 (Figure 7.10).

The Glen of Clab (Figure 7.22) is a distinctive NW-SE trending (286°) over 1km long elongate depression located north of Carran on Gortaclare Mountain. Feehan (1997) states that the Glen of Clab is an unroofed collapsed cave passage with Poulawallan immediately to the northwest being an old doline or swallow hole. Drew (pers comm. 2003), believes that given the size of the depression at the Glen of Clab, 1km long, 350m wide and >60m deep, it is unrealistic that it is in fact a collapsed cave passage and is a feature created by a coalescing of a series of NW-SE trending dolines. The Glen of Clab is of interest as the majority of depressions found in the Burren are oriented NNE, also of interest is that it is oriented in the same direction as Aillwee cave (286°) and a series of colls in the hillside to the immediate south-east of the Glen of Clab link it to the Glencolmcille Depression and to the Gort Lowlands. The Topographic profile was done perpendicular to this distinctive depression, oriented 197° and 3600m long. The Glen of Clab cuts through the Slievnaglasha Formation into the upper Aillwee Member of the Burren Limestone Formation. The depression is over 1km long, 350m wide and has apparent vertical depth of 60m from the surrounding hillsides. There are a number of minor depressions on the hillsides to the north and south of the glen, which appear to increase in frequency towards the glen. To the north of the glen there is a NW-SE trending minor topographic feature apparent on aerial photographs, marked on the profile as a possible topographic feature. The Glen of Clab is orientated along a NW-SE trending fracture system.

7.6.5 Topographic profile 5: Ballyiny Depression TPB1 (Figure 7.11).

The Ballyiny Depression (Figure 7.11.a) is a closed, narrow elongate depression orientated NNE on the west side of Slieve Elva. It is the largest enclosed depression in this area. The main part of the depression is a narrow, under a 100m at its widest, long, approximately 1000m long, trending 018°. The main depression has two subsidiary depressions at either side. The shorter depression is an EW trending depression located on the west side of the main depression. The longer depression is located on the east side of the main depression and consists of a number of segments trending EW, NNE and NE-SW. This longer depression appears to be a composite depression linking two smaller NNE trending depressions to the larger main Ballyiny depression through local joints. There are two large cave systems in the region, Pollballiny that drains for the NE and terminates under the depression at one of the NNE trending factures controlling the location and size and shape of the depression. The other cave in this region is Poll Na gCéim (Section 6.5.4.1), which can be traced along the western edge of the depression and is orientated NNE; this cave is the second deepest cave in Ireland at 18 m deep. Lloyd & Self (1982) described the depression and considered that it was controlled either by the regionally dominant NNE trending fractures or that these fractures were faults, Judd and Mullan (1994) state that the NNE trending fracture that control the orientation of Poll na gCéim is a fault. There is little evidence elsewhere in the Burren for faulting and there is no apparent stratigraphic off set visible on the geological map of this region, Mullan in a follow up paper in 1995 acknowledges that this is a debatable point.

The Ballyiny Depression has the same characteristics as the depression observed on Cappanawalla and Sheyshmore being narrow and elongate in the direction of the regionally dominant vein system. It therefore seems more likely that the depression is located along a vein cluster and the two NNE segments of the longer

subsidiary depression are located along vein clusters. The topographic profile (Figure 7.11.b) taken perpendicular to the depression is 933m long and orientated 107°. The main depression appears as a low relief zone.

Conclusion: The Ballyiny depression has similar geometrical properties as the smaller scale features described on Cappanawalla, a swell as the regionally dominant vein system. The depression formed along a cluster of NNE trending veins. To the north of the depression there are a series of smaller enclosed depression of then same orientation (Lloyd & Self 1981). There is a direct spatial correlation between the NNE trending Poll Na gCéim cave system and the NNE trending Ballyiny Depression. Both features are formed along a NNE trending vein cluster.

7.7 Enclosed depressions:

As has been previously stated the Eastern Burren is dominated by large enclosed depressions with the largest cluster of depression being located on the western side Aillwee Hill (Figure 7.12). These depressions are narrow elongate features that trend north-north-east and continue upslope and down the northern flank of the hill in an uninterrupted sequence and appear to be developed along one major fracture zone (Drew 1973). The orientation and shape of the depressions, labelled on the diagram as BC 1-6, BA 1-10, and B 1-5 when combined with the information gathered from the investigation of depressions on Cappanawalla and Sheyshmore, supports Drew's hypothesis. The depressions are formed on a cluster of NNE trending non strata-bound veins. As on Cappanawalla the depressions have similar geometric properties to the veins they are confined to particular areas are narrow and are non strata-bound. The depressions on the west of Aillwee Hill cut through a number of geological units and continue along the hill and over the northern side. The vein clusters terminate in the large Glensleade Depression, but the vein cluster has a significant control on the location and shape of this depression and the large Kilcorney Depression to the south. These depressions have a marked NNE trending component, with the large NNE trending aspect of the depression in Glensleade corresponding to the marked NNE component of Kilcorney to then south and to the series of smaller depressions to the north. The vein cluster can be traced, via the depressions, for over 7km and is at most 120m wide. In addition to these two large depressions having NNE trending depressions they also have a strong NW-SE trending component. There are a number of subsidiary topographic features in the vicinity of the main set of depressions. To the north the Aillwee depression, A 1-14, appear from a distance to have a trend of 060°, further south the Gleninsheen depressions, GS 1-11, have a stepped appearance and have an overall orientation of 030°, a third subsidiary set are the Ballymahill group, BM 1-8, which are orientated 060°. On the eastern side of Aillwee Hill there are a number of elongate NNE trending depressions, to the north six depressions, Deelin More, DM 1-5, and Deelin Bed, DB, have been identified from aerial photograph analysis and confirmed by topographic profiles across the area. To the south Poulbaun, PB and Poulaphuca, PP, are narrow, elongate NNE trending depressions, which are picked out by both aerial photographs and the DTM of the region. These two depressions are located along the same orientation as the Deelin More and Deelin Beg depressions and can tentatively be linked by a minor NNE trending feature visible on aerial photographs. These depressions seem to be located along NNE trending vein clusters. To the immediate southwest of Deelin More on the summit of Aillwee there is an old working of argentiferous galena along a NNE trending vein cluster. Another feature of interest from this diagram is geographical

spread of caves in this region. Of the thirty-two caves in the region fourteen are located along the Namurian boundary, of the remainder they are mainly confined to the depression. The two largest cave networks in the region both coincide with the large NNE trending vein cluster, which controls the largest cluster of depression and is physical evidence of a NNE trending vein system being present. Aillwee cave, marked 32 on the diagram, is composed broadly of two sections a NW-SE trending section and a NNE trending section that is coincident with the northern most Ballyallaba depression, the Cave of Wild Horses, cave number 17, coincides with the NNE trending aspect of the Kilcorney Depression. The Cave of Wild Horses has a strong NNE control with minor NW-SE and EW controls on cave passages.

Conclusion: The large cluster of NNE trending depression to the west of Aillwee Hill is controlled by a NNE trending vein cluster. The evidence for this is as follows, the depression are narrow elongate features, the depressions are all orientated 015°, the location of the depression does not vary more than 100m over the course of 7km either side of a line orientated 015° linking the most northerly and southerly depressions, NNE trending veins controlled cave passages in Aillwee cave and the Cave of wild horse coincide with surface topographic features trending 015°, the depressions are not strata-bound features. Detail work on Cappanawalla shows that the depressions exhibit the same geometrical parameters as the veins in that they are narrow elongate features trending in the same direction as the veins, are not strata-bound and whose location is controlled by the vein clusters. The same processes have formed the depressions seen along the side of Aillwee Hill as the smaller scale features analysed elsewhere. The topographic features on the east of Aillwee Hill exhibit similar properties and appear to be formed along a series of vein clusters. Drew (1973) contends that these features are confined to the central and Eastern Burren due to the greater maturity of the karst in these regions. .

7.7.1 Orientation Analysis of Enclosed Depression:

The orientation of the enclosed depression in the vicinity of Aillwee Hill were analysed in detail in order to use them to analyse the fracture pattern of the region.

7.7.1.1: Ballycahill, Ballyallba and Aillwee depressions (Figure 7.13)

The depressions in Figure 7.13 have been divided into three groups, Ballycahill (BC) Ballyallba (BA) and Aillwee (A) (Figure 7.13.a). The depressions vary in width between 20 and 50m and in depth between 4 and 10m with individual depressions separated from each other by rock colls (Drew 1973). The longest axis of the depressions was delineated by a line, where a depression consisted of sections of different orientation, such as Aillwee 1, lines were drawn the length of one of the section, when the depression changed orientation another line was draw (Figure 7.13.b). The dominant fracture orientation for these three depression groups in NNE, with a minor component of NE-SW fractures. The Aillwee group depression have a wider variation in orientation, they appear to be composite depression, with NNE trending sections being linked to adjacent NNE sections by NE-SW trending fractures, these correlate to cross joint orientation seen on Cappanawalla. The NNE trending section of Aillwee cave (Section 6.5.1.1) coincides with the northern most depression of the Ballyallba group, which has a coincident trend. The veins define a narrow zone of high fracture connectivity – due to the increased proportion of cross terminations- in which flow will be concentrated thereby creating the narrow nature of vein controlled passages. The NNE trending cave passages are

geographically coincident with this series of depressions on the surface directly above the cave, demonstrating that the vein cluster has a vertical extent in excess of 110m. Drew & Cohen (1980) noted that a number of small streams exist in this latter section and that after heavy rainfall large amounts of water quickly percolate from the surface to swell these streams, presumably utilising this long, over 6km, vertically extensive, highly connected NNE, >110m, trending vein system. The hydrological setting for the formation of Aillwee cave was different from the present hydrological setting, where the regional flow is along dip. The dry valley network in the Aillwee group appears to be following this drainage.

7.7.1.2: Berneens and Gleninsheen Depression (Figure 7.14)

The depressions in Figure 7.14 have been divided into two groups the NNE trending Berneens group (B) and the 030°trending Gleninsheen group (GS) (Figure 7.14.a). The Berneens depressions are controlled by a NNE trending vein cluster. The Gleninsheen group consists of a series of NNE trending sections, GS2, being linked by NE-SW joints (Figure 7.14.b). An increase in the frequency of vein clusters towards the centre of a larger vein cluster has been recognised on Cappanawalla where like here it is associated with an increase in the frequency of minor elongate depressions towards a larger depression. The northeasterly end of the Gleninsheen depression, GS2 at an elevation of 220m OD is along strike from Poulawallan and the Glen of Clab. This could be the most northwesterly-recoded depression of a string of NW-SE trending depressions, which continue into the Gort Lowlands. The overall fracture pattern is dominated by NNE trending fractures.

7.7.1.3: Glensleade and Kilcorney Depression (Figure 7.15)

The depressions in Figure 7.15 have been divided into three groups Glensleade depression, Kilcorney Depression and a group of seven smaller depressions, GKP 1-7 (Figure 7.15.a). The Glensleade depression is composed of two segments a NNE trending segment that is controlled by the same NNE trending vein cluster that controls the smaller scale enclosed depressions to the north and the NNE aspect of Kilcorney depression to the south (Figure 7.15.b). The second segment of the depression is a WNW-ESE trending segment that extends for 1400m and is over 200m wide. Kilcorney depression is similar in layout; the central portion is a NNE trending depression with the southerly part of the depression a WNW-ESE trending depression. The NNE section is composed of a number of parallel components, there are a number of indentations along the southern side of the depression that are controlled by NNE trending scarps, reflecting then cluster nature of the vein pattern. The WNW-ESE sections correspond to the same orientation as the WNW-ESE trending cave passage in Aillwee cave. The rose diagram of the depressions is dominated by NNE trending fractures with a sizeable proportion of WNW-ESE fractures. The rose diagram resulting from the fracture analysis of the Cave of Wild Horses (Section 6.5.11.1) shows that the NNE fractures are the dominant fracture followed by NWN-ESE fractures and then E-W fractures in controlling cave passage orientation. The southern portion of the NNE trending central section is coincident with NNE trending cave passages, indicating that as with Aillwee cave the NNE trending veins are vertically persistent. These major depressions are older than the last glaciation with drift deposits *in situ* in Kilcorney and Glensleade as well as in Meggagh and Carran (Drew 1973). A stalagmite sample from the Cave of Wild Horses has been dated to 41,000 BP, implying that the passage pre dates glaciation (Drew 1983 pers comm. in Boycott *et al* 1983). The lowest point in Kilcorney is at 103m OD (Figure TP1), Drew (1988) notes that evidence from drilling suggests that the bedrock floor of the depression is at an elevation of less that 50m OD, which would place it in the upper

Aillwee member of the Burren Limestone Formation, the same lithology that is at the base of the Glensleade depression.

7.7.1.4: Ballymihill Depression (Figure 7.16)

The Ballymihill depressions are a series of elongate narrow NE-SW trending series of depressions. The rose diagram is dominated by NE-SW fractures (Figure 7.16.a). As in the Aillwee depressions, which have a similar overall orientation, there are a number of NNE trending sections connected to each other by NW-SE fractures (Figure 7.16.b). The Meggagh and Carran depression to the south and southeast are orientated NE-SE along fold axis. This region of the Burren is host to a number of NE-SW trending monoclines, which swing into the Fergus Shear Zone in the Gort Lowlands. They are the cause of topographic features such a Meggagh, Carran, the Lough Aleeaun depression, scarps at Cathair Comhain and Mullagh More. Fracture analysis at Sheyshmore shows that a set of NE-SW trending fractures increase in frequency towards the centre of these fold axis. Ballymihill may be related to the fold axis responsible for the Meggagh depression.

7.7.1.5: Depressions to the east of Aillwee Hill (Figure 7.17 &7.18)

The depression of Deelin More, Deelin Beg (Figure 7.17.a), Poulaphuca and Poulbaun (Figure 7.18.a) are a series of elongate narrow NNE trending depression which are located along vein clusters (Figures 7.17.b & 7.18b) on the eastern side of Aillwee Hill. The two more southerly features Poulaphuca and Poulbaun can be continued along the trend of the depressions into the Deelin More set of depressions with a faint linear feature apparent of aerial photographs to suggest this.

7.7.1.6: Poulawillin Depression (Figure 7.19).

Poulawillin depression is an elongate NE-SW depression to the north of the Meggagh depression (Figure 7.19.a). The rose diagram is dominated by NE-SW fractures with some minor NNE segments along the depression (Figure 7.19.b), notably in the middle of the main depression. Poulawillin may be related to the fold axis responsible for the Meggagh depression.

The orientation of all the large enclosed depressions (Figure 7.20) in the Burren was studied with a view to determining what the dominant orientation of the depressions in the Burren is, and as a result what is the dominant fracture orientation responsible for the depressions. Ninety-eight depressions were investigated, the majority being located in the cluster on the west side of Aillwee Hill. The resultant rose diagram shows that the NNE veins are the dominant control on depression orientation. WNW-ESE fractures also have a control, principally in the Glensleade and Kilcorney depression, the other set of fractures that had a strong influence trended NE-SW. This is the orientation of the monocline fold axes and their associated fractures as well as being the orientation of minor joints across the Burren. The NNE trending veins are the regionally dominant fracture pattern in the Burren, the joint pattern while locally consistent varies throughout the Burren, in Cappanawalla the joints trend WNW-ESE while at Sheyshmore they trend EW. The clustered nature of the depression is a result of the clustered nature of the vein population.

The location and orientation of 1477 enclosed depression (Figure 7.21) complied from an unpublished MSc thesis from the Geography Department at Trinity College Dublin were analysed in order compare the results to the results obtained in this study. The clustered nature of the smaller enclosed depressions is apparent

from a visual inspection of the data. The largest cluster is again the area to the west of Aillwee Hill. The resultant rose diagram shows that a large percentage of the depressions are orientated NNE.

7.8 WNW-ESE trending depressions:

A number of topographic features are orientated WNW-ESE (Figure 7.22) apparently at odds with the dominant fracture control on the formation and location of depressions in this area. The Glen of Clab in the Eastern Burren is the largest of these features along with the southern extent of Glensleade and Kilcorney Depression which both have pronounced WNW-ESE aspects. The Glen of Clab is a distinctive WNW-ESE trending (286°) over 1km long elongate depression located north of Carran on Gortaclare Mountain. Feehan (1997) states that the Glen of Clab is an unroofed collapsed cave passage with Poulawallan immediately to the northwest being an old doline or a swallow hole. Drew (pers. comm. 2003) believes that given the size of the depression at the Glen of Clab, 1km long, 350m wide and >60m deep, it is unrealistic that it is in fact a collapsed cave passage and is a feature created by a coalescing of a series of NW-SE trending dolines. The Glen of Clab is oriented in the same direction as Aillwee cave (286°) (Figure 7.23) and a series of colls in the hillside to the immediate south-east of the Glen of Clab link it to the Glencolmcille Depression and to the Gort Lowlands, to the north-west the NNE fracture dominated Gleninsheen depression, GS2 at an elevation of 220m OD is along strike from Poulawallan and the Glen of Clab. Drew and Cohen (1980) describe Aillwee cave as having extensive phreatic development in contrast to the recent caves of the Burren, suggesting that the hydrological conditions that formed Aillwee cave, and presumably the Glen of Clab, were very different to the present down dip to the SW flow. To the east of the Glen of Clab a series of colls aligned WNW-ESE are visible between Doomore and Fahee North (grid reference 131100 201850) linking it the Glencolmcille depression, and on Turlough More Mountain (grid reference 133500 2012500) linking it to the Gort Lowlands. These features are aligned along the same orientation as fractures resulting from the termination of the Fergus Shear zone and a series of karstic features to the northeast along the Gort Lowlands (Figures 7.23 &7.28).

7.9: Gort Lowlands:

The Gort Lowlands forms a NNE trending corridor of low land from Galway Bay in the north to the Shannon Estuary in the south; lying between two areas of high relief Slieve Aughty to the east and to the west by the Burren and the Namurian capped hills of West Clare. It is over 40km long and at it narrowest is less than 12km wide. It is an exceptionally flat feature with a maximum elevation of 27m along its length, as can be seen in Figure 7.24. The Gort Lowlands is an intriguing feature, as the geology of the region it lies in is similar to that of the, comparatively, high relief Burren, and Dinantian limestone. It has a similar geology to the Burren but a remarkably different landscape. Cross sections across the Gort Lowlands from the Burren in the west to Slieve Aughty in the east show the dramatic change in topography once you move off the Burren plateau, Figures 7.25 & 7.26.

To the north the lowlands are underlain by a series of large phreatic passages, which connect surface drainage features. These phreatic passages represent a once vast cave system now partly destroyed by surface lowering (Simms 2001). The Lowlands have been exposed longer than the limestone on the Burren which

has until the recent past, and still is in a number of location, been protected by the overlying Namurian strata. Folding across Slieve Aughty exposed the Limestones and Old Red Sandstone (Williams 1964, Simms 2001) allowing for rivers to flow from the ORS onto the limestone where they formed caves passages. Ford & Williams (1989) consider the Gort Lowlands to be a classic example of a corrosion plain. Corrosion plains develop by solutional removal of material down to a surface controlled by the water table-the epiphreatic surface. Once the topography has corroded down to this surface the plain expands by the gradual retreat of adjoining karst uplands.

The Gort Lowlands corresponds to the location of the Fergus Shear Zone a sinistral NNE trending structural feature. The Fergus Shear Zone creates a more complex than the regional fracture pattern along its length. In the Gort Lowlands there are four dominant fracture patterns at high angles to each other. This leads to high fracture connectivity along the length of the Fergus Shear zone. On the Burren increased fracture connectivity is correlated to topographic depressions at a number of scales from the centimetre scale to the hundreds of metres scale. The Gort Lowlands may have been formed along the Fergus Shear Zone due to its increased connectivity.

Fractures can be seen to be controlling both the surface and subsurface flow in the region. The Gort River, Figure 7.27, resembles the cave patterns of the Burren that have been formed along a fracture backbone. The properties of the river are similar to what has been observed in the caves. The river is narrow, less than 500m wide, and elongate, over 4km long and trends NNE with a low sinuosity value of 1.06. When the segments of the river are analysed the resultant pattern is dominated by NNE trending fractures with NW-SE, NE-SW and EW. The fracture patterns "recorded" by the river are the same as those from the aerial photograph analysis of the Gort region (Section 2.2).

The subsurface drainage of the Gort Lowlands, Figure 7.28, was obtained from the OPW report on the flooding in the Gort –Ardrahan area (OPW 1998). As has been previously discussed fractures provide high permeability pathways through a system and in an impermeable matrix, flow is confined to the fracture backbone (Odling *et al* 1999). The catchment is bounded to the east by the Slieve Aughty Mountains, to the south by the Fergus river catchment, to the west by the Eastern Burren and to the north by Galway Bay. Recharge to the system is either via concentrated inputs from streams off the Slieve Aughty Mountains to the east or via diffuse inputs, rainfall, over the limestone of the Gort Lowlands and the Kinvarra catchment area of the Eastern Burren (see Figure. 6.57 for location of Kinvarra catchment). The system drains to Kinvarra and to Corranoo. This area is subject to periodic flooding of varying magnitude, and on a number of occasions, particularly in the 1990's, to high magnitude floods, which cover large areas of the region (Section 1.1). Flooding in this region occurs when sinking streams, sourced on the Slieve Aughty Mountains, are backed up when the flow exceeds the capacity of the underground flow channels and by enclosed depressions (Figure 7.29) filling up with rising ground water. The large-scale floods in the 1990's were a result of very high rainfall over a prolonged period, which lead to the finite capacity of the karstic flow system being exceeded (OPW 1998).

The flow channels marked in Figure 7.28 are a record of the fracture backbone of the region. When the direction of the channels is analysed (Figure, 7.28), the system is composed of five principal orientations (Table 7.2)

From Groundwater flow		From Aerial photos	
WNW-ESE	110-130°	NE-SW	030-050°
NE-SW	030-050°	WNW-ESE	110-130°
NS	350-010°	NW-SE	150-160°
NW-SE	150-160°	NS	350-010°
EW	090	EW	090

Table 7.2: Orientation of the fracture patterns controlling groundwater flow in the Gort Lowlands.

These orientations correspond to the fracture patterns mapped for the Fergus Shear Zone, in Chapter 5. The fracture patterns from the Fergus Shear zone explain the direction of flow in the region. In particular they explain the unexpected flow of the system to Corranoo. A series of cave passages, 25 metres below ground level, which accept flow from the entire system are orientated WNW-ESE. This corresponds to fractures mapped from the Shear Zone termination region. The most distinctive topographic features in this otherwise flat landscape are a series of large enclosed depression, dolines, and cave passages, which lie in a line extending from Caherglassaun Lough to Quinn's Cave (135680 208230) 6.5km to the west-northwest. A number of the caves along this linear trend have lengths in excess of km, such as Morans Cave (1160m long) and Pollaloughabo/Pollbehan cave system (1500m long). Drew (2003) contends that the dolines are the result of the collapses into a major, narrow, 25m wide, water filled karst conduit, of which the cave passages are part of, that carries all of the underground drainage from the Gort area. The conduit continues to an "ancient outlet in Galway Bay west of Corranroo"(Drew 2003). The majority of the modern drainage leaves this WNW trending conduit along the Pollaloughabo/Pollbehan cave passage and flows to a series of springs at Kinvarra. These cave passages have the same orientation as that of Aillwee Cave and the collapsed feature, or features that makes up the Glen of Clab. The OPW report describes these as being older features, possibly late Tertiary in age. Aillwee Cave is over 1 Ma (Drew pers.comm 2003) if these features are associated with the same environment that was responsible for the formation of Aillwee Cave then these features are at least 1 Ma.

Sediment found in a karstified collapse feature in Pollnahalla in north Co. Galway, and analyzed by Coxon & Coxon (1997), has yielded a late Pliocene / early Pleistocene age. This indicates that the surface underlying the deposits is at least of this age, implying that karstification must have taken place in later Tertiary times. The fact that the surface and sub-surface features at Pollnahalla have survived recent glaciations gives rise to the possibility that other surface, and sub-surface, features along the Western Lowlands may be pre glacial in age (Coxon & Coxon 1997). This lends itself to the idea that the Gort Lowlands are a mid to later Tertiary feature. Williams (1964) calculated, in a mathematical exercise based on the "impossible assumption" that if

current solution rates were maintained during the past, that the Gort Lowlands would have taken 4.9 Million years to form.

The Gort Lowlands are an ancient surface, c. Mid Tertiary, whose location and extent are controlled by the zone of increased connectivity created by the Hercynian Fergus Shear Zone.

7.10 Conclusions:

- Depressions are non randomly located, they occur where the are located along vein clusters
- They exhibit similar spatial characteristics to the vein sets, narrow, elongate NNE trending features
- Depressions are controlled by the vein set over a wide range of scale from centimetre to kilometre.
- The depressions unlike the cave systems, are not strata-bound they can be traced through a number of units, following the vertical persistence of the veins.
- The principal control on the depressions are the vein clusters.
- Depressions are coincident with vein controlled cave passages, as can be seen with the Ballyiny depression and Poll Na gCéim, Ballycahill depressions and the vein controlled sections of Aillwee cave and Kilcorney depression and Kilcorney cave.
- The depressions exhibit similar characteristics as the caves- narrow, elongate, NNE trending zones.
- The Gort Lowlands corresponds to the location of the Fergus Shear Zone, with its fracture pattern controlling the flow of groundwater and the development of surface and subsurface features.

7.11 Summary:

Depressions in the Burren are non-randomly located, their location being controlled by fracture patterns. The regionally dominant NNE trending vein clusters exert a strong influence on the size, shape, extent and spatial relationship of depressions. This can be seen at all scales from the centimetre scale, as seen along TP 4Z on Cappanawalla, to the kilometre scale, as seen along TP1, TP2 and TP3 on Aillwee Hill and on the Gort Lowlands. Depressions form along a well connected fracture backbone defined by the vein clusters due to a combination of the following parameters: the vein clusters are spatially well linked through interaction with the joint pattern; they have a large proportion of cross terminations, a low proportion of blind terminations and a high intersection density, providing a fracture backbone with a high connectivity; the length of fractures per unit area is large, creating a large surface area for solution to act on; and correspondingly, the block size is dramatically smaller compared to the surrounding pavement.

The largest cluster of enclosed depressions in the Burren is on the western side of Aillwee Hill. These depressions are formed along a NNE trending vein cluster and exhibit the same properties as the depressions studied on the tens of metres scale on Cappanawalla. On Cappanawalla, the depressions can be seen to form along the vein clusters. The depressions are elongated, narrow features which are orientated NNE, reflecting the vein parameters. They occur in clusters and increase in frequency towards the largest depression in the area. In the study area to the west of Aillwee, the depressions are also elongated, narrow features aligned NNE. To the east of the study area, it can be seen that there is an increase in the frequency of depressions

towards the main cluster of depressions, mirroring both the depression on Cappanawalla and the behaviour of the vein system.

The joint patterns of the Burren, while locally consistent, are regionally variable. Whereas the veins have a consistent orientation throughout the Burren. Combined with the spatial characteristic of the veins, which are the controlling influence of the location of topographic features in the Burren. For the Gort Lowlands the more complex fracture pattern associated with the Fergus Shear Zone define and control its extent.

In order to understand the location and formation of topographic features in the Burren, it is necessary first to have a detailed understanding of the fracture patterns in the region, their spatial characteristics, and regional variability and how they interact with each other. This involves detailed fracture analysis at a number of locations and scales and an understanding of fracture connectivity and percolation theory.

The depressions reflect the dominant fracture pattern of the region, and once a mechanism for their location and formation has been developed, they are useful tools in analyzing the fracture pattern of the region.

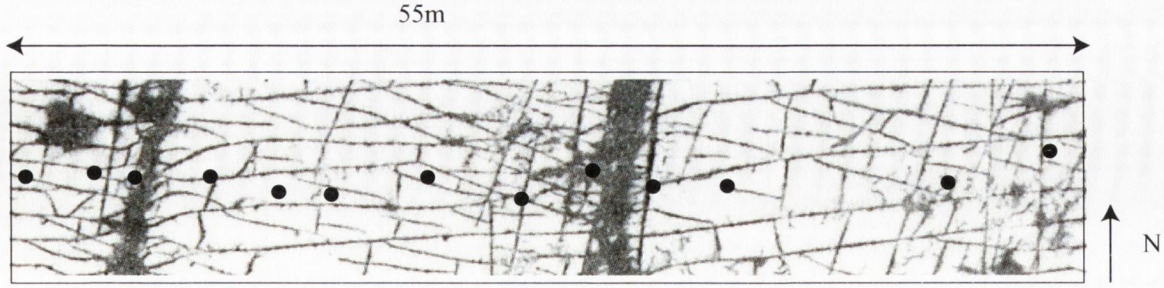

7.1a: Aerial Photograph showing location of topographic profile SM EW.

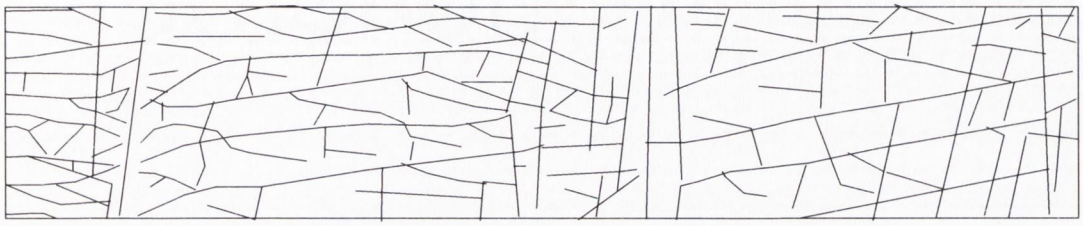

7.1b: Fractures along topographic profile SM EW.

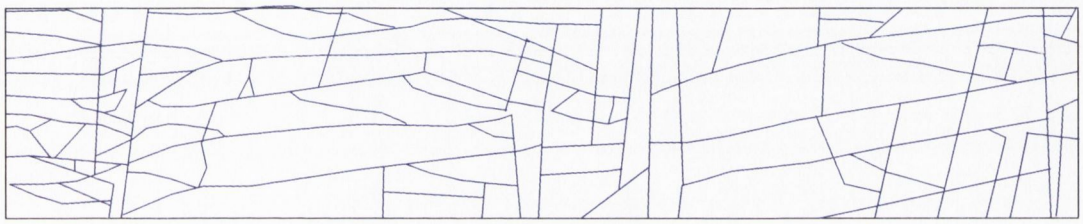

7.1c: Fracture backbone along topographic profile SM EW.

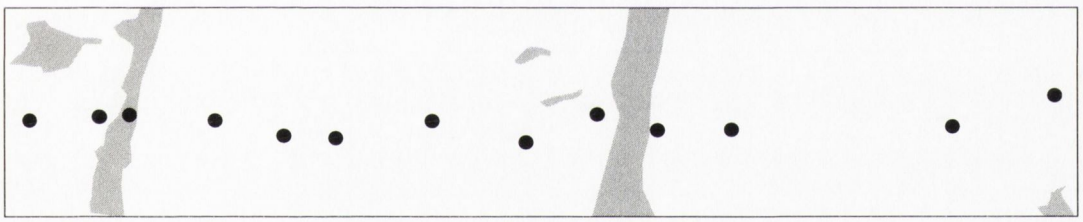

7.1d: Location of depressions along topographic profile SM EW.

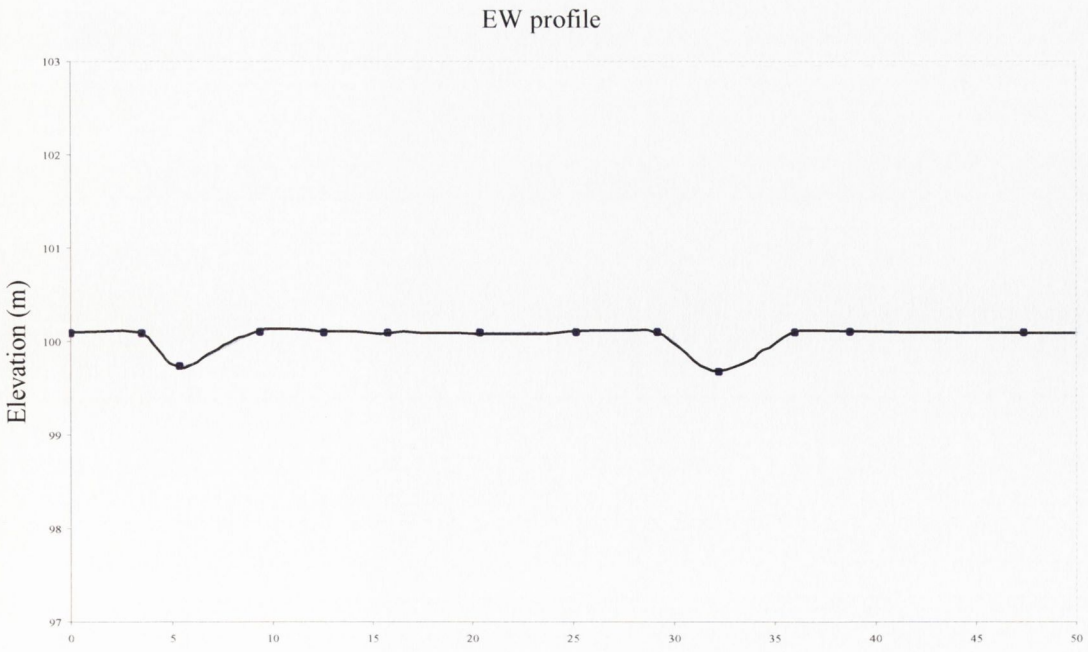

7.1e: Toographic profile SM EW, note minor topographic depression at 5m and 33m which are coincident with clusters of NNE trending veins.

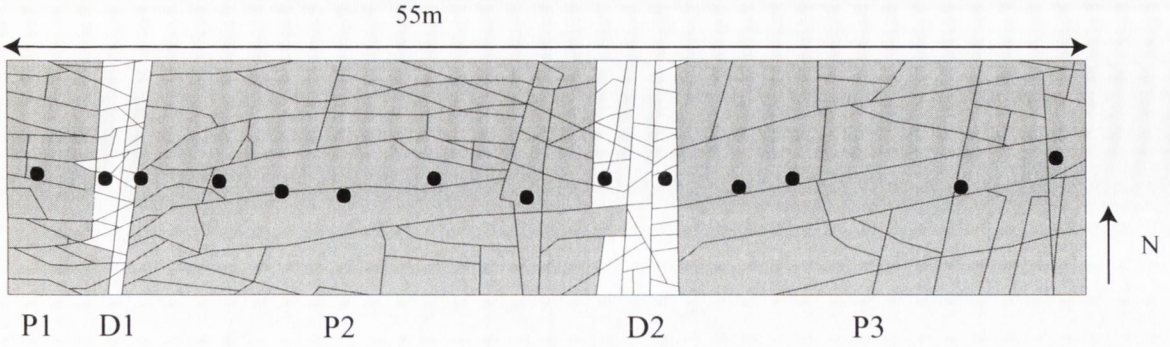

7.2a: Diagram of block size along topographic profile SM EW. Pavements are shaded depressions are un shaded.
P1: pavement 1, D1: Depression1, P2: pavement 2, D2: Depression1, P3: pavement 3.

P1: n= 21, Surface Area= 55.21 m^2, mean block size= 2.629 m^2, median block size: 2.11m^2
Fractures: n = 22, Σl = 161 m^2, Σl /A = 2.97 m/m^2
P2: n= 54, Surface Area= 284.21 m^2, mean block size= 5.26 m^2, median block size: 3.91 m^2
Fractures: n = 54, Σl = 577.15 m^2, Σl /A = 2.03 m/m^2
P3: n= 42, Surface Area= 250.36 m^2, mean block size= 5.96 m^2, median block size: 3.66 m^2
Fractures: n = 43, Σl = 420.5 m^2, Σl /A = 1.69 m/m^2
All P: n= 117 Surface Area= 589.78m^2, mean block size= 5.04 m^2, median block size: 3.616m^2
Fractures: n = 119, Σl = 1159.3 m^2, Σl /A = 1.96 m/m^2

D1: n= 35, Surface Area= 25.54 m^2, mean block size= 0.70 m^2, median block size: 0.636 m^2
Fractures: n = 35, Σl = 118.59 m^2, Σl /A = 4.64 m/m^2
D2: n= 40, Surface Area= 47.75 m^2, mean block size= 1.19 m^2, median block size: 1.056 m^2
Fractures: n = 40, Σl = 183.74 m^2, Σl /A = 3.85m/m^2

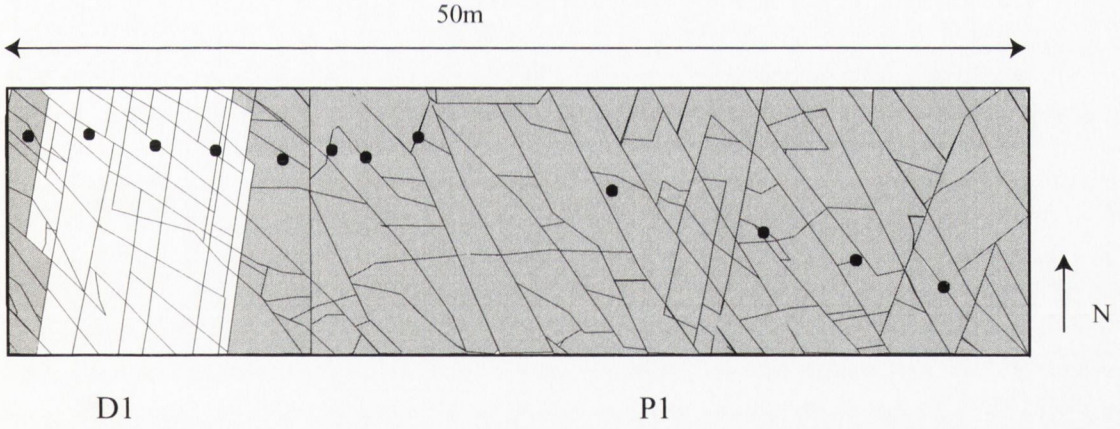

7.2b: Diagram of block size along a section of the topographic profile Cap 4-5-6. Pavements are shaded depressions are un shaded.
P1: pavement 1, D1: Depression1,

P1: n= 298, Surface Area= 1172.072 m^2, mean block size= 3.933 m^2, median block size: 2.282 m^2
Fractures: n = 451, Σl = 593.512 m^2, Σl /A = 0.383 m/m^2
D1: n= 209 Surface Area= 257.539 m^2, mean block size= 1.65 m^2, median block size: 1.216 m^2
Fractures: n = 209, Σl = 212.248 m^2, Σl /A = 0.824 m/m^2

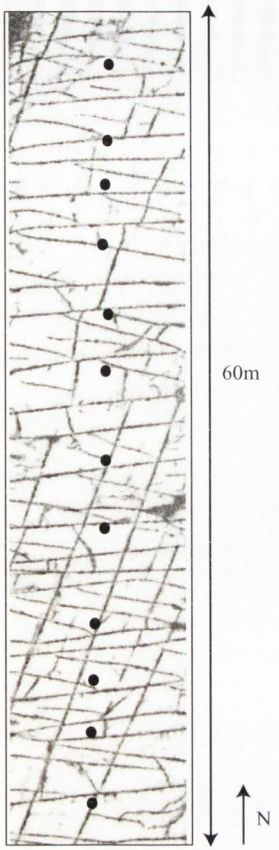

7.3a: Aerial Photograph showing location of topographic profile SM NS.

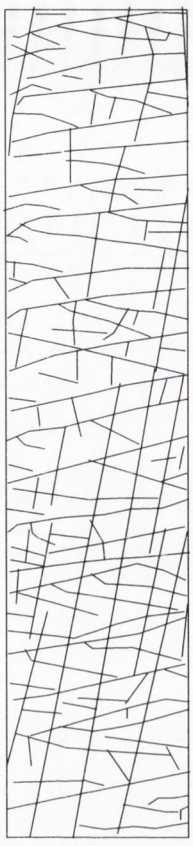

7.3b: Fractures along topographic profile SM NS.

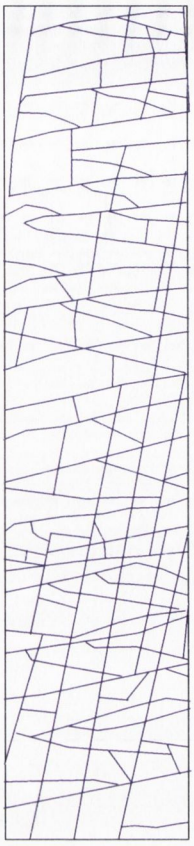

7.3c: Fracture Backbone along topographic profile SM NS.

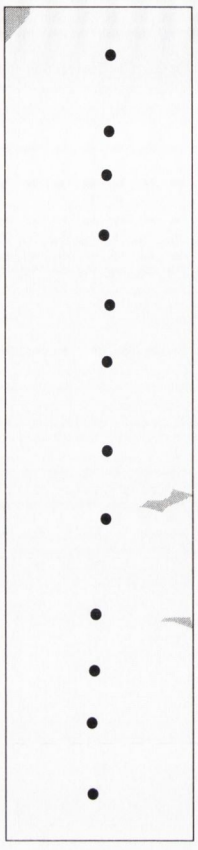

7.3d: Location of depressions along topographic profile SM NS.

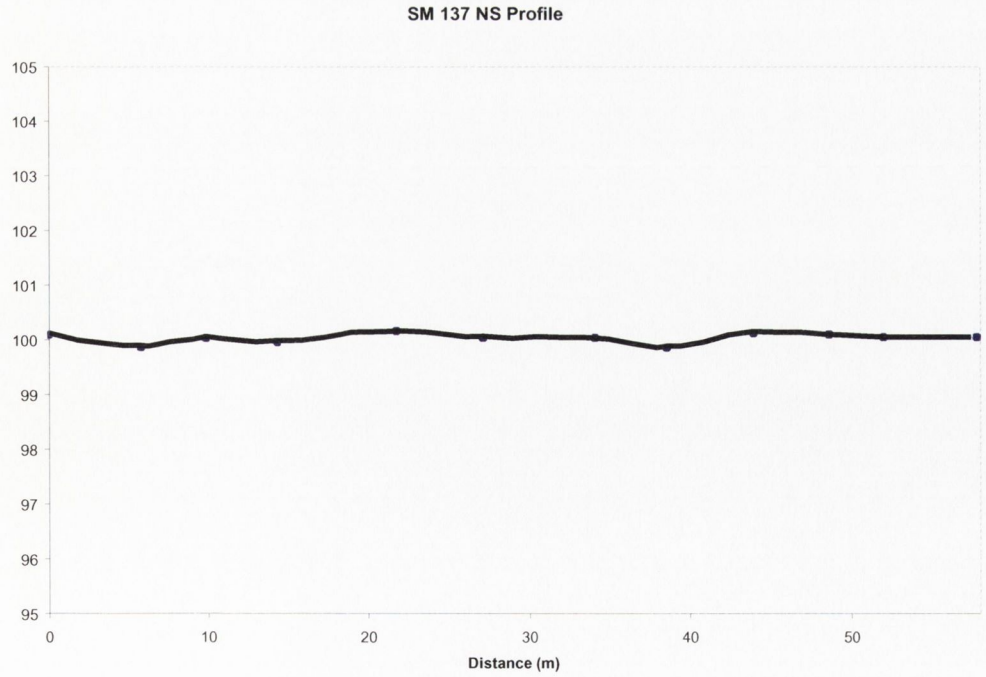

7.3e:Topographic profile SM NS, note the profile is very flat with no depressions present
The backbone illustrates the block size along the profile.
n = 120, Surface Area= 769.45m^2, mean block size = 6.412 m^2, median block size = 4.937m^2 with a maximun block size of 40 m^2.

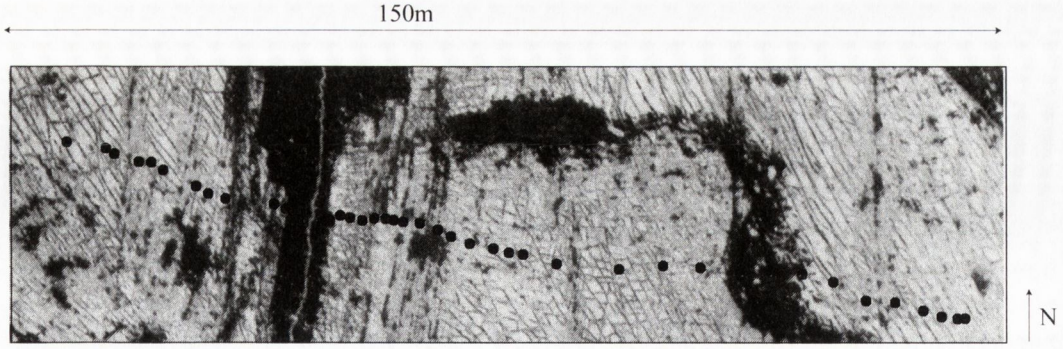

7.4a: Aerial Photograph showing location of topographic profile CAP 3-7(marked by the black dots).

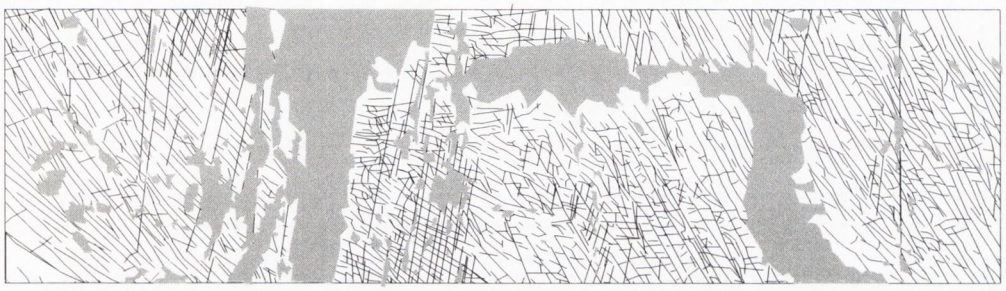

7.4b: Fracture pattern along topographic profile CAP 3-7.

7.4c: location of depressions along topographic profile CAP 3-7 (marked by the black dots).

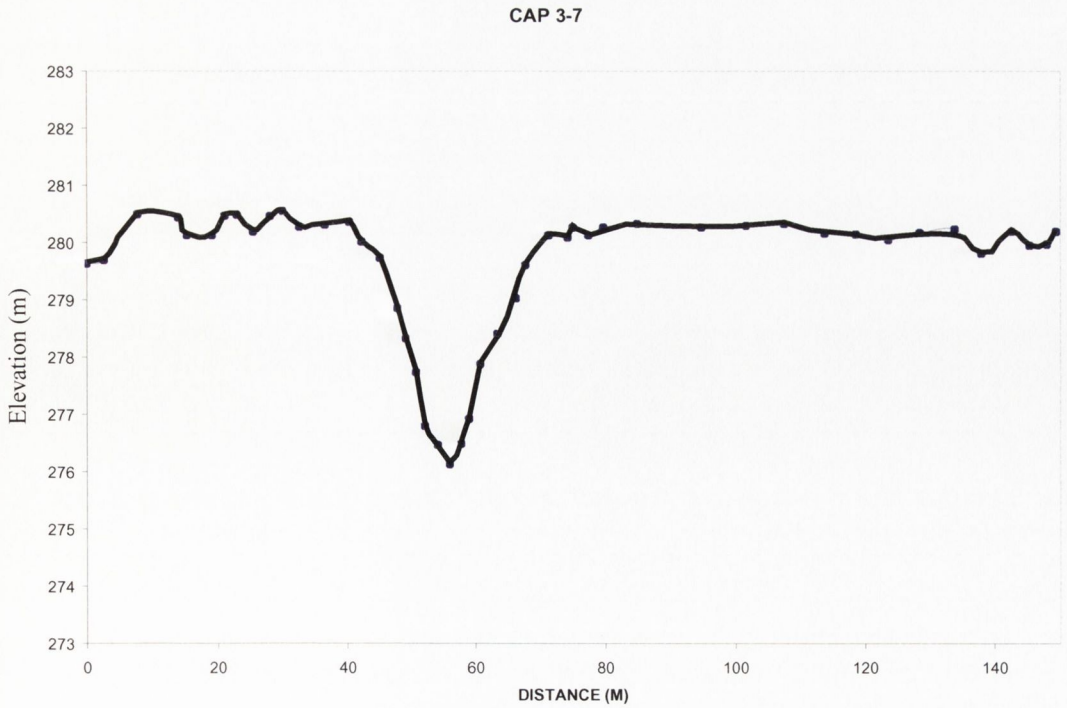

7.4d: Topographic profile CAP 3-7, the main depression correlates with a cluster of NNE trending veins.

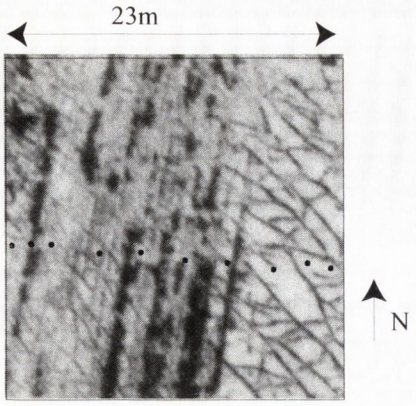

7.5a: Aerial Photograph showing the location of topographic profile CAP 4z (marked by black dots).

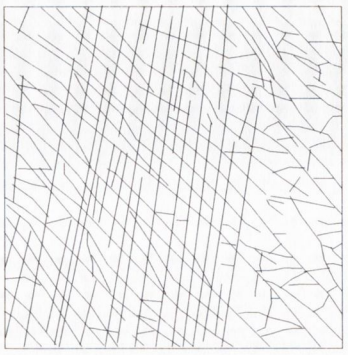

7.5b: Fractures along topographic profile CAP 4z (marked by black dots).

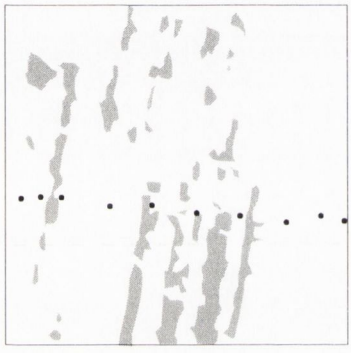

7.5c: Location of depressions along topographic profile CAP 4z (marked by black dots).

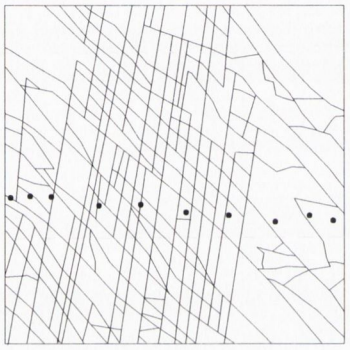

7.5d: Fracture backbone along topographic profile CAP 4z (marked by black dots).

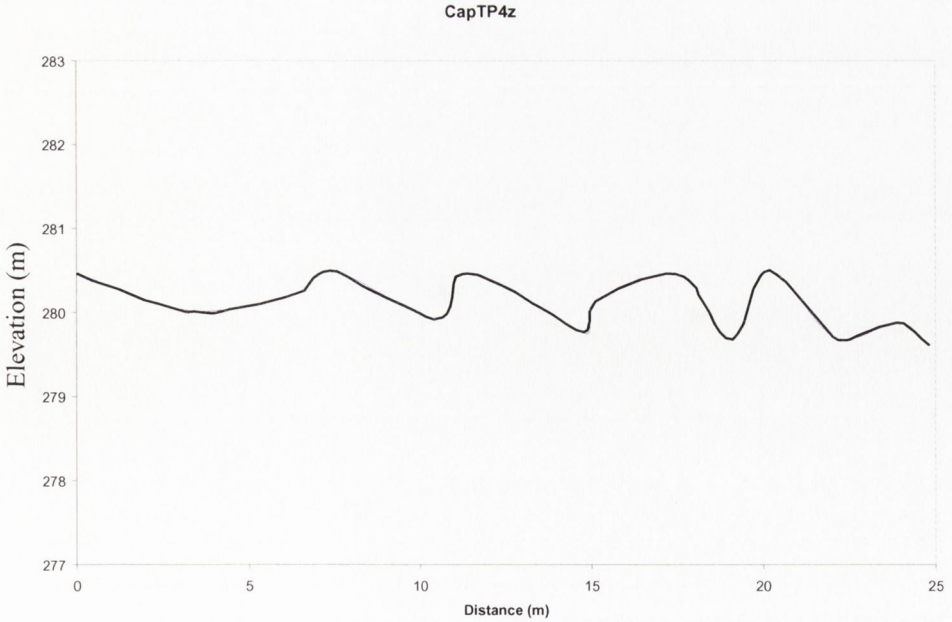

7.5e: Topographic profile CAP 4z, the depressions correlate with clusters of NNE fractures.

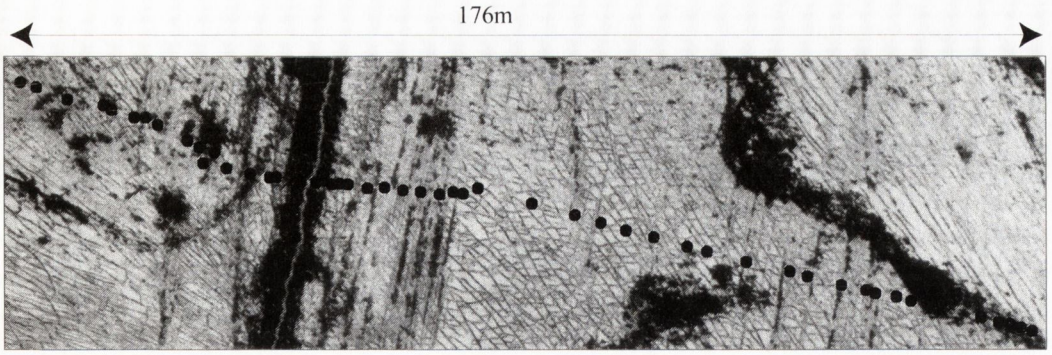

7.6a: Aerial Photograph showing location of topographic profile CAP 4-5-6 (marked by the black dots)

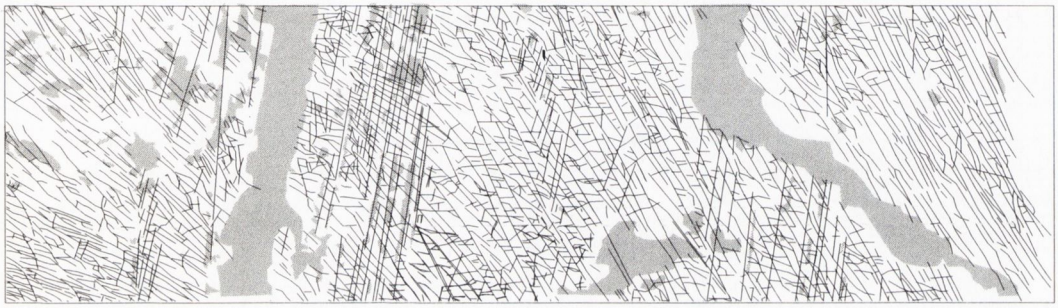

7.6b: Fracture pattern along topographic profile CAP 4-5-6 (marked by the black dots)

7.6c: Location of depressionsalong topographic profile CAP 4-5-6 (marked by the black dots)

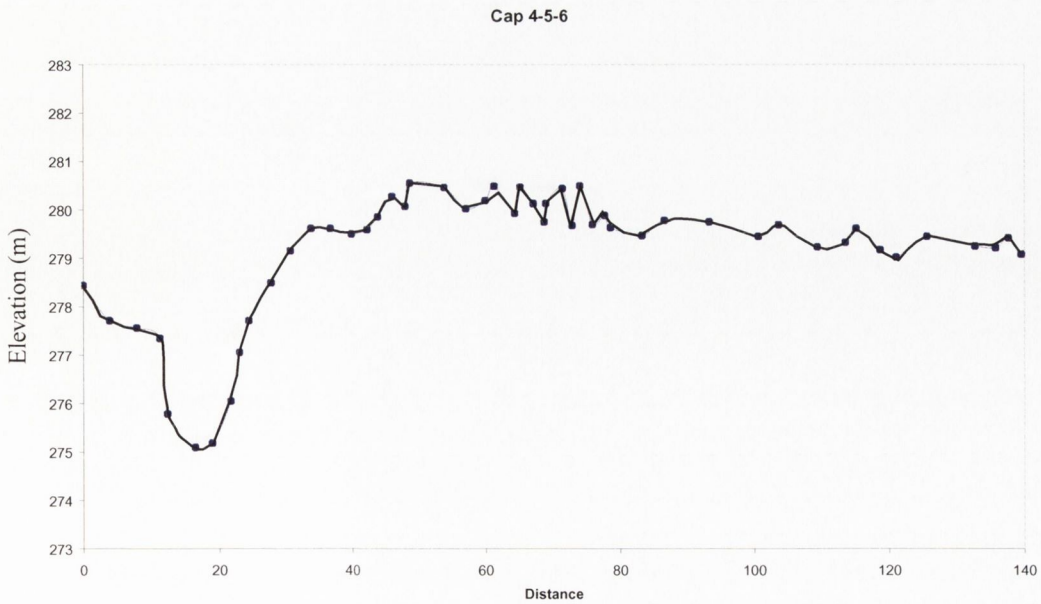

7.6d: Topographic profile CAP 4-5-6, the main depression correlates with a cluster of NNE trending veins. Minor depressions from 60m to 80m coincide with minor clusters of NNE veins as shown in 6b and 6c.

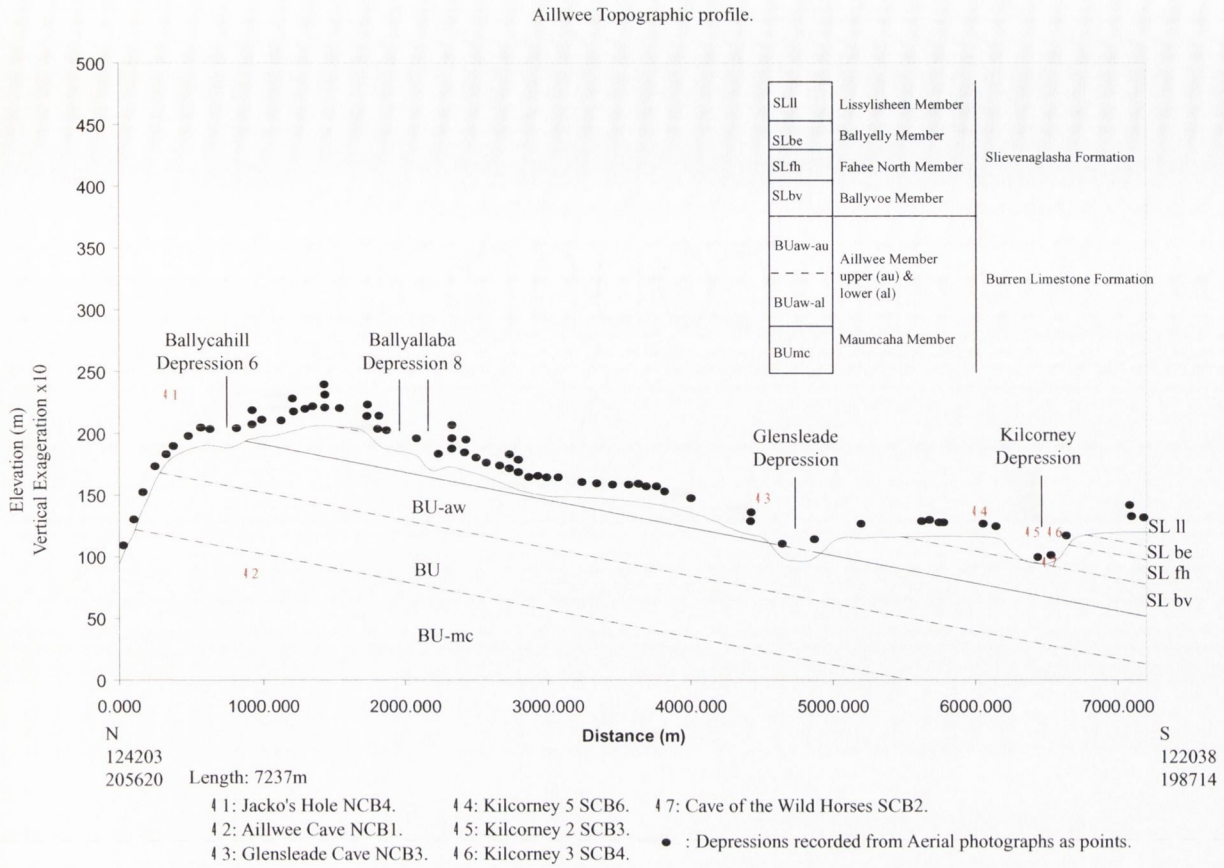

Figure 7.7: See text for detail on depressions and diagram.

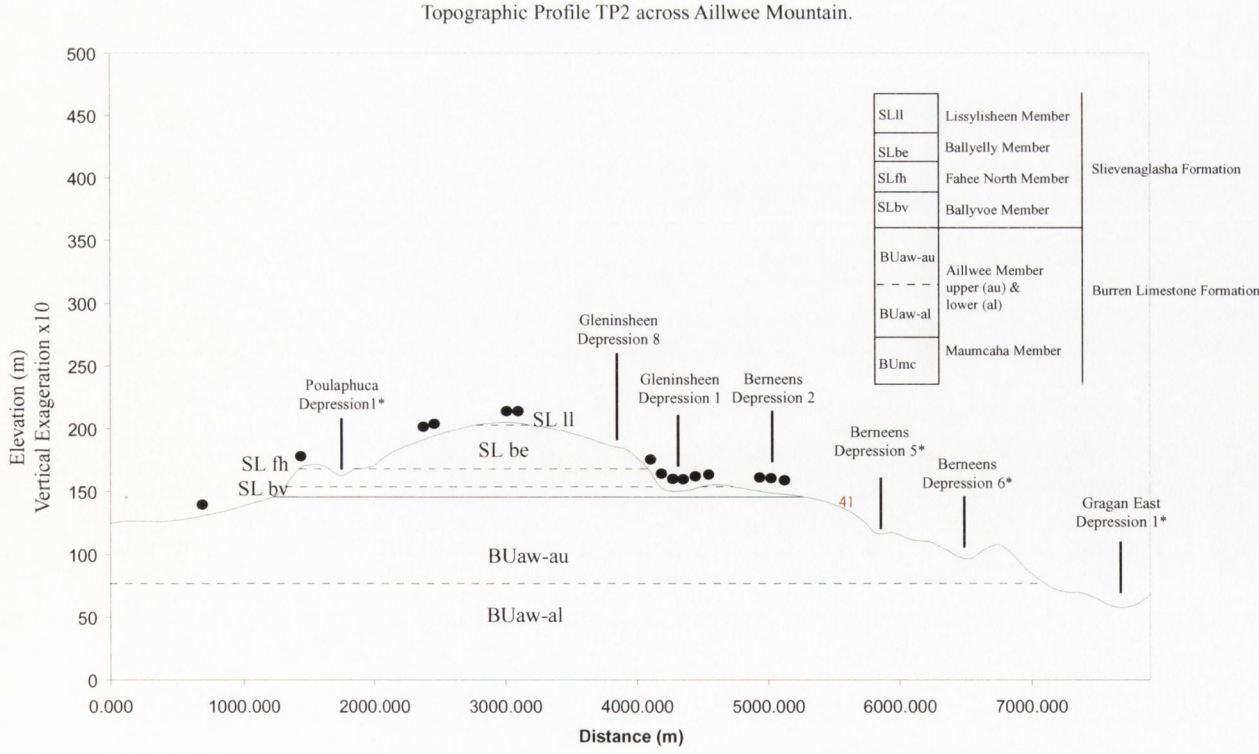

Figure 7.8: Topographic profile 2.

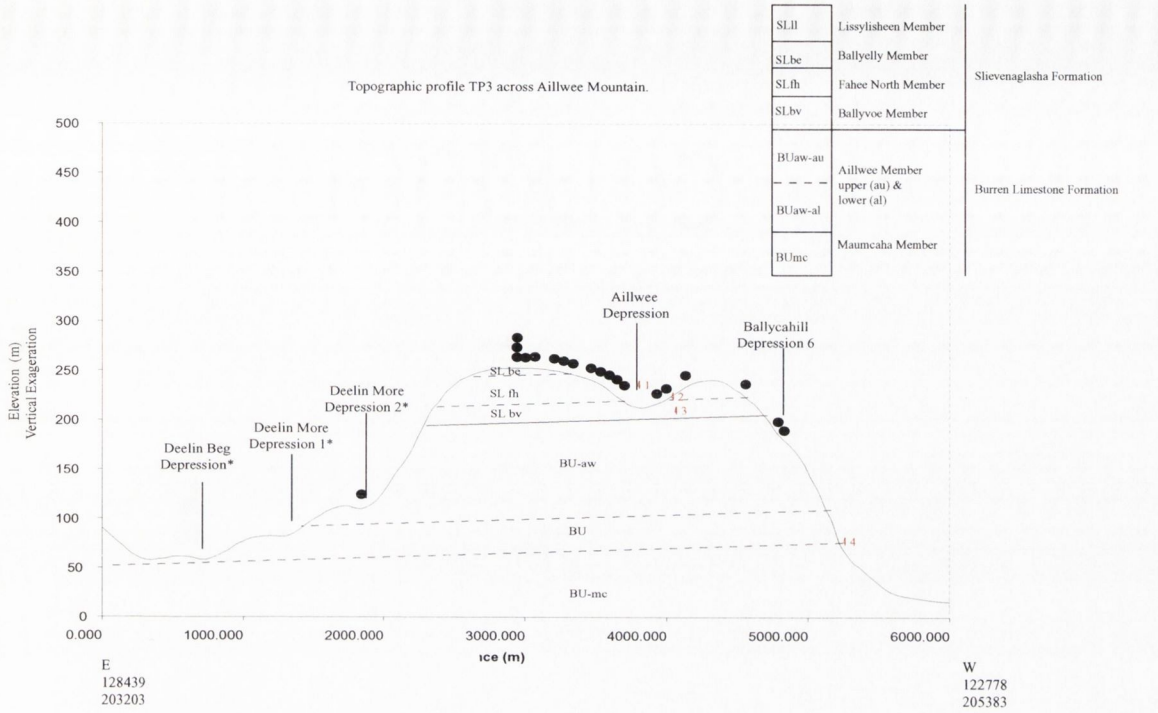

Length: 6066m

1: Maze Hole NCB6.
2: Spur Hole NCB15.
3: Mill Sink NCB8.
4: Aillwee Cave NCB1.
: Depressions recorded from Aerial photographs as points.
* : Depressions confirmed from aerial photographs.
• : Depression mapped from aerial photographs.

Figure 7.9: Topographic Profile 3.

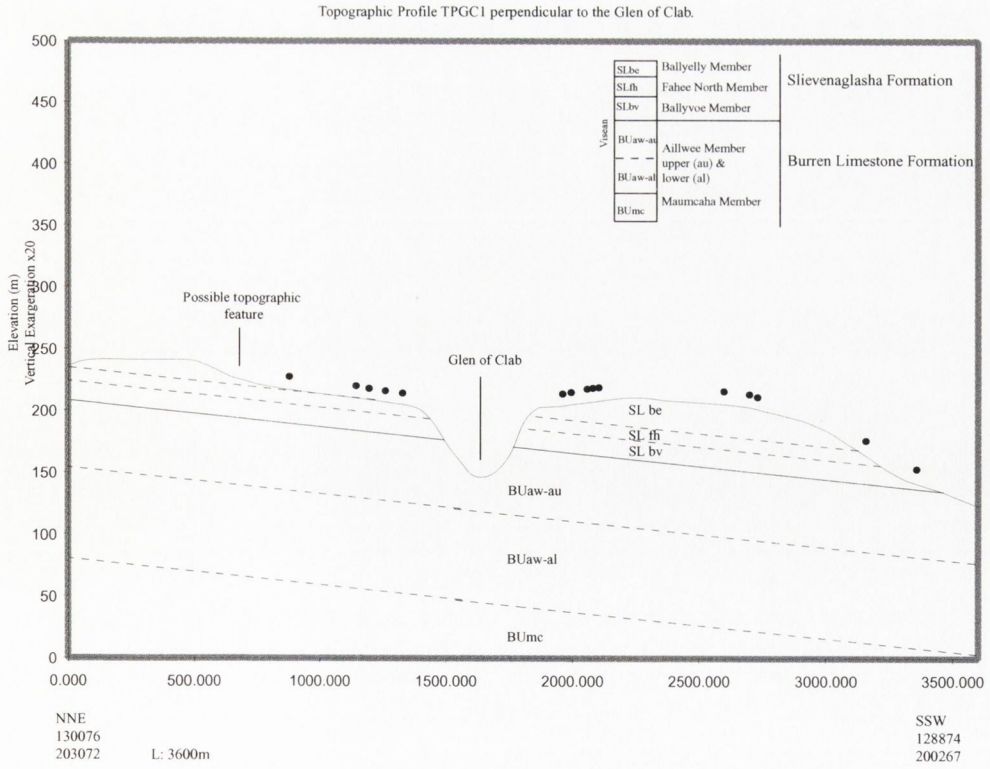

Figure 7.10: Topographic profile perpendicular to Glen of Clab.

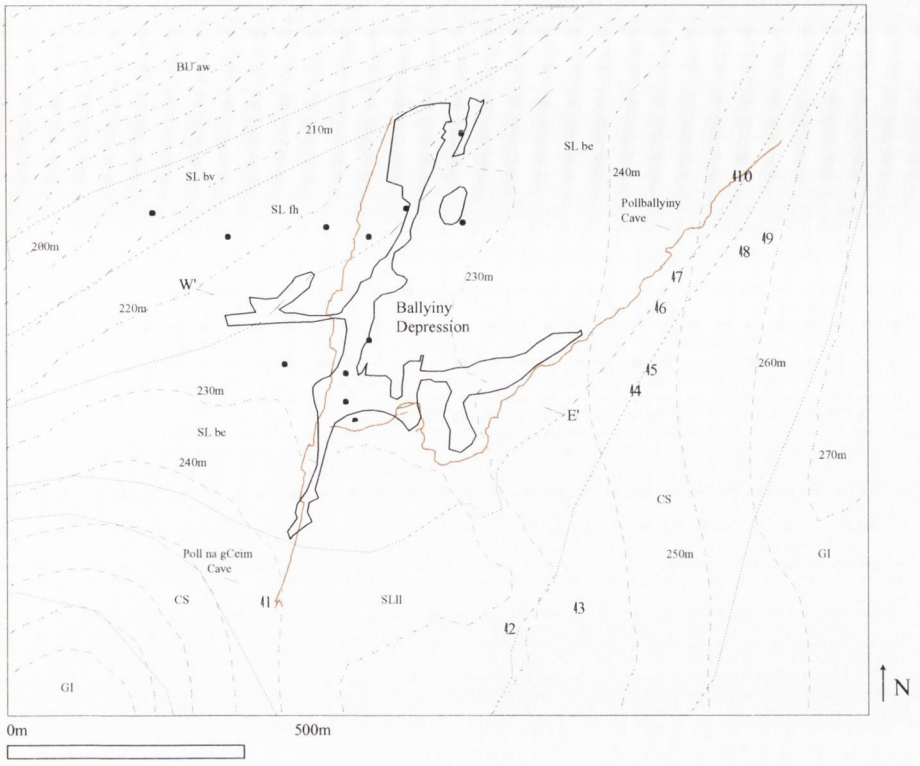

Figure 7.11a: Diagram of Ballyiny Depression and relationship with local geology, topography and cave systems. Modified from Lloyd & Self 1982, cave names and numbers from literature, Self 1981, Boycott et al 1996. Poll na gCeim cave modified from Judd & Mullan 1994, Pollballyiny cave modified from Self 1981.

E' -W': location of topographic profile TPB1
20m contour Interval: ———
Depressions identified from Yeates (1996): •
Caves: 4

1: Poll na gCeim
2: B3a
3: Polldubh South
4: B1g
5: B1f
6: Pollderren
7: B1e
8: Pollegob
9: Pollegob North
10: Pollballyiny

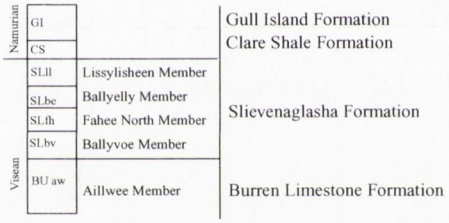

Startigraphic Column not to scale: from MacDermott pers comm

Topographic Profile TPB1-orientated 107 degrees perpendicular to the depression.

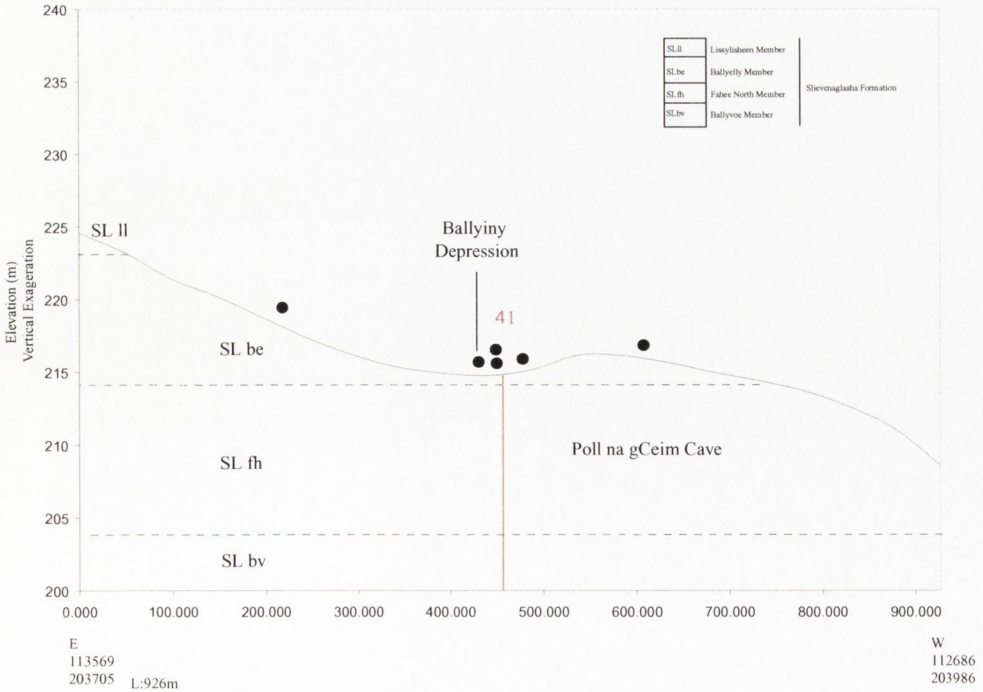

L:926m
41: Poll na gCeim Cave, Estimated Length: 890m, Estimated Depth: 181m, Judd & Mullan (1994).
Depressions identified from Yeates (1996):•

Figure 7.11b: Topographic profile perpendicular to Ballyiny Depression.

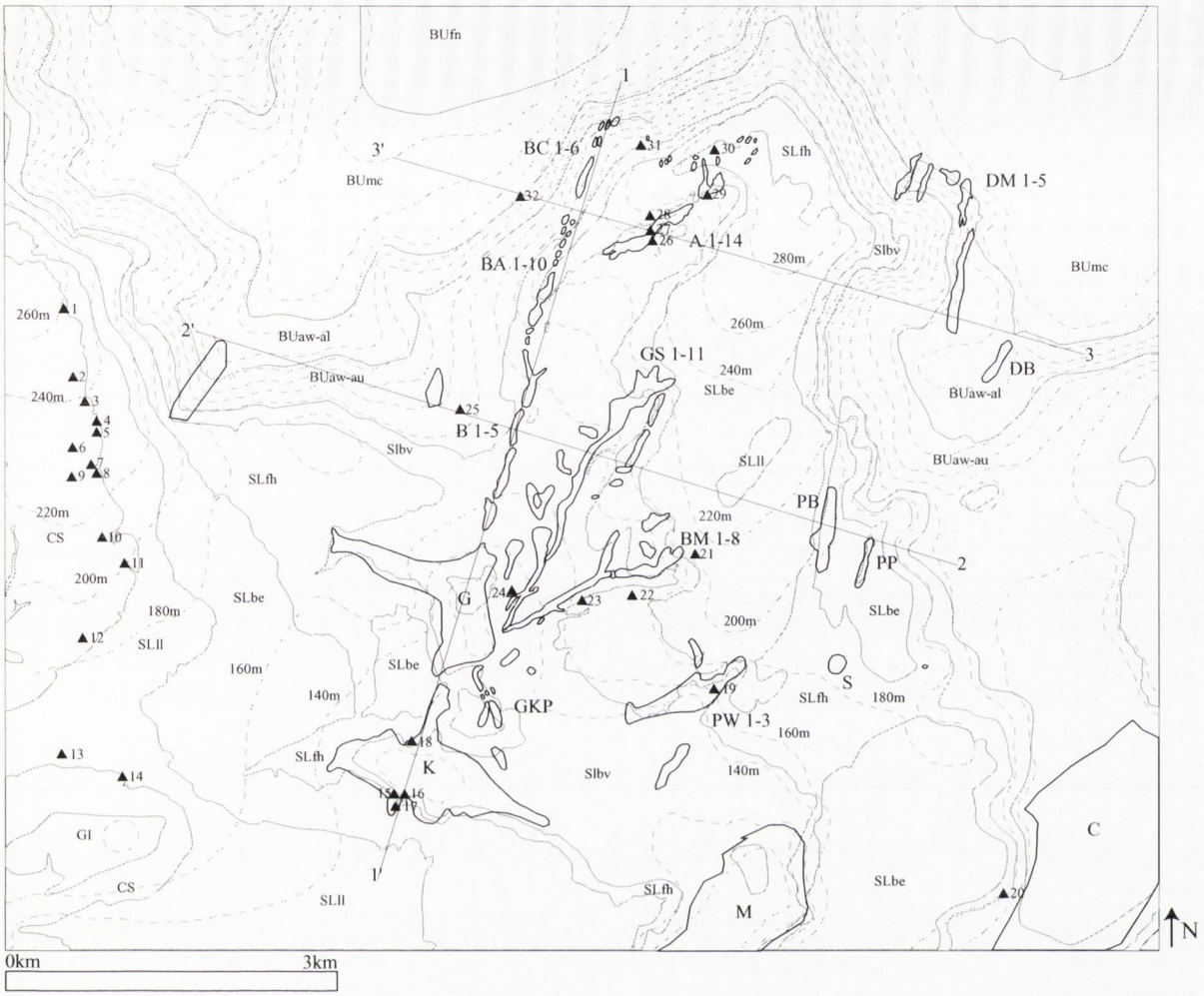

Fig 7.12: Diagram of the closed depression in the vicinity of Aillwee Mountain, with local geology, 20m contour and cave locations. Diagram modified from Drew 1973, cave locations and names fromTratman 1969, Self 1981 and Boycott *et al* 1996 Geology from MacDermott pers comm.
1 - 1', 2 - 2' and 3-3': location of topographic profiles
20m Contour Interval: _ _ _ _

Index to Depressions:

K: Kilcorney
G: Glensleade
PW: Poulawillin1-3
BM: Ballymihill 1-8
GS: Gleninsheen 1-11
B: Berneens 1-5
BA: Ballyallaba 1-10
BC: Ballycahill 1-6
A: Aillwee 1-14
GKP: Glensleade-Kilcorney-Poualwillin 1-9
M: Meggagh
C: Carran
S: Sladoo
PP: Poulaphuca
PB: Poulbaun
DB: Deelin Beg
DM: Deelin More 1-5

Cave: ▲
Index to Caves

1: Green Stream H0-1
2: Green Stream HI
3: Green Stream H2
4: Green Stream H2a
5: H2a
6: Green Stream H1
7: H3
8: H4
9: Green Stream H1a
10: Doonyvardan
11: Croagh South sink
12: Poll cahermacnaghten
13: Hammer Pot
14: Poulawillin G2
15: Kilcorney 3
16: Kilcorney 2
17: Cave of the Wild Horses
18: Kilcorney 4 & 5
19: Poulawillin NCB11
20: Ballyconry
21: Ballymihil
22: Poulgorm
23: Poulnabrone
24: Glensleade
25: Polberneens
26: Spur Holes
27: Mill Sink
28: Mill Cave
29: Maze Holes
30: Kilweeran Cave
31: Jacko's Hole
32: Aillwee Cave

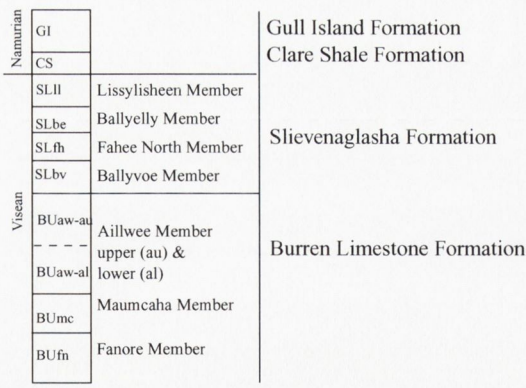

Stratigraphic column not to scale: from MacDermott pers comm.

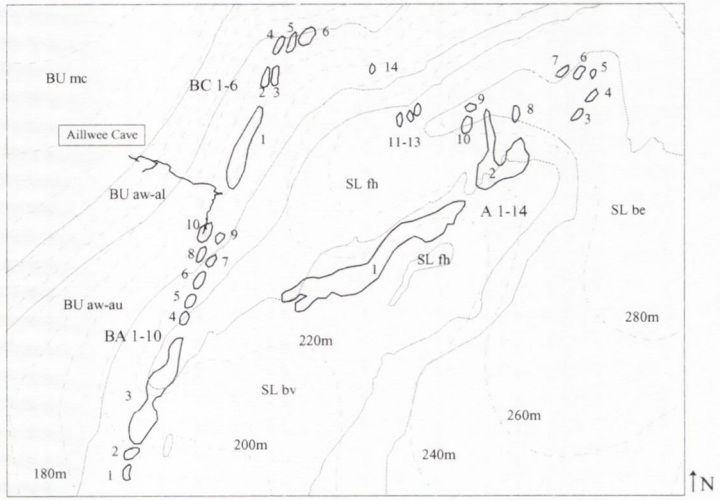

Figure 7.13a: Diagram of depressions of BC, BA and A.

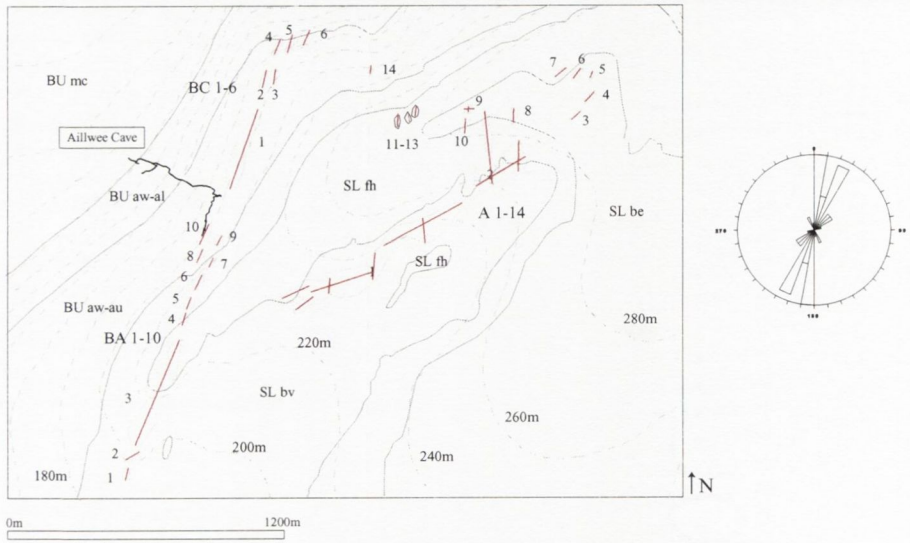

Figure 7.13b: Long axis of depressions with combined rose diagram.

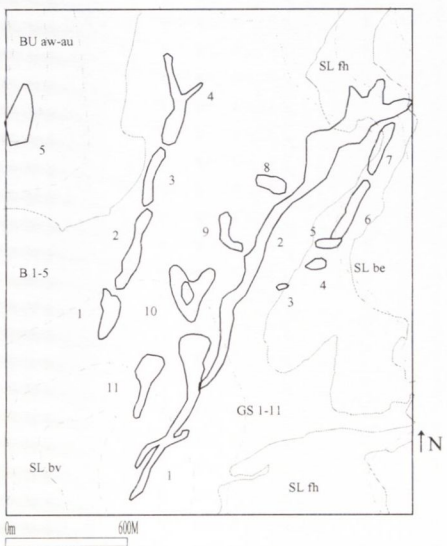

Figure 7.14a: Diagram of depressions of B and GS.

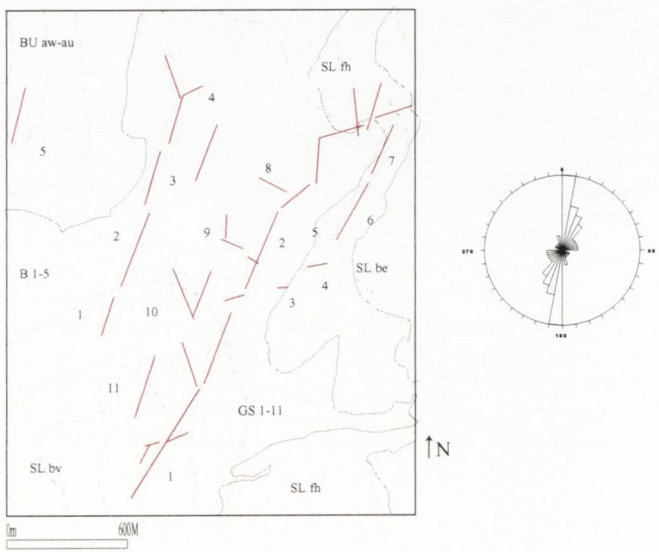

Figure 7.14b: Long axis of depressions with combined rose diagram.

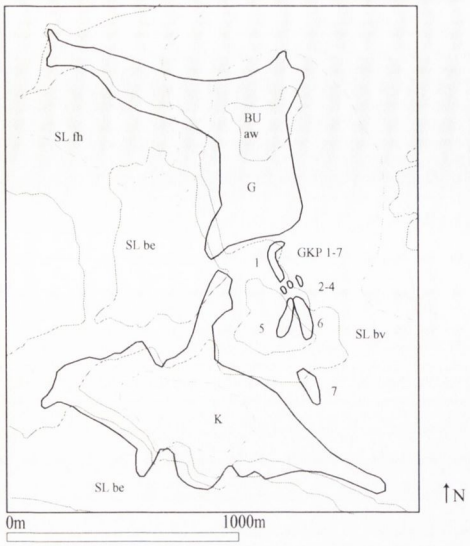

Figure 7.15a: Diagram of depressions of K, G and GKP.

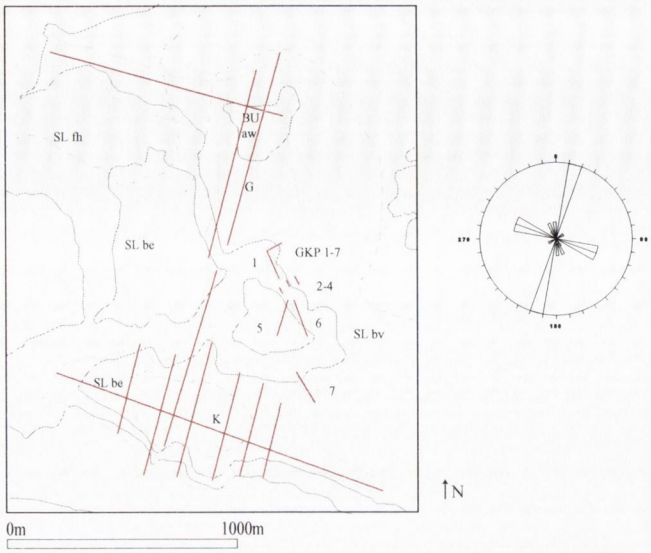

Figure 7.15b: long axis of depressions with combined rose diagram.

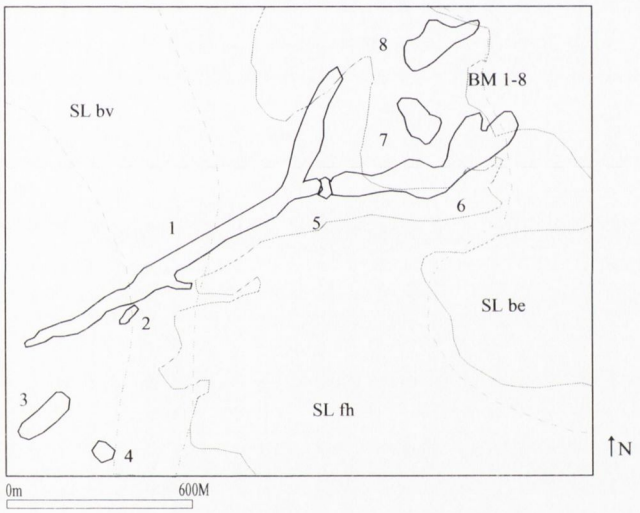

Figure 7.16a: Diagram of depressions of BM.

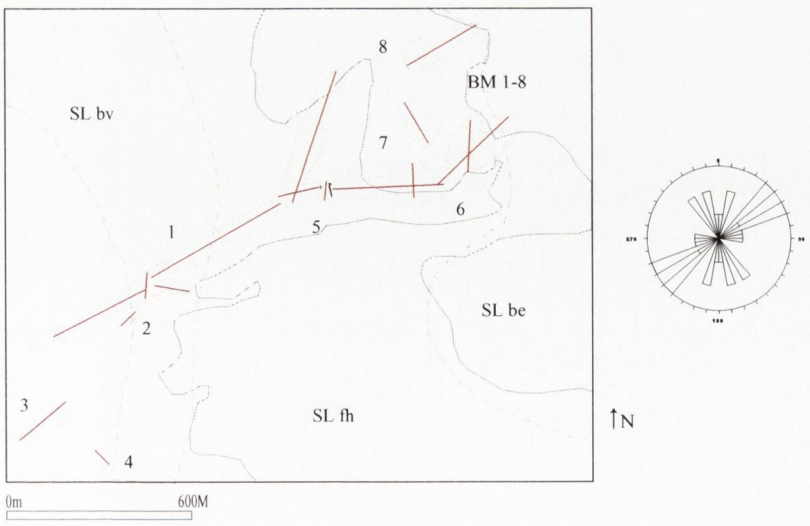

Figure 7.16b: long axis of depressions with combined rose diagram.

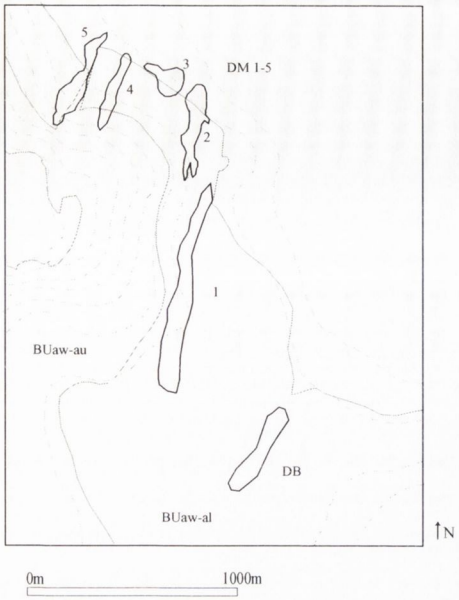

Figure 7.17a: Diagram of depressions of DM and BD.

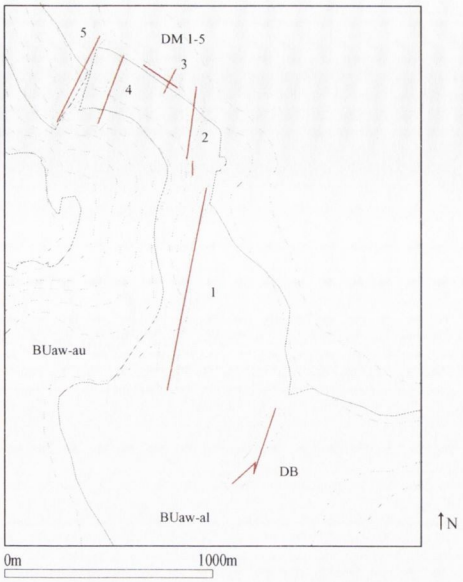

Figure 7.17b:Long axis of depressions with comined rose diagram.

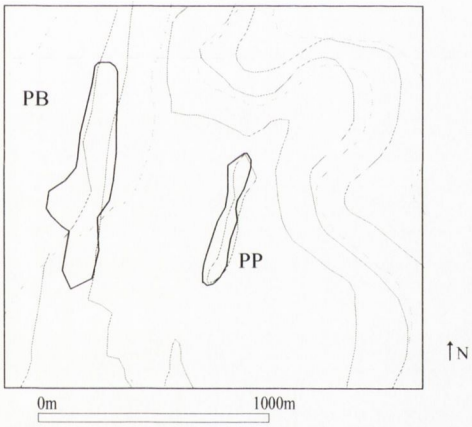

Figure 7.18a: Diagram of depressions of PB and PP.

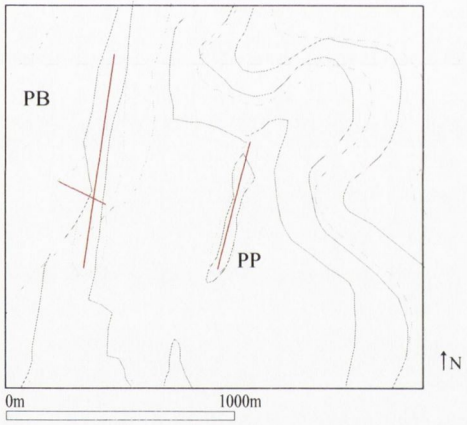

Figure 7.18b: Long axis of depressions with comined rose diagram.

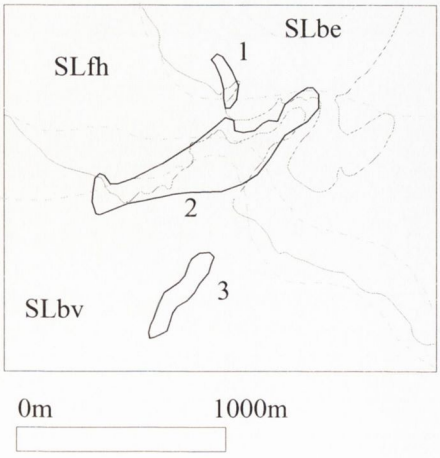

Figure 7.19a: Diagram of depressions of PW.

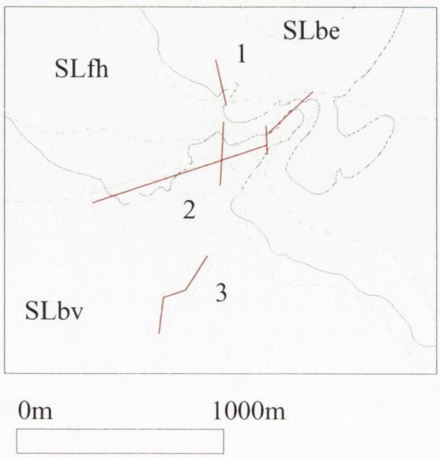

Figure 7.19b: Long axis of depressions with comined rose diagram.

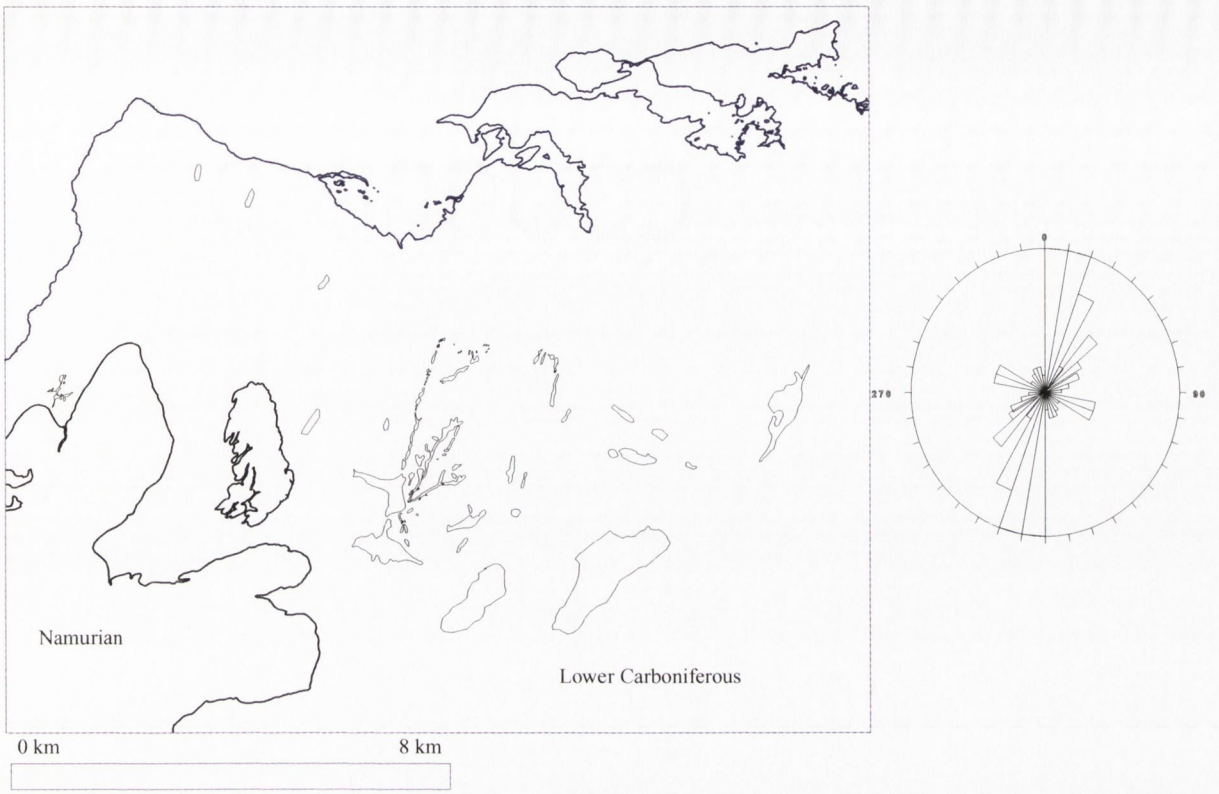

Figure 7.20: Map of location of all large enclosed depressions in the Burren, and a rose diagram based on the oreintation of the long axis of the depressions.

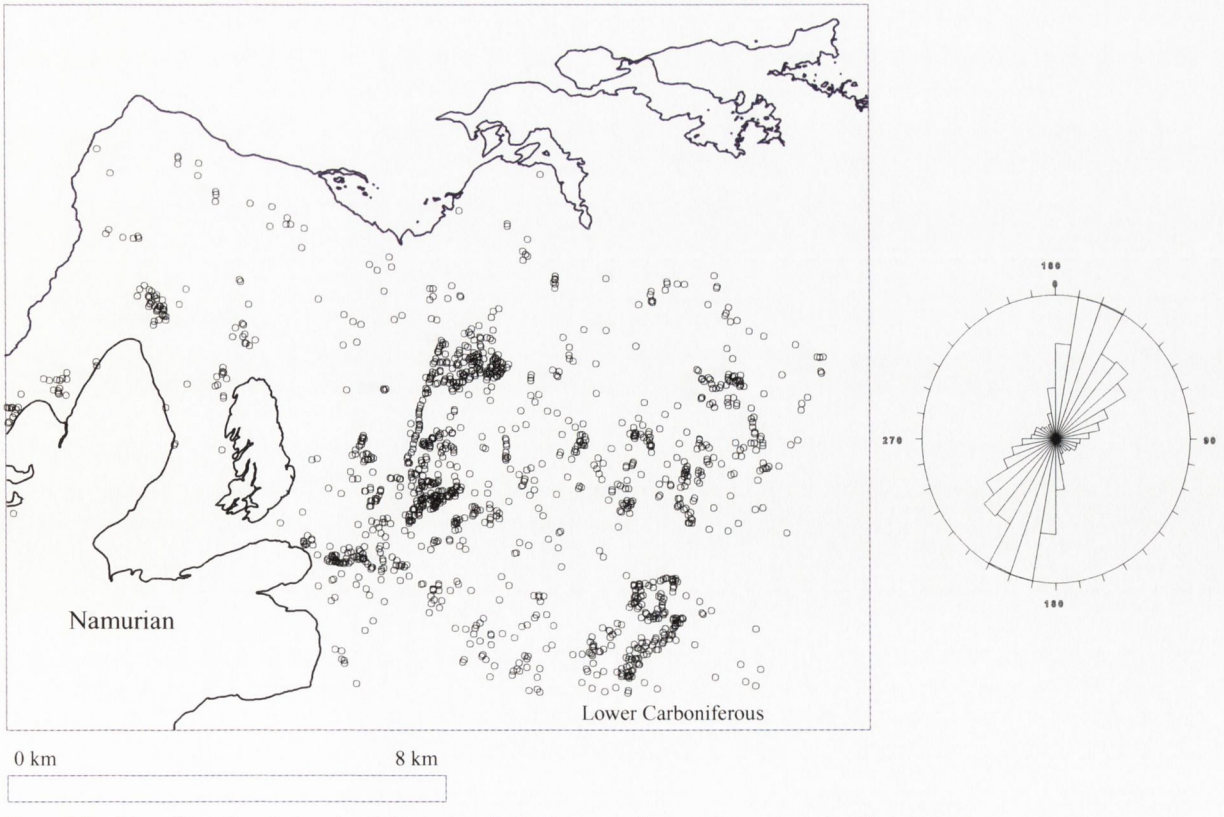

Figure 7.21: Map of location of all enclosed depressions in the Burren, and a rose diagram based on the orientation of the long axis of the depressions. Source of data unpubl MSc by Yeates.

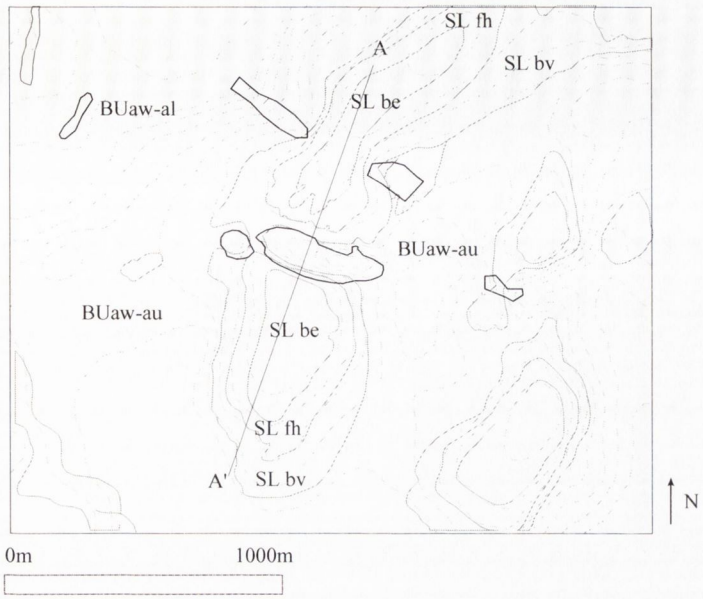

Figure 7.22: Diagram of Glen of Clab, a NW trending depression linked to the Gort Lowlands by a series of colls to the SE. A - A' marks the locationof a topographic profile perpendicular to the Glen of Clab.

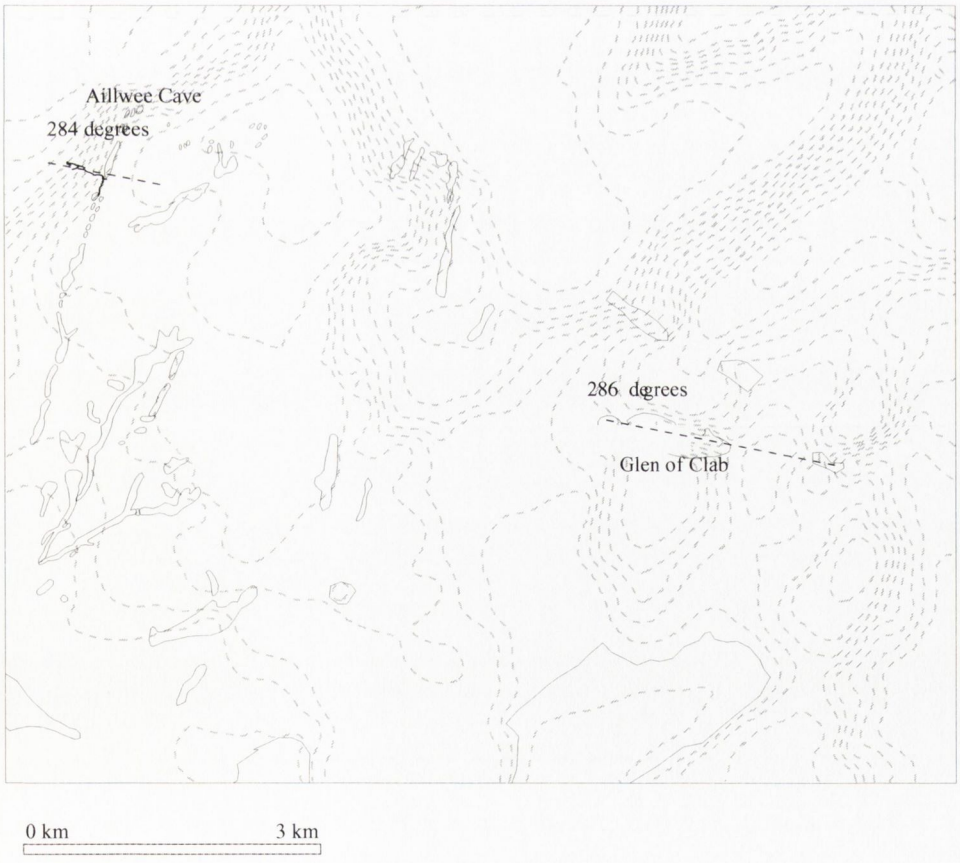

Figure 7.23: Diagram of Glen of Clab and Aillwee Cave. Both features trend NW-SE at 285 degrees.

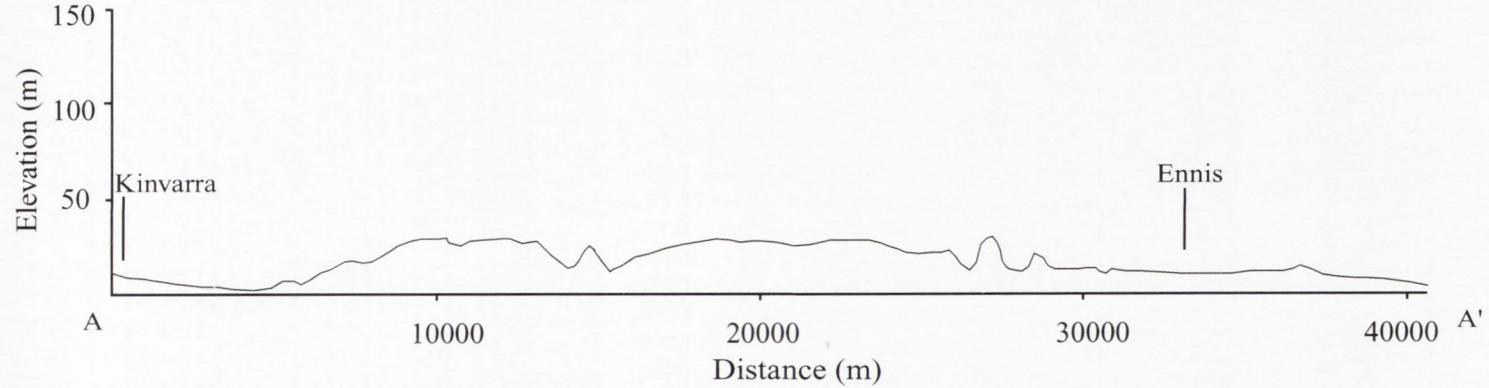

Figure 7.24: Topographic profile parallel to the Lowlands from Kinavrra in the north to the Fergus river in the south. L: 40,674 m Orientated 014 degrees.

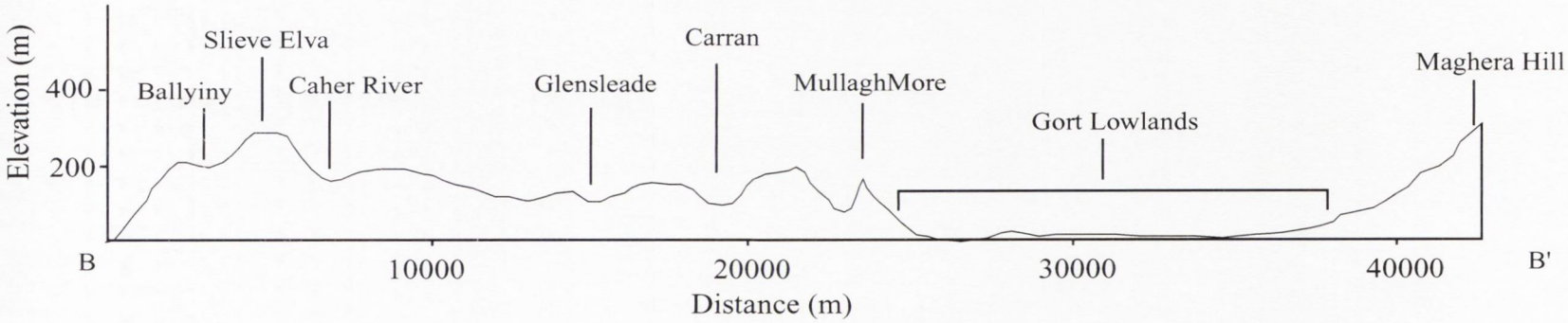

Figure 7.25: Topographic profile across the Burren and the Gort Lowlands to the foothills Maghera Hill. L: 42,762 m Orientated 115 degrees.

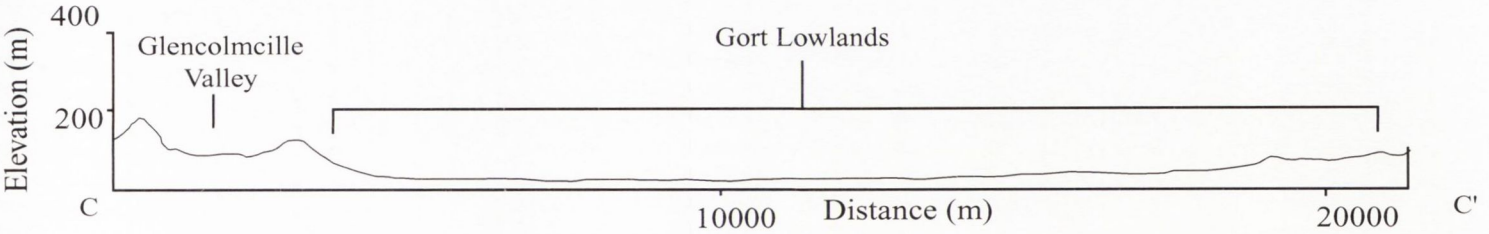

Figure 7.26: Topographic profile across the Burren and the Gort Lowlands. L: 21,429 m. Orientated 115 degrees.

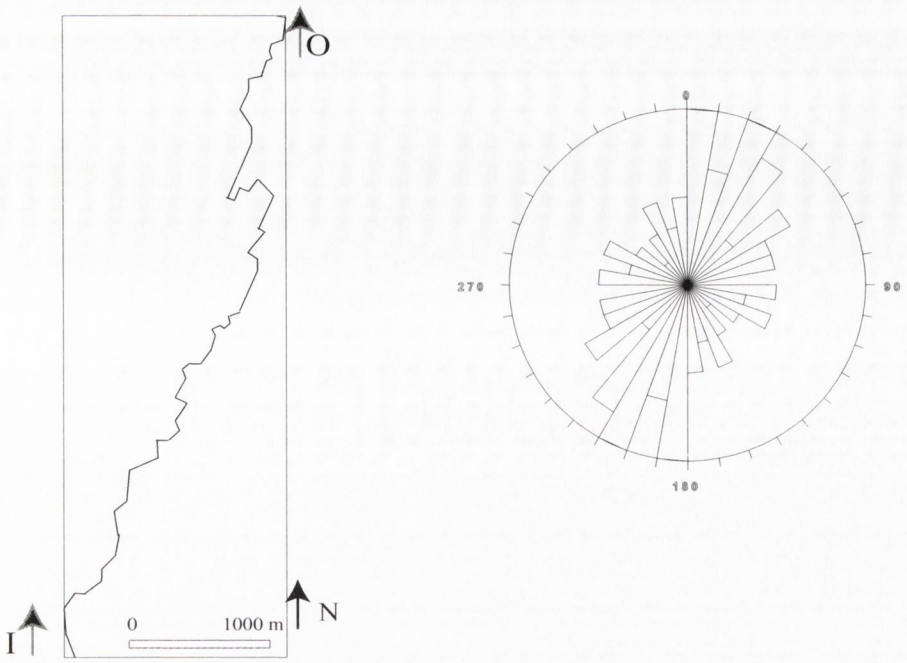

Figure 7.27: Gort River is located along the fracture backbone of the area. The backbone consists of NNE,NW-SE, NE-SW and EW fracture. The system is 4.8 km long and .5 km wide. I: Input O: Output

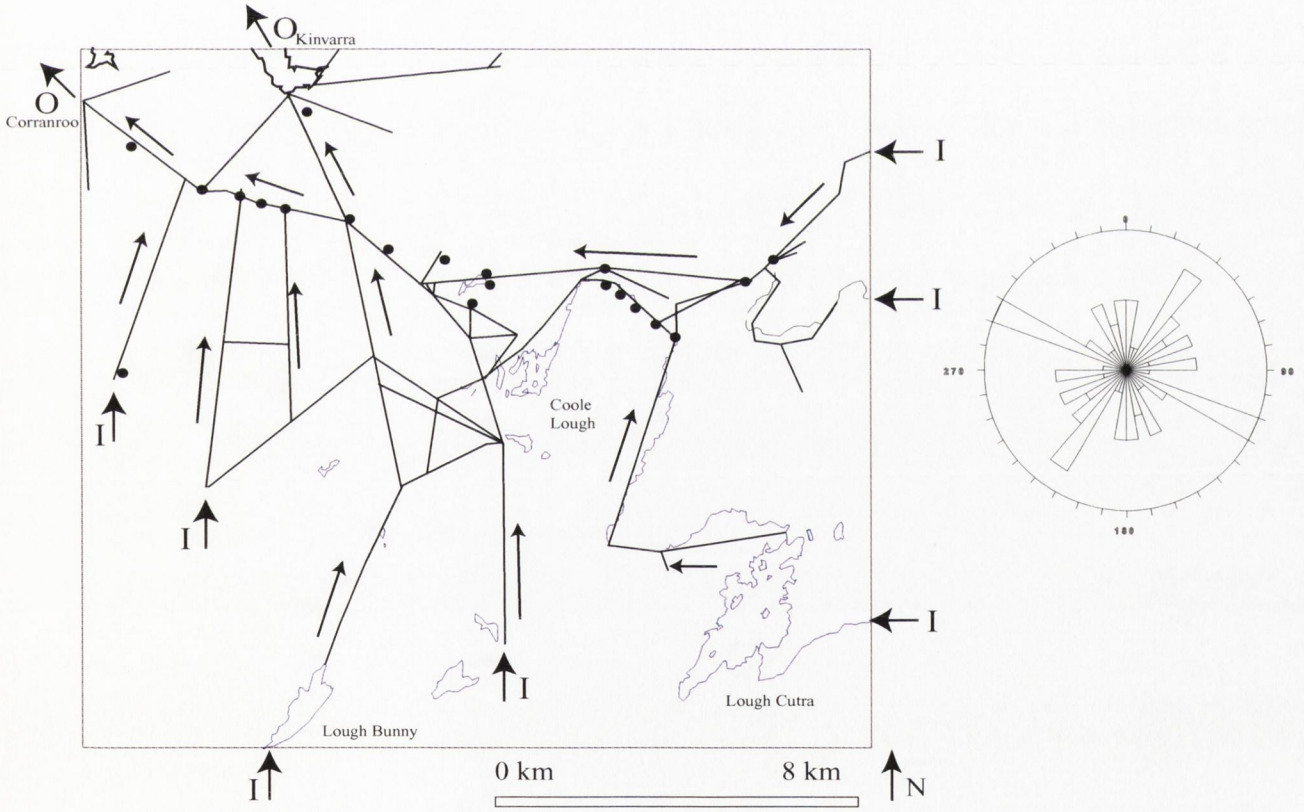

Figure 7.28: Sub-surface and surface drainage of the Gort Lowlands. The drainage is concentrated along the fracture backbone of the system. Input is from the south and east and exits via springs at Kinvarra and Corranroo to the north-west. Data for flow directions was obtained from the OPw 1998 report on the flooding of the Gort-Ardrahan area.

I: Input
O: Output
•: Caves
↑: Flow direction

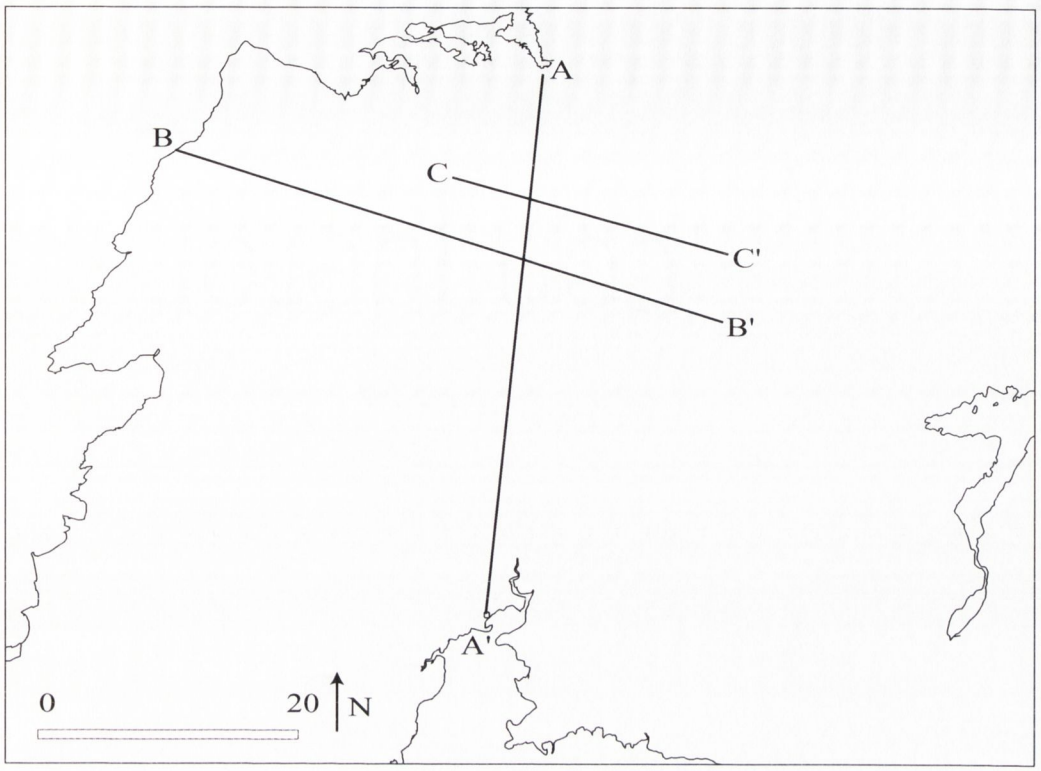

Figure 7.29: Location of traverses A-A', B-B' and C-C', figs 7.24, 7.25 & 7.26 respectively.

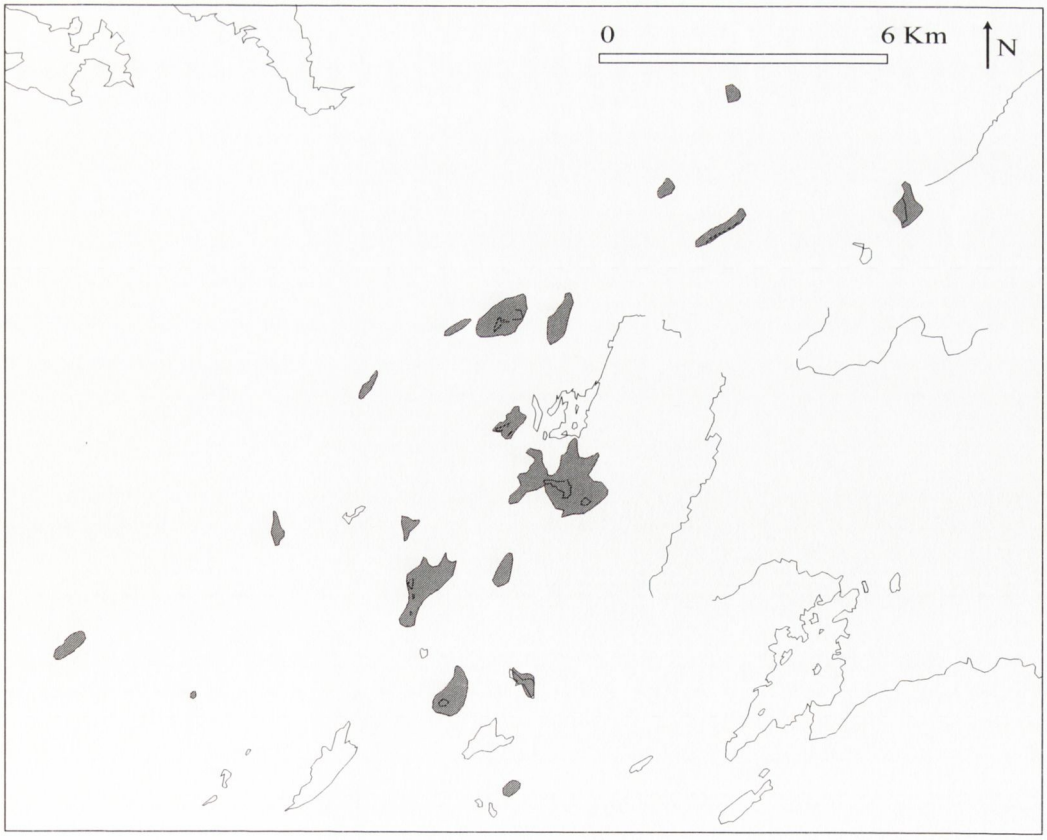

Figure 7.30: Location of the Depression and surface draiange on thw Gort Lowlands.

CHAPTER 8: DISCUSSIONS AND CONCLUSIONS

8.1: Discussion

Throughout the thesis the hypotheses outlined in Chapter 1 have been examined through analysis of three separate but inter-linked data sets- the fracture network, the cave systems and the topography of the region, with a view to proving or disproving the hypotheses. The primary hypothesis of this thesis is that "Topographic depressions are located along areas of high fracture density" the secondary, associated, hypothesis is that the "Fracture density controls the flow of fluid in the study area and the morphology of the cave systems". The results from the data to some extent prove the hypotheses but also highlight the need for modification of them. Topographic depressions are located along areas of high fracture density and fracturing does influence fluid flow in the region yet the thesis highlights the primary role of the vein set in controlling these. Fracture density is a broad ranging term, the vein clusters are areas of with a high fracture density but in this thesis it is seen that it is the interaction of the vein set and the joints with the resultant increase in connectivity that is a primary control. The original hypothesis needs to be modified to include the role of connectivity and could be better written as "Topographic depressions are located along areas of high fracture connectivity" and the secondary one rewritten as "Fluid flow and cave morphology are strongly controlled by zones of high fracture connectivity". The hypothesis should include the caveat that the regional geology needs to be investigated to highlight the effects of differential erosion on different layers, as well as the local hydrological controls being investigated. The hypotheses were tested in an area of relatively homogenous geology and a rock type that was susceptible to chemical weathering.

The principal result that comes out of the thesis is the primary importance of the veins rather than the joints in controlling karstic features such as depressions and caves. The veins are preferentially utilised due to the following characteristics, they are clustered, vertically persistent, have a regionally consistent trend, are well connected, have a high rate of intersections per units area, and are horizontally persistent along strike for over 7km. They define narrow zones of increased connectivity that enable flow to transfer across a region. By contrast the joints are regularly spaces, have a lower degree of connectivity, strata-bound and have a regionally variable trend. The veins exert a strong control on the backbone of a fracture system and therefore on regional fluid flow and resulting features. The vertical and horizontal persistence of the vein clusters allows the flow to transfer quickly and effectively between the point(s) of input and discharge. In karstic terrain's dissolution is the primary weathering agent in this region, in bedrock where the matrix is largely impermeable, fractures are the principal pathways of dissolution in the region and thus the resulting dissolution created features will be strongly controlled by the fracture pattern.

An analysis of the fracture patterns allows for an understanding of the characteristics of these cave systems and topographic depression, their locations, geometry's and spatial relationships. The two fracture sets, veins and joints, have different attributes and are utilised to differing extents. A preliminary visual analysis of the cave systems and depressions within the region shows the majority of them trend NNE (Figures 7.12, 7.20, 7.21) coincident with the regional vein trend. Analyses of the cave passages show that the NNE trending vein controlled passages are the dominant features.

The cave systems of the region are controlled by two factors, firstly the fracture network and secondly the local hydrological controls. The majority of the caves in the Burren are horizontally extensive within the one bed having formed above a series of aquitards. The Caves will preferentially form along the high connectivity vein dominated sections. These vein dominated sections start to acquire increased levels of flow and accelerate in growth as they define preferential flowpaths. The joint controlled cave passages act to connect adjacent vein controlled sections. Analysing the data within a GIS allows for the spatial distribution of the caves to be evaluated. It can be seen that vein clusters which control passages in one cave can be followed along strike to where they can be seen to control passages in separate caves such as Gragan, Green Streams and Doonyvardan caves. The local hydrological conditions, in the form of hydrological gradient, topography, location of resurgences and location of inputs, particularly localised sinking streams along the Namurian margin, exert a strong control on the shape of the cave systems in the form of the joint patterns utilised along the caves flow path.

The topographic depressions are located along vein clusters on a variety of scale from micro, metre level, (Figure 7.2) to macro, kilometre level, (Figure 7.12) scale. The depressions mirror the geometrical characteristics of the vein clusters; they are elongate narrow features, which are vertically and horizontally extensive. The surveyed profiles carried out at Cappanawalla and Sheyshmore was compared with the local fracture pattern and it is apparent that the depressions are coincident with the vein clusters. The depression surveyed on Cappanawalla (Figure 7.4) lies along the same spacing profiles discussed in Chapter 3 and shown in Figures 3.8 a, c and e, where it can be seen there is an increase in the frequency of the vein clusters towards the depression.

By utilising the different data sets within a GIS the spatial relationships between them can be investigated. When the location of all the surveyed and mapped depressions, obtained from field visits, DTM analysis and literature review, and the mapped cave systems are displayed there is a strong spatial correlation between the data sets. The vein-controlled passageway at Aillwee Cave is 110m directly below a series of vein controlled topographic depressions (Figures 7.9 and 7.13a). The NNE trending Ballyiny Depression lies directly above the vein controlled Poll Na gCéim (Figures 7.11 a and b). Both features are formed along the high connectivity zone defined by the vein cluster where solution is concentrated thus being preferentially eroded.

8.2: Future work

This thesis has raised a number of issues, which would benefit further work.

Would be of interest to undertake a similar project in different karstic regions from a number of climatic environments and to test the results from this thesis with the results from these projects. Within Ireland this could be tested in the Fermanagh/Leitrim border which has a number of well-documented cave systems. In this location the differences in regional geology, between the Burren and this region, should be taken into account. In the Burren a number of clay layers serve as aquitards forcing the caves to be horizontal, in contrast the caves of the Fermanagh/Leitrim region are principally vertically extensive. In Britain the Yorkshire Dales are a region of extensive exposed karstic landscape with a large number of mapped caves systems. To investigate how climatic variation can have an influence on the results from this thesis the

extensive karstic landscapes of Slovenia, Croatia and Bosnia-Herzegovina could be investigated. The core requirements of any of these projects would be

1. Mapping of the fracture pattern of the region through remotely sensed high quality images and field work
2. Availability of mapped cave systems and flow pathways through out the region
3. Detailed mapping of surface topography through DTM analysis and local field surveys
4. Mapping of the geological units of the region
5. Integration and analysis of the data in a GIS

There have been a number of recent advancements in technology, which would be of great benefit in undertaking this work. The development of 3D laser scanning would allow for the capture of detailed three dimensional data of the landscape and cave systems, this data in the form a point cloud can be manipulated to generate line drawings, 3D models and in conjunction with a camera mounting ortho-rectified photographs. The benefits of this system would be that initial data capture, for small areas, is very quick and that the potential outcome from the data is very detailed. The disadvantages of this system are that post-processing of the data can be lengthy and that the cost of such as system is often prohibitive. Another laser scanning system available that would be suited to covering large areas is LIght Dection and Ranging (LIDAR), this system allows for millimetre accuracy from an aerial survey and in addition this system will take aerial photographs along its flight plan so elevation data obtained from the laser scanning can be compared with the aerial photographs. This data is all obtained digitally and with some post-processing can be used directly in a GIS. As with the 3D laser scanning cost could be prohibitive in utilising this technology.

An obvious use of the data and results obtained from this thesis would be to use the fracture data in a series of computer modelled simulations on fluid flow in a karstic terrain similar to those carried out by Kaufmann & Braun (1999, 2000) and Kaufmann (2002, 2003). These models were carried out by means of finite element method on a 2D mesh of irregularly spaced nodal points. The utilisation of a mapped fracture system into such a model would be of great interest and the results could be compared with the mapped cave systems. These models should take into account the primary importance of the vein systems in conducting fluid flow through the region and their control on the morphology of cave systems and surface topography. In his 2003 paper Kaufmann states that the distribution and geometry of fractures in a karst aquifer is difficult to access by direct observation. This thesis shows that detailed fracture mapping in conjunction with the analysis of cave systems, and an understanding of the regional geology and hydrological controls, can facilitate the observation of the fracture pattern in an aquifer.

8.3: Conclusions

- The veins rather than the joints are of primary importance in controlling karstic features such as depressions and caves.
- The veins are clustered, vertically persistent, have a regionally consistent NNE trend, are well connected, have a high rate of intersections per unit area and are horizontally persistent along strike for over 7km.

Where vein fill is found it is principally sparry calcite with an assortment of fill. It is postulated that the veins formed as a result of north south-directed compression during the Variscan orogeny.

- The joints are regularly spaced, strata-bound, barren, have a regionally variable strike. The joints are younger than the veins. The variable trend and geometrical characteristics of the joints indicate they formed in response to low differential stress, possibly arising from the uplift of weakly folded beds (Gillespie *et al.* 2001). The joints are constrained by mechanical layers in the form of layer interfaces and pre-existing veins. When the Fracture Spacing Ratio (FSR) for each layer is calculated and plotted against the mechanical layer thickness there is a linear relationship between these variables (Figure 3.10), as the MLT increase so does the FSR. This relationship seems to hold true up to a layer thickness of 30m, beyond this it breaks down. The average spacing for the joints from the layers that obey this relationship is 1.77m; this appears to indicate that the joints reach a saturation point at this mean spacing.
- The presence of veins increases the proportion of cross terminations and leads to a corresponding increase in connectivity. There is a positive linear correlation between increased proportion of cross terminations and an increase in connectivity. Correspondingly there is a negative linear correlation between the proportion of blind terminations and a decrease in connectivity.
- The backbone can have different directional characteristics than the fracture network. Where veins occur they have a strong influence of the over all length of the back bone system e.g. location B1, the proportion of the length of the system that is composed of NNE trending fractures/line segments increases from the fracture network where they account for <5% of the total length to the backbone where they accounts for <24% of the total length. The resulting rose diagrams display this change. In the backbone within the vein clusters the vein-controlled sections are linked by shorter joint controlled passages, the clusters are connected to adjacent clusters by longer joint controlled sets.
- NNE trending vein controlled passages are the dominant control on the cave passages. The veins can be followed along strike to be seen to have an influence of other caves along strike; these vein-controlled passages are narrow, long, parallel features similar to the geometrical characteristics of the veins. Calcite filled veins are occasionally seen in caves
- The direction of flow has a strong control on the orientation of the joints that are utilised to make up the cave system. South-westward flow utilises the NE-SW and EW cross joints, with the passages having a higher sinuosity, this is the case at Doolin, Western Knockauns, Coolagh Valley, North West Slieve Elva and Western Poulacapple. Southeastward flow utilises the NW-SE joint set producing longer passages with a lower sinuosity, this is the case along the eastern side of Slieve Elva, eastern and southern side of Poulacapple.
- There is a correlation between the NNE trending cave passages and surface features, the Ballyiny Depression is coincident with Poll Na gCéim, Aillwee Cave is coincident with a series of depressions on the surface.
- Depressions are located along vein clusters. They exhibit similar spatial characteristics to the vein sets, narrow, elongate NNE trending features. Depressions are controlled by the vein set over a wide range of scale from centimetre to kilometre. The depressions unlike the majority of the cave systems, are not strata-bound they can be traced through a number of units, following the vertical persistence of the veins. Solution is concentrated at the highly connected zones defined by the vein clusters.

Bibliography:

Aarseth, E.S, Bourgine, B., Castaing, C., Chilès, J.P, Christensen, N.P., Eeles, M, Fillion, E., Genter, A., Gillespie, P.A., Håkansson, E., Zinck Jørgensen, K, Lindgaard, H.F, Madsen, L., Odling, N.E., Olsen, C, Reffstrup, J, Trice, R, Walsh, J.J., & Watterson, J. 1997. Interim guide to fracture interpretation and flow modelling in fractured reservoirs. European Commission Report EUR 17116 EN (Joule II Contract No. CT93-334)

Alkattan, M, Oelkers, E.H., Dandurand, J-L, Schott, J. 1998. An experimental study of calcite and limestone dissolution rates as a function of pH from –1 to 3 and temperature 25 to 80°C. *Chemical Geology*, **151**, 199-214

Antonelli, M. & Aydin, A. 1995. Effect of faulting on fluid flow in porous sandstones: geometry and spatial distributions *AAPG Bulletin*, **79**

Atkinson, B.K. 1987. Introduction to fracture mechanics and its geophysical applications. In: *Fractures Mechanics of Rock (*Ed: Atkinson, B.K). Academic Press, London. 1-26.

Bai, T. & Pollard, D.D. 2000. Fracture spacing in layered rocks: a new explanation based on the stress transition. *Journal of Structural Geology,* **22**, 43-57

Bai, T, Pollard, D.D. & Gross, M, R. 2000. Mechanical prediction of fracture aperture in layered rocks *Journal of Geophysical Research* **105 B1,** 707-721.

Balberg, I. 1986. Connectivity and conductivity in 2D and 3D fracture systems, *In:* Englman, R & Jaeger, Z (Eds) *Proceedings of international conference on fragmentation, form and flow in fractured media. Ann. Isr.Pys.Soc Vol 8.* 89-101

Balberg, I, Berkowitz, B & Drachsler, G.E. 1991. Application of a percolation model to flow in fractured hard rocks. *Journal of Geophysical Research* **96, B6,** 10015-10021.

Barton, C., Hsieh, P.A, Angelier, J, Bergerat, F., Bouroz, C., Dettinger, M.D. & Weeks, E.P. 1989. Physical and Hydrolic Flow properties of fractures. Field Trip Guidebook T385. *In:* 28th International Geological Congress, "Environmental Engineering and Urban Geology in the United States" Vol. 2, Am. Geophysics. Union

Becker, A. & Gross. M.R 1996. Mechanism for joint saturation in mechanically layered rocks: an example from southern Israel. *Tectonophysics,* **257**, 223-237.

Berkowitz, B & Balberg, I., 1993. Percolation Theory and its application to groundwater hydrology. *Water Resources Research* **29,** 4, 775-794

Boycott, A., Mullan, G.J & Wilson, L.J. 1983. The Cave of the wild Horses, Kilcorney, Co. Clare, Ireland, the 1983 extensions. *Proc. Univ. Bristol Spelaeol. Soc.* **16** (3) 215-220

Boycott, A., Mullan, G.J & Wilson, L.J. 1996. Cave notes: County Clare and County Galway, Ireland, 1996. *Proc. Univ. Bristol Spelaeol. Soc.* **20** (3) 215-237

Boyce, A.J., Anderson, R& Russell, M.J. 1983. "Rapid Subsidence & early carboniferous base metal mineralisation in Ireland", *Trans. Inst. Min. Metall Sec B Applied Earth Science* 92 pp55-66

Bour, O. & Davy, P. 1997. Connectivity of random fault networks following a power law fault length distribution. *Water Resources Research* **33,** 7, 1597-1583

Brown, S.R. & Bruhn, R.L 1998. Fluid permeability of deformable fracture networks *Journal of Geophysical Research,* **103, b2**, 2489-2500.

Bunce, C. 1991. Seven Streams, Co. Clare, *Irish Speleology* **14,** 3

Bunce, C. 1995. Poultalloon, Co. Clare, *Irish Speleology* **15,** 2-5

Clayton, K.M. 1997, The rate of Denudation of some British Landscapes. *Earth Surface Processes and Landforms* **22,** 721-731

Coats, J. S. & Wilson, J. R. 1971. The Eastern end of the Galway Granite. *Mineralogical Magazine* **38**, 138-51

Cobbing, E.J. 1969. The geology of the district north wets of Clifden, Co. Galway. *Proceedings of the Royal Irish Academy,* **67B**, 303-325

Coller, D.W. 1984. Variscan Structures in the Upper Palaeozoic rocks of west-central Ireland. *In:* Hutton, D. H.W & Sanderson, D.J. (Eds) Variscan tectonics of the North Atlantic region. *Special Publication Geological Society, London,* **14,** 185-194

Collingridge, B.R. 1960. Pol-an Ionian. *Proceedings of the Univ. Bristol Spelaeol. Soc* **9,** 47-57

Collingridge, B.R. 1969. Geomorphology of the Area. *In;* Tratman E.K. (ed) *The caves of North-West Clare, Ireland. Univ. Bristol Spelaeol. Soc* Newton Abbot : David & Charles,

Collinson, J. D., Martinsen, O., Bakken, B. & Kloster, A. 1991. Early Fill of the Western Irish Namurian Basin: A complex relationship between turbidites and deltas. *Basin Research* Vol. 3, No 4

Cooke, M.L & Underwood, C,A. 2001. Fracture termination and step-over at bedding interfaces due to frictional slip and interface opening. *Journal of Structural Geology* **23**, 223-238

Cope, J.C.W, Guion, D.D., Sevastopulo, G. D. & Swan, A. R. H. 1992 The Lower Carboniferous, *In:* (Ed) Cope, J. C. W., Ingham, J. K. & Rawson, P. F. *Atlas of Palaeogeography and litho-facies: The Geological Society Memoirs no.* 13

Cox, D.R. & Lewis, P.A.W. 1966. The statistical analysis of series of events *Chapman & Hall, London.*

Coxon, P. & Flegg. A.M. 1987. A Late Pliocene/ Early Pleistocene deposit at Pollnahalla, near Headford, Co. Galway. *Proc. Royl Ir. Acd* 87**B** 15-42

Coxon, P. & Coxon. C. 1997. A pre-Pliocene or Pliocene land surface in County Galway. *In.* (Eds) Widdowson, M, *Palaeosurfaces: recognition, reconstruction and palaeoenvironmental interpretation.* Geological Society, London Special Publication, **120,** 37-55

Cremin, B. 1991. Extension of Robbers Den Cave, Co. Clare. *Irish Speleology* **14**, 8-9

Croker, P.F. 1995. The Clear basin: A geological and geophysical outline. *In The petroleum geology of Irelands offshore basins.* (Ed): Croker, P. F. & Shannon, P. M. *Geological Society Special Publication* No. 93

Crowley, Q. & Feely, M. 1997. New perspectives on the order and style of granite emplacement in the Galway Batholith , Western Ireland. *Geological Magazine.* **134** (4) pp 539 - 548.

Cruikshank. K.M & Aydin, A. 1995. Unweaving the joints in Entrada Sandstone, Arches national Park, Utah, USA.. *Journal of Structural Geology.* **17**, 3, 409-421

Dershowitz, W.C. & Einstein, H.H. 1988. Characterising rock joint geometry with joint system models. *Rock Mech. And Eng.*, **21**, 21-51

Dewey, J.F 2000. Cenozoic tectonics of western Ireland. *Proceedings of the Geologists Association* **111**, 291-306

Dolan, J.M. 1983. A structural cross section through the Carboniferous of North-West Kerry. *Irish Journal of Earth Science*, **6**, 95-108

Douglas, J. A. 1909. The Carboniferous of County Clare Ireland. *The Quarterly Journal of the Geological Society of London 260* **65** pp538-583

Drew, D.P. 1973. A preliminary study of geomorphology of the Aillwee area, Central Burren, Co. Clare. *Proceedings of the Univ. Bristol Spelaeol. Soc* **13**, 2, 277-244

Drew, D.P. & Cohen, J.M. 1980. Geomorphology and sediments of Aillwee Cave, Co. Clare, Ireland. *Proceedings of the Univ. Bristol Spelaeol. Soc* **15,** 3, 277-240

Drew, D.P. 1988. The Hydrology of the Upper Fergus river catchment, Co. Clare. *Proceedings of the Univ. Bristol Spelaeol. Soc.* **18**, 2, 265-277

Drew, D.P. 1990. The hydrology of the Burren, Co. Clare. *Irish Geography* **23**, 2, 69-89

Drew, D.P. & Daly. D. 1993. Groundwater and karstification in Mid-Galway, South Mayo and North Clare. *Geological Survey of Ireland Report Series* **93/3**

Drew, D.P & Jones, G. Ll. 2000. Post-Carboniferous pre-Quaternary karstification in Ireland. *Proceedings of the Geologists' Association,* **111**, 345-353.

Drew, D.P. 2003. *Hydrology of the Burren & Gort Lowlands*. In Mullan, G & Drew, D.P. (2003) (Eds) Caves of County Clare and South Galway. Univ. Bristol Spelaeol. Soc

Dyer, R. 1988. Using joint interactions to estimate palaeostress ratios. *Journal of Structural Geology*, **10,** 685-699.

Engelder, T. 1985. Loading paths to joint propagation during a tectonic cycle: an example from the Appalachian Plateau, U.S.A. *Journal of Structural Geology,* **7**, 359-476.

El Desouky, M., Feely, M. & Mohr, P. 1996. Diorite - granite magma mingling and mixing along the axis of the Galway Granite batholith, Ireland. *Journal of the Geological Society of London* 153, 361 - 74.

Eyal, Y, Gross, M.R., Engelder, T. & Becker, A. 2001. Joint development during fluctuation of the regional stress field in Southern Israel. *Journal of Structural Geology* **23,** 279-796

Farrington, A. 1956. The last Glaciation in the Burren Co. Clare. *Proc. Royl Ir. Acd* **B** 64

Feehan, J. 1991. The rocks and Landforms of the Burren. *In:* O'Connell, J.W, Korff, A. (Eds) *The Book of the Burren.* Tir Eolas.

Fleischmann, K, H. 1991. Interaction between jointing and topography: a case study at Mt Acutney, Vermont, U.S.A. *Journal of Structural Geology,* **13,** 357-361

Ford, D.C. & Williams, P.W. 1989. *Karst geomorphology and hydrology*. Unwin Hyman

Friedrich, A.M, Bowring, S.A. & Hodges, K.V. 1997. U-Pb geo-chronological constraints on the duration of arc magmatism and metamorphism from Connemara, Irish Caledonides. *Abstract supplement No. 1 Terra Nova* **9**, 331

Friedrich, Hodges, K.V., A.M, Bowring, S.A. & Martin, M.W. 1999. Geo-chronological constraints on the magmatic, metamorphic and thermal evolution of the Connemara Caledonides, Western Ireland. *Journal of the Geological Society, London* **156**, 1217-1230

Gallagher, S.J. 1996. The Stratigraphy and cyclicity of the later Dinantian platform carbonates in parts of southern and western Ireland. *In:* Strogen, P, Somerville, I.D & Jones, G. Ll. (Eds) *recent Advances in Lower Carboniferous Geology.* Geological Society Special Publication **107,** 239-251

Gill, W.D. 1979. Syn-depositional Sliding and slumping in the West Clare Namurian Basin, Ireland. *Geological Survey of Ireland, Special Paper No. 4*

Gillespie, P, Howard, C.B, Walsh, J.J, & Watterson, J, 1993. Measurement and characterisation of spatial distributions of fractures. *Tectonophysics,* **226**, 116-141

Gillespie, P, Johnston, J.D, Loriga, M.A, McCaffrey, K.J.W, Walsh, J.J. & Watterson, J. 1999. Influence of layering on vein systematics in line samples In Ed: McCaffrey, K.J.W, Lonergan, L & Wilkinson, J.J. *Fractures, Fluid Flow & Mineralisation.* Geol. Soc. Spec. Pub. **155**.

Gillespie, P, Walsh, J.J, Watterson, J, Bonson, C & Manzocchi, T. 2001 Scaling relationships of joint and vein arrays from the Burren, Co. Clare, Ireland *Journal of Structural Geology* **23,** 183-201

Goodhue R. 1996. Maturation rates of the West Clare Basin. Unpublished PhD thesis . University of Dublin

Glover, P.W.J, Matsuki, K, Hikima, R. & Hayash, K. 1998. Synthetic rough fractures in rocks *Journal of Geophysical Research,* **103, B5,** 9609-9620.

Graham, J.R. 2002. Variscian Structures *In:* Holland, C.H. (Ed) *A Geology of Ireland.* Scottish Academic Press, Edinburgh.

Griffiths, J.T. 1980. Hawthorn Cave, Co. Clare, Ireland. *Proceedings of the Univ. Bristol Spelaeol. Soc.* **15**, *3, 241-244*

Gross, M.R. & Engelder, T. 1991. A case for neotectonic joints along the Niagara Escarpment *Tectonics*, **10,** 631-641.

Gross, M.R. 1993. The origin and spacing of cross joints; examples from the Monterey Formation, Santa Barbara Coastline, California. *Journal of Structural Geology*, **15,** No. **6,** 737-751.

Gross, M.R. 1995. "Fracture partitioning: Failure mode as a function of lithology in the Monterey Formation of coastal Californian". *GSA Bulletin,* **107,** No, 7, 779-792.

Gross, M.R. & Engelder, T. 1995. Strain accommodated by brittle failure in adjacent units of the Monterey Formation, U.S.A.: scale effects and evidence for uniform displacement boundary conditions. *Journal of Structural Geology*, **17,** No. 9. 1303-1318.

Gross, M.R, Fischer, M.P, Engelder, T and Greenfield, R.J. 1995. Factors controlling joint spacing in interbedded sedimentary rocks: integrating numerical models with field observations from the Monterey Formation, U.S.A. In: Ed: Ameen, M.S. *Fractography: Fracture topography as a tool in fracture mechanics and stress analysis.* Geol. Soc. London, Spec Publ. **92**. 215-233

Gross, M.R, Bahat, D. & Becker, A. 1997a. Relations between jointing and faulting based on fracture-spacing ratios and fault slip profiles: A new method to estimate strain in layered rocks. *Geology*, **25**, No. 10, 887-890

Gross, M.R, Gutiérrez-Alonso, G, Bai, T, Wacker, M.A, Collinsworth, K.B. & Behl, R.J. 1997b. Influence of mechanical stratigraphy and kinematics on fault scaling relations. *Journal of Structural Geology*, **19,** No.2, 171-183

Halliday, A.N. & Mitchell, J.G. 1983. K-Ar ages of clay concentrates from Irish orebodies & their bearing on the timing of mineralisation. *Trans. Royal Soc. Edinb. Earth Science*, **74**, 1-14

Hancock, P.L. 1985. Brittle microtectonics: principles and practice. *Journal of Structural Geology,* **7**, 437-457.

Hancock, P.L. 1991. Determining contemporary stress directions from neo-tectonic joint systems. *Phil. Trans. R. Soc. Lond.* A **337,** 29-40

Häuselmann, P, Jeannin, P.Y., & Bitterli, T. 1999. Relationship between karst and tectonics: case study of the cave system north of Lake Thun (Bern, Switzerland). *Geodinamica Acta.* **I 12.**, 377-388

Helgeson, D.E. & Aydin, A. 1991. Characteristics of joint propagation across layer interfaces in sedimentary rocks. *Journal of Structural Geology,* **13,** 897-911.

Hermann, G.C. 1997. Digital Mapping of fractures in the Mesozoic Newark basin, New Jersey; Developing a geological framework for interpreting movement of groundwater contaminants. *Environmental GeoSciences* **4,** 2, 68-84

Hobbs, D.W. 1967, The formation of tension joints in sedimentary rocks: an explanation. *Geological Magazine*, **104**. 550-556

Hodson. F, 1954.a The beds above the Carboniferous Limestone in NW Co. Clare, Eire. *The Quarterly Journal of the Geological Society of London* **109** pp 259-283.

Hodson. F, 1954.b The Carboniferous Rocks of Foynes Island, Co. Limerick. *The Geological Magazine* **91,** 153-160

Hodson, F. & Lewarne, G.C 1961. A Mid-Carboniferous (Namurian) Basin in parts of the counties of Limerick and Clare, Ireland. *The Quarterly Journal of the Geological Society of London* **117**, 307-323

Huang, Q. & Angelier, J. 1989. Fracture spacing and its relation to bed thickness. *Geological Magazine.* **126,** 355-362.

Jacques, J. M. & Reavy, R. J. 1994. Caledonian plutonism and major lineaments in the SW Scottish Highlands. *Journal of the Geological Society, London* 151, 955-69

Johnston, J.D., McCaffrey, K.J.W, Loriga, M.A., Watterson, J, Walsh, J.J. & Gillespie, P. 1994. A manual describing: Recording , analysis and prediction of vein and related fracture distributions. *MIRO,* Linchfield, UK.

Johansson, M., Migon, P & Olvmo, M. 2001. Development of joint controlled rock basins in Bohus granite, SW Sweden. *Geomorphology* **40**, 145-161

Judd, B. & Mullan. G.J. 1994. Poll na gCéim, County Clare, Ireland. *Proc. Univ. Bristol Spelaeol. Soc.* **20** (1) 3-13

Kaufmann, G. & Braun, J. 1999. Karst aquifer evolution in fractured rocks. *Water Resources Research.* **35**, 3223-3238

Kaufmann, G. & Braun, J. 2000. Karst aquifer evolution in fractured, porous rocks. *Water Resources Research.* **36**, 1381-1392

Kaufmann, G. 2002. Karst aquifer evolution in a changing water table environment. *Water Resources Research.* **38**, 6, 10.1029/2001

Kaufmann, G. 2002. Karst Landscape Evolution. *Speleogenesis and Evolution of Karst Aquifers, The virtual scientific journal (www.speleogenesis.info).* Republished from Gabrovšek, F. (Ed.) 2002. Evolution of karst: from prekarst to erosion. Postonja-Ljubljana, Zalozba ZRC, 243-258.

Kaufmann, G. 2003. A model comparison of karst aquifer evolution for different matrix-flow formulations. *Journal of Hydrology*, **283**, 281-289

Lawn , B.R. & Wilshaw, T.R. 1975. Fracture of brittle solids. Cambridge University Press. 204 pages

Laderia, F.L. & Price, N.J. 1981. Relationship between fracture spacing and bed thickness. *Journal of Structural Geology,* **3.** 179-183

Leake, B. E. 1974. The crystallisation history and mechanism of emplacement of the western part of the Galway granite, Connemara, Western Ireland. *Mineralogical magazine* **39**, 498 - 513

Leake, B. E. 1978. Granite emplacement: the granites of Ireland and their origin. *In:* Bowes, D. R. & Leake, B. E. (Eds) *Crustal Evolution in Northwest Britain and Adjacent Regions. Geological Journal, Special Issue* **10**, 21-248

Leake, B. E. 1989. The metagabbros, orthognesisses and paragnesisses of the Connemara complex, Western Ireland. *Journal of the Geological Society, London* **146**, 575-96.

Leake, B. E. 1990. Granite Magmas: their sources, initiation and consequences of emplacement. *Journal of the Geological Society, London,* **147**, 579-89

Leake, B. E., & Tanner, P.W.G. 1994. *The Geology of the Dalradian and Associated Rocks of Connemara, Western Ireland.* Dublin: Royal Irish Academy.

Leeder, M.R. 1987. Tectonic & Paleaogeographic models for Lower Carboniferous Europe, In: Eds. Miller, J., Adams, A.E & Wright, V.P. *European Dinantian Environments.* Geological Journal Special Issue **No. 12**

Lees, A & Miller, J. 1995 Waulsortian Mudbanks pp191-273. In Ed. Monty, C.L.V, Bosence, D.W.J., Bridges, B.H. & Pratt, B. R., *Carbonate Mudmounds: their origins and evolution. Special Publication No. 23 of the International association of Sedimentologists.*

Long, J.C.S & Witherspoon, P.A. 1985. The relationship of the degree of interconnection to permeability in fracture networks. *Journal of Geophysical Research.* **90 B4,** 3087-3098

Lloyd, O.C. & Self. C.A. 1982. The Ballyiny Depression, Co. Clare, Ireland. *Proc. Univ. Bristol Spelaeol. Soc* **16**, 2, 123-131

Mabee , S.B, Hardcastle, K.C. & Wise , D.U. 1994. A method of collecting and analyzing lineaments for regional scale fractured bedrock aquifer studies. *Ground Water* **32**, 884-894

Manzocchi, T. 2002. The Connectivity of two-dimensional networks of spatially correlated fractures. *Water Resources Research*, **38**,9, 1162

Max, M. D. Long, C. B, Keary, R., Ryan. D., Geoghegan, M. O'Grady, M., Inamdar, D. D., McIntyre, T. & Williams, C. E. 1977. *Preliminary report on the geology of the north-western approaches to Galway Bay and part of its landward area.* Geological Survey of Ireland. Series no. RS75/3.

Max, M. D. Long, C. B. & Geoghegan, M. 1978. The Galway Granite. *Bulletin of the Geological Survey of Ireland.* 2, 223-33

Max, M. D., Ryan, P. D. & Inadar, D. D. 1983. A magnetic structural geology interpretation of Ireland. *Tectonics.* **2**

McCaffrey, K.J.W, & Johnston, J.D. 1996 Fractal analysis of a mineralised vein deposit: Curraghinalt gold deposit, County Tyrone. *Mineralium Deposita,* **31,** 52-58

Mc Kerrow, W. S. & Campbell, C. J. 1960. The stratigraphy and structure of the Lower Palaeozoic rocks of north west Galway. *Scientific Proceedings of the Royal Dublin Society.* A1. 27 - 52

McQuillan, H. 1973. Small scale fracture density in Asmari Formation of southwest Iran and its relation to bed thickness and structural setting. *AAPG Bulletin,* **57,** 2367-2385

Meere, P.A. 1995, High and low density fluids in quartz veins from the Irish Variscides. *Journal of Structural Geology*, **17**, 3, pp 435-446

Menuge, J.F., Feely, M., O'Reilly, C. 1997. Origin and granite alteration effects of hydrothermal fluid: isotopic evidence from fluorite veins, Co. Galway, Ireland. *Mineralium Deposita*, **32**, 34-43

Miller, D.J. & Dunne, T. 1996. Topographic perturbations of regional stresses and consequent bedrock fracturing. *Journal of Geophysical Research.* **101 B11** 25523-25536

Mitchell F.G 1985. The periglacial Landscape. *In* Edwards, K.J. & Waren, W.P. (Eds) *The Quaternary History of Ireland.*

Mitchell, F.G. & Ryan, M. 1998. *Reading the Irish landscape.* Town House, Dublin

Mullan, G.J. 2000. Geomorphology and exploration of Poulnagree, Co. Clare, Ireland. *Proc. Univ. Bristol Spelaeol. Soc* **22**, 1, 99-110

Narr, W. 1991.Fracture densities in the deep sub surface: Techniques with application to Point Arguello Oil field. *AAPG Bulletin*, **75**, No. 8, 1300-1323.

Narr, W & Suppe, J. 1991. Joint spacing in sedimentary rocks. *Journal of Structural Geology,* **13,** 1037-1048.

Narr, W. 1996. Estimating Average fracture spacing in sub surface rocks. *AAPG Bulletin,* **80,** No. 10, 1565-

National Research Council. 1996 *Rock Fractures and Fluid Flow: contemporary understanding and applications*. Nat. Acad. Press, Washington, D.C.

Palmer, A.V. 1991. Origin & Morphology of Limestone caves. *Geol. Soc. Amer. Bull.* **103**, 1, 1-21

Price, N.J. 1966, *Fault and joint development in brittle and semi brittle rock.* Pergammon Press, Oxford.

O'Connor, J. 1995. Sediments of Aillwee Cave. *Irish Speleology* **15**, 47-50

O'Connor, P.J, Högelsberger, H, Feely, M. & Rex, D.C. 1993 Fluid Inclusion studies, Rare earth element Chemistry and the age of Hydrothermal Fluorite mineralisation in western Ireland – a link with continental rifting? *Trans. of the Instit. of Mining & Metallurgy, Section B,* **102,** B135-216

O'Connor, P.J., Pyne, McLaughlin, Madden. 1994. Radon Exhalative properties , Radioelement content and Rare Earth Elements composition of Namurian phosphorite deposits, Co. Clare. *Geological Survey of Ireland.* RS 94/3 (Environmental Geology).

O'Raghallaigh, C, Feely, M, McArdle, P, MacDermot, C, Geoghegan, M & Keary, R. 1997. Mineral Localities in the Galway Bay area Geological Survey of Ireland Report Series **RS97/1** (Mineral Resources).

Odling, N.E. 1993. An investigation into the permeability of a 2-D natural fracture pattern" *Memoirs XXIVth Congress International Association Hydrogeologists, Oslo*, 291-300

Odling, N.E. 1997. Scaling & Connectivity of joint systems in sandstones from western Norway *Journal of Structural Geology,* **19,** 1257-1271

Odling, N.E & Roden. J.E. 1997. Contaminant transport in fractured rocks with significant permeability, using natural fracture geometries. *Journal of Contaminant Hydrology.* **27**, 263-283

Odling. N.E, Gillespie, P, Bourgine, B, Castaing, C, Chiles, J-P, Christensen, N.P, Fillion, A, Genter, A, Olsen, C, Thrane, L, Trice, R, Aarseth, E, Walsh, J.J. & Watterson, J. 1999. Variations in fracture system geometry and their implications for fluid flow in fractured hydrocarbon reservoirs *Petroleum Geoscience,* **Vol. 5, No. 4**

Olson, J. & Pollard, D.D. 1989. Inferring palaeostress from natural fracture patterns: a new model *Geology*, **17,** 345-348.

Olson, J. 1993. Joint Pattern development: Effects of sub-critical crack growth and mechanical crack interaction. *Journal of Geophysical Research,* **98, B7**, 12,251-12,265.

Plunkett Dillion, E. 1985. *The field boundaries of the Burren, County Clare.* Unpublished PhD. Thesis University of Dublin.

Pollard, D.D. & Segall, P. 1987. Theoretical displacements and stresses near fractures in rock: with applications to faults, joints, veins, dikes and solution surfaces. In; *Fractures Mechanics of Rock (*Ed: Atkinson, B.K). Academic Press, London. 277-349.

Pulham, A.J. 1989. Controls on internal structure and architecture of sandstone bodies within Upper Carboniferous deltas, County Clare, Western Ireland. *In* Whately, M.K.G and Pickering, K.T. (Eds) *Deltas; sites and traps for fossil fuels.* Geological Society, Special Publication, **41,** 179-203

Rabinovitch, A. & Bahat, D. 1999. Model of joint spacing distribution based on shadow compliance. *Journal of Geophysical Research*, **104, b3**, 4877-4886.

Rider, M. H. 1974 The Namurian of Co. Clare. *Proceedings of the Royal Irish Academy* **74B**

Rider, M.H. 1978. Growth faults in the Carboniferous of Ireland. *Bull. Am. Ass. Petr. Geol.* **62**, pp 2191-2213

Riely, N.J. 1993 Dinantian (Lower Carboniferous) bio-stratigraphy and chrono-stratigraphy of the British Isles, *Journal of the Geological Society of London* **150**, *Celebration paper* pp 427-446

Rives, T, Razack, M, Petit, J.-P. & Rawnsley, K.D. 1992. Joint Spacing; analogue and numerical simulations. *Journal of Structural Geology,* **14**, 925-937.

Sahimi, M. 1995. *Flow and Transport in Porous Media and Fractured Rock: from classical methods to modern approaches.* VCH

Sahimi, M. 1996. Linear and non linear, scalar and vector transport processes in heterogeneous media: Fractals, percolation and scaling laws. *The Chemical Engineering Journal* **64**, *21-44*

Self, C.A. [Ed] 1981. *Caves of County Clare.* Univ. Bristol Spelaeol. Soc

Self, C.A, Miller, K.E. & Lloyd. O.C. 1980. The caves of Oughtdarra, Co. Clare, Ireland. *Proc. Univ. Bristol Spelaeol. Soc* **15**, 3, 245-257

Sevastopulo, G.D. 1981, Lower Carboniferous. *In:* Holland, C.H. (Ed) *A Geology of Ireland.* Scottish Academic Press, Edinburgh.

Sevastopulo, G.D. & Wyse Jackson, P.N. 2002, Lower Carboniferous. *In:* Holland, C.H. (Ed) *A Geology of Ireland.* Scottish Academic Press, Edinburgh.

Sharp, Jnr J.M 1993. Fractured Aquifers/reservoirs: Approaches, problems and opportunities. *Memoirs XXIVth Congress International Association Hydrogeologists, Oslo*, 23-38

Simms, M.J. 2000. Quartz rich cave sediments in the Burren Co. Clare, Ireland. *Proc. Univ. Bristol Spelaeol. Soc* **22**, 1, 81-98

Simms, M.J. 2001. *Exploring the Limestone landscapes of the Burren and the Gort Lowlands*. Burren karst.com.

Sleeman, A.G. & Pracht. M. 1999. Geology of the Shannon Estuary, a geological description of the Shannon estuary region including parts of Clare, Limerick and Kerry to accompany the bedrock geology 1:100,000 scale map series Sheet 17, Shannon Estuary. *Geological Survey of Ireland.*

Stauffer, D. & Aharrony, A. 1994. *Introduction to Percolation Theory: Revised Second Edition* Taylor & Francis, London

Tratman E.K. (1969) [Eds] *The Caves of North West Clare, Ireland.* Newton Abbot 256pp

Twiss, R.J. & Moores, E.M. 1992. *Structural Geology* W.H.Freeman & Co. USA

Van de Steen, B, Vervoort, A. & Sahin, K, 2002. Influence of internal structure of crinoidal limestones on fracture paths. *Engineering Geology.***67**, 109-125

Van der Pluijm, B.A. & Marshak, S. 1997. Earth Structure: An ntroduction to Structural Geology. McGraw Hill

Vincent, P. 1995. Limestone Pavements in the British Isles: A review. *The Geographical Journal*. **161**, 3, 265-274

Walsh, P., Bouulter, M. & Morawiecka, I. 1999. Chatian and Miocene elements in the modern landscape of Western Britain and Ireland. *In:* Smith , B.J., Whalley, W.B. & Warke, P.A (Eds). *Uplift, Erosion & Stability: perspectives on long term landscape development.*

Waltham, A.C, Simms, M.J., Farrant, A.R. & Goldie, H.S. 1997. *Karst and caves of Great Britain.* Geological conservation review series, Chapman & Hall. .

Weaver, J. 1974. Jointing along the Swansea Valley Disturbance (SVD) between Clydach and Hay-on-Wye, South Wales. *The Geological Magazine.* **111** 329-336

Weertman, J, Lin, I. & Thomson, R. 1983. Double slip plane crack model *Acta Metallurgica.* **31,** 473-482.

White, W.B. 1988. *Geomorphology and Hydrology of Karst terrains.* Oxford Uni Press.

Wignall, P.B. & Best. J.L. 2000. The Western Irish Namurian Basin reassessed. *Basin Research.* **12**, 59-78.

Wilkins, A.G., Walford, J,D. & Boycott. A. 1972. The Fergus River Cave, Co. Clare, Ireland *Proc. Univ. Bristol. Spelaeol. Soc.* **13**, 1, 119-128.

Williams, P.W. 1964. *Aspects of the Limestone physiography of parts of Counties Clare and Galway, Western Ireland* Unpublished PhD thesis, University of Cambridge.

Williams, P.W. 1966. Limestone Pavements with special reference to western Ireland. *Trans. Of the Instit. Of British Geographers,* **40,** 155-172

Wu, H & Pollard, D.D. 1995. An experimental study on the relationships between joint spacing and layer thickness. *Journal of Structural Geology.*

Yeates. B. 1997. Enclosed Depressions in the Burren Co. Clare, Ireland. Unpublished MSc. Department of Geography, University of Dublin

Zhang, X & Sanderson, D.J. 1998. Numerical study of critical behaviour of deformation and permeability of fractured rock masses. *Marine and Petroleum Geology*. 15, 535-548

Zhang, X & Sanderson, D.J. 1994. Fractal structure and deformation of fractured rock masses. *In* Kruhl, J,H, (Ed) *Fractal and Dynamic systems in Geosciences* (pp37-52).

Appendix 3.1: Vein Fill data for North Co. Clare / South Co. Galway (O'Raghallaigh et al 1997)

Location	Northing	Easting	Fill	Lithology	Info	Sheet	County
Addergoole	139300	191300	Pb, F	Burren Limestone (Lwr Carb)	Pd, F occur in a N-S trending vein	18	Clare
Aghawinnaun	131400	204800	Ca	Burren Limestone (Lwr Carb)	N trending calcite vein	6	Clare
Ailwee	126200	204700	Ag	Slievenaglasha Fm	Argentiferous galena was once present	5,6	Clare
Ballybrit	134100	226800	Cu	Burren Limestone (Lwr Carb)	Finely disseminated chalcopyrite and malachite	82	Galway
Ballyhehan	126900	205600	Ca	Burren Limestone (Lwr Carb)	The main feature os a N-S trending vein over 1 km long, varying between 2m and 4.5m wide. Parallel offshoots in the limestone can be seen along the edges of the vein. Very pure Calcite	6	Clare
Ballymaquiff North	145100	209600	Pb, Bi, Ca	Burren Limestone (Lwr Carb)	Galena (Kinahan 1865, Cole 1922). The main calcite vein is relatively pure and has a maximum thickness of 9m	113	Galway
Caherglassaun	140600	206300	Pb, Cu	Burren Limestone (Lwr Carb)	N-S trending vein, galena is the main sulphide, Chalcopyrite, malachite, azurite and buronite have been reported	122	Galway
Cappagh	131400	201800	Cu	Burren Lmst/Slievenaglasha Fm	N-S trending chalcopyrite and malachite bearing veins	6	Clare
Castletown	127500	196700	Pb, Zn, Ag, F	Slievenaglasha Fm	(Kinahan 1889)	10	Clare
Commons North	125800	194600	Pb, Cu	Slievenaglasha Fm	Galena, Chalcopyrite and malachite in a narrow 2.5cm N-S trending calcite vein	9,10	Clare

Crossard	125400	191300	Pb, Zn, F	Slievenaglasha Fm	Galena and Sphalerite are found in a 0.5m wide vein which contains fluorite in addition to quartz and Calcite ganggue.	16	Clare
Crumlin	110200	204000	Ag	Burren Limestone (Lwr Carb)	veins trend NW-SE, silver bearing galena.	4	Clare
Curragrean	135700	224900	F	Burren Limestone (Lwr Carb)		94	Galway
Doolin	106900	197600	Zn, Pb, F	Slievenaglasha Fm	Sphalerite and minor galena are found in a Ca-F vein	8	Clare
Drumminacloghaun	143700	201300	Fe, F, Ca	Visean Muddy Fossiliferous Lmst	Thick E-W striking calcite veins.	122	Galway
Fahee North	131000	199900	Ca	Slievenaglasha Fm		10	Clare
Fahygalvan	125700	196500	Cu	Slievenaglasha Fm	NNE 30m calcite vein, 0.4m wide, containing malachite	9	Clare
Garryland	141900	203500	F	Burren Limestone (Lwr Carb)		122	Galway
Glennascaul	138000	228000	F	Burren Limestone (Lwr Carb)		83	Galway
Gortlecka	131800	194400	Ca	Burren Limestone (Lwr Carb)	Ne trending calcite vein	10	Clare
Gortmore	123500	238400	Pb, Zn, Fe	Burren Limestone (Lwr Carb)	Galena, Sphalerite pyrite in a N-S trending vein	68	Galway
Gortmore-2	123800	239200	Pb	Burren Limestone (Lwr Carb)		55	Galway
Kileey More-1	142400	218200	Ca	Burren Limestone (Lwr Carb)	Pure calcite vein extending for 150m	103	Galway
Kileey More-2	142100	217800	Ca	Burren Limestone (Lwr Carb)	continuation of Kileey More 1	103	Galway
Kilweelran	125900	206600	F	Burren Limestone (Lwr Carb)	N-S trending vein 350m long	5	Clare
Kylecreen	137100	197900	Ca	Burren Limestone (Lwr Carb)		11	Clare
Kylecreen-2	136600	197500	Ca	Burren Limestone (Lwr Carb)	Dolomite-calcite vein 3m wide	11	Clare
Laban	146000	210000	Ca	Burren Limestone (Lwr Carb)		114	Galway
Lismoher	120300	296000	Phosphate	Clare Shales-Namurian	Bedded Phosphate	9	Clare
Lisnanroum	122100	198100	Pb, Cu, F	Slievenaglasha Fm	120m long NNW Ca-F vein,containing disseminated galena and chalcopyrite	9	Clare

Merlin Park	134400	225600	Cu, F	Burren Limestone (Lwr Carb)	fluorite and chalcopyrite replacing fossils	94	Galway
Moguohy	127400	198400	Pb, Cu, F	Slievenaglasha Fm	>100m N-S vein (Cole 1922)	10	Clare
Moguohy-2	127200	198400	Ca	Burren Limestone (Lwr Carb)	N-S vein	10	Clare
Moheraroon	125600	195600	Pd, Zn	Slievenaglasha Fm	Near Sheshymore,Galena and Sphalerite	9	Clare
Moneen-1	127300	207000	Ca	Burren Limestone (Lwr Carb)	1m wide N-S calcite vein, thinning to the N	3	Clare
Moneen-2	127300	207400	Ca	Burren Limestone (Lwr Carb)	Northern continuation of Moneen-1	3	Clare
Mortyclogh	128100	211200	Ca	Burren Limestone (Lwr Carb)	N-S veins at least 70 long	3	Clare
Murrooghtoohy North	114700	210700	Ca	Burren Limestone (Lwr Carb)	Major N-S vein of almost 1km length. At this locality the vein is almost 14m wide. Percussion drilling indicates that the vein extends to a depth of 10m.	1	Clare
Murrooghtoohy South	115000	211600	Ca	Burren Limestone (Lwr Carb)	Northern termination of vein exposed at Murroghtoohy North. It occurs 1km SM of Blackhead lighhouse.	1	Clare
Noughaval	120500	196400	Phosphate	Clare Shales-Namurian	Bedded Phosphate	9	Clare
Parknabinna	125100	192800	Cu, Pb	Slievenaglasha Fm	N-S trending veins bearing chalcopyrite, malachite and galena in a Ca gangue	16	Clare
Poulawack	123700	198500	Ca	Slievenaglasha Fm	N trending calcite vein	9	Clare
Pullagh	131800	203300	Cu	Burren Limestone (Lwr Carb)	Quartz- Calcite vein, bear minor amounts of malachite and chalcopyrite	6	Clare
Rakebin	146900	203200	Zn	Burren Limestone (Lwr Carb)	Sphalerite in calcite veinlets and calcite-quartz vugs along with pyrite	123	Galway

Rinville	134500	222700	Pb, Zn, Fe	Dolomitized Burren Limestone	Pyrite and limonite occur as fracture fill mineralisation	94	Galway
Roo	139000	203800	Ca	Burren Limestone (Lwr Carb)		122	Galway
Sheshodonnell East	126900	197000	Zn, Pb, F, Cu	Slievenaglasha Fm	Foot (1863). Comprises 4 NNE trending en echeon calcite veins. Sphalerite, Smithsonite, Hydrated Smithsonite, cerrussite and galena were recodered from the Ca-F gangue (Cole 1922). Also Malachite. Cadmium is present which could be due to secondary enrichment. minor greenockite (CdS)	10	Clare
Sladoo	127400	198700	Pb, Cu, F	Slievenaglasha Fm	N-S trending veins of galena and chalcophyrite bearing Ca-F veins.This is a northwards continuationof the Moguohy vein system.	10	Clare
Streamstown	148600	205600	Pb, F	Burren Limestone (Lwr Carb)	Galena bearing Ca-F veins	123	Galway
Teergonean	208200	197000	Phosphate	Clare Shales-Namurian	Bedded Phosphate	8	Clare
Tullycommon	126900	199700	Zn, Pb, Cu, F	Slievenaglasha Fm	130m long, N trending Ca-F vein bearing Galena, Cerrusite and Smithsonite	10	Clare

Appendix 4.1: Pa:Pb:Px and connectivity *n* data for Cappanawalla and Sheyshmore.

Location	A	B	X	Area m2	Total Term.	% A	%B	%X	Pa	Pb	Px	N	*n*	Σ L (m)	Mean L (m)	ρ	Dc	Max L
Cappanawalla																		
A2	200	79	42	1200	321	62.31	24.61	13.08	0.623	0.246	0.131	321	3.47	1548.587	4.82426	1.29049	3.32948	29.391
B1	359	72	73	1200	504	71.23	14.29	14.48	0.712	0.143	0.145	383	4.009	1391.864	3.63411	1.15989	2.24036	23.009
BB2	309	229	153	1200	691	44.72	33.14	22.14	0.447	0.331	0.221	658	3.435	2614.632	3.9736	2.17886	4.72507	29.271
B4	265	98	164	1200	527	50.28	18.6	31.12	0.503	0.186	0.311	557	4.727	2727.381	4.89655	2.27282	5.59596	29.479
B11	413	266	59	1200	738	55.96	36.04	7.995	0.56	0.36	0.08	468	2.781	1772.425	3.78723	1.47702	2.42621	24.695
A3	298	208	13	1200	519	57.42	40.08	2.505	0.574	0.401	0.025	359	2.458	1612.059	4.49042	1.34338	3.33363	29.738
89A2	554	223	128	1200	905	61.22	24.64	14.14	0.612	0.246	0.141	517	3.511	1662.705	3.21606	1.38559	3.17477	30.388
89A3	221	265	15	1200	501	44.11	52.89	2.994	0.441	0.529	0.03	345	1.942	1757.108	5.09307	1.46426	3.90782	38.593
89A1	111	79	189	1200	379	29.29	20.84	49.87	0.293	0.208	0.499	205	6.316	1541.658	7.52028	1.28472	4.1813	33.516
A6	318	173	122	1200	613	51.88	28.22	19.9	0.519	0.282	0.199	351	3.585	1883.508	5.36612	1.56959	4.84035	35.439
A7	405	162	170	1200	737	54.95	21.98	23.07	0.55	0.22	0.231	395	4.056	2059.005	5.21267	1.71584	4.88657	39.034
B6	147	138	189	1200	474	31.01	29.11	39.87	0.31	0.291	0.399	228	4.716	1648.929	7.23214	1.37411	5.52697	35.561
B7	180	108	91	1200	379	47.49	28.5	24.01	0.475	0.285	0.24	245	3.764	1285.608	5.24738	1.07134	2.75712	25.656
B8	375	165	223	1200	763	49.15	21.63	29.23	0.491	0.216	0.292	905	4.43	3287.462	3.63255	2.73955	5.877	36.037
B9	222	97	74	1200	393	56.49	24.68	18.83	0.565	0.247	0.188	283	3.712	1302.594	4.60281	1.0855	3.27642	35.939
B1	469	246	246	1600	961	48.8	25.6	25.6	0.488	0.256	0.256	576	4	2610.298	4.5331	1.63144	4.43	
B7 no NNE	359	160	21	1200	540	66.48	29.63	3.889	0.665	0.296	0.039	376	2.929					
Sheyshmore																		
B1	48	45	74	900	167	28.74	26.95	44.31	0.287	0.269	0.443	96	5.247	848.271	8.83616	0.94252	3.59757	30.017
B2	63	60	50	900	173	36.42	34.68	28.9	0.364	0.347	0.289	112	3.675	739.919	6.60642	0.82213	2.77181	30.204
B3	63	89	27	900	179	35.2	49.72	15.08	0.352	0.497	0.151	84	2.368	853.373	10.1592	0.94819	4.07365	30.352
B4	116	83	100	900	299	38.8	27.76	33.44	0.388	0.278	0.334	179	4.342	978.817	5.46825	1.08757	2.53181	28.868
B5	205	64	140	900	409	50.12	15.65	34.23	0.501	0.156	0.342	236	5.13	1147.983	4.86433	1.27554	2.98291	30.512
B6	171	81	114	900	366	46.72	22.13	31.15	0.467	0.221	0.311	199	4.524	1072.795	5.39093	1.19199	3.12857	30.279
B7	44	52	56	900	152	28.95	34.21	36.84	0.289	0.342	0.368	96	4.167	783.175	8.15807	0.87019	2.93474	29.918
B8	125	55	34	900	214	58.41	25.7	15.89	0.584	0.257	0.159	143	3.533	820.570	5.73825	0.91174	2.59443	29.850
B9	155	48	30	900	233	66.52	20.6	12.88	0.665	0.206	0.129	156	3.645	832.31	5.33532	0.92479	2.8457	30.111

	788																
All	3	3050	5796	115,000	16729	47.12	18.23	34.65	0.471	0.182	0.346	32905	5.005	67785.88	2.06005	0.58944	0.65911	57.195
134B1	77	30	29	900	136	56.62	22.06	21.32	0.566	0.221	0.213	101	3.963	676.144	6.6945	0.75127	3.15419	29.456
134B2	67	79	47	900	193	34.72	40.93	24.35	0.347	0.409	0.244	144	3.123	683.340	4.74542	0.75927	1.83556	30.277
134B3	63	32	35	900	130	48.46	24.62	26.92	0.485	0.246	0.269	77	4.126	590.239	7.66544	0.65582	2.63865	26.902
134B4	59	18	39	900	116	50.86	15.52	33.62	0.509	0.155	0.336	100	5.091	632.966	6.32966	0.7033	1.94622	30.322
GLEN	20	61	29	100	110	18.18	55.45	26.36	0.264	0.555	0.182		2.178					
OU1	16	32	6	100	54	29.63	59.26	11.11	0.111	0.593	0.296		2.316					
OU2	28	36	12	100	76	36.84	47.37	15.79	0.158	0.474	0.368		3.333					
CC	23	18	6	100	47	48.94	38.3	12.77	0.128	0.383	0.489		4.833					

A: Abutment termination

B: Blind termination

X: Cross termination

Pa/b/x: Proportion of ..

N: Number of fractures

n: Connectivity ($n = 4(1-P_B)/(1-P_X)$)

ΣL: Sum of the length in metres

ρ: Density measured as ΣL/Area

Dc: Critical Density $(1/4A\sum_{L\min}^{L\max} N_L L^2)$

Appendix 6.1: Location data for Cave and swallow hole in North Co. Clare / South Co. Galway (Tratman 1969, Self 1981. Boycott et al 1996

Cave Name	Length (m)	Depth (m)	Symbol	Altitude (m)	Area	Easting	Northing
Derreen West S5	0		S5	-10	West Coast	111975	205610
Derreen West S6	12		S6	4	West Coast	112000	205010
Poulavaud	0		S7	2	West Coast	111220	204860
Poulsallagh	16		S1	4	West Coast	108590	201770
Ballyryan S1b	6		S1b		West Coast	108539	201888
Ballyryan S3	0		S3	2	West Coast	108450	201495
Ballyryan S4		4	S4	8	West Coast	108530	201450
Glasha More	30		S9	4	West Coast	107745	200210
Lackglass caves	18		S10B	4	West Coast	107210	198820
Lackglass caves	40		S10C	4	West Coast		
Lackglass caves	8		S10D	4	West Coast		
Teergonean	10		S12	4	West Coast	106790	198570
Poulcraveen	250		S2	4	West Coast	106300	198020
Hot Tip Cave			Sballa1		West Coast	105650	197670
Joe's Cave			Sballa2		West Coast	105600	197630
Mermaids Hole	1500		Sballa3		West Coast	105650	197500
Poulcaoeen/Mermaids Hole			Sballa4		West Coast	105760	197780
Poulnagree system	1255	70	A3a	235	Knockauns	112200	203700
Tri eagnai Mouncai Inlet	120		A3d	245	Knockauns	112170	203540
Upper Poulnagree	25		A3	245	Knockauns	112190	203610
Poll Ballynahown	635	75	A4a	213	Knockauns	111640	202740
Poulomega	280	70	A4	210	Knockauns	111580	202545
Lackaniska resurgence	0		A16	107	Oughtdarra	110350	202660
Yellow Cave	10		A16b	137	Oughtdarra	110000	202430
Robbers Den Cave	130		A16c	140	Oughtdarra	110950	202430
Animal Den cave	6		A16d	137	Oughtdarra	110120	202430

Through & Through	43		A16e	137	Oughtdarra	110150	202480
Fairweather	7		A16f	137	Oughtdarra	110195	202480
Moonmilk cave	250		A16g	140	Oughtdarra	110195	202480
Ivy Cave	15		A16h	140	Oughtdarra	110290	202320
Rubbish Cave	12		A16i	154	Oughtdarra	110260	202520
Oughtdarra west resurgence	0		A19	88	Oughtdarra	110040	202590
Lysachts Cave	10		A17a	80	Oughtdarra	110055	202330
Goat Cave	20		A17b	80	Oughtdarra	110070	202150
Loop Cave	7		A17c	80	Oughtdarra	110170	202150
Oughtdarra resurgence	0		A17	58	Oughtdarra	110095	201930
Oughtdarra East Resurgence	0		A18	73	Oughtdarra	110450	201570
Doolin cave system	10050	55	D1-D5		Doolin		
Fisherstreet Pot			D1	20	Doolin	107420	196870
Aran View swallet			D2	60	Doolin	108470	198260
St Catherines One			D5	60	Doolin	109550	198330
St Catherines Two	460		D4	60	Doolin	110435	198206
Pollapooka 3		10	A1c	261	NW Slieve Elva	114910	205350
Pollapooka 1		26	A1	268	NW Slieve Elva	114870	205210
Pollballyelly	178	68	A1d	254	NW Slieve Elva	114720	205150
Pollapooka 2	5		A1b	262	NW Slieve Elva	114720	205060
Goat Hole		5	A1a	276	NW Slieve Elva	114740	205010
Faunarooska cave	1690	94	A2	262	NW Slieve Elva	114240	204500
Hawthorn Swallet	255		A2a	263	NW Slieve Elva	114180	204440
Pollballiny	2065		B1a	253	NW Slieve Elva	113950	204260
Pollegob North	30		B1i	250	NW Slieve Elva	114010	204120
Pollegob	20		B1h	250	NW Slieve Elva	113970	204095
Pollderreen	80		B1j		NW Slieve Elva	113790	203980
Polldubh system	1430				NW Slieve Elva		

Polldubh North	970		B1f B1g B3a	244	NW Slieve Elva	69.6 69.2 66.6	28.9 28.8 23.4
			B1f	244	NW Slieve Elva	113760	203830
			B1g	244	NW Slieve Elva	113730	203810
			B3a	244	NW Slieve Elva	113460	203295
Polldubh South	460		B3	236	NW Slieve Elva	113610	203340
B1e cave	10		B1e		NW Slieve Elva	113820	204040
Poll na gCeim	890	181	B5a		NW Slieve Elva	112920	203340
Coolagh River cave	5285	72	B7-b10		Coolagh River Valley		
Upper Coolagh Valley cave	10		B6	207	Coolagh River Valley	64.8 to 60.4	17.9 to 11.5
			B6a	207	Coolagh River Valley	113310	202710
			B6b	207	Coolagh River Valley	112900	202010
Polldonough	1780		B7	172	Coolagh River Valley	112510	201410
Polldonough North	1530		B8	183	Coolagh River Valley	112290	201780
Polldonough South	720		B9	168	Coolagh River Valley	112500	201090
Pollclabber	475		B10	152	Coolagh River Valley	111960	200750
Polldonough west	270		B8a	178	Coolagh River Valley	112020	201570
Poll an Chaisc	875		B8b		Coolagh River Valley	116900	201810
B10b	3		B10b	150	Coolagh River Valley	111790	200760
Pollcloghaun	256	25	B10f	149	Coolagh River Valley	116200	200760
School house sink	3		B10d	137	Coolagh River Valley	111510	200700
Poulnagun B11	225	38	B11	128	Coolagh River Valley	111425	200300
Poulnagun B12	6		B12	122	Coolagh River Valley	111060	200400
Poulnagun B13	10		B13	131	Coolagh River Valley	111130	200300
Poulnagun B14	55	25	B14	122	Coolagh River Valley	110730	200210
Ballynalackan B19	10		B19	122	Coolagh River Valley	110550	200280
Ballynalackna B19a	20		B19a	120	Coolagh River Valley	110540	200260
Ballynalackan B20	13		B20	122	Coolagh River Valley	110380	200350
Pol Dorian	8		A5g	91	Coolagh River Valley	110060	199850
Pol an Ionain	550		A5g	72	Coolagh River Valley	109800	199830
Cregg Lodge swallet	10		A6	70	Coolagh River Valley	109750	199990

Coolmeen E2	550		E2	274	Eastern Slieve Elva	115520	204820
Poulnagollum - Poulelva Cave System	1168	100	E3- E10		Eastern Slieve Elva		
PP E3			E3	272	Eastern Slieve Elva	115625	204500
PP E3a			E3a	272	Eastern Slieve Elva	115630	204420
PP E3b			E3b	272	Eastern Slieve Elva	115640	204400
Pollnua			E4	260	Eastern Slieve Elva	115770	203870
Pollbinn			E6	250	Eastern Slieve Elva	115910	203610
Poulnagollum Pothole	14468		E7	225	Eastern Slieve Elva	116100	203750
Pollismorahaun			E9	226	Eastern Slieve Elva	116235	202750
PP E9a			E9a	225	Eastern Slieve Elva	116140	202750
Poulelva pothole			E10	198	Eastern Slieve Elva	116360	202280
Pollbeg	0		E8	220	Eastern Slieve Elva	116205	203500
Bullock pot	1000		E11	213	Eastern Slieve Elva	116270	202380
PP E11b	23		E11b	191	Eastern Slieve Elva	116210	201670
Cragreagh Rd Swallet	30		E11c	188	Eastern Slieve Elva	116150	202630
Pollcragreagh	430	36	E12	183	Eastern Slieve Elva	116050	202430
Poll cahercloggaun East	3		E13	181	Eastern Slieve Elva	115960	202310
Poll cahercloggaun West	10		E14	179	Eastern Slieve Elva	115780	202220
Poll cahercloggaun west one	3170		E14a	179	Eastern Slieve Elva	115640	202110
Poll Kilmoon East	230		E18	159	Eastern Slieve Elva	115220	200550
Killeany rising	10		F1	140	Eastern Slieve Elva	116390	200800
Owentoberlea swallet	0		F2	137	Eastern Slieve Elva	116300	200450
Murphys Bridge Stream Cave	0		F8	120	Lisdoonvarna	112950	199390
Kilmoon stream cave	90		F6	120	Lisdoonvarna	113620	199260
Poultalloon	1910		F5	143	Lisdoonvarna	114160	200010
Owenacloggaun Cave	0		F9	146	Lisdoonvarna	114470	200050
St Brendan's Dig	100	10	F4b	103	Lisdoonvarna	114630	198635
St Brendan's Well	0		F4b	92	Lisdoonvarna	114710	198430
Poll gowlaun	80	15	F4a	106	Lisdoonvarna	114800	198700

F3a sink			F3a		Lisdoonvarna	115080	198770
F3b			F3b		Lisdoonvarna	115090	198780
F3c			F3c		Lisdoonvarna	114900	198880
Cullaun 0-1	65		C0-1	240	W. Poulacapple	118120	203170
Cullaun 0	410		C0	220	W. Poulacapple	17 16.6 16.6 16.4	17.1 16.4 16.2 15.3
Cullaun 0 a			a			117970	202420
Cullaun 0 b			b			117930	202350
Cullaun 0 c			c			117930	202330
Cullaun 0 d			d			117900	202240
Cullaun 1	3100		C1	218	W. Poulacapple	118110	202400
Cullaun 2	3335		C2 C2a C2e	210	W. Poulacapple	19 19.5 21.7	11.4 12.4 16.1
			C2			118195	201820
			C2a			118250	201920
			C2e			118480	202320
Caullaun 3	3500	78	C3 C3b	210	W. Poulacapple	21.8 21	10 8.2
			C3			118490	201660
			C3b			118410	201470
Ballyconnoe N C2d	0		C2d	190	W. Poulacapple	117950	200880
Croagh South sink	20				E. Poulacapple	119700	201420
Poulacapple Pot	10		H0	268	E. Poulacapple	118730	204119
Green Stream cave	300		H0-1	256	E. Poulacapple	119140	203720
Gragan West Cave	2255		H1 H1a H2 H2a	250	E. Poulacapple	28.2 28.4 29.2 30.2	25.9 23.4 21.4 19.8
			H1			119220	202400
			H1a			119240	202140

			H2			119310	202890
			H2a			119420	202710
Forestry sink		10	H1b	244	E. Poulacapple	119160	203030
H2b	0		H2b	235	E. Poulacapple	119420	202610
H3	0		H3	220	E. Poulacapple	119420	202250
H4	10		H4	218	E. Poulacapple	119470	202170
Doonyvardan Cave	1740		H8	210	E. Poulacapple	119520	201665
Poll Cahermacnaghten	1800		G1a	180	S.Poulacapple	119370	200740
Cullaun 5	5950		C5 C5b C5c C5d	190	S.Poulacapple	22.6 22.6 23.4 24.1	4.3 1.8 6.9 58.4
			C5			118570	201050
			C5b			118570	200790
			C5c			118650	201330
			C5d			118635	200520
Cahermacnaghten C5a	70		C5a	190	S.Poulacapple	118800	201000
Ballyconnoe N C5e	0		C5e	190	S.Poulacapple	118470	201010
Poll Cahermaan	1000		C6	170	Knockavoarheen Ridge	118650	199540
Hammer Pot	10		C14	174	Knockavoarheen Ridge	119025	199650
Boulder Pot	8		C19	174	Knockavoarheen Ridge	119150	199670
Poulawillin	2000		G2	171	Knockavoarheen Ridge	119700	199460
Ballymahony Cave	175		G5	138	Knockavoarheen Ridge	118700	198060
Poulnagollum Ballyshanny	150		G10	83	Knockavoarheen Ridge	118650	195540
Pollballygoonaun	200		G11	92	Knockavoarheen Ridge	117250	194990
Black Head caves	10		NWB1	30	North Western Burren	115510	212250
Caher Valley Cave	15		NWB2	100	North Western Burren	115250	209010

Fanore cave	22		NWB3	57	North Western Burren	114800	208710
Lighthouse Cave	10		NWB6	2	North Western Burren	115390	212170
St Johns Well	0		NWB7	115	North Western Burren	119420	206200
Toberdhu	5		NWB8	160	North Western Burren	117570	206060
Toberdhu South	25		NWB9	176	North Western Burren	117670	205050
Ailwee Cave	1070		NCB1	92	North Central Burren	123400	204870
Ballymihil Cave	23		NCB2	195	North Central Burren	124860	201510
Glensleade Cave	20		NCB3	140	North Central Burren	123210	201160
Jacko's Hole	10		NCB4	214	North Central Burren	124370	205210
Kilweerlan Cave	10		NCB5	281	North Central Burren	125030	205110
Maze Holes	140		NCB6	244	North Central Burren	124970	204840
Mill cave	12		NCB7	226	North Central Burren	124490	204570
Mill sink	0		NCB8	207	North Central Burren	124470	204430
Polberneens	12		NCB9	140	North Central Burren	122680	202770
Poll gorm	76		NCB10	61	North Central Burren	127400	206900
Poulawillin cave	5		NCB11	152	North Central Burren	124980	200330
Poulgorm Cave	14		NCB12	178	North Central Burren	124330	201115
Poulnabrone Cave	6		NCB13	153	North Central Burren	123790	201050
Skeleton Cave	10		NCB14	23	North Central Burren	123270	206770
Spur Holes	25		NCB15	220	North Central Burren	124490	204340
Coskeam Cave	30		NEB1	159	NE Burren	130960	202000
Fahee Cave	14		NEB2	152	NE Burren	130460	200360
Poulcarra cave	10		NEB3	55	NE Burren	132230	199990
Glen of Clab cave			NEB4		NE Burren	129920	202190
Pollnaluchnacrua	15		NEB5	125	NE Burren	129770	210980
Poulbaun cave	2		NEB66		NE Burren	134140	204570
Cave of the Wild Horses (Kilcorney 1)	520	40	SCB2	103	S Central Burren	122200	199330
Kilcorney 2	18		SCB3	122	S Central Burren	122220	199320
Kilcorney 3	0		SCB4	122	S Central Burren	122130	199320
Kilcorney 4	23		SCB5	131	S Central Burren	122295	199805
Kilcorney 5	8		SCB6	131	S Central Burren	122290	199805
Moheraroon cave	12		SCB7	101	S Central Burren	125760	195840

Poulcarry caves	25		SCB8	153	S Central Burren	124620	197150
Ballyconry Cave	19		SEB1	152	SE Burren	127770	198430
Carran mine cave	80		SEB2	153	SE Burren	127390	198260
Cashlaungarr cave	7		SEB3	116	SE Burren	127770	196500
Castletwon river sink	0		SEB4	116	SE Burren	128410	198010
Clooncoose Cave	31		SEB5	116	SE Burren	127920	195860
Commons north caves	10		SEB6	152	SE Burren	127720	194450
Glencurran cave	400		SEB7	110	SE Burren	127390	196310
Gortlecka cave	123		SEB8	33	SE Burren	131820	194560
Seven streams of Teeskagh	75		SEB9		SE Burren	128530	196120
Monocline holes	10		SEB8	150	SE Burren	127810	194630
Sheshodonnell West Cave	60		SEB9	104	SE Burren	126250	195920
Morans Cave	1160		GL4	21	Gort Lowlands	138940	207620
Pollaloughabo	1500 incGL18		GL6	15	Gort Lowlands	136860	208010
Polldeelin	10		GL7	15	Gort Lowlands	141810	205640
Pollnadirk	40		GL9	20	Gort Lowlands	140050	206930
Pollnapasty	45		GL11	18	Gort Lowlands	141220	206550
Quinn's Cave	10		GL12	15	Gort Lowlands	135680	208230
The Bridge			GL14		Gort Lowlands	144790	205870
Coole river main rising 2			GL16		Gort Lowlands	144340	206190
Pollaleen			GL17		Gort Lowlands	148030	206610
Pollbehan	1500 incGL6		GL18		Gort Lowlands	136170	208230
Pollanoween			GL19		Gort Lowlands	147490	206150
Polldalagha			CL20		Gort Lowlands	141810	206170
Polldeelin spring			GL21		Gort Lowlands	145100	205670
Pollhoish	50 +		GL22		Gort Lowlands	138150	209820
Pollnageanh	60	30	GL23		Gort Lowlands	133870	209490

Pollnamona			GL24		Gort Lowlands	141680	206260
Polltoophill sinks							
Polltoophill main sink			GL25		Gort Lowlands	145920	204900
Polltoophill Kiltaran Castle sink			GL26		Gort Lowlands	145960	204740
Raheen Hse Flood rising			GL27		Gort Lowlands	144380	206490
Skelpnahooey	25		GL28		Gort Lowlands	137340	207860
Tom Murray' sink			GL29		Gort Lowlands	144670	206050
Fergus river cave	2300	56	F1	50	Fergus area	125198	192267
Fergus resurgence	0		F2	29	Fergus area	124987	191878
Poulnaboe	0		F3	30	Fergus area	124359	191790
Elmvale Risings	10		F4	27	Fergus area	125757	191776
Chamber pot	7		F5	61	Fergus area	125916	190828
Nooan pothole	95	15	F6	60	Fergus area	125758	190589
Vigo cave	100		F7	55	Fergus area	126020	190514
Boulder Pot	10		F8	46	Fergus area	126095	190582
Nooan cave	8		F9	41	Fergus area	126144	190718
Drummoher pot East	17		F10	61	Fergus area	124958	190696
Drummoher pot West	90	25	F11	61	Fergus area	124846	190699